

องค์ประกอบชนิดและการแพร่กระจายของสัตว์เลื้อยคลานด้วยน้ำนมในสมัยไพลสโตซีนตอนกลางในตำบล
โคกสูง จังหวัดนครราชสีมา และการมีส่วนร่วมในชุมชนสัตว์มีกระดูกสันหลัง



นายกันตภณ สุระประสิทธิ์

จุฬาลงกรณ์มหาวิทยาลัย

CHULALONGKORN UNIVERSITY

บทคัดย่อและแฟ้มข้อมูลฉบับเต็มของวิทยานิพนธ์ตั้งแต่ปีการศึกษา 2554 ที่ให้บริการในคลังปัญญาจุฬาฯ (CUIR)
เป็นแฟ้มข้อมูลของนิสิตเจ้าของวิทยานิพนธ์ ที่ส่งผ่านทางบัณฑิตวิทยาลัย

The abstract and full text of theses from the academic year 2011 in Chulalongkorn University Intellectual Repository (CUIR)
are the thesis authors' files submitted through the University Graduate School.

วิทยานิพนธ์นี้เป็นส่วนหนึ่งของการศึกษาตามหลักสูตรปริญญาวิทยาศาสตรดุษฎีบัณฑิต

สาขาวิชาวิทยาศาสตร์ชีวภาพ

คณะวิทยาศาสตร์ จุฬาลงกรณ์มหาวิทยาลัย

ปีการศึกษา 2558

ลิขสิทธิ์ของจุฬาลงกรณ์มหาวิทยาลัย

SPECIES COMPOSITION AND DISTRIBUTION OF MIDDLE PLEISTOCENE MAMMALIAN
FAUNA IN KHOK SUNG SUBDISTRICT, NAKHON RATCHASIMA PROVINCE
AND ITS CONTRIBUTION TO VERTEBRATE COMMUNITY

Mr. Kantapon Suraprasit



A Dissertation Submitted in Partial Fulfillment of the Requirements
for the Degree of Doctor of Philosophy Program in Biological Sciences

Faculty of Science

Chulalongkorn University

Academic Year 2015

Copyright of Chulalongkorn University

Thesis Title SPECIES COMPOSITION AND DISTRIBUTION OF
MIDDLE PLEISTOCENE MAMMALIAN FAUNA IN KHOK
SUNG SUBDISTRICT, NAKHON RATCHASIMA
PROVINCE AND ITS CONTRIBUTION TO VERTEBRATE
COMMUNITY

By Mr. Kantapon Suraprasit

Field of Study Biological Sciences

Thesis Advisor Professor Somsak Panha, Ph.D.

Thesis Co-Advisor Professor Jean-Jacques Jaeger, Ph.D.

Accepted by the Faculty of Science, Chulalongkorn University in Partial
Fulfillment of the Requirements for the Doctoral Degree

.....Dean of the Faculty of Science
(Associate Professor Polkit Sangvanich, Ph.D.)

THESIS COMMITTEE

.....Chairman
(Noppadon Kitana, Ph.D.)

.....Thesis Advisor
(Professor Somsak Panha, Ph.D.)

.....Thesis Co-Advisor
(Professor Jean-Jacques Jaeger, Ph.D.)

.....Examiner
(Assistant Professor Tosak Seelanan, Ph.D.)

.....Examiner
(Assistant Professor Thasinee Charoentitirat, Ph.D.)

.....External Examiner
(Yaowalak Chaimanee, Ph.D.)

กันตภณ สุระประสิทธิ์ : องค์ประกอบชนิดและการแพร่กระจายของสัตว์เลี้ยงลูกด้วยนมในสมัยไพลสโตซีนตอนกลางในตำบลโคกสูง จังหวัดนครราชสีมา และการมีส่วนร่วมในชุมชนสัตว์มีกระดูกสันหลัง (SPECIES COMPOSITION AND DISTRIBUTION OF MIDDLE PLEISTOCENE MAMMALIAN FAUNA IN KHOK SUNG SUBDISTRICT, NAKHON RATCHASIMA PROVINCE AND ITS CONTRIBUTION TO VERTEBRATE COMMUNITY) อ.ที่ปริกษาวิทยาพนธ์หลัก: ศ. ดร. สมศักดิ์ ปัญหา, อ.ที่ปริกษาวิทยาพนธ์ร่วม: ศ. ดร. ฌอง ฌาคส์ เจเกอร์, 266 หน้า.

เมื่อปีพ.ศ. 2548 ซากดึกดำบรรพ์สัตว์มีกระดูกสันหลังจำนวนมากถูกค้นพบที่บ่อทรายบริเวณบ้านโคกสูง จังหวัดนครราชสีมา ตัวอย่างที่ค้นพบประกอบไปด้วยกะโหลกศีรษะ ฟัน และกระดูกของสัตว์เลี้ยงลูกด้วยนมและสัตว์เลื้อยคลานที่ถูกเก็บรักษาในสภาพที่ค่อนข้างสมบูรณ์ไปจนถึงเป็นเศษชิ้นส่วนที่แตกหัก จากการศึกษาลักษณะทางสัณฐานวิทยาของตัวอย่างที่ค้นพบโดยทำการเปรียบเทียบกับสัตว์ปัจจุบันและกับซากดึกดำบรรพ์ของสัตว์ที่สูญพันธุ์ไปแล้ว พบว่ากลุ่มสัตว์เลี้ยงลูกด้วยนมในบริเวณนี้สามารถจัดจำแนกทางอนุกรมวิธานได้ทั้งสิ้นออกเป็น 15 ชนิด 13 สกุล ประกอบไปด้วยสัตว์ในกลุ่มไพรเมต ช้าง ไฮยีน่า หมา แรด หมู วัว ควาย และกวาง ซึ่งสัตว์บางสายพันธุ์ได้สูญพันธุ์ไปแล้ว นอกจากนั้นซากดึกดำบรรพ์ของสัตว์เลื้อยคลาน 3 สายพันธุ์ คือ จระเข้ น้ำจืด งูหลามไม่ระบุชนิด และตะกวดไม่ระบุชนิดได้ถูกบรรยายเพิ่มเติมขึ้นจากการศึกษาก่อนหน้านี้ ทั้งนี้สายพันธุ์ที่ค้นพบในบริเวณบ้านโคกสูงนี้มีความสอดคล้องกับกลุ่มสัตว์เลี้ยงลูกด้วยนมโบราณที่ประกอบด้วยช้างสเตโกดอนและแพนด้ายักษ์ ซึ่งมีการกระจายตัวอย่างกว้างขวางในภาคพื้นทวีปเอเชียตะวันออกเฉียงใต้และในตอนใต้ของประเทศจีนตลอดสมัยไพลสโตซีน ซากดึกดำบรรพ์ของกวางดาวซึ่งเป็นหนึ่งในสัตว์ปัจจุบันที่อาศัยอยู่บริเวณอนุทวีปอินเดียได้ถูกค้นพบเป็นครั้งแรก โดยกลุ่มสัตว์มีกระดูกสันหลังบริเวณบ้านโคกสูงนี้มีอายุอยู่ในสมัยไพลสโตซีนตอนกลางหรือประมาณ 2 แสนปีที่ผ่านมาจากหลักฐานการเทียบสัมพันธ์ของชั้นแม่เหล็กบรรพกาลและการเปรียบเทียบกลุ่มสิ่งมีชีวิตกับบริเวณแหล่งซากดึกดำบรรพ์อื่นๆที่เคยมีการค้นพบมาก่อนหน้านี้ จากการวิเคราะห์ความคล้ายคลึงกันของกลุ่มสิ่งมีชีวิตพบว่ากลุ่มสัตว์เลี้ยงลูกด้วยนมบริเวณบ้านโคกสูงมีความคล้ายคลึงกับกลุ่มสิ่งมีชีวิตในสมัยไพลสโตซีนตอนกลางที่ค้นพบบริเวณถ้ำวิมานนาคินจังหวัดชัยภูมิมากที่สุด ซากดึกดำบรรพ์ของสัตว์เลี้ยงลูกด้วยนมที่ค้นพบในบริเวณบ้านโคกสูงประกอบไปด้วยสายพันธุ์ที่อาศัยอยู่ในบริเวณภาคพื้นทวีปเอเชียตะวันออกเฉียงใต้ทั้งสิ้น โดยสัตว์เลี้ยงลูกด้วยนมกลุ่มนี้ได้มีการอพยพไปยังเขตหมู่เกาะชวาในช่วงปลายสุดของสมัยไพลสโตซีนตอนกลางด้วยเส้นทางโบราณจากจีนตอนใต้ไปยังเกาะชวาผ่านทางบริเวณไหล่ทวีปซุนดาของอ่าวไทย เนื่องจากช่วงยุคน้ำแข็งนั้นมีการลดลงของระดับน้ำทะเลประมาณ 100 ถึง 150 เมตรจากระดับน้ำทะเลในปัจจุบัน จึงก่อให้เกิดลักษณะภูมิประเทศแบบแผ่นดินบริเวณไหล่ทวีปซุนดาที่เชื่อมต่อกับแผ่นดินใหญ่เอเชียตะวันออกเฉียงใต้กับเขตหมู่เกาะอินโดนีเซีย การศึกษาองค์ประกอบชนิดของกลุ่มสัตว์เลี้ยงลูกด้วยนมในภาคตะวันออกเฉียงเหนือของประเทศไทยนี้จึงเป็นหลักฐานหนึ่งของการแลกเปลี่ยนกันของกลุ่มสัตว์บกขนาดใหญ่ในยุคน้ำแข็งระหว่างภาคพื้นทวีปกับเขตหมู่เกาะของเอเชียตะวันออกเฉียงใต้ สภาพแวดล้อมโบราณบริเวณบ้านโคกสูงเป็นทุ่งหญ้าใกล้กับแม่น้ำสายหลัก ซึ่งประกอบไปด้วยสัตว์เลี้ยงลูกด้วยนมขนาดใหญ่จำนวนมากอาศัยอยู่ จากการวิเคราะห์การกระจายตัวของน้ำหนักของกลุ่มสัตว์เลี้ยงลูกด้วยนมที่ค้นพบบริเวณบ้านโคกสูงและถ้ำวิมานนาคิน บ่งบอกว่าภาคตะวันออกเฉียงเหนือของประเทศไทยเป็นบริเวณที่มีอากาศค่อนข้างชื้นในช่วงสมัยไพลสโตซีนตอนกลาง

สาขาวิชา วิทยาศาสตร์ชีวภาพ

ลายมือชื่อนิสิต

ปีการศึกษา 2558

ลายมือชื่อ อ.ที่ปรึกษาหลัก

ลายมือชื่อ อ.ที่ปรึกษาร่วม

5472889223 : MAJOR BIOLOGICAL SCIENCES

KEYWORDS: LARGE MAMMAL / TAXONOMY / PALEOBIOGEOGRAPHY / QUATERNARY / NORTHEASTERN THAILAND

KANTAPON SURAPRASIT: SPECIES COMPOSITION AND DISTRIBUTION OF MIDDLE PLEISTOCENE MAMMALIAN FAUNA IN KHOK SUNG SUBDISTRICT, NAKHON RATCHASIMA PROVINCE AND ITS CONTRIBUTION TO VERTEBRATE COMMUNITY. ADVISOR: PROF. SOMSAK PANHA, Ph.D., CO-ADVISOR: PROF. JEAN-JACQUES JAEGER, Ph.D., 266 pp.

The terrace deposit of Khok Sung, Nakhon Ratchasima province, has yielded the richest Pleistocene vertebrate fauna of Thailand, where abundant fossil mammals and reptiles (skulls, isolated teeth, and postcranial remains) were recovered. The mammalian fauna consists of at least 15 recognized species in 13 genera, including a primate, proboscideans, carnivores rhinoceroses, suids, bovids, and cervids, characterized by mostly extant elements associated to some extinct (*Stegodon cf. orientalis*) and extirpated (*Crocota crocuta ultima*, *Rhinoceros unicornis*, *Sus barbatus*, and *Axis axis*) taxa. Three reptilian taxa: *Crocodylus cf. siamensis*, *Python* sp., and *Varanus* sp. are also identified. The Khok Sung mammalian taxa characterize the Pleistocene *Ailuropoda–Stegodon* faunal complex found throughout the subtropical to tropical forested regions of South China and mainland Southeast Asia. A chital, *Axis axis*, whose distribution is today restricted to the Indian Subcontinent, is reported here for the first time in Southeast Asia during the Pleistocene. The age of the Khok Sung fauna is tentatively attributed to the late Middle Pleistocene as either 188 or 213 ka, based on the paleomagnetic data and on the faunal comparisons. According to an analysis of the faunal similarity using the Simpson index, the Khok Sung mammalian fauna is most similar to that of Thum Wiman Nakin (northeastern Thailand), whose age has been dated to older than 169 ka. Compared to other Southeast Asian Pleistocene and extant faunas, the Khok Sung mammal assemblage yields most of mainland Southeast Asian taxa that migrated to Java during the latest Middle Pleistocene, supporting the hypothesis that Thailand was a part of the Sino-Malayan migration route from South China to Java. The Sunda shelf, forming when the sea-levels dropped during glacial stages, is supposed to provide the only possible route of mammalian dispersal between Southeast Asian mainland and islands. The Khok Sung fauna illustrates an open grassland landscape with abundant and diversified herbivores, close to the main river channel. A cenogram analysis of the mammalian fauna reflects a relatively humid condition for Khok Sung, similar to that of Thum Wiman Nakin, during the late Middle Pleistocene.

Field of Study: Biological Sciences

Academic Year: 2015

Student's Signature

Advisor's Signature

Co-Advisor's Signature

ACKNOWLEDGEMENTS

I would like to thank all of the supervisors and colleagues who have helped me to complete this research and to attain my Doctor of Philosophy degree in Biological Sciences program. I would like to express deepest gratitude to my thesis supervisor, Prof. Dr. Somsak Panha (Chulalongkorn University), for his guidance, encouragement, and financial supports throughout this research project. I would like to extend special thanks to my co-supervisor, Prof. Dr. Jean-Jacques Jaeger, who led me down research avenues and supported me to maintain the necessary persistence to explore them. I would particularly like to thank Dr. Olivier Chavasseau for his constructive improvements and reviews of the thesis manuscript. I am indebted to Dr. Yaowalak Chaimanee, who encouraged and inspired me to step beyond the traditional field of geology into the fantastic world of vertebrate paleontology. I am grateful to Dr. Noppadon Kitana, Assistant Professor Dr. Tosak Seelanan, and Assistant Professor Dr. Thasinee Charoentitrat for serving on my thesis committee and for generously offering their time and guidance.

The completion of this research would not have been possible without the assistances of several museums, departments, and laboratories and their associated personnel. I would like to thank all of the curators, who permitted me access to the collection and provided me the comparative fossil and extant material, including Dr. Joséphine Lesur (MNHN), Chen Jin (IVPP), Natasja den Ouden (RMNH), Dr. Frank Zachos (NMW), Alexander Bibl (NMW), Gassner Georg (NMW), Dr. Reinhard Ziegler (SMNS), Michael Hiermeier (ZSM), and Cholawit Thongcheroenchakit (THNHM). I would like to express our grateful thanks to Dr. Mouloud Benammi for his paleomagnetic analysis and to Dr. John de Vos (NBC) who provided me some additional information regarding the Pleistocene mammalian taxonomy during my visit to the Dubois collection. I am grateful to Mana Rugbumrung (DMR), Pannipa Tian (DMR), Chotima Yamee (DMR), and Bernard Marandat (ISEM) for their works during the excavation. I also thank Dr. Ekgachai Jiratthitikul (MU) for his assistances with the geometric-morphometric analysis. I take this opportunity to record my sincere thanks to all members from the Animal Systematics Research Unit (Chulalongkorn University) for scientific discussions and communications, as well as for our friendship.

I am obligated to my dad, mom, brothers, and Miss Armooh, who gave me financial and moral supports, as well as encouragement, when I needed them. I also thank my beloved friends and cousins: Aphinand, Chatchalerm, Manit, Chonlada, Patchara, Chawin, Karanta, and Suppharun, who graciously helped me collect the data at the museums and generate the PhD thesis database. I especially thank Preusamon for her encouragement and dissertation assistance.

I especially acknowledge the following academic institutions and departments: Department of Biology (Faculty of Science, Chulalongkorn University) and iPHEP (Université de Poitiers) for all facilities and financial supports through the research study and Department of Mineral Resources and the Khok Sung subdistrict municipality for allowing me access to the collection. Finally, this research could not have succeeded without the financial supports funded by the following grants: “The 90th Anniversary of Chulalongkorn University Fund” (Ratchadaphiseksomphot Endowment Fund), “60/40 Support for Tuition Fee”, “Support for the Overseas Presentations of Graduate Level Academic Thesis”, “ED Gay Lussac”, and “La Fondation Poitiers Université”.

CONTENTS

	Page
THAI ABSTRACT	iv
ENGLISH ABSTRACT	v
ACKNOWLEDGEMENTS	vi
CONTENTS	vii
LIST OF FIGURES	xiii
LIST OF TABLES	xxv
CHAPTER 1.....	1
Introduction	1
Rationale.....	1
Objectives of the study	4
CHAPTER 2.....	5
Literature reviews	5
Southeast Asian history and biogeographic provinces	5
Zoogeographic history of Southeast Asian mammalian faunas	8
Pleistocene mammalian faunas in mainland Southeast Asia	11
The Republic of the Union of Myanmar (Myanmar)	13
The Lao People’s democratic Republic (Laos)	15
The Kingdom of Cambodia (Cambodia).....	16
The socialist Republic of Vietnam (Vietnam).....	17
The Federation of Malaysia (Peninsular Malaysia).....	19
The Kingdom of Thailand (Thailand)	21
CHAPTER 3.....	25

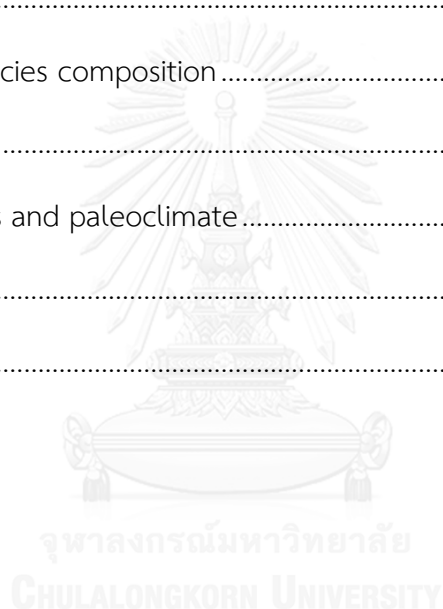
	Page
Study area and geological background.....	25
The discovery of the Khok Sung fossiliferous site.....	25
Geologic setting.....	27
Lithostratigraphy.....	28
Previous chronological framework and magnetostratigraphic analysis	31
CHAPTER 4.....	34
Material and methods	34
Material and measurements.....	34
Taxonomic study (identification, classification, and nomenclature).....	49
Dental nomenclatures	49
3D geometric-morphometric analysis.....	55
Samples and 3D scans.....	55
Landmark acquisition.....	57
Statistical analyses.....	58
Species composition and distribution analyses.....	59
Faunal similarity measures and cluster analysis	59
Body mass estimation and cenogram analysis.....	60
CHAPTER 5.....	62
Results and discussion.....	62
Taxonomic study.....	62
<i>Macaca</i> sp.....	62
Material description	62
Taxonomic remarks and comparisons	63

	Page
<i>Crocota crocuta ultima</i> (Matsumoto, 1915)	64
Material description	65
3D geometric-morphometric analysis of fossil and recent hyaenid crania	70
Size differences between hyaenid taxa.....	70
Shape differences between hyaenid taxa.....	71
Taxonomic remarks and comparisons	72
<i>Cuon</i> sp.....	77
Material description	77
Taxonomic remarks and comparisons	77
<i>Stegodon cf. orientalis</i> Owen, 1870.....	80
Material description	80
Taxonomic remarks and comparisons	86
<i>Elephas</i> sp.....	92
Material description	92
Taxonomic remarks and comparisons	93
<i>Rhinoceros sondaicus</i> Desmarest, 1822.....	94
Material description	94
Taxonomic remarks and comparisons	98
<i>Rhinoceros unicornis</i> Linnaeus, 1758.....	99
Material description	99
Taxonomic remarks and comparisons	100
<i>Sus barbatus</i> Müller, 1838.....	101

	Page
Material description	101
Taxonomic remarks and comparisons	106
<i>Axis axis</i> (Erxleben, 1777).....	108
Material description	109
Taxonomic remarks and comparisons	117
<i>Panolia eldii</i> (M'Clelland, 1842).....	121
Material description	122
Taxonomic remarks and comparisons	125
<i>Rusa unicolor</i> (Kerr, 1792).....	128
Material description	128
Taxonomic remarks and comparisons	131
<i>Bos sauveli</i> Urbain, 1937.....	132
Material description	132
Taxonomic remarks and comparisons	136
<i>Bos gaurus</i> (Hamilton-Smith, 1827).....	139
Material description	140
Taxonomic remarks and comparisons	143
<i>Bubalus arnee</i> (Kerr, 1792).....	144
Material description	145
Taxonomic remarks and comparisons	152
<i>Capricornis sumatraensis</i> (Bechstein, 1799).....	153
Material description	153
Taxonomic remarks and comparisons	155

	Page
<i>Crocodylus cf. siamensis</i> Schneider, 1801	156
Material description	157
Taxonomic remarks and comparisons	159
<i>Python</i> sp.	159
Material description	159
Taxonomic remarks and comparisons	160
<i>Varanus</i> sp.	161
Material description	161
Taxonomic remarks and comparisons	162
Faunal composition of Khok Sung vertebrate assemblage.....	163
Individual species distribution patterns.....	166
Stegodontids and elephantids.....	167
Javan and Indian rhinoceroses.....	169
Bearded pigs	172
Chitals (Axis deer)	174
Eld's and sambar deer	175
Koupreys, gaurs, and wild water buffaloes	178
Sumatran serows	181
Faunal comparisons of the assemblage with other penecontemporaneous assemblages.....	183
Cenogram analysis.....	186
CHAPTER 6.....	188
Discussion	188

	Page
Contribution to the age of Khok Sung.....	188
Evolutionary and biogeographic affinities of Khok Sung fauna	190
Paleoecological, paleoenvironmental and paleoclimatic implications of Khok Sung.....	194
CHAPTER 7.....	197
Conclusion and perspectives	197
Chronology.....	197
Taxonomy and species composition.....	199
Paleobiogeography	201
Paleoenvironments and paleoclimate.....	203
REFERENCES	205
VITA.....	266



LIST OF FIGURES

- Figure 1.** Map of Southern Asia showing the biogeographical regions and subregions (modified from Lekagul and McNeely, 1988; Corbet and Hill, 1992; Antoine, 2012).....6
- Figure 2.** Map of Southeast Asia showing the land exposure (sky blue color), at sea level of 120 m below the present day, over Sundaland and Indochina during the Pleistocene (modified from Voris, 2000).9
- Figure 3.** Map of mainland Southeast Asian countries showing the location of the Early (blue square), Middle (red star) and Late (yellow circle) Pleistocene fossil sites. 14
- Figure 4.** Map of Thailand showing the location of the Khok Sung fossiliferous site in Nakhon Ratchasima province, northeastern Thailand (modified from the Royal Thai Survey Department topographic map: scale 1:50,000, sheet 5439III, series L7017). Red lines indicate highways of Thailand. 25
- Figure 5.** The sand pit of Khok Sung during the paleontological excavation (in March, 2005): (A) a general view of the sand pit, (B) an area of vertebrate fossil recovery, and (C) *in situ* remains of *Stegodon*. The photos were taken by Yaowalak Chaimanee during the fieldwork. The blue arrow indicates the location of the fossiliferous layer (above the dark gray layer) and the black one points to the non-marine Mesozoic bedrock. 26
- Figure 6.** Geological map of Nakhon Ratchasima province. A star indicates the Khok Sung fossil site and red lines refer to main roads. Abbreviations: **Qa** (Quaternary alluvium), **Qt** (Quaternary terrace), **KTms** (Late Cretaceous to Early Palaeogene? Mahasarakam Formation), and **Kkk** (Early to Late Cretaceous Khok Kruat Formation) (modified from Department of Mineral Resources, 2007). 28
- Figure 7.** Magnetostratigraphic and lithostratigraphic profiles of the Khok Sung sand pit, Nakhon Ratchasima province, unit A-I from top to bottom in descending order (after Suraprasit et al., 2015). 30
- Figure 8.** Paleomagnetic data: (A) and (B) examples of orthogonal vector diagrams of progressive alternating field demagnetizations, solid and open circles are projections on horizontal and east-west vertical planes, respectively, (C) a stereographic projection of the sample KS-1A, (D) an equal-area projection of magnetization directions related to horizons of the normal polarity, solid circles are plotted on the lower hemisphere. Overall mean directions and their 95% error limits are given in boxes, and (E) examples of IRM acquisition. 32

Figure 9. Metrical methods and parameters used for the lower third molar of <i>Stegodon</i> . Lengths and widths of the molar ridges are abbreviated as “LR” and “WR”, respectively. An illustration of two right m3 (lateral and occlusal views) of <i>Stegodon orientalis</i> is duplicated from the specimen IVPP V5216-15 (above) and IVPP V5216-13 (below).....	35
Figure 10. Methods of measurements for the hyaenid cranium, mandible, and upper fourth premolar: a cranium in dorsal (A), ventral (B), lateral (C), and posterior (D) views; (E) a mandible in medial view; (F) an upper fourth premolar in occlusal view. Red dash lines indicate the reconstruction of missing parts. The basion (the orobasal border of the foramen magnum in the median plane) is abbreviated as “b”. The number corresponds to the metrical parameters used in Tab. A2.....	36
Figure 11. Methods of measurements for the cranium of <i>Bos</i> in dorsal (A), ventral (B), lateral (C), and posterior (D) views (from von den Driesch, 1976).....	37
Figure 12. Methods of measurements for the cranium of <i>Cervus</i> in dorsal (A), lateral (B), and ventral (C) views (from von den Driesch, 1976).....	38
Figure 13. Methods of measurements for the mandible of ruminants in lateral view (from von den Driesch, 1976).....	39
Figure 14. Methods of measurements for the mandible of <i>Sus</i> in lateral view (from von den Driesch, 1976).	39
Figure 15. Methods of measurements for the scapulae (from von den Driesch, 1976): (A) scapula of <i>Bos</i> in lateral view; (B) scapula of <i>Bos</i> in distal view. Abbreviations: L=left side and R=right side.....	42
Figure 16. Methods of measurements for the humeri (from von den Driesch, 1976): (A) humerus of <i>Equus</i> in posterolateral view; (B) humerus of <i>Bos</i> in anterior view; (C) humerus of <i>Ursus</i> in anterior view; (D) humerus of <i>Cervus</i> in anterior view; (E) proximal humerus of <i>Canis</i> in lateral view. Abbreviations: L=left side and R=right side.....	43
Figure 17. Methods of measurements for the radii and ulnae (from von den Driesch, 1976): (A) radius and ulna of <i>Equus</i> in anterior view; (B) radius and ulna of <i>Bos</i> in lateral view; (C) ulna of <i>Canis</i> in medial view; (D) radius of <i>Canis</i> in anterior view; (E) radius of <i>Equus</i> in proximal view; (F) radius of <i>Equus</i> in distal view; (G) proximal ulna of <i>Cervus</i> in anterior view. Abbreviations: L=left side and R=right side.	44

Figure 18. Methods of measurements for the pelvises (from von den Driesch, 1976): **(A)** pelvis of *Ovis* in dorsal view; **(B)** pelvis of *Sus* in lateral view; **(C)** acetabulum of *Bos*; **(D)** acetabulum of *Equus*. Abbreviations: L=left side and R=right side..... 45

Figure 19. Methods of measurements for the femora (from von den Driesch, 1976): **(A)** femur of *Equus* in posterior view; **(B)** femur of *Ovis* in anterior view; **(C)** proximal femur of *Lepus* in anterior view; **(D)** femur of *Canis* in proximal view. Abbreviations: L=left side and R=right side. .. 46

Figure 20. Methods of measurements for the tibiae (from von den Driesch, 1976): **(A)** tibia of *Equus* in anterior view; **(B)** tibia of *Capra* in proximal view; **(C)** tibia of *Equus* in distal view. Abbreviations: L=left side and R=right side..... 47

Figure 21. Methods of measurements for the metapodial bones (from von den Driesch, 1976): **(A)** metacarpus III of *Equus* in anterior view; **(B)** metatarsus III of *Equus* in anterior view; **(C)** metacarpus III+IV of *Bos* in proximal view; **(D)** metatarsus III+IV of *Ovis* in proximal view; **(E)** metatarsi III+IV of *Bos* in anterior view; **(F)** metatarsus III+IV of *Bos* in proximal view; **(G)** metatarsi III+IV of *Capra* in lateral view. Abbreviations: L=left side and R=right side..... 48

Figure 22. Dental nomenclatures of cheek teeth of hyaenids (modified from Werdelin and Solounias, 1991)..... 50

Figure 23. Dental nomenclatures of cheek teeth of Elephantoidea (from van den Bergh, 1999): **(A)** a lower molar of stegodontids in occlusal view; **(B)** a lower molar of elephantids in occlusal view; **(C)** a molar plate of elephantids in anterior view. Arabic and roman numbers indicate a sequence of molar ridges which are counted, starting from the anterior to posterior direction for the former and from the posterior to anterior direction for the latter. Abbreviations: L=maximum length; W=maximum width; w=maximum width of ridges; h=maximum height; 1=a contact facet with the preceding molar; 2= anterior half ridge; 3=double median expansions of enamel loop; 4=molar ridge; 5=apical digitations of molar ridges; 6=posterior half ridge; 7=complete enamel wear pattern or enamel loop of occlusal surfaces; 8=inner enamel layer; 9=outer enamel layer; 10=dentine; 11=median cleft or median sulcus; 12=transverse valley filled by cementum; 13=anterior median sinus of enamel loop; 14=posterior median sinus of enamel loop; 15=median pillar; 16=molar plate; 17=median digitations; 18=lateral digitations; 19=root. 51

Figure 24. Dental nomenclatures of cheek teeth of rhinoceroses (from Yan et al., 2014): **(A)** upper left third premolar; **(B)** upper left third molar; **(C)** upper right first molar; **(D)** lower left second molar..... 52

Figure 25. Dental nomenclatures of cheek teeth of suids (from van der Made, 1996): **(A)** upper left third premolar; **(B)** upper left fourth premolar; **(C)** upper left third molar; **(D)** lower left premolar; **(E)** lower left second molar; **(F)** lower left third molar. Legends: 0, primocone; 1, paracone/protoconid; 1B", protoprestyle; 1B'D, postcrista of the protopreconule; 1'C, protoendoconulid; 2, protocone/metaconid; 2B', protopreconule; 3, metacone/hypoconid; 3A', hypopectoconulid; 3B', metapreconule/hypopreconulid; 4, tetracone/entoconid; 5, pentacone/pentaconid; 5A', pentaectoconulid; 5B', pentapreconule; 6, hexacone/hexaconid; 7, heptaconid; 7A', heptaectoconulid; 7B', heptapreconulid; 8, octaconid; A, ectocrista; B, precrista/precristid; B', preconule; B", prestyle; B'B, precrista of the preconule; D, postcrista; D", poststyle ; I, profossa..... 52

Figure 26. Dental nomenclatures of upper cheek teeth of ruminants: **(A)** upper second deciduous premolar; **(B)** upper third premolar; **(C)** upper fourth premolar; **(D)** upper third molar. The dental terminology is modified from Heintz (1970), Gentry et al. (1999) and Bärmann and Rössner (2011). 53

Figure 27. Dental nomenclatures of lower cheek teeth of ruminants: **(A)** lower fourth deciduous premolar; **(B)** lower fourth premolar; **(C)** lower third molar. The dental terminology is compiled from Heintz (1970), Gentry et al. (1999), and Bärmann and Rössner (2011). 54

Figure 28. Landmarks digitized in lateral **(A)** and ventral **(B)** views (for anatomical description, see table 3). 57

Figure 29. Schematic representation of categories of cenograms (after Legendre, 1989). 61

Figure 30. Postcranial remains of *Macaca* sp. **(A–D)** and *Cuon* sp. **(E–H)** from Khok Sung: **(A–D)** DMR-KS-05-04-04-1, a right tibia in anterior **(A)**, medial **(B)**, proximal **(C)**, and distal **(D)** views; **(E–F)** DMR-KS-05-04-11-34, a right ulna in medial **(E)** and anterior **(F)** views; **(G–H)** DMR-KS-05-04-28-13, a right femur in proximal **(G)** and posterior **(H)** views..... 63

Figure 31. Remains of *Crocota crocuta ultima* from Thailand. **(A–H)** material from Khok Sung, Nakhon Ratchasima province (northeastern Thailand)—DMR-KS-05-04-2-1: a cranium in dorsal **(A)**, ventral **(B)**, lateral **(C)**, and posterolateral **(D)** views; a right mandible in mesial **(E)** and lateral **(F)** views; an upper left tooth row on occlusal **(G)** view a right tooth row in occlusal **(H)** view, **(I–L)** material from Thum Wiman Nakin—TF-3400: a half right fragmentary m1 in labial **(I)** view; TF-3762: a right p2 in labial **(J)** view; TF-3974: a left p2 in occlusal **(K)** and lingual **(L)** views, and **(M)** material from Thum Phedan, a right fragmentary mandible with P3 and P4 in lingual view. Only the image **D** is not scaled. Abbreviations: **Pal.F**—palentine

foramen; **Inf.O.Ca**—infraorbital canal; **Op.C**—optic canal; **O.Fi**—orbital fissure; **F.R**—foramen rotundum; **Sph.F**—sphenoid foramen; **Inf.Ob**—inferior oblique muscle (fossa); **La.F**—lacrimal foramen; **PostPal.F**—postpalatine foramen; **Ma.F**—mandibular foramen; **Men.F**—mental foramen..... 67

Figure 32. Box plot showing centroid sizes of fossil and recent hyaenid taxa. Each box plot shows the median, first and third quartiles, and maximum and minimum values for the species..... 70

Figure 33. Principal components 1 and 2 with wireframes of cranial shapes represented by positive and negative extremities of each axis in dorsal (dash line) and lateral (solid line) views. The same color refers to the same species, as same as in Fig. 32. 71

Figure 34. Log-ratio diagrams of fossil and extant representatives of *Crocuta crocuta* (measurements standardized to 6 individuals of *Hyaena hyaena*): **(A)** upper dentition and **(B)** lower dentition, comprising Khok Sung *C. c. ultima*, Phnom Loang *C. c. ultima*, Taiwanese *C. c. ultima* including specimens from the Penghu Channel (Ho et al., 1997; Tseng and Chang, 2007), Chinese *C. c. ultima* including specimens from Guanyindong, Xianrendong, Laochihe, Huainan (Tseng et al., 2008) and Zhoukoudian (Pei, 1940), Chinese *C. c. honanensis* including specimens from Henan (Zdansky, 1924), Yushe, Longdan, and Nihewan, and African extant spotted hyaenas (8 individuals). Dental measurements of fossil spotted hyaenas used here are given in Tab. A3..... 74

Figure 35. Dental remains of *Stegodon cf. orientalis* from Khok Sung: **(A–B)** DMR-KS-05-03-28-14, a right DP4 in occlusal **(A)** and buccal **(B)** views; **(C)** DMR-KS-05-03-19-7, an anterior lobe of DP4 in occlusal view; **(D)** DMR-KS-05-04-01-8, a left dp3 in occlusal view; **(E–F)** DMR-KS-05-03-29-1, a left posterior fragment of M2 in occlusal **(E)** and buccal **(F)** views; **(G–H)** DMR-KS-05-03-22-19, a right posterior fragment of M3 in occlusal **(G)** and buccal **(H)** views; **(I–K)** DMR-KS-05-03-15-2, a fragmentary upper tusk in proximal **(I–J)** and dorsal **(K)** views; **(L)** DMR-KS-05-03-08-1, a right mandible with m3 in occlusal view; **(M)** DMR-KS-05-03-08-2, a left mandible with m3 in occlusal view. 82

Figure 36. Postcranial remains of *Stegodon cf. orientalis* from Khok Sung: **(A–B)** DMR-KS-05-03-10-6, a left distal humerus in anterior **(A)** and distal **(B)** views; **(C–D)** DMR-KS-05-03-10-4, a right femur posterior **(C)** and distal **(D)** views; **(E)** DMR-KS-05-03-00-124, a right fibula in posterior view; **(F)** DMR-KS-05-03-10-11, a right pelvis in dorsal view; **(G)** DMR-KS-05-03-10-12, a left pelvis in lateral view; **(H)** DMR-KS-05-03-09-18 and **(I)** DMR-KS-05-03-10-7, vertebrae in

anterior view; (J) DMR-KS-05-03-10-8, a sacrum in ventral view; (K) DMR-KS-05-03-10-14 and (L) DMR-KS-05-03-10-13, ribs in anterior view..... 85

Figure 37. Dental remains of *Elephas* sp. from Khok Sung: (A–C) DMR-KS-05-03-22-1, a fragmentary upper tusk in proximal (A, C) and ventral (B) views; (D–F) DMR-KS-05-03-17-12, a posterior fragment of a right lower molar in occlusal (D), lingual (E), and anterior (F) views. 93

Figure 38. Cranial, mandibular, dental remains of *Rhinoceros sondaicus* from Khok Sung: (A) DMR-05-03-00-128, a left P2 in occlusal view; (B) DMR-KS-05-03-22-17, a left P3 in occlusal view; (C) DMR-KS-05-03-00-129, a left M1 in occlusal view; (D) DMR-KS-05-03-00-127, a left M3 in occlusal view; (E–G) DMR-KS-05-03-00-126, a mandible in lateral (E), occlusal (F) and ventral (G) views; (H–I) DMR-KS-05-03-31-28, a fragmentary mandible in occlusal (H) and lateral (I) views; (J–K) DMR-KS-05-03-00-56, a nasal in dorsal (J) and lateral (K) views. 95

Figure 39. Postcranial remains of *Rhinoceros sondaicus* from Khok Sung: (A–B) DMR-KS-05-03-00-58, a left scapula in lateral (A) and distal (B) views; (C–E) DMR-KS-05-03-31-3, a left humerus in anterior (C), proximal (D), and distal (E) views; (F–H) DMR-KS-05-04-05-15, a right metacarpus IV in posterior (F), proximal (G), and distal (H) views; (I) DMR-KS-05-04-27-19, a right calcaneus in lateral view; (J) DMR-KS-05-03-26-23, a left astragalus in dorsal view. 97

Figure 40. Remains of *Rhinoceros unicornis* from Khok Sung: (A) DMR-KS-05-03-18-X, a right M1 in occlusal view; (B) DMR-KS-05-03-19-4, a left p2 in occlusal view; (C–E) DMR-KS-05-03-17-13, a left mandible in occlusal (C), medial (D), and lateral (E) views; (F–G) DMR-KS-05-03-00-63, a left femur in posterior (F) and distal (G) views..... 100

Figure 41. Remains of *Sus barbatus* from Khok Sung: (A) DMR-KS-05-04-19-2, a left upper cheek tooth row in occlusal view; (B) DMR-KS-05-04-19-5, a left M2; (C) DMR-KS-05-03-18-23, a left fragmentary M2; (D) DMR-KS-05-04-03-4, a right M3; (E) DMR-KS-05-04-19-4, a right M3; (F–G) DMR-KS-05-03-15-1, a mandible in occlusal (F) and lateral (G) views; (H–I) DMR-KS-05-04-19-1, a mandible in occlusal (H) and lateral (I) views; (J) DMR-KS-05-04-19-3, a left fragmentary m3; (K–N) DMR-KS-05-03-26-8, a right humerus in proximal (K), posterior (L), anterior (M), and distal (N) views. Cross-sections of canines are given. All isolated teeth are shown in occlusal view. 102

Figure 42. Cranial remains of *Axis axis* from Khok Sung: (A–B) DMR-KS-05-04-18-50, a cranium with nearly complete antlers in dorsal (A) and ventral (B) views; (C–D) DMR-KS-05-03-00-30, a cranium in lateral (C) and ventral (D) views; (E) DMR-KS-05-03-18-X9, a cranium in anterior view; (F–G) DMR-KS-05-03-27-1, a cranium in dorsal (F) and ventral (G) views; (H) DMR-KS-05-03-31-30, a right antler in anterior view; (I) DMR-KS-05-03-22-4, a right antler in lateral view;

(J) DMR-KS-05-03-18-21, a left antler fragment in lateral view; (K) DMR-05-03-22-2, a left antler fragment in lateral view; (L) DMR-KS-05-03-19-81, a left antler fragment in medial view.. 110

Figure 43. Dental remains of *Axis axis* from Khok Sung: (A) DMR-KS-05-03-08-31, an upper left P3 and P4 in occlusal view; (B) DMR-KS-05-03-28-6, a left upper molar row in occlusal view; (C) DMR-KS-05-04-01-3, a right P4 in occlusal view; (D) DMR-KS-05-04-28-5, a left M1 in occlusal view; (E) DMR-KS-05-03-14-5, a left M2 in occlusal view; (F–G) DMR-KS-05-03-29-1, a left mandible in occlusal (F) and lateral (G) views; (H–I) DMR-KS-05-03-26-10, a right mandibular fragment in occlusal (H) and medial (I) views; (J–K) DMR-KS-05-04-03-1, a right mandible in occlusal (J) and lateral (K) views; (L–M) DMR-KS-05-03-20-1, a right mandible in occlusal (L) and lateral (M) views; (N–O) DMR-KS-05-03-22-7, a right mandible in occlusal (N) and lateral (O) views; (P–Q) DMR-KS-05-03-08-33, a left m3 in occlusal (P) and buccal (Q) views..... 111

Figure 44. Postcranial remains of *Axis axis* from Khok Sung: (A–B) DMR-KS-05-04-11-32, a right distal humerus in anterior (A) and distal (B) views; (C–E) DMR-KS-05-03-18-2, a right metacarpus in proximal (C), anterior (D), and distal (E) views; (F–H) DMR-KS-05-03-19-37, a left metacarpus in proximal (F), anterior (G), and distal (H) views; (I–J) DMR-KS-05-03-27-4, a right distal femur in posterior (I) and distal (J) views; (K–M) DMR-KS-05-03-26-3, a right metatarsus in proximal (K), anterior (L), and distal (M) views..... 117

Figure 45. Scatter diagrams of upper cheek tooth (P3–M3) lengths and widths of recent and fossil *Axis*. Data of *Axis javanicus* (Trinil H. K.) and *Axis porcinus* (Thum Wiman Nakin) are from von Koenigswald (1933) and Tougard (1998), respectively..... 119

Figure 46. Scatter diagrams of lower cheek tooth (p2–m3) lengths and widths of recent and fossil *Axis*. Data of *Axis javanicus* (Trinil H. K.) and *Axis porcinus* (Thum Wiman Nakin and Thum Prakai Phet) are from von Koenigswald (1933), Tougard (1998), and Filoux et al. (2015), respectively..... 120

Figure 47. Remains of *Panolia eldii* from Khok Sung: (A–C) DMR-KS-05-04-20-4, a cranium in dorsal (A), lateral (B), and ventral (C) views; (D) DMR-KS-05-03-15-11, a right P2; (E) DMR-KS-05-03-00-24, a left M1; (F) DMR-KS-05-03-00-23, a right M2; (G) DMR-KS-05-03-27-6, a left M3; (H) DMR-KS-05-04-9-2, a left M3; (I) DMR-KS-05-03-29-2, a right i1 in lingual view; (J–K) DMR-KS-05-03-27-2, a left mandible in lateral (J) and occlusal (K) views; (L–M) DMR-KS-05-04-9-5, a left mandible in occlusal (L) and lateral (M) views. All teeth are shown in occlusal view..... 123

Figure 48. Postcranial remains of *Panolia eldii* from Khok Sung: (A–B) DMR-KS-05-06-24-4, a right scapula in lateral (A) and distal (B) views; (C–E) DMR-KS-05-03-18-1, a right proximal

humerus in proximal (C), anterior (D), and posterior (E) views; (F–H) DMR-KS-05-03-31-10, a right radius in proximal (F), anterior (G), distal (H) views; (I–K) DMR-KS-05-03-24-2, a right metacarpus in proximal (I), anterior (J), and distal (K) views; (L–N) DMR-KS-05-03-25-8, a left metatarsus in proximal (L), anterior (M), distal (N) views; (O–Q) DMR-KS-05-03-17-36, a right femur in proximal (O), posterior (P), distal (Q) views. 124

Figure 49. Scatter diagrams of upper cheek tooth (P2, M1, M2, and M3) lengths and widths of some recent and fossil large cervids. The measurements of fossil cervids from the caves of Phnom Loang, Thum Wiman Nakin, and Ma U’Oi are obtained from Beden and Guérin (1973), Tougard (1998), and Bacon et al. (2004), respectively. 126

Figure 50. Scatter diagrams of lower cheek tooth (p2–m3) lengths and widths of some recent and fossil large cervids. The measurements of fossil cervids from the caves of Thum Wiman Nakin, Thum Prakai Phet, and Ma U’Oi are obtained from Tougard (1998), Filoux et al. (2015), and Bacon et al. (2004), respectively. 127

Figure 51. Remains of *Rusa unicorn* from Khok Sung: (A) DMR-KS-05-03-20-11, a right antler in lateral view; (B) DMR-KS-05-03-26-2, a right antler fragment in lateral view; (C) DMR-KS-05-03-28-23, a right antler fragment in medial view; (D) DMR-KS-05-04-9-3, a left M2; (E) DMR-KS-05-03-31-1, a left M3; (F–G) DMR-KS-05-03-13, a right mandible in lateral (F) and occlusal (G) views; (H–I) DMR-KS-05-03-00-101, a left mandible in lateral (H) and occlusal (I) views; (J) DMR-KS-05-03-00-5, a right m1; (K) DMR-KS-05-03-27-4, a left m3. All isolated teeth are shown in occlusal view. 129

Figure 52. Postcranial remains of *Rusa unicorn* from Khok Sung: (A–C) DMR-KS-05-03-15-43, a left humerus in anterior (A), posterior (B), and distal (C) views; (D–E) DMR-KS-05-03-19-14, a right proximal radius in proximal (D) and anterior (E) views; (F–G) DMR-KS-05-03-26-19, a right distal radius in anterior (F) and distal (G) views; (H–J) DMR-KS-05-03-17-26, a left metacarpus in proximal (H), anterior (I), and distal (J) views; (K–L) DMR-KS-05-03-19-7, a right proximal femur in proximal (K) and anterior (L) views; (M–N) DMR-KS-05-04-30-9, a left distal femur in posterior (M) and distal (N) views; (O–Q) DMR-KS-05-03-28-16, a right tibia in proximal (O), anterior (P), and distal (Q) views; (R–T) DMR-KS-05-03-19-11, a right metatarsus in proximal (R), anterior (S), and distal (T) views. 130

Figure 53. Remains of *Bos sauveli* from Khok Sung: (A) DMR-KS-05-03-29-8, a left DP3; (B) DMR-KS-05-04-01-4, a left P3; (C–D) DMR-KS-05-03-23-2, a left M1 or M2 in occlusal (C) and lingual (D) views; (E) DMR-KS-05-03-29-6, a right M3; (F) DMR-KS-05-04-01-6, a right p2; (G) DMR-KS-05-04-28-4, a broken right m3; (H–I) DMR-KS-05-04-9-1, a left mandible in occlusal

(H) and lateral (I) views; (J–K) DMR-KS-05-03-9-1, a right mandible in occlusal (J) and lateral (K) views; (L–N) DMR-KS-05-03-20-2(1), a left humerus in anterior (L), posterior (M), and distal (N) views. All isolated teeth are shown in occlusal view. 133

Figure 54. Scatter diagrams of upper cheek tooth (P2–M3) widths of recent and fossil large bovids. Fossil data from Phnom Loang, Lang Trang, Thum Wiman Nakin, and Tam Hang South are from Beden and Guérin (1973), de Vos and Long (1993), Tougard (1998), and Bacon et al. (2011), respectively. 137

Figure 55. Scatter diagrams of lower cheek tooth (p2–m3) widths of recent and fossil large bovids. Fossil data from Phnom Loang, Lang Trang, Thum Wiman Nakin, Thum Prakai Phet, Duoi U’Oi, and Tam Hang South are from Beden and Guérin (1973), de Vos and Long (1993), Tougard (1998), Filoux et al. (2015), and Bacon et al. (2008b, 2011), respectively. 138

Figure 56. Remains of *Bos gaurus* from Khok Sung: (A–B) DMR-KS-05-03-26-22, a left horn core in posterior (A) and anterior (B) view; (C) DMR-KS-05-03-20-1, a right DP2; (D) DMR-KS-05-03-19-27, a right P2; (E) DMR-KS-05-04-03-03, a right P2; (F) DMR-KS-05-03-20-3, a right DP3; (G–H) DMR-05-03-17-3, a right DP4 in occlusal (G) and lingual (H) views; (I) DMR-05-03-17-1, a right M3; (J) DMR-05-03-19-26, a left m2; (K–L) DMR-KS-05-04-3-1, a left mandible in and occlusal (K) and lateral (L) views; (M) DMR-KS-05-03-00-1, a fragmentary mandible in occlusal view. All isolated teeth are shown in occlusal view. 141

Figure 57. Postcranial remains of *Bos gaurus* from Khok Sung: (A–D) DMR-KS-05-05-1-1, a right humerus in proximal (A), posterior (B), anterior (C), and distal (D) views; (E–G) DMR-KS-05-03-26-27, a right metacarpus in proximal (E), anterior (F), and distal (G) views; (H–J) DMR-KS-05-03-9-2, a left femur in proximal (H), distal (I), and anterior (J) views. 142

Figure 58. Cranial and upper dental remains of *Bubalus arnee* from Khok Sung: (A–C) DMR-KS-05-03-20-1, a cranium in dorsal (A), ventral (B), and lateral (C) views and (D–E) DMR-KS-05-03-21-1, a cranium in dorsal (D) and ventral (E) views; (F–G) DMR-KS-05-03-11-1, a right upper jaw in lateral (F) and occlusal (G) views; (H–I) DMR-KS-05-03-16-3, a partial cranium in ventral view (H) with a right tooth row (I); (J) DMR-KS-05-03-16-2, a right horn core in dorsal view; (K) DMR-KS-05-03-18-14, a left P2; (L) DMR-KS-05-03-00-103, a left DP3; (M) DMR-KS-05-04-29-8, a right DP4; (N) DMR-KS-05-03-00-7, a right M3. Cross-sections of basal horn cores are given. All isolated teeth are shown in occlusal view. 148

Figure 59. Mandibular and lower dental remains of *Bubalus arnee* from Khok Sung: (A–B) DMR-KS-05-03-20-1, a right mandible in lateral (A) and occlusal (B) views; (C–D) DMR-KS-05-03-10-3, a left mandible in mesial (C) and occlusal (D) views; (E–F) DMR-05-03-20-2, a right

mandible in lateral **(E)** and occlusal **(F)** views; **(G–H)** DMR-05-03-20-10, a left mandible in lateral **(G)** and occlusal **(H)** views; **(I)** DMR-KS-05-03-20-20, a left fragmentary mandible with m1 and m2 in occlusal view; **(J)** DMR-KS-05-03-18-8, a right i1 in lingual view; **(K)** DMR-KS-05-03-00-106, a left i3 in lingual view; **(L)** DMR-KS-05-03-16-3, a right i4; **(M)** DMR-KS-05-03-00-4, a left dp4 in occlusal view; **(N–O)** DMR-KS-05-03-00-105, a left m1 in occlusal **(N)** and buccal **(O)** views..... 149

Figure 60. Articulated postcranial skeletons of *Bubalus arnee* from Khok Sung: **(A)** thoracic (abbreviated as “T”) vertebrae in lateral view: DMR-KS-05-04-1-11 (T3), DMR-KS-05-04-1-26 (T4), DMR-KS-05-04-1-13 (T5), DMR-KS-05-04-1-14 (T6), DMR-KS-05-04-1-15 (T7), DMR-KS-05-04-1-16 (T8), DMR-KS-05-04-1-12 (T9), DMR-KS-05-04-1-17 (T10), DMR-KS-05-04-1-18 (T11), DMR-KS-05-04-1-19 (T12), and DMR-KS-05-04-1-20, (T13); **(B)** lumbar (L) vertebrae in dorsal view: DMR-KS-05-04-1-24 (L1), DMR-KS-05-04-1-23 (L2), DMR-KS-05-04-1-22 (L3), and DMR-KS-05-04-1-21 (L4); **(C–E)** a left forelimb in anterior view: **(C)** DMR-KS-05-02-20-4, a scapula in lateral and distal views; **(D)** DMR-KS-05-03-31-8, a humerus in proximal and distal views; **(E)** DMR-KS-05-03-31-9, an ulna and a radius in proximal and distal views; **(F)** DMR-KS-05-03-26-3(1), a right metacarpus in proximal, anterior, and distal views; **(G)** DMR-KS-05-04-1-25, a pelvis in ventral view; **(H–R)** hindlimbs in anterior view: **(H)** DMR-KS-05-04-1-1, a right femur in proximal and distal views; **(I)** DMR-KS-05-4-1-11, a right tibia in proximal and distal views; **(J)** DMR-KS-05-04-1-7, a right 4th tarsal bone in dorsal view; **(K)** DMR-KS-05-04-1-8, a right metatarsus in proximal and distal views; **(L)** DMR-KS-05-04-1-2, a left femur; **(M)** DMR-KS-05-04-1-3, a left tibia; **(N)** DMR-KS-05-04-1-4, a left astragalus in plantar view; **(O)** DMR-KS-05-04-1-5, a left 4th tarsal bone; **(P)** DMR-KS-05-04-1-6, a left metatarsus; **(Q)** DMR-KS-05-04-1-9, a left phalanx I in lateral view; **(R)** DMR-KS-05-04-1-10, a left phalanx II in lateral view..... 151

Figure 61. Dental remains of *Capricornis sumatraensis* from Khok Sung: **(A–B)** DMR-KS-05-03-18-16, a left M2 in occlusal **(A)** and lingual **(B)** views; **(C–D)** DMR-KS-05-04-05-4, a right m3 in occlusal **(C)** and buccal **(D)** views; **(E–F)** DMR-KS-05-03-27-5, a left m3 in occlusal **(E)** and buccal **(F)** views; **(G–H)** DMR-KS-05-03-28-10 in occlusal **(G)** and buccal **(H)** views..... 154

Figure 62. Scatter diagrams of M2 and m3 lengths and widths of recent and fossil serows and gorals. The measurements of fossil specimens from Lang Trang, Thum Wiman Nakin, Thum Prakai Phet, and Tam Hang South are from de Vos and Long (1993), Tougaard (1998), Filoux et al. (2015), and Bacon et al. (2011), respectively..... 155

Figure 63. Remains of non-mammalian vertebrates from Khok Sung: *Crocodylus cf. siamensis*—**(A–B)** DMR-KS-05-03-30-30, a cranium in dorsal **(A)** and ventral **(B)** views; **(C)** DMR-KS-05-03-21-1, a tooth in lingual view; **(D–E)** DMR-KS-05-03-29-57 and **(F–G)** DMR-KS-05-

03-27-25, osteoderms in dorsal (D, F) and ventral (E, G) views; <i>Python</i> sp.—(H-I) DMR-KS-05-03-00-16, a trunk vertebra in anterior (H) and ventral (I) views; <i>Varanus</i> sp.—(J-K) DMR-KS-05-03-08-36, a trunk vertebra in anterior (J) and ventral (K) views; Galliformes indet.—(L-M) DMR-KS-05-04-05-40, a cervical vertebra fragment in dorsal (L) and ventral (M) views; Siluridae indet.—(N-O) DMR-KS-05-03-22-76, a vertebra in anterior (N) and lateral (O) views; (P) DMR-KS-05-04-11-20, a pectoral spine in dorsal view; (Q) DMR-KS-05-04-05-25, a pectoral spine in medial view. Anatomical abbreviations: al , alveolus; pmx , premaxilla; en , external naris; n , nasal; mx , maxilla; pal , palatine ; palp , palatine process.	158
Figure 64. Pie chart showing the species richness of Khok Sung vertebrate fauna.....	164
Figure 65. The Middle (red circle) and Late (yellow circle) Pleistocene records of stegodontids and relative fossil elephants, and the current distribution (green area) of <i>Elephas maximus</i> (Indian elephant). Stars indicate the co-occurrence of sympatric proboscideans. The current distribution of Indian elephants is compiled from Lekagul and McNeely (1988).....	168
Figure 66. The Early (blue square), Middle (red star), and Late (yellow circle) Pleistocene records and the current distribution (green area) of <i>Rhinoceros sondaicus</i> (Javan rhinoceros). The current distribution of the species is compiled from Groves (1967), Rookmaker (1980), and Groves and Leslie Jr (2011).	170
Figure 67. The Middle (red star) and Late (yellow circle) Pleistocene records and the current distribution (green area) of <i>Rhinoceros unicornis</i> (Indian rhinoceros). “?” indicates the possible record of <i>R. unicornis</i> according to Antoine (2012). The current distribution of the species is modified from Laurie et al. (1983).	171
Figure 68. The Middle Pleistocene (red star) and Late Pleistocene to Holocene (yellow circle) records and the current distribution (green area) of <i>Sus barbatus</i> (bearded pig). The current distribution of the species is compiled from Corbet and Hill (1992).	173
Figure 69. The Middle Pleistocene record (red star) and the current distribution (green area) of <i>Axis axis</i> (chital). The current distribution of the species is compiled from Duckworth et al. (2008a).	175
Figure 70. The Middle (red star) and Late (yellow circle) Pleistocene records and the current distribution (green area) of <i>Panolia eldii</i> (Eld’s deer). The current distribution of the species is compiled from Lekagul and McNeely (1988).	176

- Figure 71.** The Middle Pleistocene (red star) and Late Pleistocene to Holocene (yellow circle) records and the current distribution (green area) of *Rusa unicolor* (sambar deer). The current distribution of the species is compiled from Lekagul and McNeely (1988)..... 177
- Figure 72.** The Middle (red star) and Late (yellow circle) Pleistocene records and the current distribution (green area) of *Bos sauveli* (kouprey). The current distribution of the species is compiled from Lekagul and McNeely (1988) and Timmins et al. (2008)..... 179
- Figure 73.** The Middle (red star) and Late (yellow circle) Pleistocene records and the current distribution (green area) of *Bos gaurus* (gaur). The current distribution of the species is compiled from Lekagul and McNeely (1988) and Duckworth et al. (2008b)..... 179
- Figure 74.** The Middle (red star) and Late (yellow circle) Pleistocene records and the current distribution (green area) of *Bubalus arnee* (wild water buffalo). The current distribution of the species is compiled from Lekagul and McNeely (1988) and Hedges et al. (2008)..... 180
- Figure 75.** The Early Pleistocene (blue square), Middle Pleistocene (red star), and Late Pleistocene (yellow circle) records and the current distribution (green area) of *Capricornis sumatraensis* (Sumatran serow). The current distribution of the species is compiled from Lekagul and McNeely (1988)..... 182
- Figure 76.** Cluster analysis of the Middle Pleistocene mammalian fossil records in Southeast Asian and some central-eastern and southern Chinese localities based on the Simpson coefficients..... 186
- Figure 77.** Illustration of the Khok Sung cenogram. Dash lines refer to missing data on the medium- (between 8 kg and 500 g) and small- (<500 g) sized mammals that indicate a characteristic of habitats (Legendre, 1989). The Y-axis represents the log-transformed mean body weight of a mammalian species in the community. The X-axis refers to a species rank, starting from large to small sizes in order descending..... 187
- Figure 78.** Map of Southeast Asia showing the Sundaland boundaries and the migration route hypothesis: Siva-Malayan route (black), Sino-Malayan route (red), and Taiwan-Philippine Archipelago route (blue). The boundaries of the Sunda shelf at the sea level of about 120 m lower than the present day are compiled from Voris (2000)..... 191

LIST OF TABLES

Table 1. Metrical abbreviations for the postcranial bones (from von den Driesch, 1976).	40
Table 2. Scanned hyaenid crania used for the 3D geometric-morphometric analysis.....	56
Table 3. Cranial landmarks used in this study. Numbers correspond to the landmark illustrated in Figure 28.....	58
Table 4. Ratios of the greatest lengths of tibiae (GL) to the lengths and widths of proximal and distal tibiae (Bp, Dp, Bd, and Dd) of Khok Sung macaques compared to recent Southeast Asian primates.	64
Table 5. Dental measurements (L, length and W, width) of Thai <i>Crocuta crocuta ultima</i> including Khok Sung (DMR-KS-05-04-2-1), Thum Phedan (Yamee and Chaimanee, 2005), and Thum Wiman Nakin (Thai fossil-numbers (TF); Tougard, 1998) specimens. The blade width of upper carnassials is abbreviated as “Wbl”.....	68
Table 6. Measurements of upper carnassials of <i>Crocuta crocuta ultima</i> from Khok Sung in Thailand (DMR-KS-05-04-2-1), Phnom Loang in Cambodia (PNL 179; Beden and Guérin, 1973) , Xianrendong in South China (V05234.19 and V05198.3), and Penghu Channel in Taiwan (CJ-0038 and HL-0001; Tseng and Chang, 2007), see Fig. 10 for the abbreviations of metrical parameters.	69
Table 7. Measurements (in millimetres) of ulnae and femurs of Khok Sung and other extant and fossil canids. * indicates a subadult individual. Metrical data of fossil canids are from Baryshnikov (2012, 2015).....	78
Table 8. Measurements (in millimeters) of cheek teeth of Khok Sung proboscideans, including a number of preserved ridges (NR), lengths (L), widths (W), heights (H), enamel thickness (ET), H/W indices ($100 \times H/W$), and laminar frequencies (LF). The laminar frequencies are expressed as the following formula: $LF = n \cdot 100 / d_l + n \cdot 100 / d_b / 2$, where “ d_l ” and “ d_b ” are referred to distances at the lingual and buccal side of the tooth, respectively, and “ n ” is equivalent to the number of ridges between two measuring points (van den Bergh, 1999). * indicates measurements of the maximum preservation according to incomplete specimens. The H/W index is calculated for each ridge. The laminar frequency is measured based on the maximum number of preserved ridges.....	83
Table 9. Ridge dimensions (lengths and widths in millimeters) of upper fourth deciduous premolars between Khok Sung <i>Stegodon</i> and <i>Stegodon orientalis</i>	86

Table 10. Ridge dimensions (lengths and widths in millimeters) of lower third deciduous premolars between Khok Sung <i>Stegodon</i> and <i>Stegodon orientalis</i>	87
Table 11. Ridge dimensions (lengths and widths in millimeters) of upper second and third molars between Khok Sung <i>Stegodon</i> and <i>Stegodon orientalis</i> . The total ridge number of upper molars of Khok Sung stegodontids used for our comparisons follows that of <i>Stegodon orientalis</i>	89
Table 12. Ridge dimensions (lengths and widths in millimeters) of lower third molars of derived <i>Stegodon</i> in Southeast Asia. The ridge formula of each taxon follows van den Bergh et al. (2008: table. 3). The ridge number of <i>Stegodon insignis</i> is considered as representing a total of twelve.....	90
Table 13. Measurements (in millimeters) of cheek teeth of Khok Sung rhinoceroses, <i>Rhinoceros sondaicus</i> and <i>Rhinoceros unicornis</i> , compared to recent specimens (data from Guérin (1980)). “(i)” refers to an isolated tooth and “(m)” indicates a tooth attached to the mandible.....	96
Table 14. Measurements (lengths and widths in millimeters) of cheek teeth of Khok Sung <i>Sus barbatus</i> compared to the recent and fossil species. The number of specimens is given within the parentheses. The measured specimens of recent <i>Sus scrofa</i> include three subspecies: <i>S. s. scrofa</i> , <i>S. s. vittatus</i> , and <i>S. s. attila</i>	104
Table 15. Measurements (in millimeters) of lower canines of <i>Sus barbatus</i> from Khok Sung. The canine index is expressed by the following formula: labial surface*100/posterior surface (Groves, 1981).....	107
Table 16. Measurements (lengths and widths in millimeters) of cervid teeth from Khok Sung. N=number of specimens.	113
Table 17. Proportional indices of postcranial remains of identified ruminant taxa from Khok Sung.....	114
Table 18. Body mass prediction of Khok Sung ruminants using second molar variables, compared to relative sizes of the recent population (Grzimek, 1975; Lekagul and McNeely, 1988; Nowak, 1999). The predictive equations follow Janis (1990: table. 16.8).	118
Table 19. Measurements (lengths and widths in millimeters) of cheek teeth of large bovids from Khok Sung. N=number of specimens.....	134
Table 20. Measurements (lengths and widths in millimeters) of cheek teeth of Khok Sung <i>Capricornis sumatraensis</i> . N=number of specimens.....	154

Table 21. Measurements (in millimeters) of vertebrae of <i>Python</i> and <i>Varanus</i> from Khok Sung. Abbreviations: CL , centrum length (measured at the ventral midline); H , maximum height (measured from the tip of the neural spine to the ventral rim of the cotyle); WPP , width between pre- and postzygapophyseal processes; Wpre , width across zygapophyseal processes; Wpost , width across postzygapophyseal processes; Wcd , width of the condyle; Hcd , height of the condyle (measured from the dorsal to ventral rim); Wct , width of the cotyle; Hct , height of the cotyle. ⁺ refers to the measurement of 2 attached vertebrae and * indicates an incomplete preservation.	160
Table 22. Fauna list of Khok Sung vertebrate fauna.....	164
Table 23. Similarity matrix based on the Simpson coefficients. Locality abbreviations: YCK , Yenchingkou; KLS , Koloshan; DX , Daxin; HJ , Hejiang; GX , Ganxian; PXDD , Panxian Dadong; WY , Wuyun; MB , Maba; HST , Hoshantung; KS , Khok Sung; TWN , Thum Wiman Nakin; TPKP , Thum Phra Khai Phet; TK , Tham Khuyen; TO , Tham Om; BDB , Boh Dambang; KDBB , Kedung Brubus; TNHK , Trinil Hauptknochenschicht; ND , Ngandong.....	185

CHAPTER 1

Introduction

Rationale

The Middle Pleistocene (781 to 126 ka) is a critical period in the history of Earth characterized by a cyclic occurrence of high amplitude glacial periods alternating with interglacial periods (Huybers, 2007), whose intensity is under the control of astronomic cycles and oceanic paleocurrents. The climatic characteristics of that period have been largely analyzed in the Northern Hemisphere, where the glaciations are directly expressed by the variation of inlandis surface and extension (e.g., Versteegh, 1997; Jahn et al., 2003). Paleoclimatic evidence has been also deeply investigated in the world oceans (e.g., Billups and Schrag, 2003; Ferreira et al., 2014; DeNinno et al., 2015) because of the possibility of having access to more global information, which is less affected by continental and coastal conditions. These important data contribute to understanding of the climatic changes that have occurred in the world. The impact of these climatic events on the biodiversity is also well-known in the Northern hemisphere continents and surrounding oceans, having considerably modified the composition of the living communities, by the way of distribution, extinction, and speciation events, reduction and/or extension of landscapes and habitats. However, the understanding of these events is much less advanced in tropical areas. In Africa, in relation to human evolution, a great number of data have been collected so far and have shown the close relationships between vertebrate and plant communities, composition, distribution, and climatic changes. It is now clear that, at least in tropical Africa, the glacial periods corresponded to significantly more open environments than during the interglacial phrase, stable isotopes and microfossils from lake sedimentary cores

having broadly contributed to that understanding (e.g., Smith et al., 2004; Lézine et al., 2005; Lee-Thorp et al., 2007). On the other hand, the current situation is much more confused in Asia, where only two regions (Northern China and Indonesia) have been investigated in details. In Northern China, the study of loess deposits (e.g., An et al., 1990; Sun et al., 2006; Peng et al., 2015) and the stable isotopic analysis of terrestrial mammal tooth enamel (e.g., Gaboardi et al., 2005; Biasatti et al., 2010) have allowed to unravel some aspects of climatic changes in the Northern part of Asia. Some proxy data have been obtained from Sundaland (Indonesia), mostly the island of Java, in relation to the rich records of fossil hominids (*Homo erectus*) (Dubois, 1894) in that island (e.g., van der Kaars and Dam, 1995; van der Kaars and Dam, 1997; van der Kaars, 1998; Bettis et al., 2009; Sémah et al., 2010; Brasseur et al., 2015). However, the data obtained from extensive chronological stages (Early to Late Pleistocene) are still scarce, often limited to short time intervals, and become only more detailed for the late Pleistocene, since 126,000 years ago.

Since Southeast Asia has been currently known as a “biodiversity hotspot” with a high diversity of plants and animals including rare and unique species and/or even specific landforms, glacial refugia could contain the last remaining individuals of species that were widely distributed but have now mostly disappeared. It is possibly hypothesized that some population of animals and plants have been separated from the rest of their species within these refugia in this region during the glacial events and have subsequently increased or decreased their genetic diversity. In Thailand and neighbouring countries, this information is poorly known due to the extreme scarcity of data. In addition, this current geographic area is under the control of the monsoon, which is classically considered to have been directly related to the uplift of the Tibetan plateau since the last 20 million years ago (Ruddiman and Kutzbach, 1989, 1990; Passey et al., 2009). The paleobotanic evidence obviously demonstrates that the vegetation zones dropped about 1,000

meters of elevation and that lowlands were mostly covered by grasslands with tropical Dipterocarp forests relicts in some areas during the last glacial maximum (e.g., Morley, 1982; Sun et al., 2002; Harrison and Prentice, 2003; Morley, 2012; Raes et al., 2014). However, the fragmentation of the Dipterocarp forest did not reach the maximum levels at all of the periods, as exemplified by the fact that orangutans and giant pandas were widespread in mainland Southeast Asia (e.g., Olsen and Ciochon, 1990; Tougaard et al., 1996; Tougaard and Ducrocq, 1999; Ibrahim et al., 2013; Harrison et al., 2014). But this iterative mechanism of contraction and extension of Dipterocarp forests has been considered as the source of numerous allopatric speciation events whose evidence has to be still demonstrated. Therefore, the fauna and flora enclosed on the Pleistocene deposits play an important role to understand these environmental and climatic phenomena. Mammals are known as sensitive indicators of changes in terrestrial climate and environments that have significant impacts on their species distribution and diversity patterns.

To examine the regional scale of Southeast Asian paleoclimatic dynamics, Thailand is a critical position because it is located at the intermediate zone between different mammal communities from South China and from Java (Lekagul and McNeely, 1988; Corbet and Hill, 1992; Tougaard, 1998, 2001). Studies on Thai Middle Pleistocene faunas are therefore crucial to understand the distribution patterns of large mammals across Southeast Asia in relation to the climate changes during the glacial-interglacial cycles. However, the information regarding the species composition, chronology, and paleogeographical affinities of Thai Pleistocene faunas is poorly known due to the inappropriate taxonomic identification, to the lack of radiometric dating, and to the scarcity of substantial fossil sites.

In 2005, the Khok Sung sand pit (Nakhon Ratchasima province, northeastern Thailand) was excavated (Fig. 2). This locality, an ancient fluvial terrace, constitutes the richest

Pleistocene vertebrate fauna of Thailand with thousand vertebrate remains. The Khok Sung fauna is tentatively attributed to the Middle Pleistocene (Chaimanee et al., 2005). The Khok Sung locality yields a unique and diverse fossil assemblage of plant remains, fish, reptiles, and mammals. Plant remains (fruits, seeds, leaves, wood, tubers, ambers, and pollens) suggest the presence of tropical mixed deciduous and dry green forests (Grote, 2007). Some reptilian fossils were also described including turtles: *Batagur cf. trivittata*, *Heosemys annandalii*, *Heosemys cf. grandis*, and *Malayemys sp.*, soft-shelled turtles: *Chitra sp.* and *cf. Amyda sp.* (Claude et al., 2011), and a gavial, *Gavialis cf. bengawanicus* (Martin et al., 2012). The mammalian assemblage consists of rhinoceroses, pigs, bovids, cervids, and an extinct elephant *Stegodon*, whose taxonomic attribution in generic and specific levels is poorly known (Chaimanee et al., 2005).

Objectives of the study

The proposed subject of this research is to study the species composition and distribution of the Middle Pleistocene mammalian fauna in Khok Sung subdistrict, Nakhon Ratchasima province and its contribution to the vertebrate community.

CHAPTER 2

Literature reviews

Southeast Asian history and biogeographic provinces

Southeast Asia constitutes a subregion of Asia and is divided into two geographic regions (mainland and insular Southeast Asia). Mainland Southeast Asia consists of six countries including Myanmar, Thailand, Peninsular Malaysia, Laos, Cambodia, and Vietnam, whereas insular or maritime Southeast Asia includes the countries of Malaysian Borneo, Singapore, Brunei, East Timor, Indonesia, and the Philippines. The Southeast Asian continental block largely comprises elements, which have been broken off from the southern supercontinent Gondwanaland (Gatinsky and Hutchison, 1987). Tectonically, the extant geography of Southeast Asia has been formed by the collision between Sinoburmalaya and Cathaysia plates from the event of the Late Triassic Indosinian Orogeny (Hutchison, 2005). Additionally, the collisions between Burma plate and Shan highlands during the Cretaceous and between India and Eurasia during the Early Tertiary have been evidenced (Hutchison, 2005). Until the Miocene, the latter collision gradually resulted in the North-South trending mountain ranges of Western Yunnan, Myanmar, the eastern part of Peninsular Malaysia, and in the uplift of the Himalayas and the northern part of the Qinghai-Tibetan Plateau (Whitmore, 1987). The uplift of the Himalayas and the Qinghai-Tibetan Plateau causing the alteration of climates has resulted in the development of the Asian monsoon system during the Miocene (25-22 Ma). However, the existence of the older Asian monsoon related to the enhanced greenhouse conditions is supposed to have occurred in the north and southern part of the Tibetan-Himalayan orogen during the late Eocene (Licht et al., 2014). Another relatively more recent tectonic collision occurred between Southeast Asia and Australia

at about 15 Ma, leading to the formation of the Lesser Sunda islands, as well as the appearance of islands of Sulawesi and the Philippine Archipelago (Hutchison, 1989).

With regards to biogeographical terms, Southern Asia coincides with the Indo-Malayan region (Udvardy, 1975), which is divided into 5 subregions: the Indian, Indochinese, Sundaic, Philippines, and Wallacean subregions (Lekagul and McNeely, 1988; Corbet and Hill, 1992) (Fig. 1). The Indochinese subregion includes the Indochinese Peninsula (Myanmar, Thailand, Laos, Cambodia, and Vietnam and South China). The Sundaic subregion comprises the southern part of Thailand, Malaysia, Sumatra, Java, and Borneo (Lekagul and McNeely, 1988).

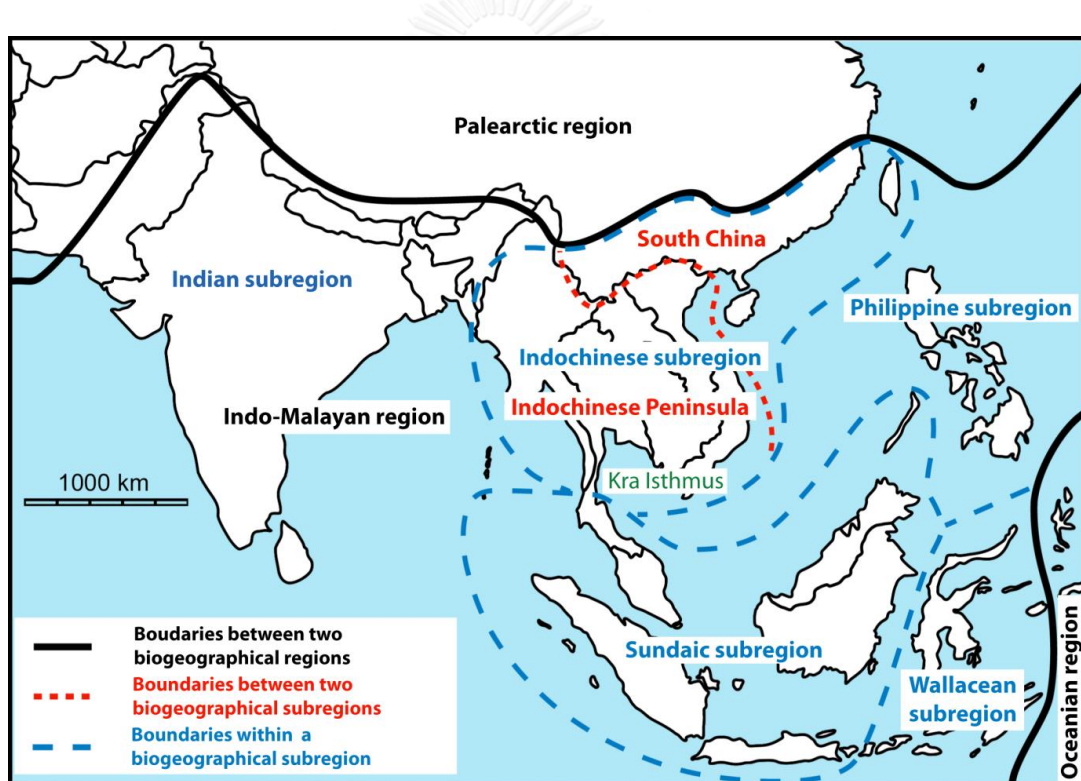


Figure 1. Map of Southern Asia showing the biogeographical regions and subregions (modified from Lekagul and McNeely, 1988; Corbet and Hill, 1992; Antoine, 2012).

Climate between these two subregions is markedly different, the Indochinese province displaying a stronger seasonality with lower rainfall (Whitmore, 1984; Gray et al., 1994). According to Wallace (1869), biogeographers defined a major transition between Indochinese and Sundaic zoogeographic subregions at the Thai-Malay Peninsula near the Isthmus of Kra ($10^{\circ} 30' N$,

Peninsular Thailand), where both of the northern and southern faunas meet (Fig. 1). This biogeographic boundary is defined by differences in biotas with a rapid turnover. There is about 50% turnover at the species level in forest-associated birds between the northern and southern of the Kra Isthmus (Hughes et al., 2003; Round et al., 2003). Botanists recognized a similar floristic pattern but more significant transition at about 500 km south, where the Southeast Asian and Malayan plants meet (e.g., Whitmore, 1984; Lekagul and Round, 1991; Ashton, 1992; Baker et al., 1998; Morley, 2000). These differences in biotas are also valid for insects, amphibians, and mammals (e.g., Corbet and M., 1992; Corbet and Hill, 1992; Gray et al., 1994; Inger, 1999).

The mammalian fauna is sufficiently rich to support biogeographic analyses due to the presence of over 500 extant species in Southeast Asia. The extant mammal transition is also suggested to occur near the Isthmus of Kra (Chasen, 1940; Musser and Newcomb, 1983; Cranbrook, 1988; Lekagul and McNeely, 1988; Corbet and Hill, 1992). The species diversity of national terrestrial mammals in Southeast Asia has been estimated: ~300 species in Myanmar, ~251 species in Thailand, ~273 species in Vietnam, and ~210 species in Malaysia (World Conservation Monitoring Centre, 1992; Southeast Asian Mammal Databank, 2006; Sterling et al., 2006). In addition, the taxonomic abundances, habitats, distributions, and natural history of these mammals are documented by a century of enquiry, atlases, and books (e.g., Chasen, 1940; Medway, 1983; Lekagul and McNeely, 1988; Corbet and Hill, 1992; Francis, 2001, 2008). However, the understanding of the history of present-day mammals in the region is most linked to information on the Pleistocene megafaunas (e.g., biodiversity, distribution, and extinction), whose evidence is still under investigation today. The Khok Sung fauna that has yielded numerous remains of large mammals possibly provides a high amount of data regarding all of those aspects.

Zoogeographic history of Southeast Asian mammalian faunas

Since the late 20th century, the Quaternary history of Southeast Asia has been sufficiently detailed and allowed for some reliable inferences of the role of the geographic events in faunal distribution. Several studies (e.g., Chaimanee, 1998; Chaimanee and Jaeger, 2000; Tougard, 2001; Tougard and Montuire, 2006) on the Pleistocene mammalian faunas in mainland Southeast Asia made the significant progress in explaining paleobiogeographic affinities and could be considered as references to the broader faunal comparisons. Fossils of murine rodents and squirrels are useful to reconstruct the regional palaeoenvironments and their data can be interpreted as an indicator for the past boundaries of forest and savannah communities in mainland Southeast Asia (Tougaard, 1998; Tougaard and Montuire, 2006). They also have evidenced past migrations between Indochinese and Sundaic subregions, which occurred in Thailand. Distribution patterns inferred from northern taxa that dispersed southward into the Sundaic subregion and from some peninsular endemic taxa, whose distribution has taken place in the Northern province, suggest severe shifts of the boundary between these two biogeographic subregions during the Pleistocene. Similar to those of large mammals, their fossil records have indicated that the transition between Indochinese and Sundaic taxa was located further south of the Isthmus of Kra during some parts of the Pleistocene. Some species dispersed further north or south than they do today (e.g., Tougaard, 2001; Bacon et al., 2004; 2006; 2008a; 2008b; 2011) , in relation to the climatic fluctuations during the glacial-interglacial. Overall, mainland Southeast Asia appears to have been cooler and more seasonal than today during the major part of the Pleistocene (Chaimanee, 1998; Penny, 2001; White et al., 2004; Chaimanee, 2013). The vegetation type of mainland Southeast Asia during that period was dominated by evergreen, semi-evergreen and coniferous forests with considerable amounts of grasses and some herbaceous vegetation (Louys and Meijaard, 2010). However, the paleobiogeographic situation in mainland Southeast Asia is still

less advanced, compared to those of islands (e.g., Java), where the Pleistocene faunas and floras have been studied in more details in relation to the presence of *Homo erectus*. The geographical distribution of large terrestrial mammals in insular Southeast Asia has been well-documented, almost related to a land corridor (known as the “Sunda shelf”) connecting the mainland Southeast Asia and islands of Indonesia (Fig. 2), allowing an overland migration of large mammals during the glacial periods. Glacio-eustatic fluctuations therefore play a significant role on Southeast Asian geography (e.g., size, number, and degree of isolation of islands) and biota (e.g., faunal turnover and endemism rate), depending on the timing and magnitude of sea level related to the glacial-interglacial cycles.

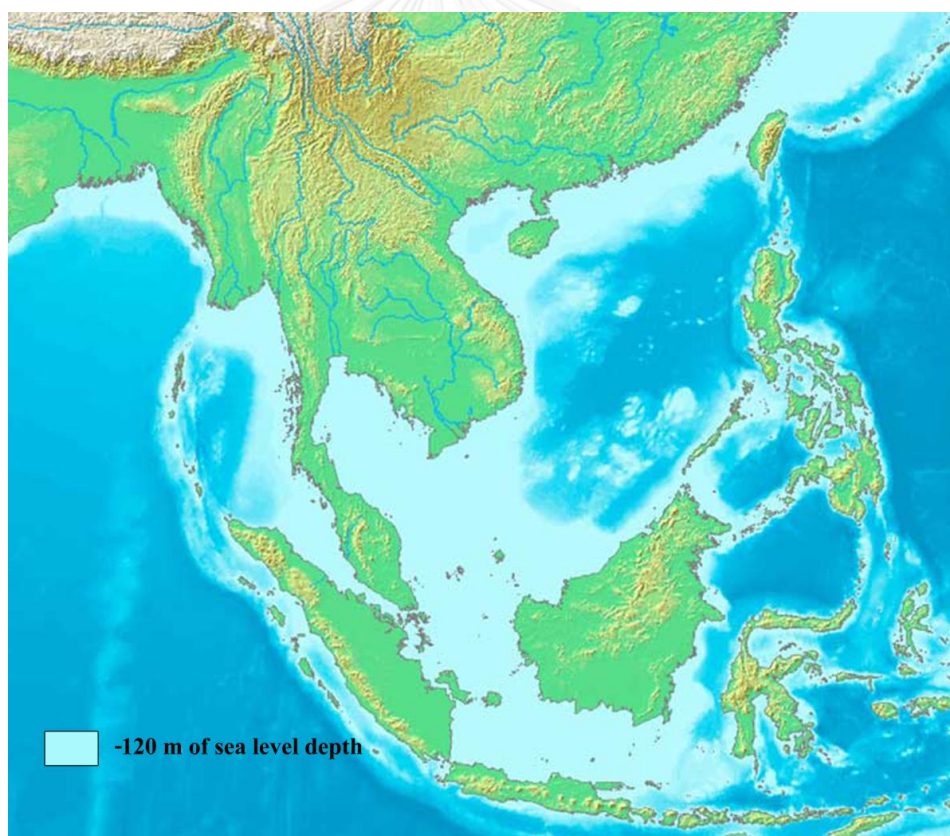


Figure 2. Map of Southeast Asia showing the land exposure (sky blue color), at sea level of 120 m below the present day, over Sundaland and Indochina during the Pleistocene (modified from Voris, 2000).

The Sundaland is a biogeographical region that comprises the Indonesian islands of Borneo, Sumatra, Java, and Bali, as well as Malay Peninsula. The largest geographic part of this region lies hidden below sea level today. Early geographic emergence of the Sunda shelf (geological term) or “Sundaland” (biogeographical term) in Southeast Asia has been first reconstructed by Molengraaff (1922) and Wallace (1876). Later on, this scene is further studied and discussed by many authors (e.g., Whitmore, 1987; Hall and Holloway, 1998; Whitmore, 1998; Woodruff, 2003; Bird et al., 2005; Meijaard and Groves, 2006). Although many details remain controversial, the major patterns of geographic and sea-level changes have been principally accepted now. Early Pleistocene faunas related to the expansion of the Sundaland are almost known exclusively from Java, where the uplift process started during the Late Pliocene due to the combination of tectonic and volcanic activities (van Bemmelen, 1949). Both the flora and the fauna between mainland and insular Southeast Asia are supposed to have been exchanged during the Early Pleistocene (before 800 ka) by dispersing through the emergence of Sundaland, when the sea level dropped about 70 m on average below the present-day sea level (Prentice and Denton, 1988; van den Bergh et al., 2001). These archaic fossils recovered from the Sangiran Formation indicate an unbalanced fauna and suggest Siva-Malayan characteristics that originated from Siwaliks and Myanmar (Sondaar, 1984). The paleoenvironmental conditions during the Early to Middle Pleistocene in Java were characterized by riparian forests, savannahs, and open woodlands (Bettis et al., 2009; Sémah et al., 2010; Janssen et al., 2016). A major environmental change that occurred in Java might have taken place toward the end of the Middle Pleistocene, as exemplified by the stable carbon isotope analyses of mammalian tooth enamel (Janssen et al., 2016) and the presence of new tropical rainforest faunas in Punung (van den Bergh et al., 2001; Westaway et al., 2007). The large expansion of Sundaland could generally provide an unequal opportunity for the distribution of mammals because forest-associated mammals are

better adapted to various types of forests (e.g., perhumid rainforest and seasonal, monsoonal, and mangrove forests) (Woodruff and Turner, 2009). The floodplain area of Sundaland might have been vegetated by *Pinus* savannah woodlands or grasslands, rather than by the rainforests (Whitmore, 1987; Heaney, 1991; Whitmore, 1998; Morley, 2000, 2007). Therefore, mammals that are restricted to the primary rainforests could have crossed this area through riparian forest corridors and subsequently became isolated by ecological barriers (Gorog et al., 2004). However, the central Sundaland exposed due to the lower sea level during the last glacial maximum (LGM, 21 ka) harbored optimal environmental conditions for Dipterocarpaceae and was probably covered by rainforests (Raes et al., 2014).

Although boundaries and ranges of the geographical distribution of savannah lands and rainforests in Southeast Asia are still controversial (Sun et al., 2000; Meijaard, 2003; Sun et al., 2003; Bird et al., 2005; Morley, 2007; Raes et al., 2014), the impacts of the habitat modification on the past mammalian geographic distribution are directly linked to these scenarios. Comprehensive studies on ancient mammals are therefore crucial to understand their distribution patterns and responses to environmental and climatic changes and needs to be taken into account in future analyses. Here we summarize the key findings from literature works and also elucidate an ongoing progress on the Pleistocene fossil records of large mammals in mainland Southeast Asia, in terms of faunal composition, chronology, paleoenvironments, and paleoclimate.

Pleistocene mammalian faunas in mainland Southeast Asia

A particular assemblage of mammals, so-called the “*Ailuropoda-Stegodon* fauna complex” or the “Sino-Malayan fauna”, has been known since the early 20th century and first described as a representative of the Middle Pleistocene in South China (Young, 1932; Pei, 1935;

Teilhard de Chardin, 1935; Bien and Chia, 1938; Granger, 1938; von Koenigswald, 1938–1939; Kahlke, 1961; de Vos, 1984). However, it represents a characteristic of the long period ranging from the Early to Late Pleistocene of the Indochinese subregion (e.g., Tougard, 2001; Rink et al., 2008; Zeitoun et al., 2010; Bacon et al., 2015). This faunal association fundamentally yields Asian taxa, which are endemic or closely related to tropical environments, including an extinct proboscidean *Stegodon*, Indian elephants, rhinoceroses, the largest primate *Gigantopithecus*, an orangutan, suids, cervids, and bovids. The carnivores commonly include a spotted hyaena (*Crocota crocuta ultima*), a tiger (*Panthera tigris*), a dhole (*Cuon alpinus*), an Asiatic black bear (*Ursus thibetanus*), and a giant panda (*Ailuropoda melanoleuca*). This faunal complex has been first identified in South China (Matthew and Granger, 1923) based on the occurrence of tropical taxa such as *Hylobates* and *Tapirus*, followed by the same discovery in Vietnam (Patte, 1928), Laos (Fromaget, 1936), Myanmar (de Terra, 1938), Cambodia (Beden and Guérin, 1973), and Thailand (Pope et al., 1981; Ginsburg et al., 1982). The distribution of the faunal complex is widespread in Indochinese subregion, expanding latitudinally from the Yangtse River (Pei, 1957) to Kra Isthmus (Tougaard, 2001). Their fossils were mostly found from the karst topologies including sinkholes, caves, and underground drainage systems. Interestingly, this faunal association was sometimes recovered together with human remains and/or stone artifacts, allowing further the understanding of the anthropic dynamics in this part of the world. The *Ailuropoda-Stegodon* faunal characteristics are highly crucial to establish a regional biochronology and stratigraphy, at least for the Pleistocene. However, nowadays its precise duration and subdivision are peculiarly nonspecific. In mainland Southeast Asia, the absolute datings are scarce and rather inaccurate. Bacon et al. (2015) proposed a Middle to Late Pleistocene biochronological division in mainland Southeast Asia with three evolutionary stages: (1) the presence of lineages of extant mammals (modern faunas), (2) the occurrence of some extinct

taxa (e.g., *Megatapirus augustus* and *Stegodon orientalis*) (archaic faunas), and (3) the appearance of new incomers. However, the biochronological ages based on the evolutionary stages have not been justified yet. A precise biochronologic time scale will become critical to reconstruct scenarios of the mammalian evolution and extinction, as well as paleoenvironments and paleoclimates of the region, if such a well constrained timing is more finely subdivided.

Since the late 20th century, numerous paleontological and archaeological discoveries of Pleistocene fossil sites in mainland Southeast Asia have dramatically raised new information. Numerous pieces of the puzzle involving the faunal composition, chronology, and paleoenvironments are stepwise reconstructed. The latest information on these aspects is hereby updated for the following countries in mainland Southeast Asia (Fig. 3).

The Republic of the Union of Myanmar (Myanmar)

Sites along the Irrawaddy River terraces and localities of Mogok Caves are representatives of the Early to Middle Pleistocene faunas in the country (Colbert, 1943) (Fig. 3). The ages of these two faunas have been poorly established since the 20th century excavation, only based on the presence of *Stegodon* and other archaic taxa (Colbert, 1943), without radiometric dating analyses. The Upper Irrawaddy fauna, being of Early Pleistocene in age (Stamp, 1922; Colbert, 1938), obviously consists of archaic species such as *Stegodon insignis*, *Elephas hysudricus*, *Rhinoceros sivalensis* (later regarded as junior synonym of *Rhinoceros unicornis* by Antoine (2012)), *Equus yunnanensis*, and *Hexaprotodon iravaticus* (Colbert, 1943; Takai et al., 2006). However, the taxonomic validity of *Rhinoceros sivalensis* is still controversial (Yan et al., 2014). Only two modern species, *Rhinoceros sondaicus* and *Capricornis cf. sumatraensis*, are present in this assemblage (Colbert, 1938; Takai et al., 2006; Zin-Maung-Maung-Thein et al., 2006). The presence of *Hipparion cf. antelopinum* and *Stegodon elephantoides* in the Early Pleistocene of the Upper

Irrawaddy fauna (Colbert, 1943) is ambiguous. They were possibly collected from the older strata (the Lower Irrawaddy Formation, late Miocene to Pliocene in age) according to Takai et al. (2006).

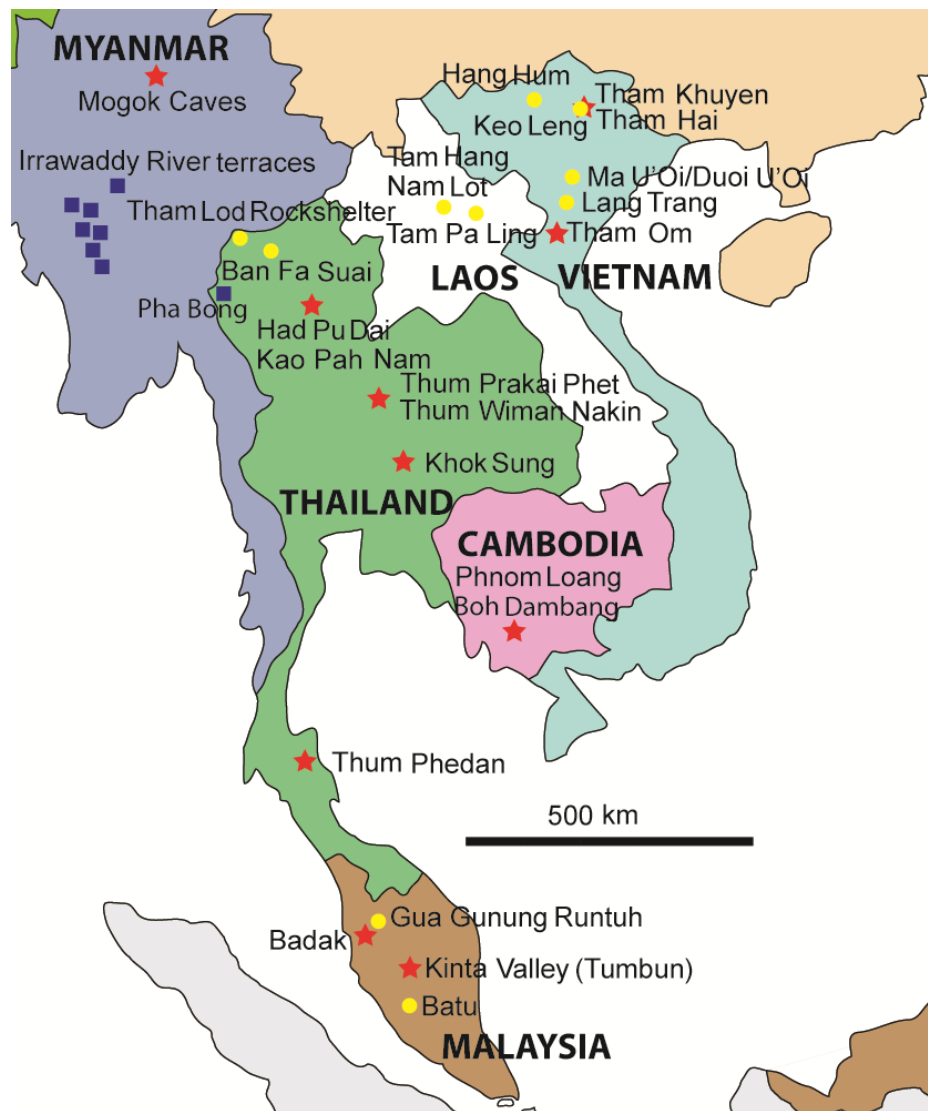


Figure 3. Map of mainland Southeast Asian countries showing the location of the Early (blue square), Middle (red star) and Late (yellow circle) Pleistocene fossil sites.

Although Hooijer (1950) considered the faunas of Mogok Caves as being of Early Pleistocene age, two extinct proboscideans, *Stegodon orientalis* and *Palaeoloxodon namadicus*, rather suggest a Middle Pleistocene age (Colbert, 1943), in agreement with Louys et al. (2007). However, Takai et al. (2006) argued that the material of *Palaeoloxodon*, described by Colbert (1943), possesses similar morphological features of extant Asian elephants and should be

assigned to *Elephas*. Moreover, the presence of a giant panda (*Ailuropoda melanoleuca*) is documented from nearby caves (Colbert, 1943). The paleoenvironments corresponded to closed habitats for these two faunas due to the synecological (community-based) methods (Louys and Meijaard, 2010). This interpretation is probably a result of the limited number of taxa recovered from the sites. Louys and Meijaard (2010) further suggested that mixed and open habitats are more consistent for these sites because the Pleistocene climatic fluctuations could result in expanding and contracting forests within a more open vegetation matrix. Palynological records indicate a more widespread expansion of savannah vegetation, as well as charred grass cuticles, during the Early Pleistocene (Morley, 1998).

The Lao People's democratic Republic (Laos)

The paleoenvironmental information for the Pleistocene of Laos is mostly achieved from the fissure filling deposits of Nam Lot (Bacon et al., 2012) and Tam Hang South (Bacon et al., 2008b, 2011) (Fig. 3). The ages of Nam Lot and Tam Hang South have been attributed to around the early Late Pleistocene (86-72 ka and 94-60 ka, respectively) on the basis of the luminescence and U-series dating methods combined with the faunal correlations (Bacon et al., 2015). The Nam Lot and Tam Hang South mammalian assemblages consist of modern and extinct taxa, the first site yielding remains of *Homo* sp. (Bacon et al., 2011, 2012). The cave of Nam Lot is younger than that of Tam Hang South according to the presence of two modern taxa (*Muntiacus muntjak* and *Sus scrofa*) that represent more advanced evolutionary stages (Bacon et al., 2015). The paleoenvironments of these two sites corresponded to mixed habitats with open seasonal deciduous forests and grassy covers based on the presence of abundant cervids, bovids, and suids (Bacon et al., 2015) and on the synecological (community-based) methods (Louys and Meijaard, 2010).

Regarding the most recent debated topics on the modern human migrations into Asia, modern man might have expanded eastward from Africa and colonized South Asia before 60 ka (after Toba volcanic eruption), and have subsequently spread across Southeast Asia around 50 ka, possibly through the past coastline based on stone artifact and genetic evidence (Appenzeller, 2012). This hypothesis supports that identifications of *Homo sapiens* remains recovered from the late Middle Pleistocene of Southeast Asian and South Chinese sites are no longer consistent. Interestingly, a human cranium from the cave of Tam Pa Ling (Fig. 3), dated between 63 and 46 ka by OSL and TL dating of sediments and U-series dating of bones, provides the first evidence of early modern humans in mainland Southeast Asia, supporting an early dispersal out of Africa and into Southeast Asia by the Late Pleistocene (Demeter et al., 2012, 2015). The presence of extinct arvicolines (Rodentia) in this cave indicates cooler environments than today (Demeter et al., 2015).

The Kingdom of Cambodia (Cambodia)

Few data documenting Cambodian Pleistocene mammal faunas are known, only some sites having been previously described (e.g., Phnom Loang in Kampot). Beden and Guérin (1973) reported a Middle Pleistocene fauna, known as “Phnom Loang” (Fig. 3), consisting of both the modern (e.g., *Panthera tigris*, *Rusa unicolor*, *Bubalus cf. arnee*) and the extinct (*Crocota crocuta ultima*, a spotted hyaena) taxa. A Middle Pleistocene age has been attributed to that site (Beden and Guérin, 1973), probably slightly older than that of Thum Wiman Nakin (>169 ka) based on the evolutionary stage of the fauna by Bacon et al. (2011). Louys and Meijaard (2010) conducted a discriminant function analysis of the community structure of the mammalian fauna and suggested a mixed habitat for this locality. In addition, thick laterites in Cambodia commonly occurred during the Middle Pleistocene (Takaya, 1967), suggesting some seasonality of the humid tropical climate (Whittow, 1984). Another late Middle Pleistocene cave, known as “Boh

Dambang”, in Kampot is reported by Demeter et al. (2013) (Fig. 3). The mammalian assemblage, as well as the age, is considered to be similar to that of Phnom Loang, containing several modern taxa: *Prionailurus bengalensis*, *Cuon alpinus*, *Ursus thibetanus*, *Axis porcinus*, *Rusa unicolor*, *Muntiacus muntjak*, *Bos* sp., *Bubalus arnee*, *Capricornis sumatraensis*, and *Macaca* sp. and locally extinct species: *Crocuta crocuta ultima* and *Pongo pygmaeus* (Demeter et al., 2013). The presence of the spotted hyaena and large bovids in the locality indicates a humid climate with relatively open environments (Demeter et al., 2013).

The socialist Republic of Vietnam (Vietnam)

Three Middle Pleistocene sites: Tham Khuyen (~475 ka, based on the U-series (performed on speleothems) and ESR (operated with tooth enamel and sediments) analyses (Ciochon et al., 1996)), Tham Hai (~475 ka based on the biochronological correlation (Olsen and Ciochon, 1990)), and Tham Om (250-140 ka based on the biochronological correlation (Olsen and Ciochon, 1990)) have been known since the late 20th century excavation (Fig. 3). Two preceding Vietnamese faunas, Tham Khuyen and Tham Hai, contain several extinct taxa (e.g., *Gigantopithecus*, *Pongo*, *Stegodon orientalis*, *Megatapirus augustus*, and a mystery ape (previously identified as belonging to *Homo erectus* (Ciochon, 2009)), but modern species (e.g., *Sus scrofa*, *Rusa unicolor*, *Muntiacus muntjak*, and *Bos gaurus*) were also present (Kha and Bao, 1967; Cuong, 1971; Olsen and Ciochon, 1990). The Tham Om fauna yields relatively similar taxa with those of Tham Khuyen and Tham Hai, but lacks *Gigantopithecus blacki*. This species became possibly extinct during the late Middle Pleistocene in Vietnam (Louys et al., 2007). Louys and Meijaard (2010) used a discriminant function analysis of the community guild structure to interpret the paleoenvironments for these caves. Their results suggest mixed habitats for those three caves.

Based on the faunal correlations, Hang Hum and Lang Trang are representatives of the late Middle to early Late Pleistocene sites in Vietnam (Fig. 3), confirmed by absolute ages tentatively estimated between 140 and 80 ka (Kha, 1976; Olsen and Ciochon, 1990) and between 100 and 80 ka (de Vos and Long, 1993; Long et al., 1996), respectively. These two faunas exhibit modern elements, especially for carnivores, associated with some extinct taxa (e.g., *Pongo pygmaeus*, *Stegodon orientalis*, *Palaeoloxodon namadicus*, and *Dicerorhinus sumatrensis*). Archaic *Homo* sp. and Chinese suids (*Sus* cf. *officinalis* and *Sus* cf. *lydekkeri*) are additionally reported from Hang Hum (Kha and Bao, 1967; Cuong, 1985; Olsen and Ciochon, 1990), while a giant panda (*Ailuropoda melanoleuca*) is present in Lang Trang (de Vos and Long, 1993). The presence of *Pongo* in Hang Hum and Lang Trang suggests a tropical to sub-tropical vegetation cover. The temperate species preferring bamboos are possibly present according to the occurrence of *Ailuropoda melanoleuca* in the latter site (de Vos, 1983; Tougaard et al., 1996; Louys et al., 2007). The synecological analysis based on discriminant function methods indicates also mixed habitats for these two localities (Louys and Meijaard, 2010). For the late Middle to Late Pleistocene site of Ma U’Oi in northern Vietnam (Fig. 3), the *in situ* mammalian fossils (dated to the Late Pleistocene, >49 ka based on the U/Th dating performed on the fossiliferous breccia) belong to an extinct proboscidean, *Palaeoloxodon namadicus*, and relatively modern species that are still living today in Vietnam (Bacon et al., 2004, 2006). Two teeth and skull fragments assigned to archaic *Homo* were extracted from the ground floor in rooms A2 and A3 and a corridor A (Demeter et al., 2004, 2005). Numerous remains of microvertebrates (including primates, rodents, insectivores, chiropterans, and small reptiles and amphibians) were also recovered from the roof of corridor “A” in the same cave (Bacon et al., 2006; fig. 4). The *in situ* Ma U’Oi fauna suggests open woodlands close to the present-day environments in Vietnam. The microvertebrate fauna (dated to the late Middle Pleistocene, 193 ± 17 ka) indicates a more

closed canopy (Bacon et al., 2006). With regards to the Late Pleistocene cave of Duoi U'Oi (66 ± 3 ka for the U/Th geochronology of the calcitic floor) (Fig. 3), the large mammal fauna is slightly less diversified than that of Tam Hang South and Nam Lot. A leopard, *Panthera pardus*, is additionally reported in Duoi U'Oi (Bacon et al., 2008a). Two isolated teeth assigned to *Homo* sp. were also recovered from this site (Bacon et al., 2008a). This fauna is typical of those living relatives in open seasonal forests (Bacon et al., 2015). In addition, between 62 and 19 ka, the reworking of aeolian sands along the southeastern Vietnam coast has indicated a reduction of vegetation covers and landscape instability, in relation to the climate change, in this area (Murray-Wallace et al., 2002). The possibly more recent site of Keo Leng (30-20 ka based on the faunal correlation with other Vietnamese localities, Cuong (1985)) (Fig. 3) yields most of modern faunas (including *Homo sapiens*) with some extinct taxa: *Ailuropoda melanoleuca*, *Pongo pygmaeus*, and *Stegodon orientalis* (Kha, 1976; Long and Du, 1981; Olsen and Ciochon, 1990). The paleoenvironments of this site might have corresponded to a closed habitat due to the presence of both *Pongo* and *Ailuropoda*. All of these data therefore suggest a variety of habitat types for the Late Pleistocene sites of Vietnam (Louys and Meijaard, 2010).

The Federation of Malaysia (Peninsular Malaysia)

The Kinta valley (Tambun) fauna constitutes possibly one of very few Middle Pleistocene sites in the Malay Peninsula (Fig. 3). This fauna yields some archaic species including *Hexaprotodon* sp., *Duboisia santeng*, and *Palaeoloxodon namadicus*, but a modern Javan rhinoceros, *Rhinoceros sondaicus*, is also present (Hooijer, 1962). Other modern species probably occurred, but more detailed taxonomic identification needs to be further addressed. According to the faunal correlations, the age of the site has been tentatively established as being around the Middle Pleistocene (Hooijer, 1962; Medway, 1972). However, this dating is not well-constrained, a Late Pleistocene age being possible based on the geological evidence (Kamaludin et al., 1993;

Kamaludin and Azmi, 1997; Teeuw et al., 1999). The paleoenvironments of this site corresponded to a savannah condition with some parts of rather swampy areas according to the presence of ecological mammal indicators (*Duboisia santeng* and an extinct hippopotamus (Hooijer, 1962), in agreement with Heaney (1991) who suggested a savanna corridor for the Sundaland during the Middle Pleistocene. The late Middle Pleistocene site of Badak Cave (dated between 278 and 208 ka, based on OSL and TL datings of sediments) is described by Ibrahim et al. (2013) (Fig. 3). Its fauna contains obviously a locally extinct orangutan (*Pongo* sp.) and modern elements of large mammals such as *Ursus thibetanus*, *Helarctos malayanus*, *Sus scrofa*, *Rusa unicolor*, *Muntiacus muntjak*, and *Capricornis sumatraensis*. Peat with detritus remains of *Pinus*, Gramineae, and ferns are recorded from the possible Middle Pleistocene of Sunung, an area of about 230 km south of Badak Cave C, indicating the existence of a savanna-type habitat with more seasonal climates (Batchelor, 1979; Morley and Flenley, 1987). Moreover, Morley (1998) mentioned that *Pinus* savanna was probably widespread on the Malay Peninsula at about 660, 480, 200, and 22 ka. Climate in lowlands during the interglacials was probably similar to prevailing today, as demonstrated by the palynological records deposited at about 80 and 55 ka (Kamaludin and Azmi, 1997).

Other younger caves are formed within the metamorphosed Kuala Lumpur limestone known as “Batu Caves” (Fig. 3), being of Late Pleistocene in age (between 66 and 33 ka), according to the OSL and TL datings of sediments (Ibrahim et al., 2013). These caves yield a large mammal fauna similar to Badak Cave, but some modern taxa (e.g., *Panthera tigris*, *Tapirus indicus*, *Dicerorhinus sumatrensis*, and *Sus* cf. *barbatus*) are additionally documented. The presence of *Pongo* suggests a prevailing (evergreen) forest habitat for both Badak Cave and Batu Caves, implying that sufficient forest covers persisted in the western coast of Peninsular Malaysia through the late Middle to middle Late Pleistocene (Ibrahim et al., 2013). Other late Late

Pleistocene to Holocene sites, where large mammal remains have been recovered in Peninsular Malaysia, are reported (e.g., Gua Gunung Runtuh (Davidson, 1994) and Gua Cha (Groves, 1985)) (Fig. 3). In the Quaternary deposits of Sungei Besi, western Malaysia, carbon-dated peat and wood and pollens suggest perhumid vegetation that occurred at around 41.2 and 36.4 ka (Ayob, 1970). Overall, the closed environments (evergreen vegetation) were dominating and existing in Peninsular Malaysia before the Late Glacial Maximum (LGM).

The Kingdom of Thailand (Thailand)

Large mammalian fossils have been poorly recorded from the Early Pleistocene of Thailand. Only the Late Miocene to Pleistocene sand pit of Tha Chang (Nakhon Ratchasima) and the possible Early to Middle Pleistocene cave of Pha Bong (Mae Hong Son) have been reported (Chaimanee et al., 2004; Bocherens et al., in press). In Tha Chang, fossils from the Late Miocene and from the overlying Pleistocene level were mixed and collected by locals, without stratigraphical control (Chaimanee et al., 2004). Sediments and material collected from the upper horizon of sand pits were deposited by high-energy flood pulses, contemporaneous with the tektites forming event during mid-Pleistocene at 0.7 Ma (Gentner et al., 1969; Charusiri et al., 2002; Haines et al., 2004). The Pha Bong fauna contains *Gigantopithecus*, *Pongo* sp., *Crocuta crocuta*, *Ailuropoda melanoleuca*, *Ursus* sp., *Sus scrofa*, *Rhinoceros* sp., *Capricornis* sp., cervid and bovid indet., *Hystrix* sp., and *Rhizomys* sp. (Bocherens et al., in press). The stable carbon isotope analysis of mammalian tooth enamel from Pha Bong suggests a variety of landscapes ranging from closed forests to open savannah grasslands (Bocherens et al., in press). The occurrence of Pliocene to Early Pleistocene thick laterites in the lower Central Plain of Thailand also suggests high seasonality under the humid tropical climate (Whittow, 1984; Thiramongkol, 1986).

Compared to the Early Pleistocene information in Thailand, mammal fossils have been much better known from the Middle to Late Pleistocene fissure-filling deposits (Fig. 3): Had Pu Dai (Pramankij and Subhavan, 2001a), Kao Pah Nam (Pope et al., 1981), Thum Wiman Nakin (Ginsburg et al., 1982; Chaimanee and Jaeger, 1993; Tougard, 1998, 2001), Thum Prakai Phet (Tougaard, 1998; Filoux et al., 2015), Thum Phedan (Yamee and Chaimanee, 2005), and the Cave of the Monk (Zeitoun et al., 2005, 2010). The mammalian fauna from Had Pu Dai has not been studied in details yet, but fundamentally consists of a giant panda, a hyaena, cervids, suids, and possibly a large extinct ape (*Gigantopithecus* sp.) and an orangutan (*Pongo* sp.) (Tobias, 2002). An age of 500 ka has been proposed by Pramankij and Subhavan (2001a, 2001b) on the basis of the presence of archaic taxa. However, the age of Had Pu Dai is highly doubtful due to the inaccurate taxonomic descriptions of the mammalian fauna. The Kao Pah Nam site yields extinct (*Crocota* sp., *Hippotamus*?, and *Pongo*?) and modern (e.g., *Panolia eldii* and *Bos* cf. *gaurus*) taxa. The age of the site has been dated to around 690 ka based on the geological and faunistic data by Pope et al. (1981). The paleoenvironments of this site are interpreted as corresponding to relatively open and dry Dipterocarp woodlands based on the presence of *Hippopotamus*, hyaenids, and large cervids and bovids as well as the absence of gibbons (Pope et al., 1981). However, similar to Had Pu Dai, this locality reveals an inappropriate taxonomic identification of mammalian taxa. The precise age of Kao Pah Nam is thus ambiguous. During the late Middle Pleistocene, Thum Wiman Nakin yields one of the most abundant and diversified mammal fossils in mainland Southeast Asia. It contains numerous modern (e.g., *Ursus thibetanus*, *Rhinoceros sondaicus*, *Sus scrofa*, *Axis porcinus*, *Rusa unicolor*, *Bos javanicus*, *Bubalus arnee*, *Capricornis sumatraensis*) and extinct (e.g., *Crocota crocota ultima*, *Ailuropoda melanoleuca*, *Pongo pygmaeus*, and *Rhinoceros unicornis*) taxa that are representatives of the late Middle Pleistocene fauna (Tougaard, 1998, 2001), dated to 169 ka for the minimum age based on the U-series dating of the stalagmitic floor

above the fossiliferous layer (Esposito et al., 1998, 2002) . A tooth of *Homo* sp. was also recovered from this locality (Tougaard et al., 1998). Chaimanee (1998) suggested a wetter and cooler climate than today on the basis of the rodent species and vegetation. Based on an analysis of the cenogram (Legendre, 1986, 1989), the paleoenvironments of Thum Wiman Nakin are characterized by a slightly open forest landscape with relatively humid conditions (Tougaard and Montuire, 2006). According to stable carbon isotope analysis of tooth enamel of Thum Wiman Nakin mammals, a mosaic of C3 and C4 plants in open and semi-wooded savannah with forest patches and deep forest cover was common in the area (Pushkina et al., 2010). The cave of Thum Prakai Phet is highly similar in faunal composition and age to that of Thum Wiman Nakin. Accordingly, the paleoenvironments of Thum Prakai Phet are proposed to have corresponded to a slightly open forest (Tougaard, 1998; Filoux et al., 2015). The Thum Phedan cave in southern Thailand yields some large mammalian taxa including *Crocuta crocuta ultima*, *Rhinoceros* sp., *Sus scrofa*, *Capricornis sumatraensis*, and indeterminate cervids and bovids (Yamee and Chaimanee, 2005). The age of this site has been tentatively dated to late Middle Pleistocene due to the occurrence of the spotted hyaena (Yamee and Chaimanee, 2005). The palaeoenvironments of the site likely corresponded to mixed habitats with an open savannah and forest patches based on the presence of the spotted hyaena and its associated fauna.

Several Late Pleistocene to Holocene archaeological sites in Thailand (e.g., the Cave of the Monk (Zeitoun et al., 2005, 2010) and Tham Lod Rockshelter (Shoocongdej, 2006; Marwick et al., 2013)) were discovered (Fig. 3), but only the few associated mammalian faunas have been studied in details. The Cave of the Monk (Ban Fa Suai) has been faunistically studied by Zeitoun et al. (2005, 2010). This fauna contains diverse modern (primates, carnivores, rhinoceroses, elephants, cervids, bovids, and suids) and extinct (e.g., *Ailuropoda melanoleuca*, Hyaenidae indet., *Rhinoceros unicornis*, *Pseudoryx* sp., *Pongo pygmaeus*) taxa (Zeitoun et al., 2005, 2010).

The minimal age of the fauna ranges from 32 to 19 ka, based on the ESR dating of enamel, dentine, and sediments (Zeitoun et al., 2010). The paleoenvironments of this site possibly corresponded to mixed habitats (Louys and Meijaard, 2010).

Overall, the open environments in Thailand during the Pleistocene seem to have been more extended than those in present day. Fortunately, the Khok Sung terrace deposit, presumably being of Pleistocene in age (Chaimanee et al., 2005), has been discovered in northeastern part of Thailand since the last 10 years ago. Providing more information regarding the Pleistocene history of Thailand, fossils collected from this locality needs to be studied here in details.



CHAPTER 3

Study area and geological background

The discovery of the Khok Sung fossiliferous site

The Khok Sung fossiliferous site (N 15°06'17", E 102°06'38.2") is situated in land tenure of the Korat Yongsanguan Rice Mill Co. Ltd. owned by Mr. Somchai Tirasetphakdee. This rice mill is located in Ban Khok Sung subdistrict, Nakhon Ratchasima province (also called "Khorat"), at about 15 km north of Nakhon Ratchasima city, close to the Highway no. 205 (Fig. 4).

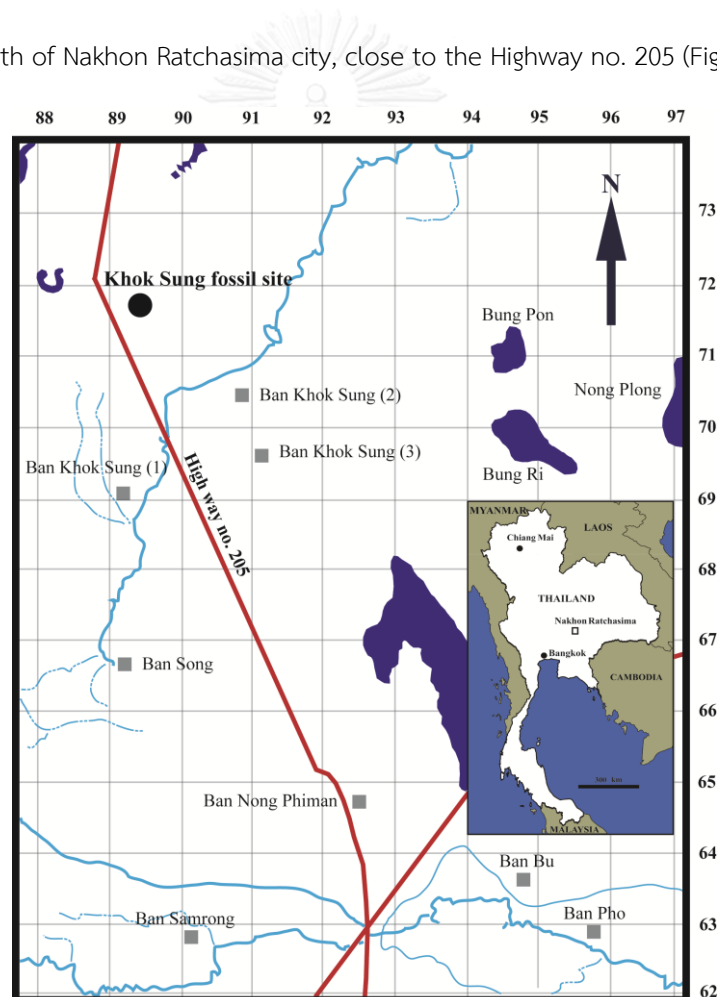


Figure 4. Map of Thailand showing the location of the Khok Sung fossiliferous site in Nakhon Ratchasima province, northeastern Thailand (modified from the Royal Thai Survey Department topographic map: scale 1:50,000, sheet 5439III, series L7017). Red lines indicate highways of Thailand.

In 2005 (March), remains of vertebrate fossils have been first recovered, at the depth of 5-7 meters below the surface, during which the fluvial terrace deposits behind the rice mill were dug out for the construction of a pond (50 long x 50 wide x 15 deep) (Fig. 5A). Following the discovery of large bone fragments by workers, this site was then rapidly excavated by the Thai-French paleontological research team and geologists from the Department of Mineral Resources. While the water was pumped out of the sand pit, the fossils have been continuously exposed and searched, using the water spraying technique (Fig. 5B). The excavation work has revealed an extraordinary discovery of vertebrate fossils, especially for mammals and reptiles, in terms of quantity and preservation (Fig. 5C).



Figure 5. The sand pit of Khok Sung during the paleontological excavation (in March, 2005): **(A)** a general view of the sand pit, **(B)** an area of vertebrate fossil recovery, and **(C)** *in situ* remains of *Stegodon*. The photos were taken by Yaowalak Chaimanee during the fieldwork. The blue arrow indicates the location of the fossiliferous layer (above the dark gray layer) and the black one points to the non-marine Mesozoic bedrock.

Geologic setting

The Khok Sung sand pit is geographically positioned on the Khorat Plateau (about 150 m above sea level for an average elevation), a north-central part of the Indochinese Peninsula. The Khorat Plateau covering an area of 180,000 km² exhibits a saucer-shaped basin that is structurally developed over the sequence of Mesozoic to Tertiary clastic sediments (Sattayarak, 1985; Sattayarak et al., 1998). It fundamentally comprises two major sedimentary basins, the large Khorat Basin (south) and the small Sakon Nakhon Basin (north), separated by the northwestern to southeastern Phu Phan Mountain Range (Dheeradilok and Kaewyana, 1986). The central part of the southern Khorat Basin with an average elevation of 120 m contains a deeply incised mature river valley filled by Quaternary sediments (Löffler et al., 1984). Other incised valleys covered by more recent sediments indicate that the flat appearance of the Khorat Plateau is today characteristics of the infilling sediments during the Late Pleistocene to Holocene (Löffler et al., 1983). The Quaternary tectonic activity on the Khorat Plateau has therefore contributed to the alteration of present-day river drainage patterns (Löffler et al., 1983; Hutchison, 1989).

The Plateau's landscape is drained by two main rivers, Mun and Chi, flowing eastward into the Mekong River. The Mun River drainage joins the Mekong River near the eastern border of the Khorat Plateau. However, the ancient Mun river drainage is likely connected to the Chao Phraya River prior to the Middle Pleistocene (Hutchison, 1989; Attwood and Johnston, 2001; Glaubrecht and Köhler, 2004). Its paleocurrent was possibly flowing from east to southwest, in the direction of Chao Phraya drainage systems (Claude et al., 2011). The Khok Sung sand pit is located closest to the Mun River. It is thus considered to have corresponded to the ancient Mun River terrace deposits that consist of Quaternary alluvial sediments underlain by the Mesozoic red beds (Chaimanee et al., 2005) (Fig. 5A). The undulating bedrock surfaces underlying the Mun

River floodplain and interfluvial areas are a result of the weathered shales and sandstones of the Maharakham Formation (Löffler et al., 1984).

Lithostratigraphy

According to the geological map of Nakhon Ratchasima province (Department of Mineral Resources, 2007), the Khok Sung site lies on a floodplain overlaying Khorat Plateau Mesozoic deposits (Fig. 6). The deposits of the Khok Sung site consist of recent alluvial sediments (**Qa**—gravel, sand, silt, and clay). The adjacent areas are represented by older sedimentary deposits including Pleistocene colluvial sediments (**Qt**—gravel, sand, silt, local laterite, and lateritic soil), unconformably overlaying the Late Cretaceous to possible Early Tertiary Maharakham Formation (**KTms**—reddish to red pale siltstone and sandstone, frequently interbedded with rock-salt and gypsum) and the Early to Late Cretaceous Khok Kruat Formation (**Kkk**—grayish red to pale red siltstone, sandstone, and fine calcareous conglomerate) (Fig. 6).

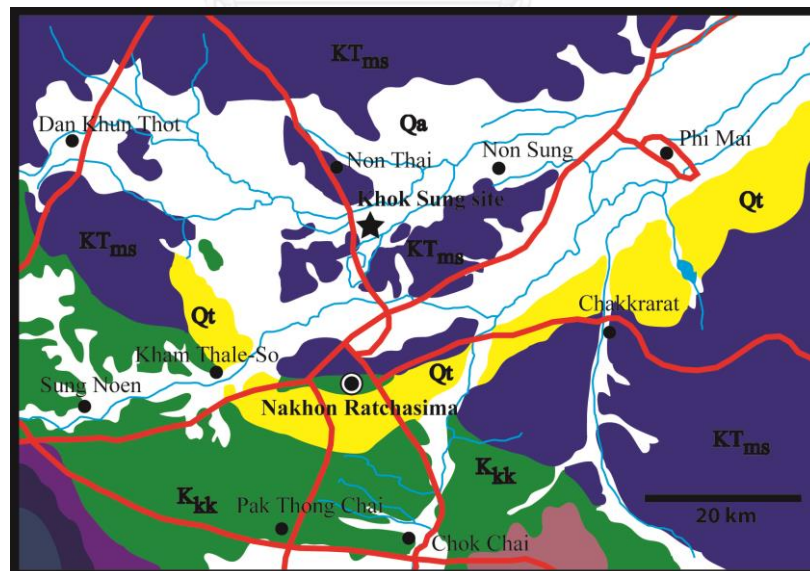


Figure 6. Geological map of Nakhon Ratchasima province. A star indicates the Khok Sung fossil site and red lines refer to main roads. Abbreviations: **Qa** (Quaternary alluvium), **Qt** (Quaternary terrace), **KTms** (Late Cretaceous to Early Palaeogene? Maharakham Formation), and **Kkk** (Early to Late Cretaceous Khok Kruat Formation) (modified from Department of Mineral Resources, 2007).

A lithostratigraphic section of the Khok Sung site figured by Chaimanee et al. (2005) has been divided into nine unconsolidated sedimentary units (A-I from top to bottom, respectively), excluding the underlying bedrock (Fig. 7). The uppermost part (unit A) is represented by dark-brownish and very poorly-sorted silty muds with a homogeneous texture and abundant root and wood fragments. Unit B consists of brownish and poorly-sorted silty muds with some root and wood fragments. Unit C contains brownish-yellow to dark-brown, fine-grained, and very poorly-sorted sandy muds with humic substances. Black manganese pisolithes, carbonate concretions, and plant remains are common in this unit. Unit D comprises light- to dark-brownish, fine- to coarse-grained, subround- to round-shaped, and well-sorted sands. Most of tree trunks found in this unit are oriented in E-W to SW-NE directions. The light-pinkish to dark-gray, fine- to medium-grained, subangular- to subround-shaped, and moderately well- to well-sorted sand is a representative of the unit E where gray carbonate mud clasts, mud lenses, and abundant petrified woods and trunks are also found. Unit F is characterized by dark-gray and coarse- to very coarse-grained sands and subround- to round-shaped, well-sorted, and matrix-supported gravels. This unit is interbedded by some layered-silty mud lenses at its upper part and by abundant remains of leaves, seeds, and vertebrates at its lowermost part. The dark-grayish, subangular- to subround-shaped, very poorly-sorted, and grain-supported gravels are recognized as the underlying unit G where rich calcareous mud clasts are recovered. Unit H is composed of dark-gray and moderately well- to well-sorted silty muds, interbedded with fine-sandy lenses. The plant remains are abundant at the upper part of this unit. Unit I contains pinkish-gray, fine- to medium-grained, subangular- to subround-shaped, and well-sorted sand and dark-gray and grain-supported gravels at the lowermost part of the section, unconformably overlying the bed rock. Vertebrate fossils were entirely collected from the layer of dark sands

and gravels (unit F) (Suraprasit et al., 2015). All fossils were deposited nearly simultaneously because they occurred within the same channel sequence (Duangkrayom et al., 2014).

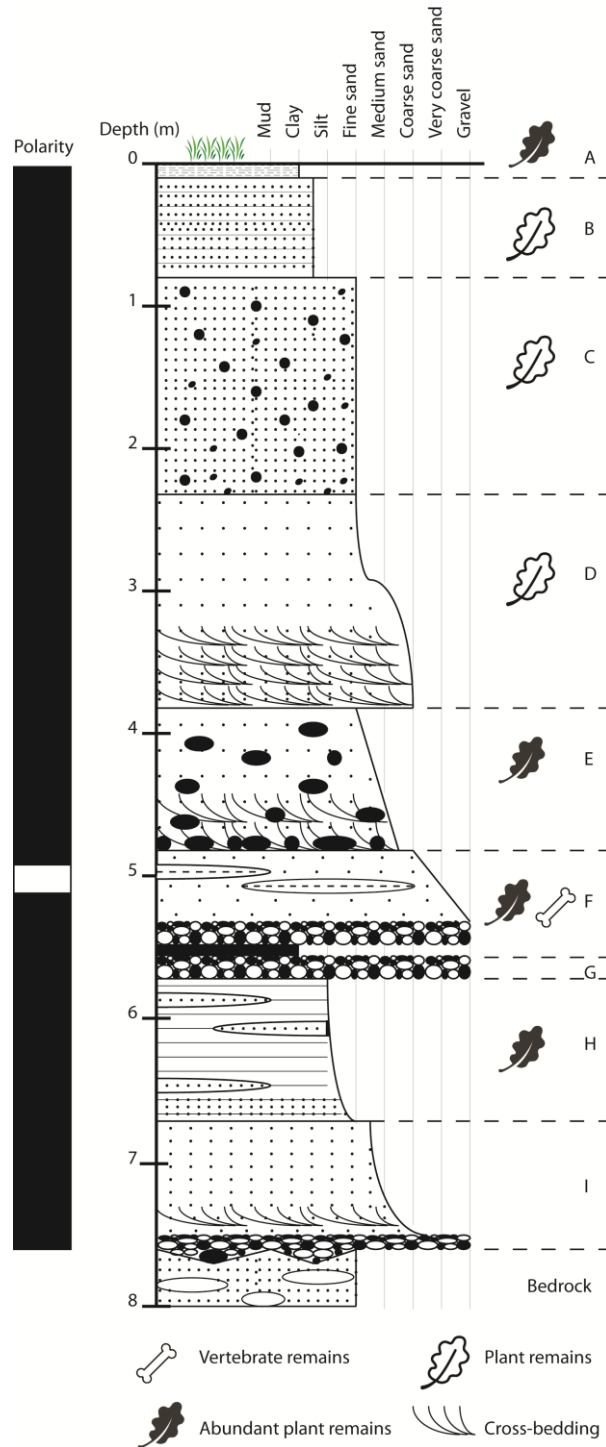


Figure 7. Magnetostratigraphic and lithostratigraphic profiles of the Khok Sung sand pit, Nakhon Ratchasima province, unit A-I from top to bottom in descending order (after Suraprasit et al., 2015).

Previous chronological framework and magnetostratigraphic analysis

The age of the Khok Sung fauna has been first suggested as being of the Early Pleistocene on the basis of the occurrence of *Gavialis cf. bengawanicus* (Martin et al., 2012). These authors argued that *Gavialis* has reached Thailand via the fluvial drainages of the Ganges, Brahmaputra, Irrawaddy, Mekong-Salween and finally Chao Phraya river before Early Pleistocene and arrived Java subsequently during a low sea-level event of the Early Pleistocene (Delfino and de Vos, 2010). Additionally, the C^{14} dating methods performed with plant seeds from the gravel beds (unit F) have only indicated that the age of this fossiliferous layer was out of the range of C^{14} ages (Chaimanee et al., 2005). The age of the Khok Sung fossiliferous layer is thus older than 40 kyr.

Although the excavation is no longer accessible according to the fact that the locality is now flooded, our paleomagnetic samples conducted on the Khok Sung locality have been collected when the outcrops were freshly excavated. Oriented block samples collected from 7 different lithostratigraphic units (Fig. 7) were analysed at the Paleomagnetic Lab, Laboratorio de Paleomagnetismo of the Universidad Nacional Autonoma de Mexico.

Alternating field demagnetization data for each specimen generated at 8 steps were plotted on orthogonal vector diagrams (Zijderveld, 1967) to identify a characteristic component (Fig. 8A, B), whose mean direction was then calculated using a principal component analysis (Kirschvink, 1980). All samples indicate a reliable primary magnetization signal, mainly showing normal polarity. However, samples collected from the unit F show either normal (sample KS-2B) or reverse (KS-1A) polarity (Fig. 8A-C). The overall mean direction of normal polarities is $D = 1.53^\circ$ $I = 13.27^\circ$ (Fig. 8D). The natural remanent magnetizations (NRM) are typically carried by low coercivity minerals, such as magnetite. The sample KS-2B was subjected to an isothermal

remanent magnetization (IRM), saturated by the field of about 150 mT (Fig. 8E). The sediments are dark gray-colored and show no obvious weathering evidence. Therefore, the magnetite may be a detrital component carrying an early acquired and original record of a fossil geomagnetic field of normal polarity.

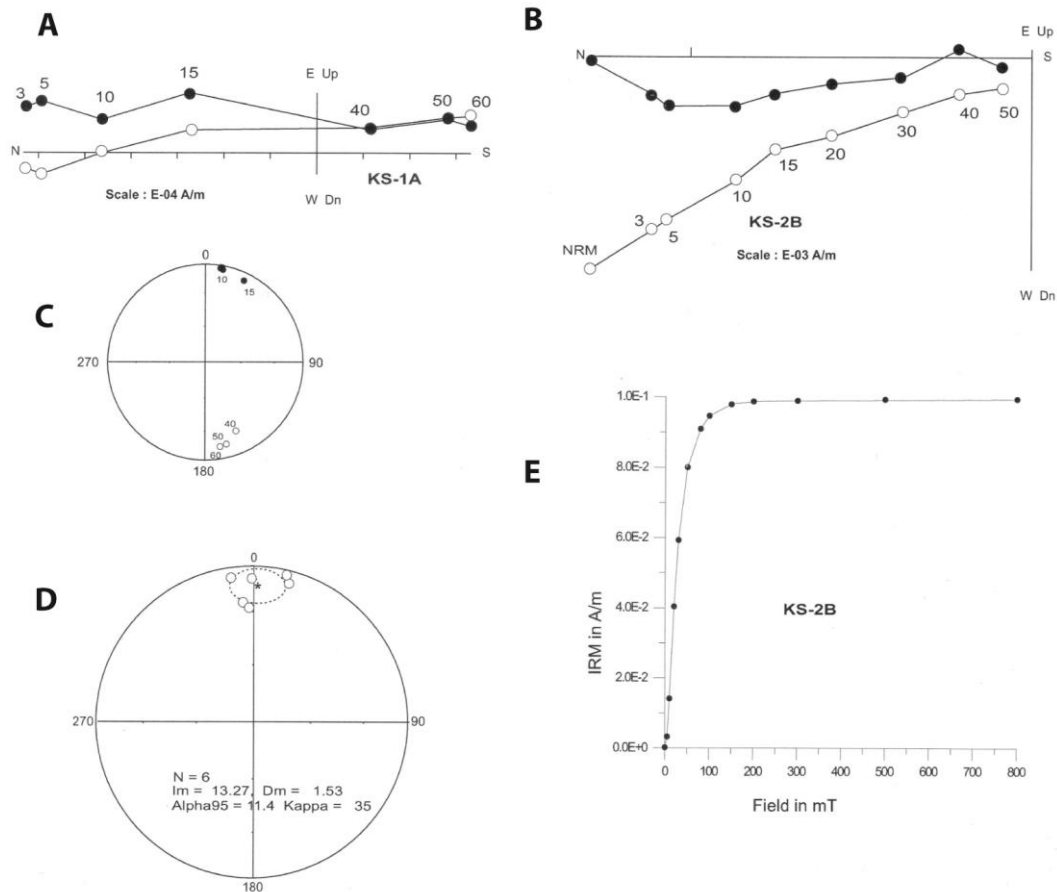


Figure 8. Paleomagnetic data: (A) and (B) examples of orthogonal vector diagrams of progressive alternating field demagnetizations, solid and open circles are projections on horizontal and east-west vertical planes, respectively, (C) a stereographic projection of the sample KS-1A, (D) an equal-area projection of magnetization directions related to horizons of the normal polarity, solid circles are plotted on the lower hemisphere. Overall mean directions and their 95% error limits are given in boxes, and (E) examples of IRM acquisition.

The magnetozone of the Khok Sung sequence shows normal polarity which can be correlated to the Brunhes normal chron according to the Geomagnetic Instability Time Scale (GITS) by Singer et al. (2005; 2006; 2008), pinpointing to a lapse of time spanning from the early

Middle Pleistocene (776 ± 2 ka) to modern day. An Early Pleistocene age for Khok Sung fauna is thus discarded because the Matuyama chron is represented by a mainly reverse polarity with two short normal subchrons (Olduvai and Jaramillo). Interestingly, *in situ* silty mud lenses interbedded within the sandy layer (sample KS-1A) which corresponds to the upper part of the unit F in the lithostratigraphic section (Fig. 7) show reverse polarity. Within the Brunhes normal chron, several well-dated excursions are recognized and named as “Laschamp” (40.4 ± 1.1 ka; Singer et al., 2005, 2006), “Blake” (120 ka; Lund et al., 2001), “Iceland Basin” (188 ka; Channell, 2006), “Pringle Falls” (211 ± 13 ka; Singer et al., 2008), and “Big Lost” (579 ± 6 ka; Singer et al., 2005, 2006). Other older excursions are also identified according to Singer et al. (2008). The reverse polarity of the silty mud lenses from the unit F can be therefore correlated to any of these excursions within the Brunhes normal chron. The age of the fossiliferous layer is presumably contemporaneous with or very slightly older than that of claimed polar reversal due to a short distance (less than 1 m in depth) between the fossiliferous layer and the reversed excursion (Fig. 7).

CHAPTER 4

Material and methods

Material and measurements

All fossil specimens are housed at the Khok Sung local museum (Nakhon Ratchasima) and at the Department of Mineral Resources (DMR) (Bangkok). Individual fossils are catalogued with the collection (DMR), locality (KS), and unique specimen number, respectively. All specimens were photographed, measured and identified. They were then compared with the extant and extinct mammalian collection and other published literatures. The comparative material is from the recent and fossil vertebrate collections housed at the following natural history museums and institutes: **IPHEP**, Institut International de Paléoprimateologie et de Paléontologie Humaine: Evolution et Paléoenvironnements, Université de Poitiers (Poitiers, France); **IVPP**, Institute of Vertebrate Paleontology and Paleoanthropology (Beijing, China); **NHMP**, National Museum (Prague, Czech Republic); **NMW**, Naturhistorisches Museum Wien (Vienna, Austria); **MNHN-ZMO**, Zoological collection of mammals and birds, Muséum National d'Histoire Naturelle (Paris, France); **RMNH DUB**, Dubois collection, Rijksmuseum van Natuurlijke Historie (Leiden, Netherlands); **THNHM-M**, Mammal collection, Thailand Natural History Museum (Pathum Thani, Thailand); **ZIN**, Zoological Institute, Russian Academy of Sciences (St. Petersburg, Russia); **ZSM**, Zoologische Staatssammlung München (Munich, Germany).

All specimens were measured using digital callipers to the nearest 0.01 mm. The tooth dimensions for all mammals were measured at the base of the crown along the anterior-posterior margins for the maximum length (L) and from the labial (incisors and canines)/buccal (premolars/molars) to lingual margins for the maximum width (W). In the case of measurements

of stegodontid cheek teeth, the methods and parameters used for molar and ridge dimensions were given in Fig. 9. The H/W index and the laminar frequency (LF) were calculated, using the formula proposed by van den Bergh (1999: p. 29–30). The ridge formula of stegodontids follows the original notation of Osborn (1942). Halfridges, whose width and height were 25% less than the succeeding or preceding ridge, at the anterior or posterior extremities of stegodontid molars are not counted and abbreviated as “x”. For the measurements ofhyaenid teeth, the widths at the position between the paracone and the metastyle (Wbl) were also measured on upper fourth premolars and the length of the anterior-(parastyle; Lps), middle- (paracone; Lpc), and posterior-(metastyle; Lms) cusps were also taken (Fig. 10), following the dental measurements by Werdelin and Solounias (1991). The measurements of cranial (Figs 10–12), mandibular (Figs 13 and 14), and postcranial (Figs 15–21) elements of fossil mammals were taken, using the methods of von den Driesch (1976) (for metrical abbreviations, see Tab. 1).

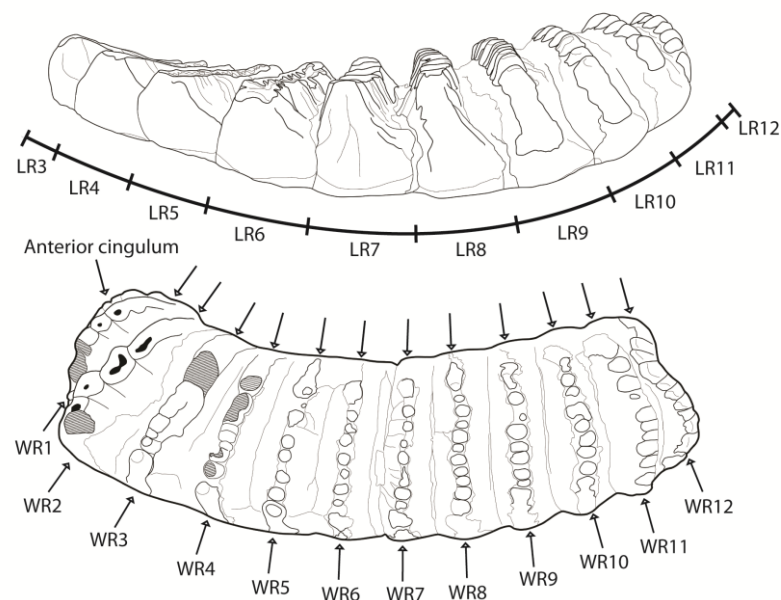


Figure 9. Metrical methods and parameters used for the lower third molar of *Stegodon*. Lengths and widths of the molar ridges are abbreviated as “LR” and “WR”, respectively. An illustration of two right m3 (lateral and occlusal views) of *Stegodon orientalis* is duplicated from the specimen IVPP V5216-15 (above) and IVPP V5216-13 (below).

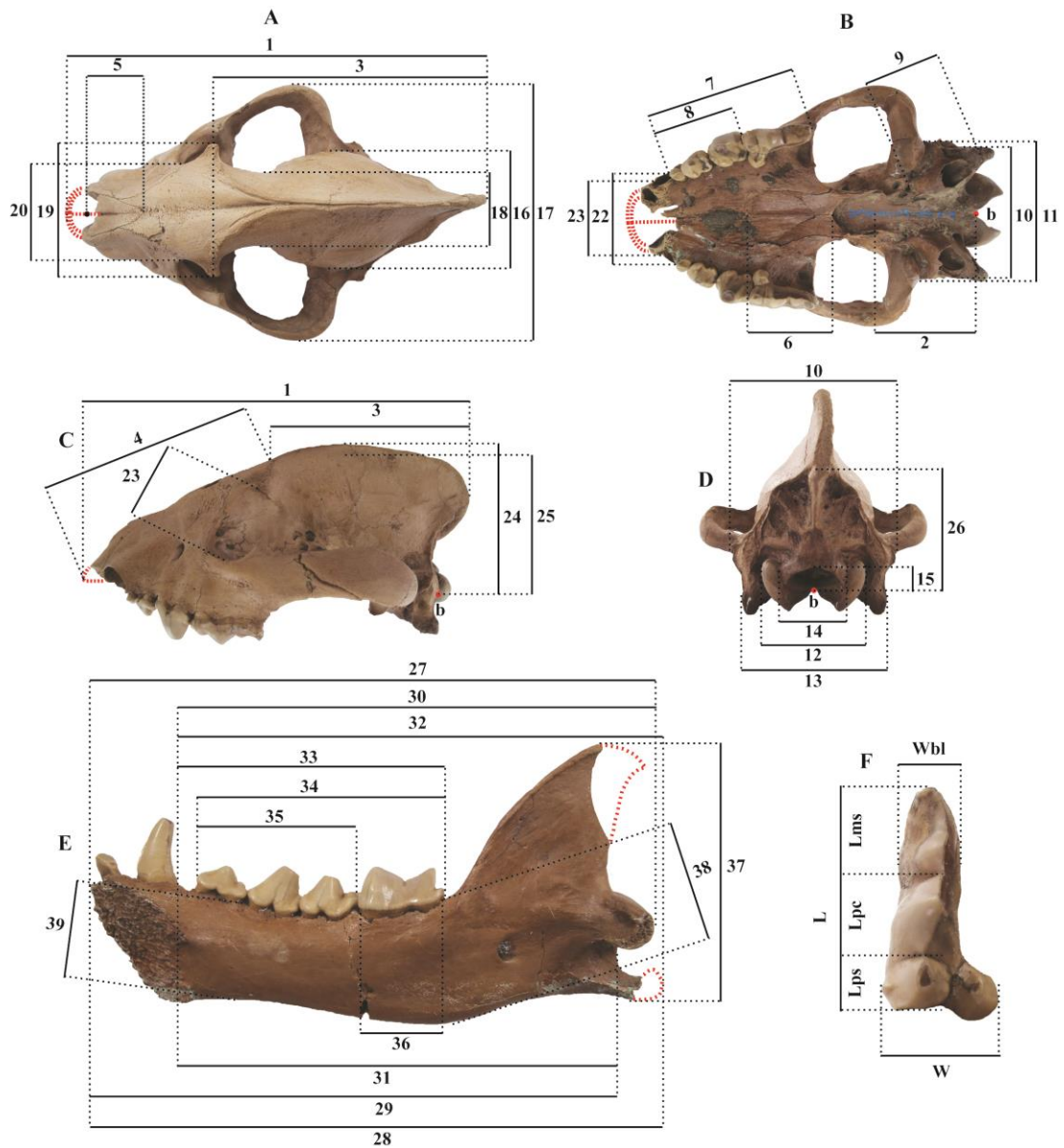


Figure 10. Methods of measurements for the hyaenid cranium, mandible, and upper fourth premolar: a cranium in dorsal (A), ventral (B), lateral (C), and posterior (D) views; (E) a mandible in medial view; (F) an upper fourth premolar in occlusal view. Red dash lines indicate the reconstruction of missing parts. The basion (the orobasal border of the foramen magnum in the median plane) is abbreviated as “b”. The number corresponds to the metrical parameters used in Tab. A2.

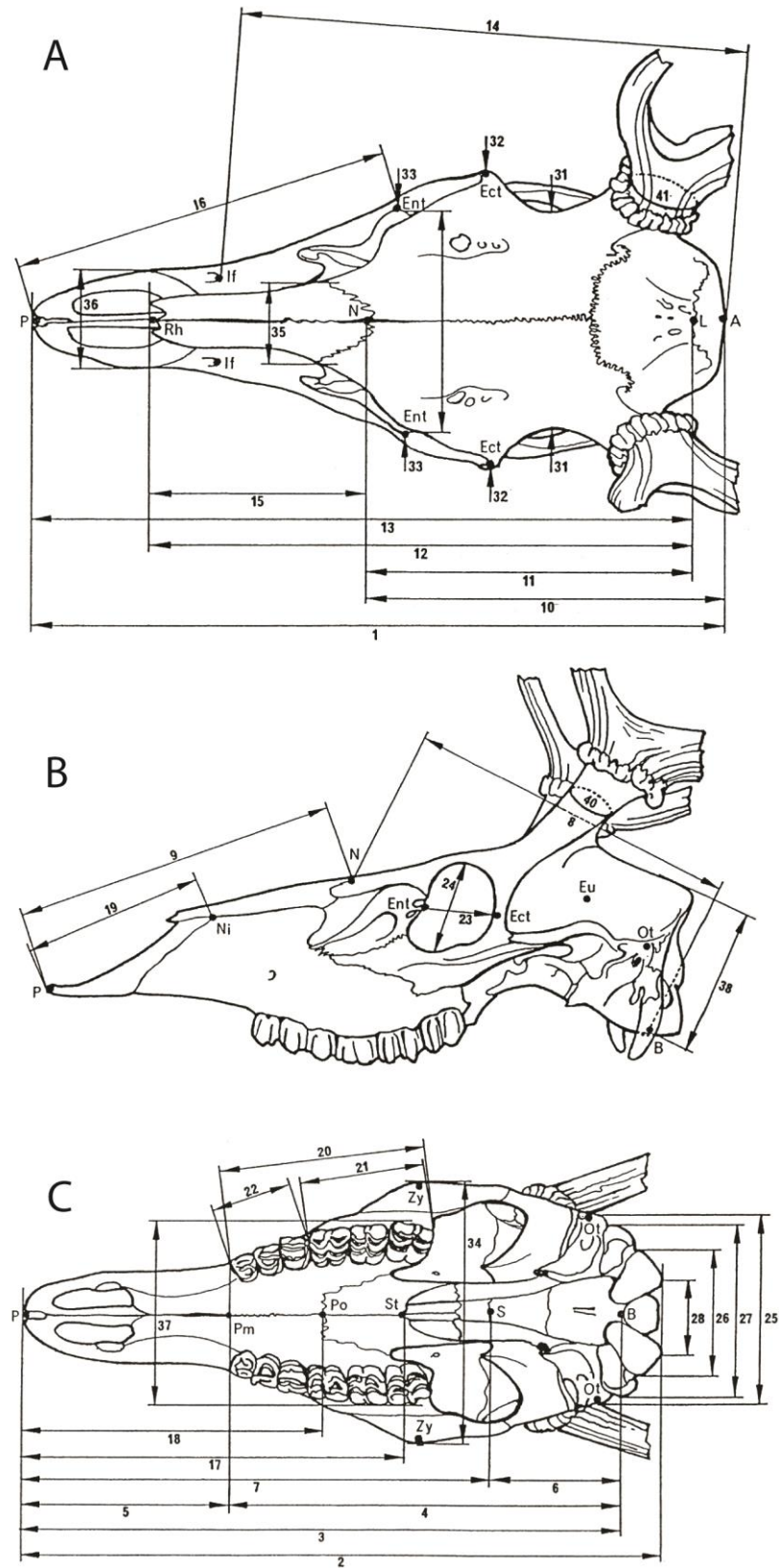


Figure 12. Methods of measurements for the cranium of *Cervus* in dorsal (A), lateral (B), and ventral (C) views (from von den Driesch, 1976).

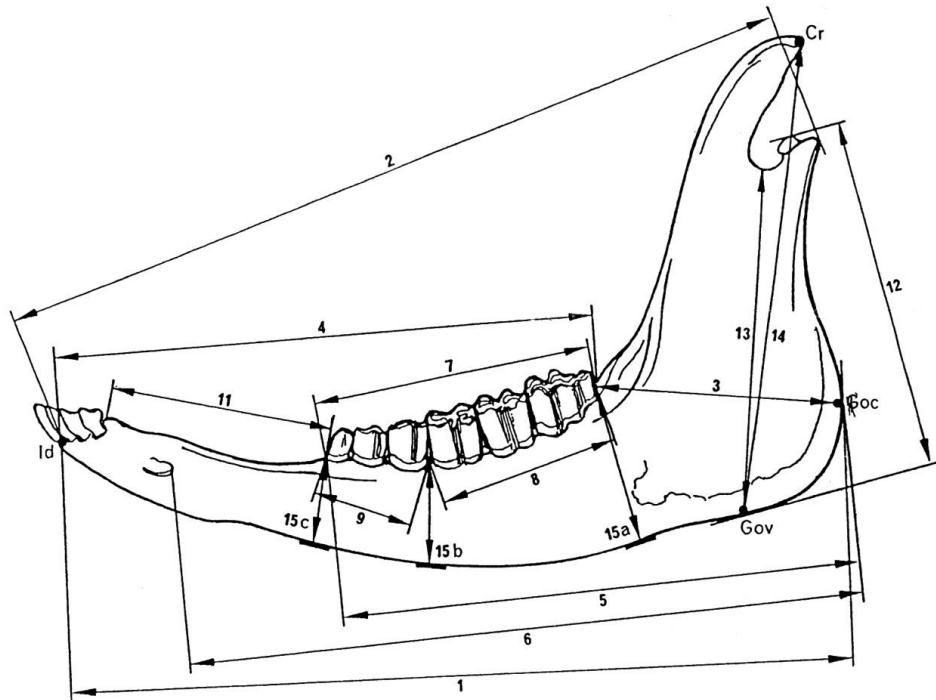


Figure 13. Methods of measurements for the mandible of ruminants in lateral view (from von den Driesch, 1976).

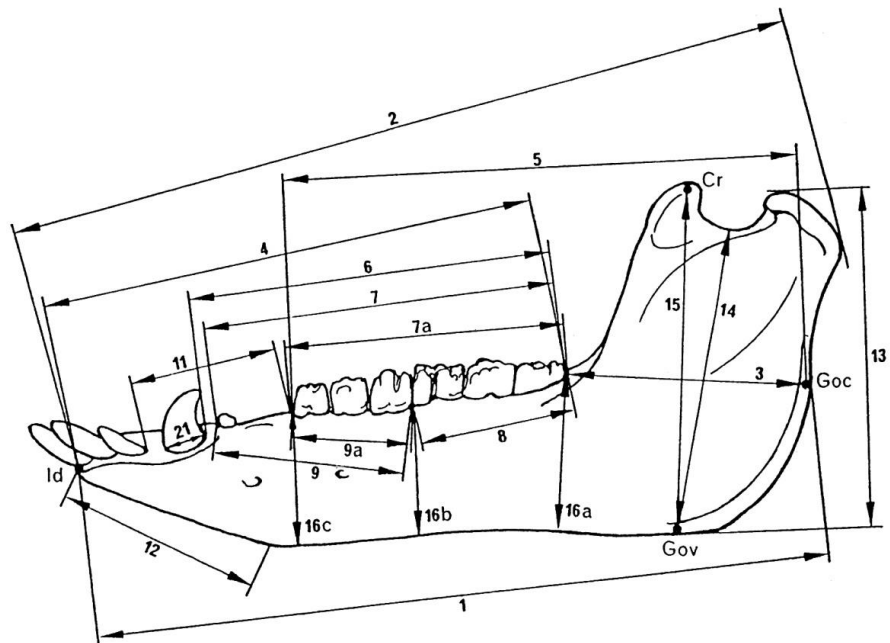


Figure 14. Methods of measurements for the mandible of *Sus* in lateral view (from von den Driesch, 1976).

Table 1. Metrical abbreviations for the postcranial bones (from von den Driesch, 1976).

Scapula	
HS	Height along the spine
DHA	Diagonal height from the most distal point of the scapula to the thoracic angle
Ld	Greatest dorsal length
SLC	Smallest length of the Collum scapulae (neck of the scapula)
GLP	Greatest length of the Processus articularis (glenoid process)
LG	Length of the glenoid cavity
BG	Breadth of the glenoid cavity
Long bones	
GL	Greatest length
GLL	Greatest length of the lateral part
GLC	Greatest length from the caput (head)
PL	Physiological length (for radius only)
LL	Length of the lateral part
Bp	Greatest breadth of the proximal end
BFp	Greatest breadth of the Facies articularis proximalis (for radius only)
BPC	Greatest breadth across the coronoid process (=greatest breadth of the proximal articular surface) (for ulna only)
SD	Smallest breadth of diaphysis
Dp	Depth of the proximal end
Bd	Greatest breadth of the distal end
BFd	Greatest breadth of the Facies articularis distalis (for radius only)

Dd	Greatest breadth of the distal end
DC	Greatest depth of the Caput femoris
DD	Smallest depth of the diaphysis (for metapodials only)
BT	Greatest breadth of the trochlea (for humerus only)
LO	Length of the olecranon (for ulna only)
DPA	Depth across the Processus anconaeus (for ulna only)
SDO	Smallest depth of the olecranon (for ulna only)

Pelvis

GL	Greatest length of one half
LA	Length of the acetabulum including the lip
LS	Length of the symphysis
SH	Smallest height of the shaft of ilium
SB	Smallest breadth of the shaft of ilium
SC	Smallest circumference of the shaft of ilium
LFo	Inner length of the foramen obturatum
GBTc	Greatest breadth across the Tubera coxarum–greatest breadth across the lateral angle
GBA	Greatest breadth across the acetabula
GBTi	Greatest breadth across the Tubera ischiadica
SBI	Smallest breadth across the bodies of the Ischia

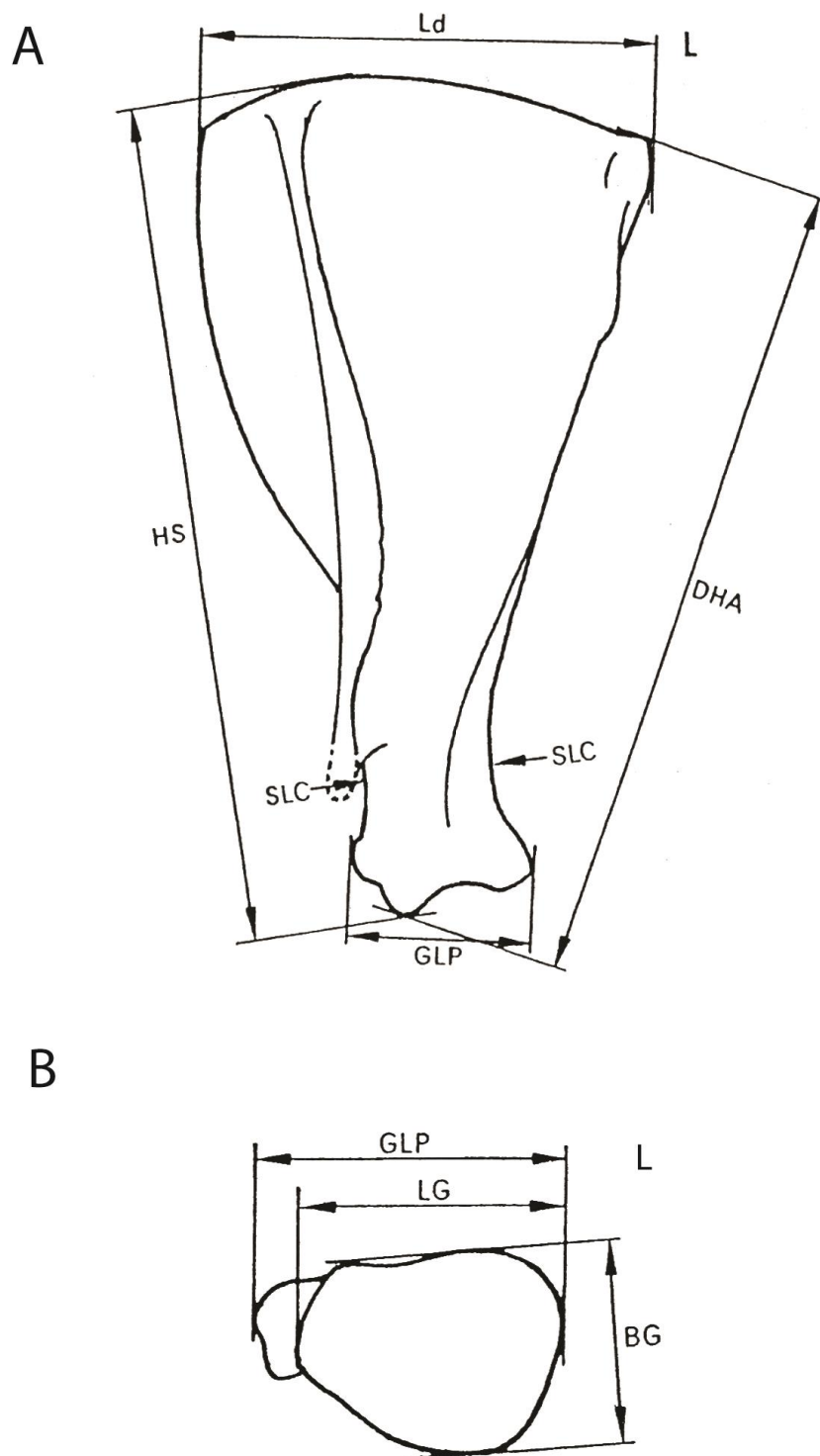


Figure 15. Methods of measurements for the scapulae (from von den Driesch, 1976): **(A)** scapula of *Bos* in lateral view; **(B)** scapula of *Bos* in distal view. Abbreviations: L=left side and R=right side.

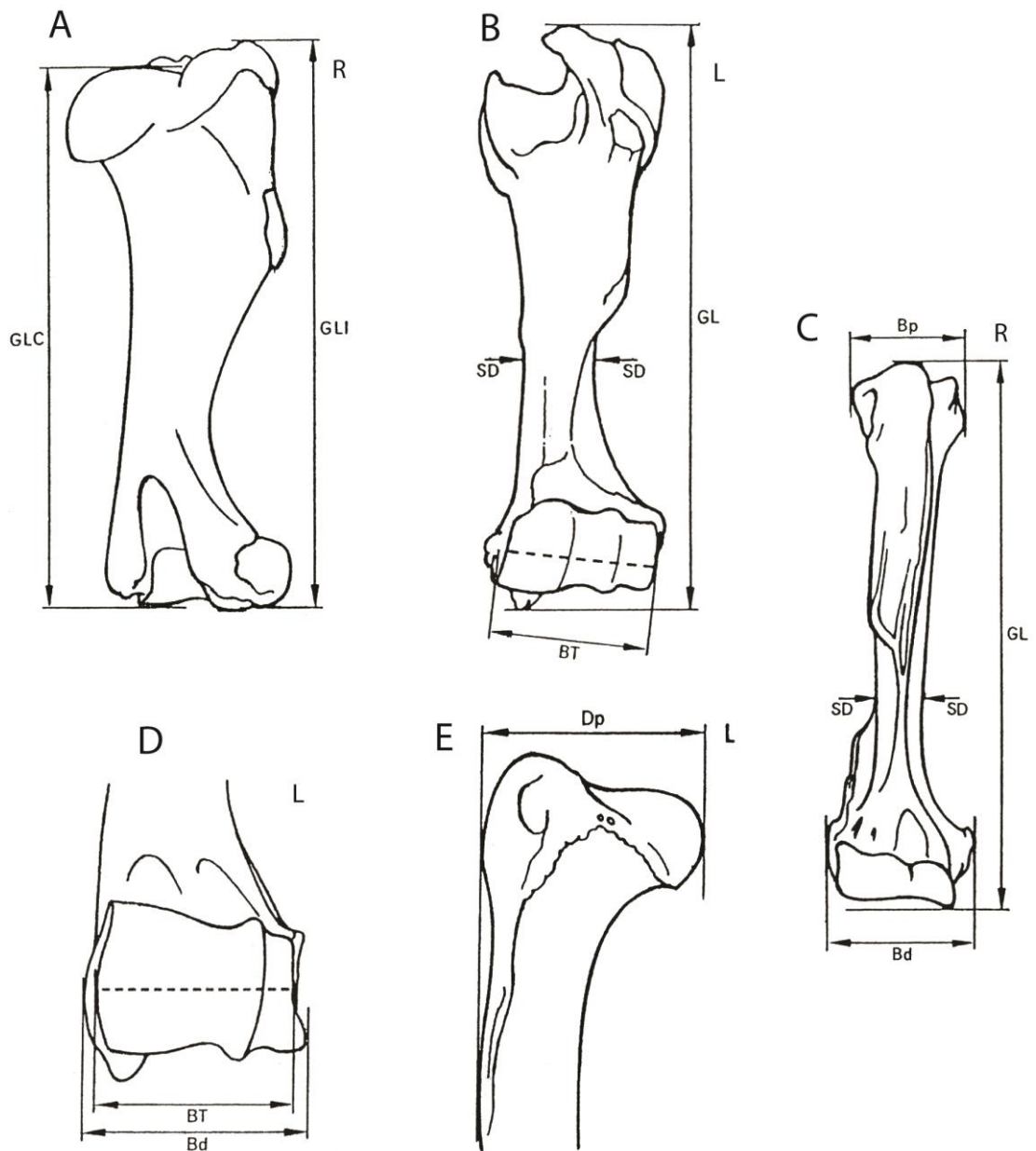


Figure 16. Methods of measurements for the humeri (from von den Driesch, 1976): **(A)** humerus of *Equus* in posterolateral view; **(B)** humerus of *Bos* in anterior view; **(C)** humerus of *Ursus* in anterior view; **(D)** humerus of *Cervus* in anterior view; **(E)** proximal humerus of *Canis* in lateral view. Abbreviations: L=left side and R=right side.

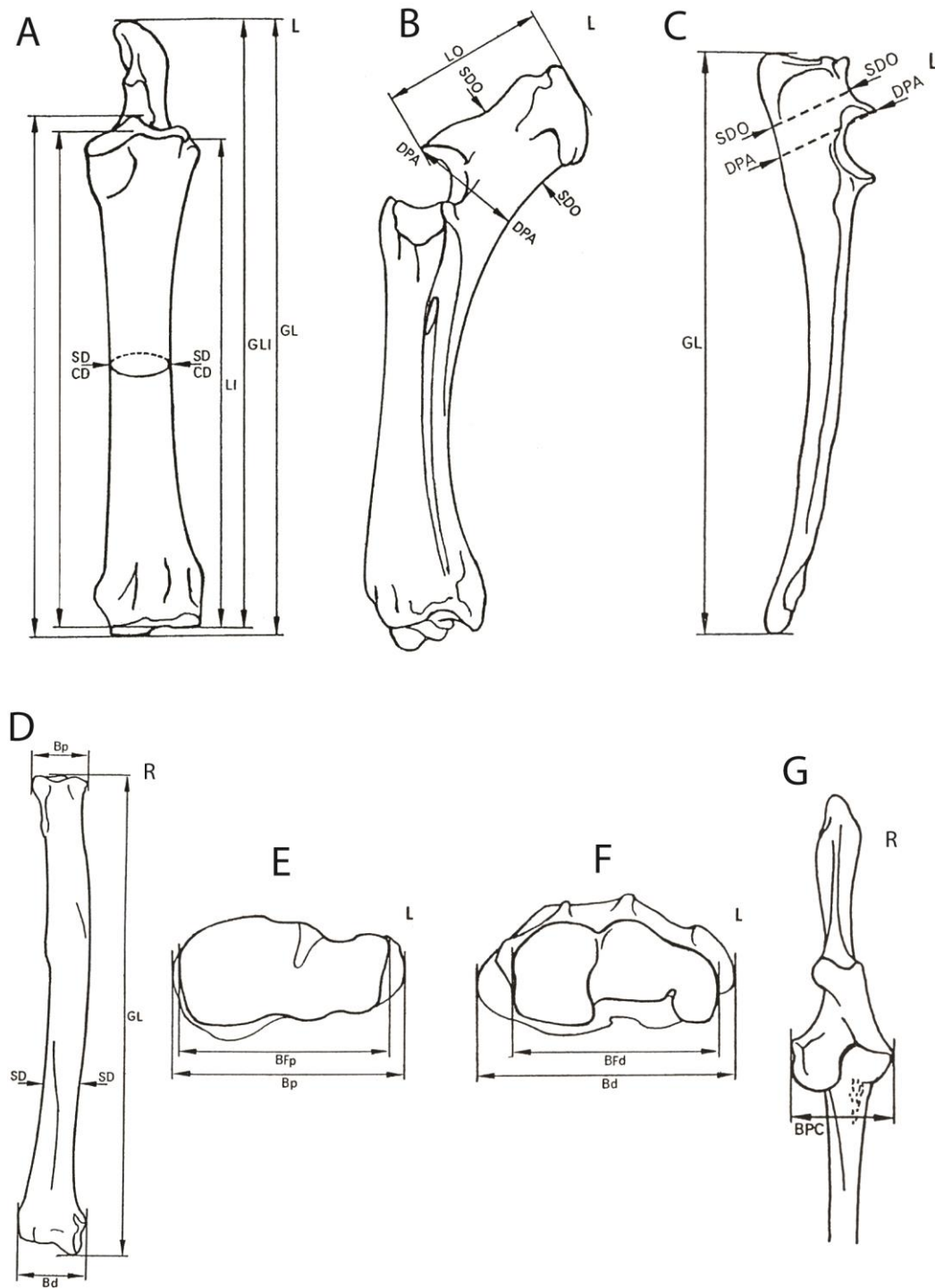


Figure 17. Methods of measurements for the radii and ulnae (from von den Driesch, 1976): **(A)** radius and ulna of *Equus* in anterior view; **(B)** radius and ulna of *Bos* in lateral view; **(C)** ulna of *Canis* in medial view; **(D)** radius of *Canis* in anterior view; **(E)** radius of *Equus* in proximal view; **(F)** radius of *Equus* in distal view; **(G)** proximal ulna of *Cervus* in anterior view. Abbreviations: L=left side and R=right side.

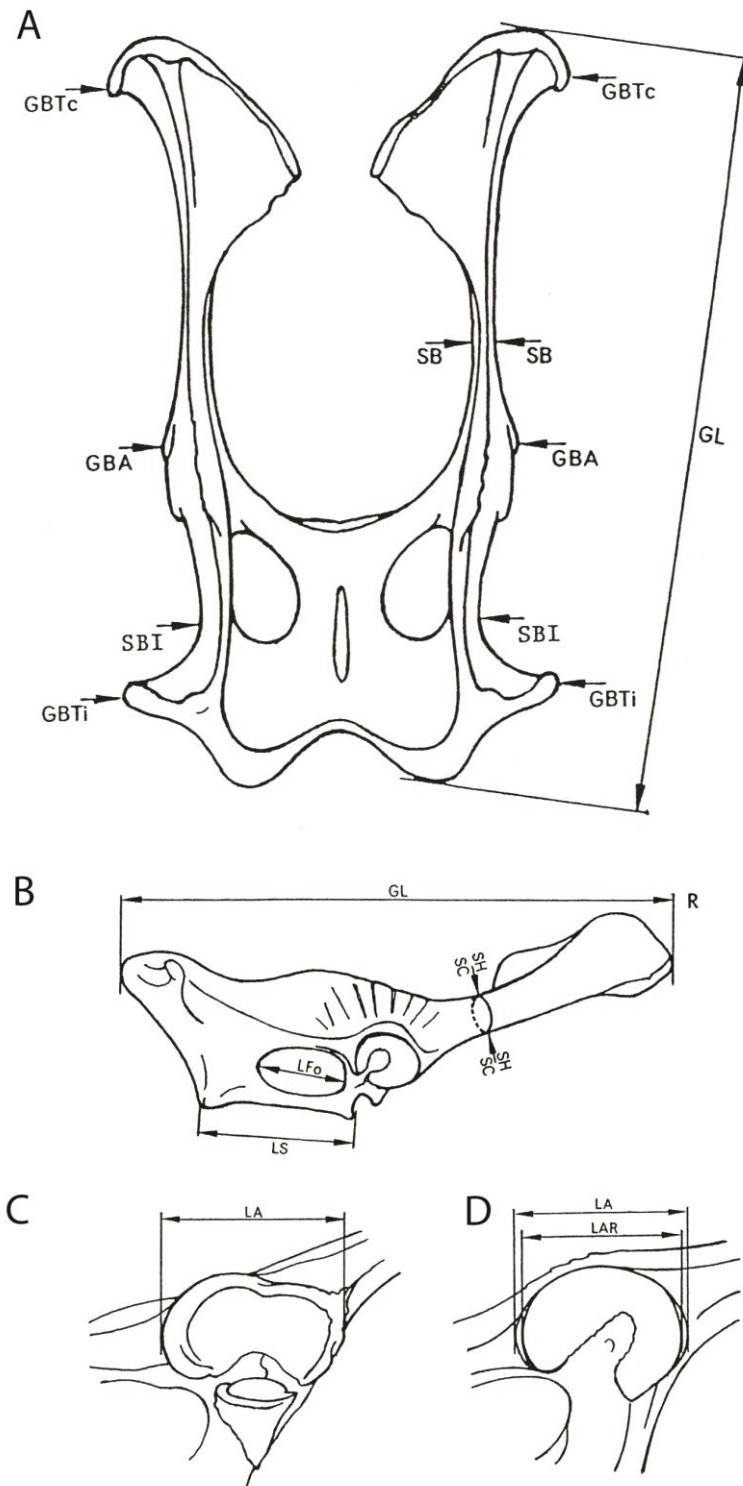


Figure 18. Methods of measurements for the pelvises (from von den Driesch, 1976): (A) pelvis of *Ovis* in dorsal view; (B) pelvis of *Sus* in lateral view; (C) acetabulum of *Bos*; (D) acetabulum of *Equus*. Abbreviations: L=left side and R=right side.

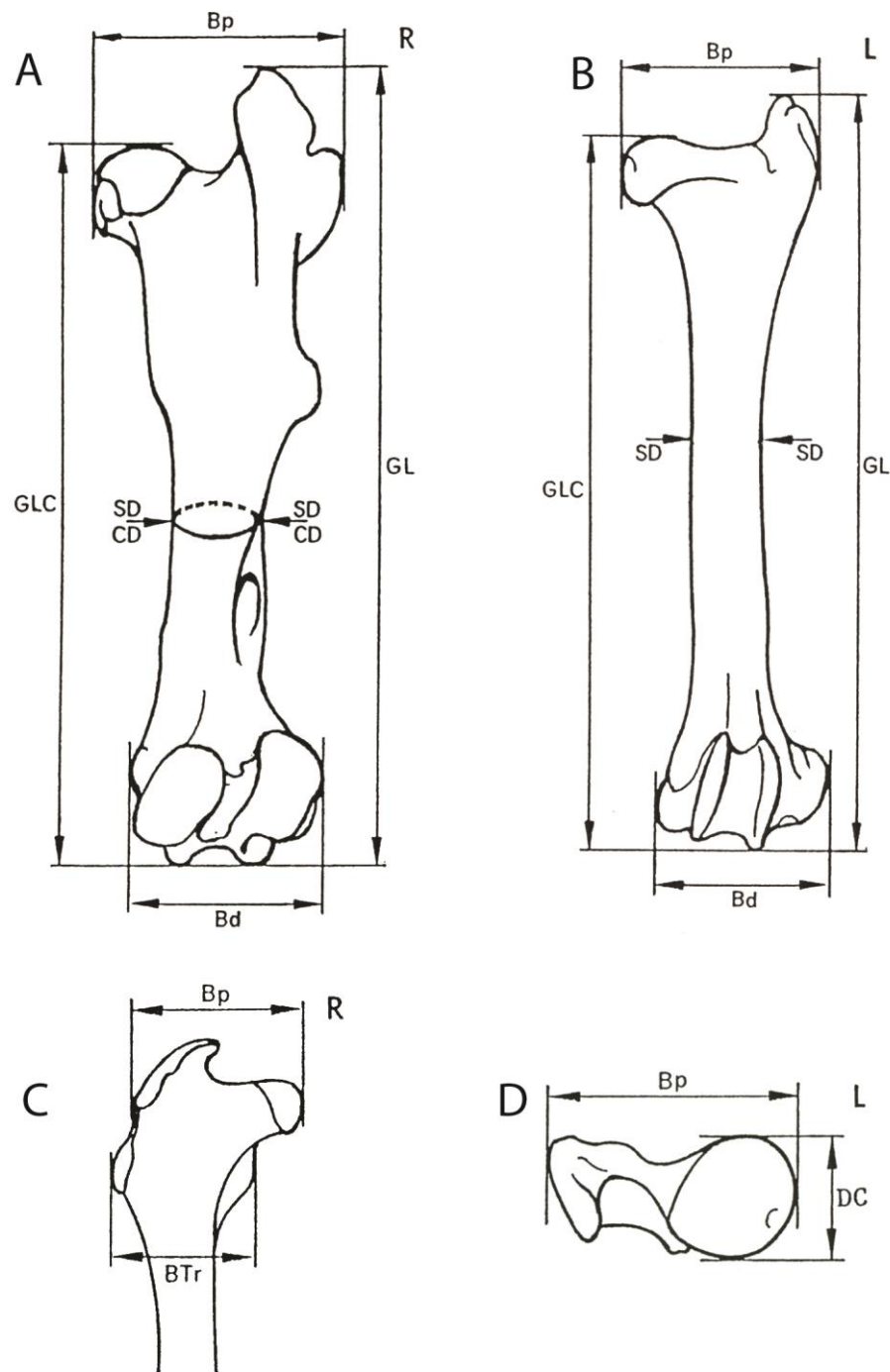


Figure 19. Methods of measurements for the femora (from von den Driesch, 1976): **(A)** femur of *Equus* in posterior view; **(B)** femur of *Ovis* in anterior view; **(C)** proximal femur of *Lepus* in anterior view; **(D)** femur of *Canis* in proximal view. Abbreviations: L=left side and R=right side.

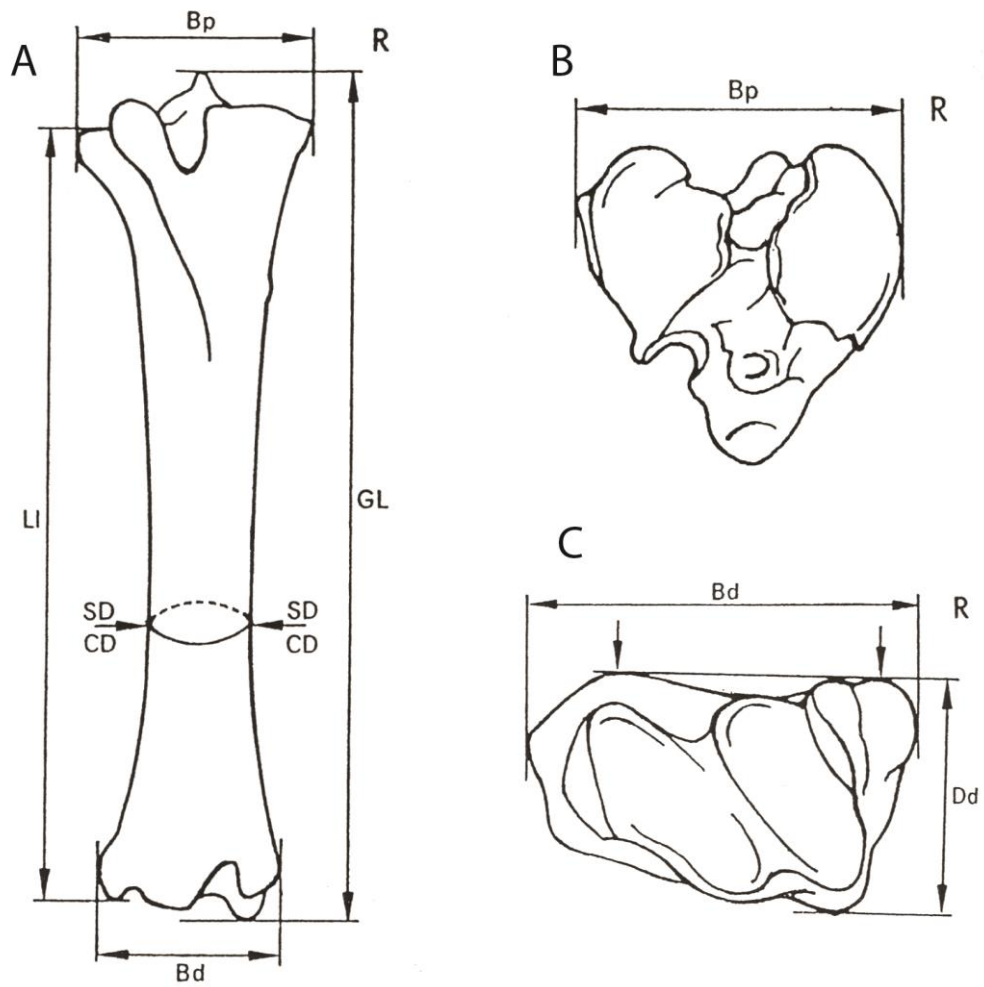


Figure 20. Methods of measurements for the tibiae (from von den Driesch, 1976): **(A)** tibia of *Equus* in anterior view; **(B)** tibia of *Capra* in proximal view; **(C)** tibia of *Equus* in distal view. Abbreviations: L=left side and R=right side.

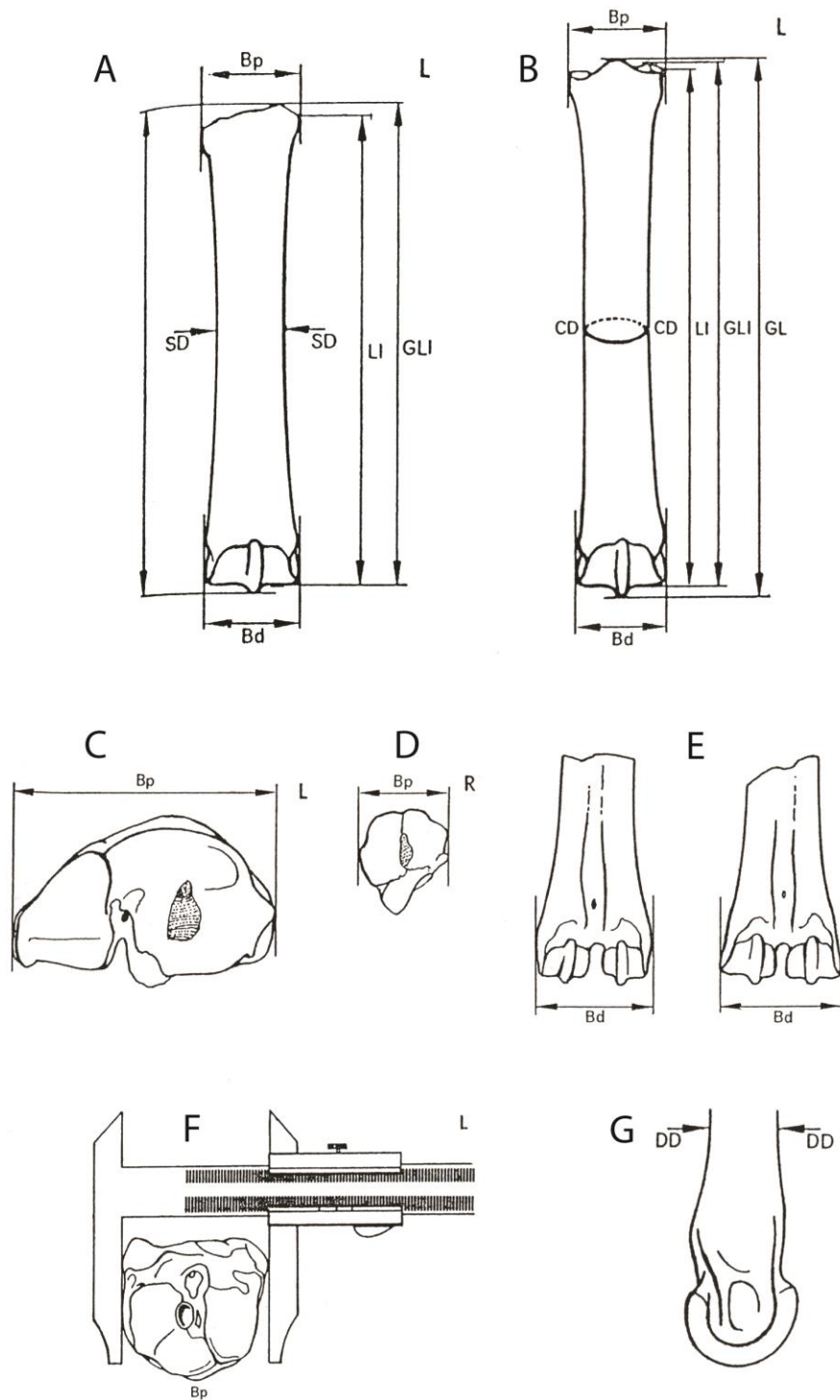


Figure 21. Methods of measurements for the metapodial bones (from von den Driesch, 1976): (A) metacarpus III of *Equus* in anterior view; (B) metatarsus III of *Equus* in anterior view; (C) metacarpus III+IV of *Bos* in proximal view; (D) metatarsus III+IV of *Ovis* in proximal view; (E) metatarsi III+IV of *Bos* in anterior view; (F) metatarsus III+IV of *Bos* in proximal view; (G) metatarsi III+IV of *Capra* in lateral view. Abbreviations: L=left side and R=right side.

Taxonomic study (identification, classification, and nomenclature)

To identify the mammals, cranial and dental remains are the most diagnostic features left from the fossil records. All complete and fragmentary specimens were compared with other related Pleistocene mammalian taxa (the holotype and all referred specimens) and with the living taxa (type specimens). Our analysis is confined to the species and generic levels, with possible subspecies determination. Taxa unassigned at higher than the generic levels were also included, whether the genus-species level identification of that taxon is limited due to the quantity and completeness of the preserved fossils. The identification of taxa is also supported by the morphological study of related postcranial skeletons. The family-level identification of postcranial remains of mammals is based on the atlases of France (2009) and Brown and Gustafson (2000). The taxonomic nomenclature of extant mammals follows Groves and Grubb (2011) for ungulates and the systems of the IUCN Red List of Threatened Species (IUCN, 2015) for primates, carnivores, elephants, and other vertebrates.

Dental nomenclatures

Dental characters are important in mammal taxonomy and systematic according to the fact that the mammalian fossil records largely consist of teeth, which show tremendous morphological diversity within and/or between the groups. The teeth also reveal sufficient variability in size and shape and are used as major classifying traits in subordinate taxa. To describe and compare tooth crown morphologies, we applied various and different dental nomenclatures for each group of mammals. The dental nomenclature follows Werdelin and Solounias (1991) for the hyaenids (Fig. 22), van den Bergh (1999) for the proboscideans (Fig. 23), Yan et al. (2014) for the rhinoceroses (Fig. 24), and van der Made (1996) for the suids (Fig. 25). The dental nomenclature for the ruminants is modified from Heintz (1970), Gentry et al. (1999), and

Bärmann and Rössner (2011) (for upper cheek teeth, see Fig. 26 and for lower cheek teeth, see Fig. 27).

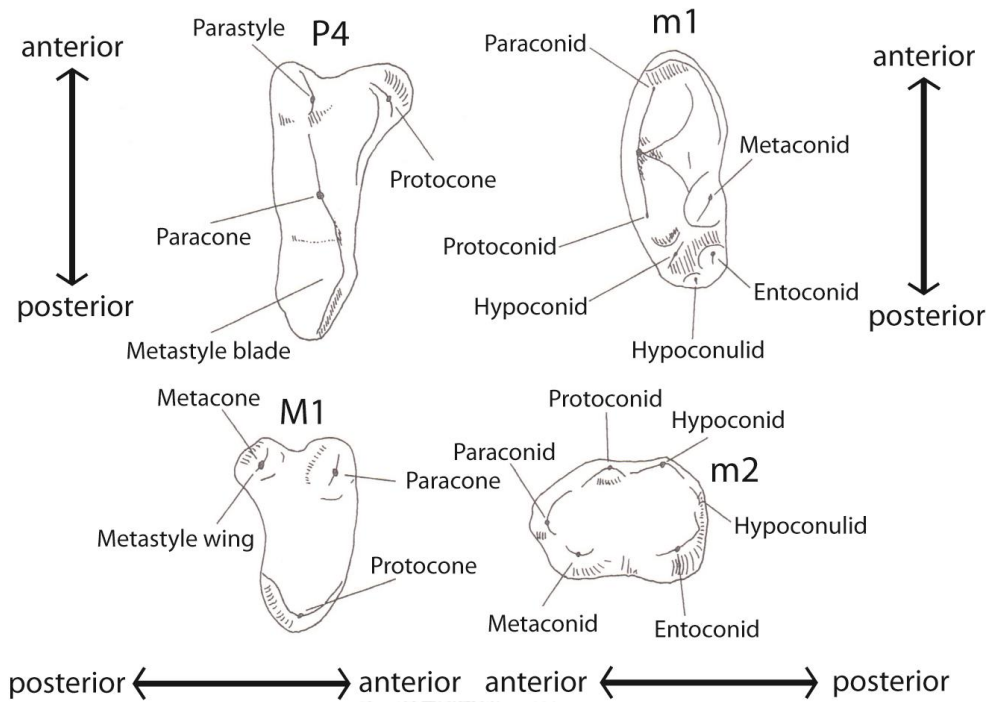


Figure 22. Dental nomenclatures of cheek teeth of hyaenids (modified from Werdelin and Solounias, 1991).

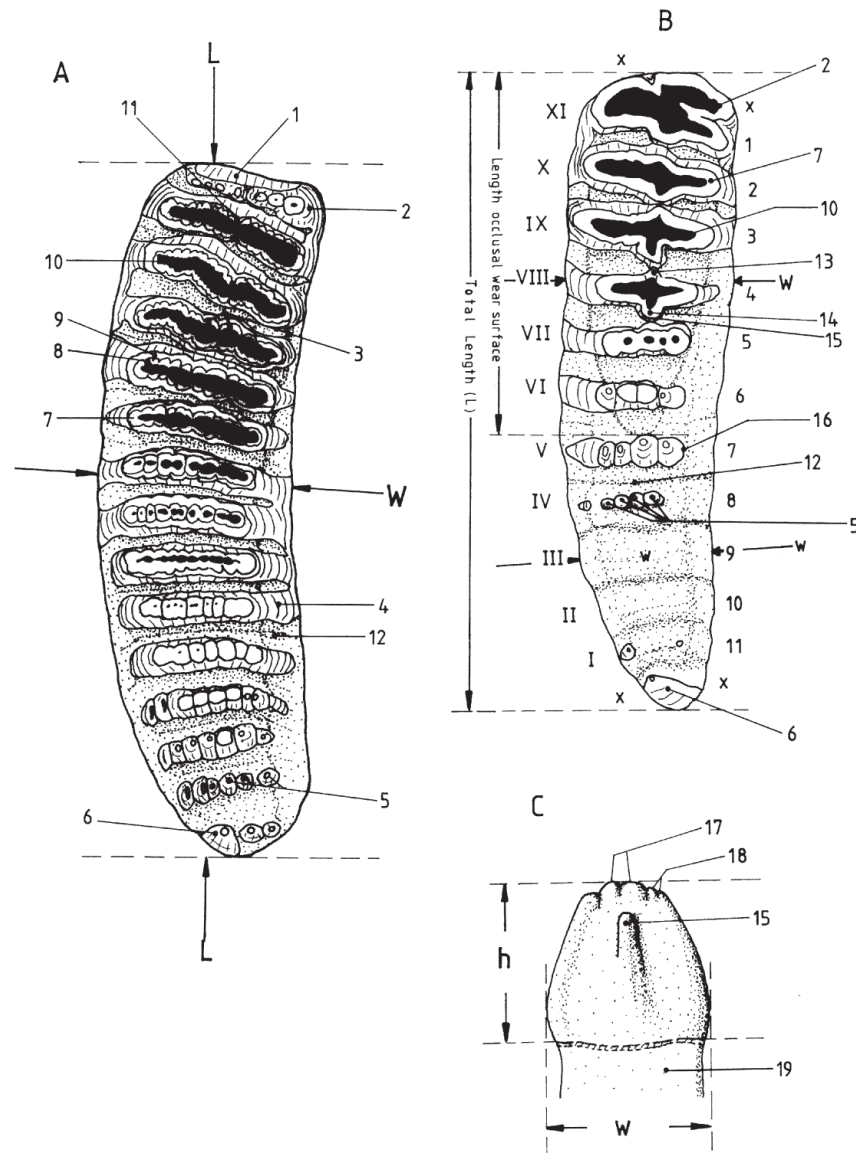


Figure 23. Dental nomenclatures of cheek teeth of Elephantoidea (from van den Bergh, 1999): (A) a lower molar of stegodontids in occlusal view; (B) a lower molar of elephantids in occlusal view; (C) a molar plate of elephantids in anterior view. Arabic and roman numbers indicate a sequence of molar ridges which are counted, starting from the anterior to posterior direction for the former and from the posterior to anterior direction for the latter. Abbreviations: L=maximum length; W=maximum width; w=maximum width of ridges; h=maximum height; 1=a contact facet with the preceding molar; 2= anterior half ridge; 3=double median expansions of enamel loop; 4=molar ridge; 5=apical digitations of molar ridges; 6=posterior half ridge; 7=complete enamel wear pattern or enamel loop of occlusal surfaces; 8=inner enamel layer; 9=outer enamel layer; 10=dentine; 11=median cleft or median sulcus; 12=transverse valley filled by cementum; 13=anterior median sinus of enamel loop; 14=posterior median sinus of enamel loop; 15=median pillar; 16=molar plate; 17=median digitations; 18=lateral digitations; 19=root.

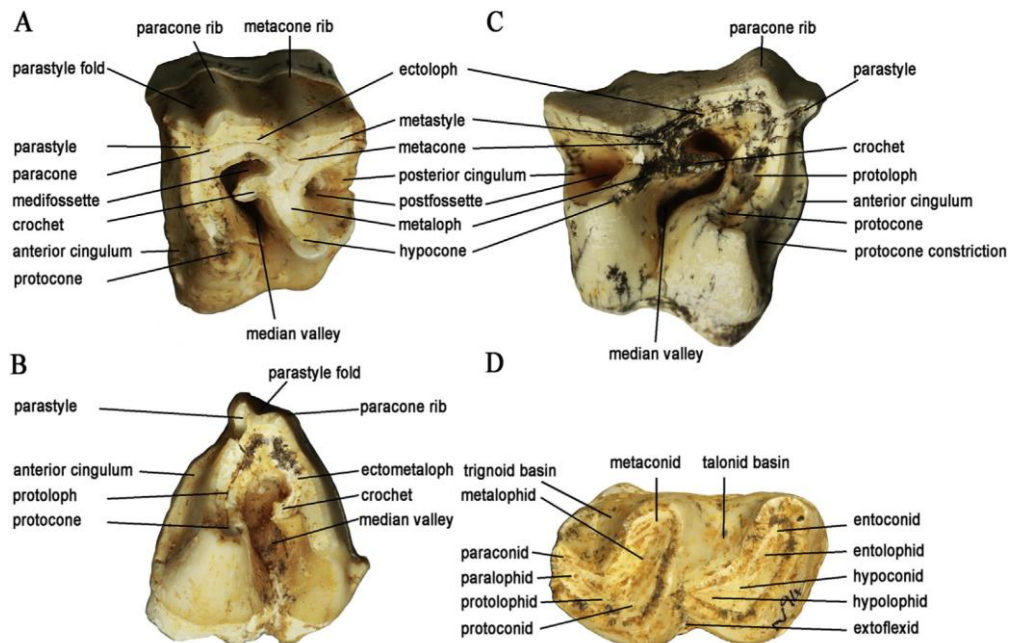


Figure 24. Dental nomenclatures of cheek teeth of rhinoceroses (from Yan et al., 2014): (A) upper left third premolar; (B) upper left third molar; (C) upper right first molar; (D) lower left second molar.

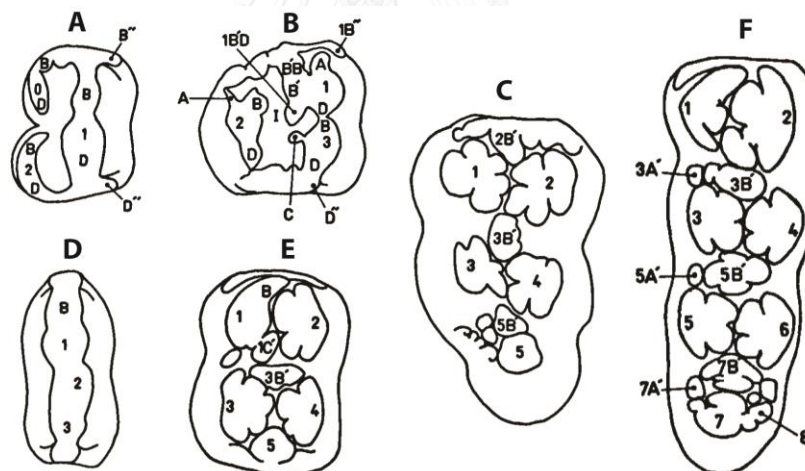


Figure 25. Dental nomenclatures of cheek teeth of suids (from van der Made, 1996): (A) upper left third promolar; (B) upper left fourth premolar; (C) upper left third molar; (D) lower left premolar; (E) lower left second molar; (F) lower left third molar. Legends: 0, primocone; 1, paracone/protoconid; 1B'', protoprestyle; 1B'D, postcrista of the protopreconule; 1'C, protoendoconulid; 2, protocone/metaconid; 2B', protopreconule; 3, metacone/hypoconid; 3A', hypoectoconulid; 3B', metapreconule/hypopreconulid; 4, tetracone/entoconid; 5, pentacone/pentaconid; 5A', pentaectoconulid; 5B', pentapreconule; 6, hexacone/hexaconid; 7, heptaconid; 7A', heptaectoconulid; 7B', heptapreconulid; 8, octaconid; A, ectocrista; B, precrista/precristid; B', preconule; B'', prestyle; B'B, precrista of the preconule; D, postcrista; D'', poststyle; I, protofossa.

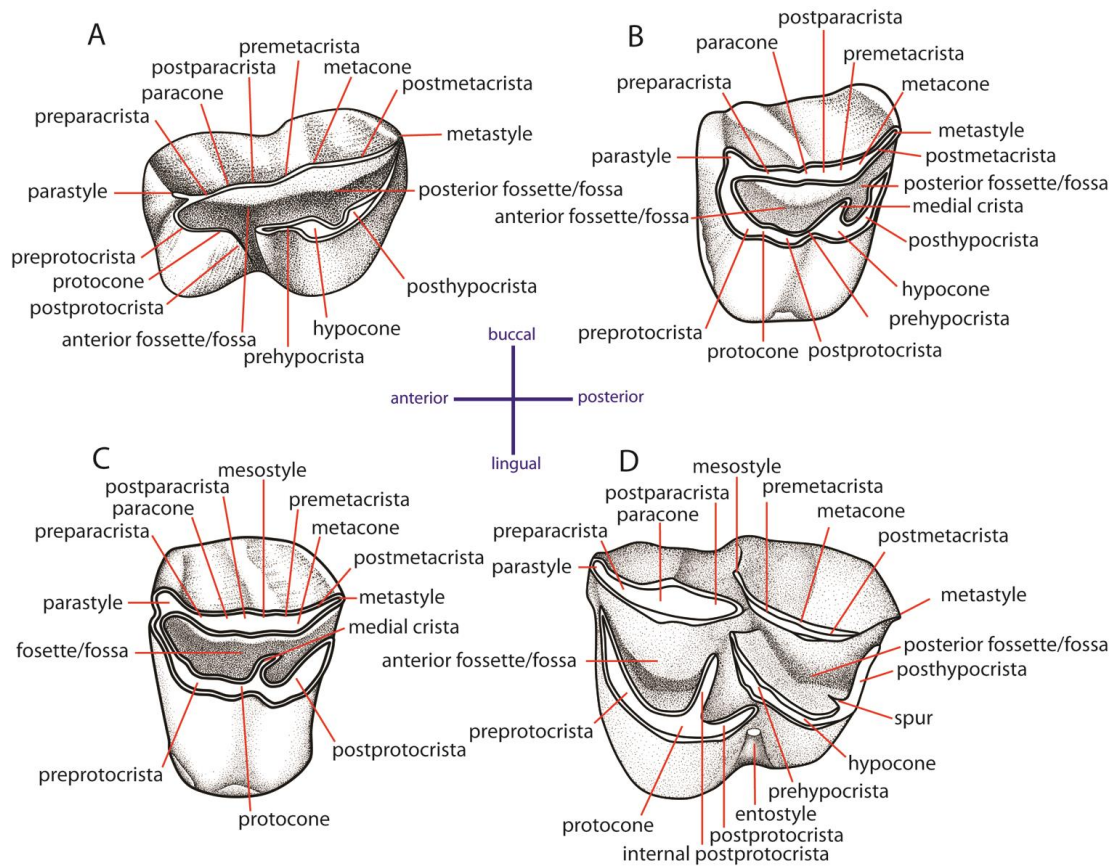


Figure 26. Dental nomenclatures of upper cheek teeth of ruminants: **(A)** upper second deciduous premolar; **(B)** upper third premolar; **(C)** upper fourth premolar; **(D)** upper third molar. The dental terminology is modified from Heintz (1970), Gentry et al. (1999) and Bärmann and Rössner (2011).

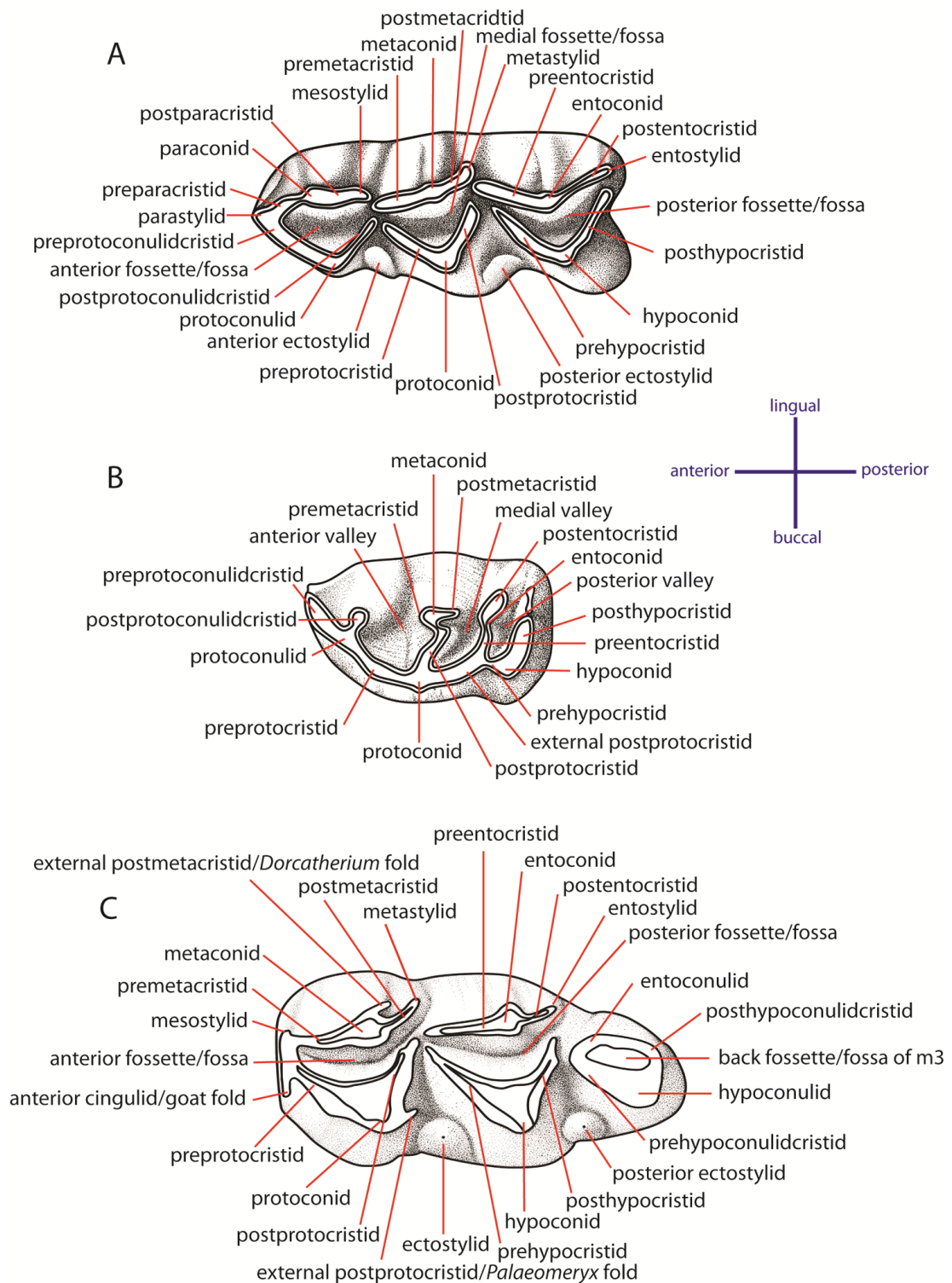


Figure 27. Dental nomenclatures of lower cheek teeth of ruminants: **(A)** lower fourth deciduous premolar; **(B)** lower fourth premolar; **(C)** lower third molar. The dental terminology is compiled from Heintz (1970), Gentry et al. (1999), and Bärmann and Rössner (2011).

3D geometric-morphometric analysis

Geometric morphometrics could be defined as the study of organism form, in two or three dimensional spaces, allowing in-depth investigation and comparison of morphological changes and addressing shape variation (Bookstein, 1982; Zelditch et al., 2004). The principal aims of the 3D geometric-morphometric analysis are to ensure that our taxonomic identification of the Khok Sung spotted hyaena is corrected, to examine the relationships between Khok Sung material and other hyaenid species, and to determine whether the cranial morphology can be used to make a distinction between fossil and recent hyaenid taxa. We assess that a geometric-based approach in cranial shape may provide more reliable and accurate discrimination among hyaenid taxa than that of an identification based on the dental morphology.

Samples and 3D scans

We sampled a total number of 35 undeformed crania of adult fossil and recent hyaenid taxa including *Crocuta crocuta ultima* (1 sample from Khok Sung), *Crocuta spelaea* (4 samples), *Crocuta crocuta* (19 samples), *Hyaena hyaena* (6 samples), and *Parahyaena brunnea* (5 samples). Sample details are listed in Table 2. The cranial surfaces were scanned with the Handyscan 3D laser scanner (EXAscan), following the protocol suggested by Fabre et al. (2013). The resolution of the surface scanner is medium with accuracy up to 30 microns. In order to obtain all the relevant information, each specimen was scanned twice in different direction: the dorsal and ventral surfaces. The two scanning surfaces were then merged into a single object in ScanStudioHD Pro (Next Engine Corporation) and exported into a PLY file. These data were subsequently imported into Geomagic Studio 2013 (Raindrop Geomagic Inc.), where the objects were aligned and fused into a single model of the whole specimen. The raw scanning data were transformed into three-dimensional polygonal surfaces. Some holes in the resulting mesh were filled using the GeoMagic hole-filling algorithm. The fossil specimen SMNS-19062 is incomplete,

preserving only a lateral half of the cranium (left side). This missing portion was reconstructed by creating a symmetry plane along the median longitudinal axis of the cranium and then mirror-imaging using the function in Geomagic software.

Table 2. Scanned hyaenid crania used for the 3D geometric-morphometric analysis.

Specimen	Species	Sex	Ontogenic stages
DMR-KS-05-04-2-1	<i>Crocuta crocuta ultima</i>	indet.	adult
SMNS-7.801	<i>Crocuta spelaea</i>	indet.	adult
SMNS-6617.7.3.62.1	<i>Crocuta spelaea</i>	male	adult
SMNS-19062	<i>Crocuta spelaea</i>	indet.	adult
SMNS-AH-248	<i>Crocuta spelaea</i>	indet.	adult
MNHN-ZMO-1894_54	<i>Crocuta crocuta</i>	indet.	adult
MNHN-ZMO-1901-662	<i>Crocuta crocuta</i>	indet.	adult
MNHN-ZMO-1910-162	<i>Crocuta crocuta</i>	male	adult
MNHN-ZMO-1936-656	<i>Crocuta crocuta</i>	indet.	adult
MNHN-ZMO-1947-7	<i>Crocuta crocuta</i>	male	adult
MNHN-ZMO-1962-1537	<i>Crocuta crocuta</i>	indet.	adult
MNHN-ZMO-1972-399	<i>Crocuta crocuta</i>	indet.	adult
MNHN-ZMO-1996-2514	<i>Crocuta crocuta</i>	indet.	adult
NMW-5584	<i>Crocuta crocuta</i>	indet.	adult
NMW-7393	<i>Crocuta crocuta</i>	indet.	adult
SMNS-2655	<i>Crocuta crocuta</i>	indet.	adult
SMNS-4457	<i>Crocuta crocuta</i>	male	adult
SMNS-4458	<i>Crocuta crocuta</i>	female	adult
SMNS-4543	<i>Crocuta crocuta</i>	female	adult
SMNS-8058	<i>Crocuta crocuta</i>	indet.	adult
SMNS-8060	<i>Crocuta crocuta</i>	male	adult
SMNS-18982	<i>Crocuta crocuta</i>	indet.	adult
SMNS-30161	<i>Crocuta crocuta</i>	indet.	adult
SMNS-31174	<i>Crocuta crocuta</i>	indet.	adult
MNHN-ZMO-1962-1531	<i>Hyaena hyaena</i>	indet.	adult
MNHN-ZMO-1938-87	<i>Hyaena hyaena</i>	indet.	adult
MNHN-ZMO-2000-1267	<i>Hyaena hyaena</i>	indet.	adult
MNHN-ZMO-2005-423	<i>Hyaena hyaena</i>	male	adult
GPIT-ME-6474	<i>Hyaena hyaena</i>	indet.	adult
NMW-1756	<i>Hyaena hyaena</i>	indet.	adult
NMW-31570	<i>Parahyaena brunnea</i>	female	adult
ZSM-1901-3011	<i>Parahyaena brunnea</i>	indet.	adult
ZSM-1901-3012	<i>Parahyaena brunnea</i>	indet.	adult
ZSM-1949-1113	<i>Parahyaena brunnea</i>	indet.	adult
ZSM-2008-0020	<i>Parahyaena brunnea</i>	indet.	adult

Landmark acquisition

We captured the 3D coordinates from 17 osteological landmarks on the lateral and ventral surfaces of the crania (Fig. 28 and Tab. 3). The landmarks plotted on the surfaces were positioned, using Landmark Editor V3.0 Software (Wiley et al., 2005), by one person (K. Suraprasit). The landmarks on each sample were selected to be homologous through all specimens (Martin, 1988). In order to remove non-shape variation (size and orientations of the landmark configurations), all landmark coordinates were processed using Generalized Procrustes analysis (GPA). This analysis superimposes multiple landmark configurations by translating them into a common origin, scaling them to unit Centroid size, and rotating them into a uniform orientation according to a least-squares criterion. The new coordinates provide the residual geometric information of which the size effect is minimized. Therefore, subsequent analyses would focus solely on the shape differences between specimens.

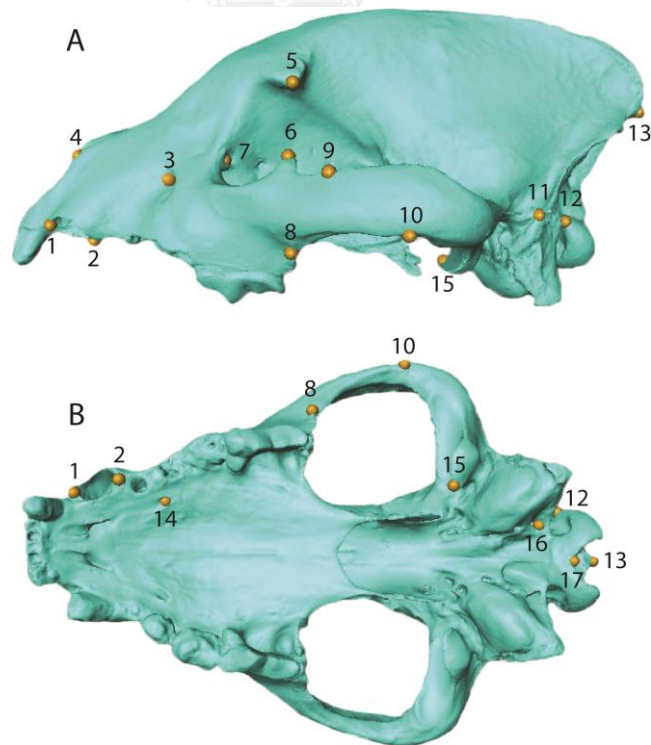


Figure 28. Landmarks digitized in lateral (A) and ventral (B) views (for anatomical description, see table 3).

Table 3. Cranial landmarks used in this study. Numbers correspond to the landmark illustrated in Figure 28.

Lateral landmarks (left side)	
1	Anteriomost point of the canine
2	Posteriormost point of the canine
3	Anteriomost point on the infraorbital foramen
4	Anteriomost point on the nasal-premaxilla suture
5	Tip of the postorbital process on the frontal bone
6	Tip of the postorbital process on the jugal bone
7	Uppermost point of the lacrimal foramen
8	Posterior edge of the premaxilla-jugal suture
9	Upper edge of the jugal-squamosal suture
10	Ventral edge of the jugal-squamosal-suture
11	Lateralmost point of the mastoid process
12	Uppermost point on the occipital condyle
Midline landmarks	
13	Posterior end of the nuchal crest
17	Anteriomost point on the foramen magnum
Ventral landmarks	
14	Anteriomost point of the anterior palatine foramen
15	Medial edge of the glenoid process
16	Medial edge of the jugular foramen

Statistical analyses

The principal component analysis (PCA) was carried out to explore the affinities of the Khok Sung hyaenid cranium with other fossil and recent hyaenas, as well as their ranges of cranial morphological variation. This procedure transforms the raw data into a set of scores on linearly uncorrected principal components. The first principal component (PC1) possesses the largest possible variance and accounts for the greatest amount of the variability in the data (Jackson, 1991). Images of hypothetical skulls related to extreme positions on the first and two principal components (relative warp scores) were illustrated as wireframes for visualizing the shape transitions (Gunz and Harvati, 2007; Mitteroecker and Gunz, 2009). All geometric-morphometric

analyses were done by MorphoJ software (Klingenberg, 2011). Centroid size, which is a proxy of the overall cranial size, between fossil and recent hyaenid taxa was compared, using Kruskal-Wallis one-way analysis of variance as implemented in SPSS software (V. 21).

Species composition and distribution analyses

The mammalian faunal list from this site was documented and the diversified fossil fauna was considered as the sample of the Middle Pleistocene mammalian community in Southeast Asia. The faunal lists of Southeast Asian mammals were compiled using the published literatures (e.g., van den Bergh et al., 2001; Louys et al., 2007) and atlases of mammalian distribution (Lekagul and McNeely, 1988; Corbet and Hill, 1992; Nowak, 1999), as principle faunal records of fossil and recent taxa, respectively. The zoogeographical distribution ranges of Khok Sung mammalian taxa were also documented. The Khok Sung mammalian assemblage was compared with other Pleistocene faunas from China and Southeast Asia (Indochinese and Sundaic provinces), in terms of the faunal composition and paleoenvironments.

Faunal similarity measures and cluster analysis

We compared differences in species composition of Southeast Asian large mammal fauna during the Middle Pleistocene, using an analysis of the faunal similarity. According to unequal sampling conditions for our data, we applied two criteria for undertaking this analysis: localities are disqualified when they have fewer than 10 taxa identified at the species level and taxa are excluded when their appearances are still doubtful (i.e. poor taxonomic description or identification). We therefore selected Simpson's Faunal Resemblance Index (FRI) because it has the smallest influence of sample size and emphasizes faunal resemblance (Simpson, 1943, 1960). When fauna lists in several localities differ evidently in size, the Simpson's FRI is the most useful

tool for eliminating the effect of size differences between two faunas, compared to other indices (Simpson, 1960). The Simpson's FRI is also applied for analysing faunal resemblances of vertebrate fossil records (e.g., Tsubamoto et al., 2004; Travouillon et al., 2006; Grossman et al., 2014). The formula of Simpson's FRI is expressed as $FRI (\%) = (N_c / N_1) \times 100$, where N_c is the number of identified taxa shared by two faunas and N_1 is the number of identified taxa in the smaller of the two faunas (Simpson, 1960). A higher score indicates a greater similarity between the faunas. We performed a dataset, transformed into a similarity matrix, to generate the dendrogram using the "PAST" statistical software version 1.61 (Hammer et al., 2001). We selected an Unweighted Pair-Group Method with Arithmetic Mean (UPGMA) as cluster algorithms for our analysis because the dendrogram represents higher values of cophenetic correlation coefficient compared to the others.

Body mass estimation and cenogram analysis

We estimated the body mass of Khok Sung ungulates in order to demonstrate size differences or similarities between Pleistocene and extant mammalian taxa. The body mass of ruminants was estimated, using the equations of Janis (1990) based on the $M2/m2$ surface area ratio. The surface area of $M2/m2$ used here is the best body mass predictor according to the high correlations with the body mass for bovids ($r^2 > 0.93$) and cervids ($r^2 > 0.95$) (Janis 1990: table 16.8). The body mass of suids was predicted based on the allometric equations of Janis (1990), using the length of $m2$ (regressions for all ungulates: $r^2 > 0.94$). The body mass estimation of rhinoceroses follows Damuth (1990) by using the molar row length for the regressions of all ungulates ($r^2 > 0.93$). The length and circumference of the femur and humerus were used to estimate the body mass of stegodontids because they represent a higher correlation than that of tooth (Roth, 1990). In case of the poor preservation of molars, the body mass of Khok Sung

Elephas sp. has been defined based on the average weight of relative present-day species (i.e. *Elephas maximus*, Sreekumar and Nirmalan (1989)).

The body mass distribution of 12 ungulate taxa from Khok Sung has been examined, using a cenogram analysis (Fig. 29). The cenogram method has been developed by Legendre (1986, 1989). This method describes the body mass distribution of herbivorous and insectivorous species in the mammalian community. Studies of extant faunas have demonstrated that this distribution is closely linked to the environments (Legendre, 1986, 1989). A cenogram method is generated by plotting the logarithm of the average body mass of each species in the community on the Y-axis, and the species rank in a decreasing order of sizes on the X-axis, allowing the recognition of 4 types of environmental (open or closed) and climatic (arid or humid) conditions. The successive distribution of the body mass reveals a characteristic of forested habitats. In open-landscape faunas, the lack of medium weight species (with a body weight between 500 g and 8 kg) is observed. The abundance of large species (body weight over 8 kg) characterises humid conditions, whereas the deep slope represents arid environments. Although this method is still under discussion, it has been extensively applied for many fossil faunas (e.g., Croft, 2001; Montuire and Marcolini, 2002; Travouillon and Legendre, 2009).

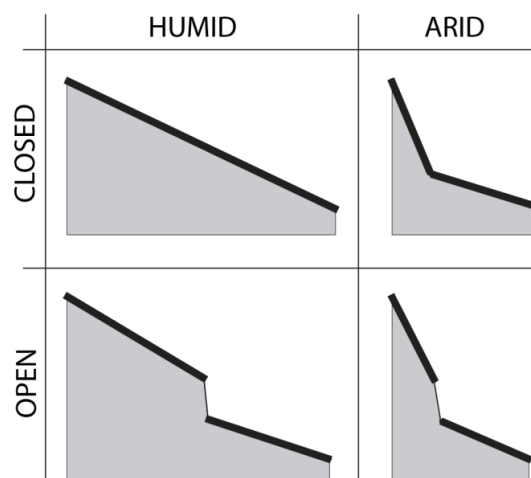


Figure 29. Schematic representation of categories of cenograms (after Legendre, 1989).

CHAPTER 5

Results and discussion

The study results are divided into five main parts: the taxonomic attribution of each vertebrate taxon, the species composition of the Khok Sung fauna, the individual species distribution patterns, the faunal comparisons between Khok Sung and other Pleistocene assemblages, and the cenogram analysis based on the body mass distribution of Khok Sung mammals.

Taxonomic study

Systematic paleontology

Class MAMMALIA Linnaeus, 1758

Order PRIMATES Linnaeus, 1758

Suborder HAPLORRHINI Pocock, 1918

Family CERCOPITHECIDAE Gray, 1821

Genus *Macaca* Lacépède, 1799

Macaca sp.

Referred material: a right tibia, DMR-KS-05-04-04-1

Material description

The right tibia is complete (Fig. 30A–D) and elongated (for measurements, see Tab. A1). On the proximal articular surface, the medial condyle is as large as the lateral one. The lateral condyle is convex anteroposteriorly (Fig. 30C). The posteromedial margin of the lateral condyle lacks a notch that indicates a single meniscus attachment. At the proximal end, the tibial

tuberosity is developed. The shaft is elongated, anteriorly and laterally bowed, and not anteroposteriorly compressed (Fig. 30A, B). Distally, the trochlear surface is trapezoid in outline (Fig. 30D). The medial malleolus is well-developed and projects more anteriorly than posteriorly. The medial and lateral parts of the trochlear surface are equally separated by a weak median keel.

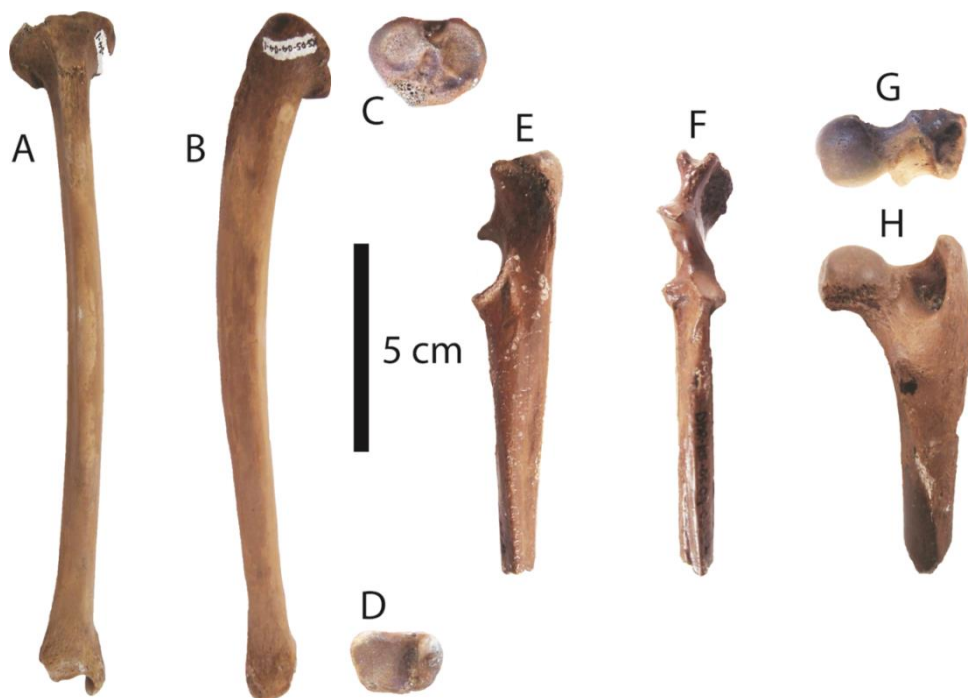


Figure 30. Postcranial remains of *Macaca* sp. (A–D) and *Cuon* sp. (E–H) from Khok Sung: (A–D) DMR-KS-05-04-04-1, a right tibia in anterior (A), medial (B), proximal (C), and distal (D) views; (E–F) DMR-KS-05-04-11-34, a right ulna in medial (E) and anterior (F) views; (G–H) DMR-KS-05-04-28-13, a right femur in proximal (G) and posterior (H) views.

Taxonomic remarks and comparisons

Tibial morphology is relatively conservative within and among primates. Particularly, the morphological differences of tibiae among cercopithecoids are minimal (Turley et al., 2011). The distal part of tibiae of arboreal primates (*Hylobates* and all arboreal cercopithecoids) is characterized by more rounded borders of the trochlear surface and a convex proximal border of the medial malleolus joining the trochlear surface (Tallman et al., 2013). The specimen DMR-KS-

05-04-04-1 shows typical characters of the recent cercopithecoids whose tibial shaft is less mediolaterally compressed than those of great apes. However, the tibia from Khok Sung represents compatible dimensions with the tibiae of *Hylobates* (gibbon), *Presbytis* (surili), and *Macaca* (macaque). We suggest here to make distinction between these genera based on the ratios of the greatest length of the tibia to the length or width of the proximal tibia (GL/Bp or GL/Dp). Based on these indices, the Khok Sung tibia falls within the range of recent *Macaca* (Tab. 4). According to the ratios, the shaft of both the surilis and gibbons is more elongated, compared to that of macaques. The distal tibia of DMR-KS-05-04-04-1 also shares some additional characters with that of macaques such as the poorly developed ball-shaped convexity and -articular facet (Sondaar et al. 2006) and the shape of the trochlear surface (Tallman et al., 2013: fig. 5). We therefore attribute this material to *Macaca* sp.

Table 4. Ratios of the greatest lengths of tibiae (GL) to the lengths and widths of proximal and distal tibiae (Bp, Dp, Bd, and Dd) of Khok Sung macaques compared to recent Southeast Asian primates.

	DMR-KS-05-04-04-1	<i>Presbytis</i> (N=30)			<i>Hylobates</i> (N=24)			<i>Macaca</i> (N=71)		
		Max	Min	Mean	Max	Min	Mean	Max	Min	Mean
GL/Bp	6.09	7.70	6.76	7.29	7.52	6.06	7.01	6.56	4.55	5.61
GL/Dp	7.81	9.89	8.15	9.07	9.95	7.96	9.43	9.62	6.36	7.67
GL/Bd	9.25	12.38	10.26	11.37	14.49	9.01	11.31	10.84	7.20	8.79
GL/Dd	12.94	16.21	12.75	14.13	16.79	10.94	14.50	12.77	7.69	10.78

Order CARNIVORA Bowdich, 1821

Family HYAENIDAE Gray, 1869

Genus *Crocota* Kaup, 1828

Crocota crocota ultima (Matsumoto, 1915)

Referred material: DMR-KS-05-04-2-1, a sub-complete cranium with left and right tooth rows (P1–P4) associated to a right mandible (i2, c1, and p2–p4)

Material description

Cranium and upper dentition: the cranium DMR-KS-05-04-2-1 is well-preserved and undeformed, lacking only most of the premaxillar portion broken away from the maxilla at the level of premaxilla-maxilla suture (Fig. 31A–C). This specimen displays prominent sagittal and supramastoid crests. The mastoid crest is long as compared to *Hyaena hyaena* and continues towards the ventral end of the external auditory meatus. The zygomatic arches are prominent (Fig. 31A). The lateral wings of the premaxilla are divergent in both dorsal (Fig. 31A) and anterior views. The internal of auditory bullae are exposed, showing two auditory chambers for each side. The anterior margin of orbits is situated above the anterior extremity of P4. The premaxilla-maxilla suture on the palate is located at the postero-lateral margin of the incisive fossa (Fig. 31B) but is positioned on the incisive fossa for *Hyaena hyaena*. The basioccipital is flat and displays two low lateral ridges and a small longitudinal groove at the central portion (Fig. 31B). The palatine foramina are well-preserved and positioned about 2 cm anterior to the palate-maxilla suture (Fig. 31B). The palatine margin ends at the level of P4 in ventral view. The maxilla-jugal sutures are straight in lateral view. Three foramina are well-preserved and aligned dorsoventrally in the wall of the orbits: the optic canal, the orbital fissure, and the foramen rotundum (Fig. 31C). The infraorbital canal is located above the central portion of P3 (Fig. 31C). The lacrimal foramen and sphenoid foramen are present. The latter is separated from the postpalatine foramen (Fig. 31D). The inferior oblique muscle fossa at the maxilla-lacrimal suture is small (Fig. 31D), similar to that of *Hyaena hyaena* (Werdelin and Solounias, 1991).

Only the sockets for I3 and C1 are preserved, I3 being presumably larger than other incisors as deduced from its larger socket (for measurements of teeth, see Tab. 5). The upper canines show oval-shaped alveoli (Fig. 31G). Most of upper premolars are slightly worn with the exception of P1 being unworn (Fig. 31G). The P1 is peg-like, bearing a single root, and is much

smaller than the others. The P2 is apparently smaller and lower-crowned than the P3. Both show posterior accessory cusps, but no anterior ones, and distinct ridges at the anterolingual side. This ridge runs from the base of the crown up to the central cusp. The posterior part of P2 and P3 is wider than the anterior one. The P3 is robust and pyramidal. The P4 is the longest tooth characterized by the sharp edges of the protocone, parastyle, paracone and metastyle blade (for measurements of upper carnassial blades, see Tab. 6). The protocone is situated very slightly more anteriorly than the parastyle in occlusal view. The parastyle is as high as the metastyle blade. In occlusal view, crests of the parastyle, paracone, and metastyle blade run along the anteroposterior midline of the tooth, starting at the anterolabial corner and ending at the posterolabial one (Fig. 31G).

Mandible and lower dentition: the right hemi-mandible (DMR-KS-05-04-2-1) preserves i2, c1, and p2-m1 (for measurements of teeth, see Tab. 5). The dentary is intact except the posterior part of the coronoid and angular processes which are slightly broken (Fig. 31E, F). The outline of the symphysis is asymmetrical and inverted heart-like (Fig. 31E). A single mental and mandibular foramen are present, the former located at mid-depth of the jaw and below the mid-point of p2 (Fig. 31E, F). The depth of the corpus increases posteriorly. In occlusal view, the tooth row is concave lingually (Fig. 31H). All lower teeth are slightly worn with the exception of the m1 which is unworn.

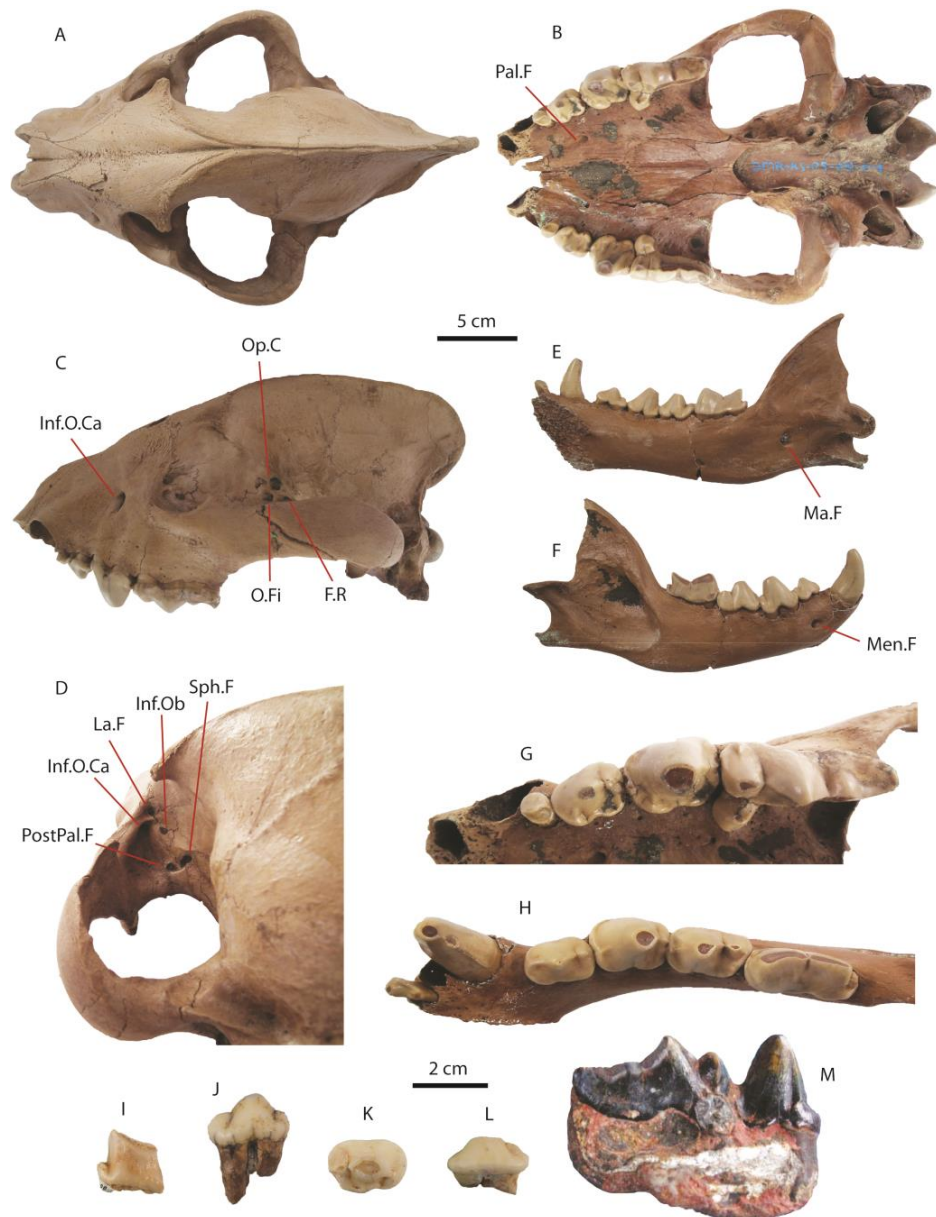


Figure 31. Remains of *Crocuta crocuta ultima* from Thailand. **(A–H)** material from Khok Sung, Nakhon Ratchasima province (northeastern Thailand)—DMR-KS-05-04-2-1: a cranium in dorsal **(A)**, ventral **(B)**, lateral **(C)**, and posterolateral **(D)** views; a right mandible in mesial **(E)** and lateral **(F)** views; an upper left tooth row on occlusal **(G)** view a right tooth row in occlusal **(H)** view, **(I–L)** material from Thum Wiman Nakin—TF-3400: a half right fragmentary m1 in labial **(I)** view; TF-3762: a right p2 in labial **(J)** view; TF-3974: a left p2 in occlusal **(K)** and lingual **(L)** views, and **(M)** material from Thum Phedan, a right fragmentary mandible with P3 and P4 in lingual view. Only the image **D** is not scaled. Abbreviations: **Pal.F**—palentine foramen; **Inf.O.Ca**—infraorbital canal; **Op.C**—optic canal; **O.Fi**—orbital fissure; **F.R**—foramen rotundum; **Sph.F**—sphenoid foramen; **Inf.Ob**—inferior oblique muscle (fossa); **La.F**—lacrimal foramen; **PostPal.F**—postpalatine foramen; **Ma.F**—mandibular foramen; **Men.F**—mental foramen.

Table 5. Dental measurements (L, length and W, width) of Thai *Crocota crocuta ultima* including Khok Sung (DMR-KS-05-04-2-1), Thum Phedan (Yamee and Chaimanee, 2005), and Thum Wiman Nakin (Thai fossil-numbers (TF); Tougard, 1998) specimens. The blade width of upper carnassials is abbreviated as “Wbl”.

Specimen no.		L	W	
		(mm)	(mm)	
Upper dentition				
DMR-KS-05-04-2-1	P1 (right)	6.33	7.57	
	P2 (right)	16.86	12.18	
	P3 (right)	20.65	15.99	
	P4 (right)	37.86	21.08	12.25
	P1 (left)	6.46	7.21	
	P2 (left)	16.85	13.49	
	P3 (left)	21.92	16.01	
	P4 (left)	37.46	20.72	12.21
Thum Phedan specimens	P3 (right)	19.68	15.76	
	P4 (right)	37.55	19.60	?
TF 3901	i2 (right)	6.10	9.00	
TF 3762	P2 (right)	17.50	10.60	
TF 3974	P2 (left)	18.00	12.30	
Lower dentition				
DMR-KS-05-04-2-1	i2 (right)	7.59	4.58	
	c1(right)	15.22	12.61	
	p2 (right)	17.17	11.77	
	p3 (right)	21.21	14.22	
	p4 (right)	22.98	12.68	
	m1 (right)	29.70	11.96	
TF 3400	m1 (right)	-	9.30	

The i2 is spatulate-shaped in occlusal view but triangular-shaped in lateral view. The i2 is apparently intermediate in size between i1 and i3 (the largest), as deduced from the size of their

respective sockets. The canine is robust and oval-shaped in cross-section. The longitudinal axis of the canine is oriented obliquely to the jugal tooth row on an anterolabial-posterolingual axis (Fig. 31H). The canine displays two ridges connecting the tip and the base of the crown on the anterolingual and posterolingual sides of the tooth. The p2 has a small posterior accessory cusp but no anterior accessory cusp (Fig. 31H). It is apparently smaller than p3 and p4 but is not relatively reduced in size. The p3 is slightly larger than the p4 and is characterized by a small posterior accessory cusp but no anterior one. The p4 displays anterior and posterior accessory cusps, the latter being larger, as well as a wide posterior cingulum. The m1 is dominated by a long and high paraconid relative to the protoconid, and a reduced talonid basin. The talonid is unicuspid, unlike *Hyaena hyaena* in which the hypoconid and entoconid are present. The metaconid is weak and is situated close to the posterolingual border of the paraconid.

Table 6. Measurements of upper carnassials of *Crocuta crocuta ultima* from Khok Sung in Thailand (DMR-KS-05-04-2-1), Phnom Loang in Cambodia (PNL 179; Beden and Guérin, 1973) , Xianrendong in South China (V05234.19 and V05198.3), and Penghu Channel in Taiwan (CJ-0038 and HL-0001; Tseng and Chang, 2007), see Fig. 10 for the abbreviations of metrical parameters.

Upper carnassials (P4)				
Specimen no.		Lps (mm)	Lpc (mm)	Lms (mm)
DMR-KS-05-04-2-1	right	8.35	13.64	17.22
	left	7.61	14.39	16.23
PNL 179	right	7.40	14.70	18.10
V05234.19	left	9.69	14.95	15.58
V05198.3	right	7.56	16.16	18.61
CJ-0038	left	8.62	14.92	18.16
HL-0001	left	10.49	14.51	20.12

3D geometric-morphometric analysis of fossil and recent hyaenid crania

To quantify the differences between fossil and recent hyaenid cranial morphologies and to explore the cranial variation for each hyaenid taxon, we applied a geometric-morphometric approach based on 3D landmarks to their crania.

Size differences between hyaenid taxa

Based on the cranial dataset, centroid size values for each hyaenid species are given in Fig. 32. Cranial sizes show statistically significant differences between fossil and recent samples (Kruskal-Wallis, $p=0.002$). The Khok Sung spotted hyaena, *C. c. ultima*, has a medium-sized cranium compared to other species. It is placed within the ranges of variation for recent *C. crocuta* but outside the ranges for the other species. The fossil samples of *C. spelaea* are clearly larger than Khok Sung *C. c. ultima*, *H. hyaena*, and *P. brunnea*, but overlap with upper tier samples of recent spotted hyaenas.

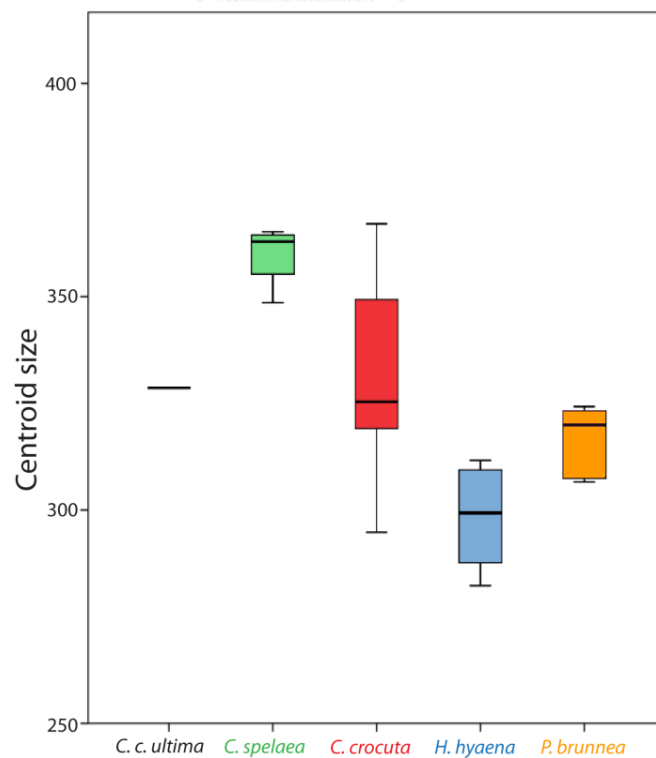


Figure 32. Box plot showing centroid sizes of fossil and recent hyaenid taxa. Each box plot shows the median, first and third quartiles, and maximum and minimum values for the species.

Shape differences between hyaenid taxa

The first two principal components (PC1 and PC2) based on recent and fossil hyaenid crania account for 39% of the total shape variation (Fig. 33). They therefore provide a considerable estimation of the total variation because no other PCs account for more than 10%. The first and second axes of the PCA represent 26.32% and 12.68% of the variance, respectively. The percentage of variance of the third axis is 9.31%.

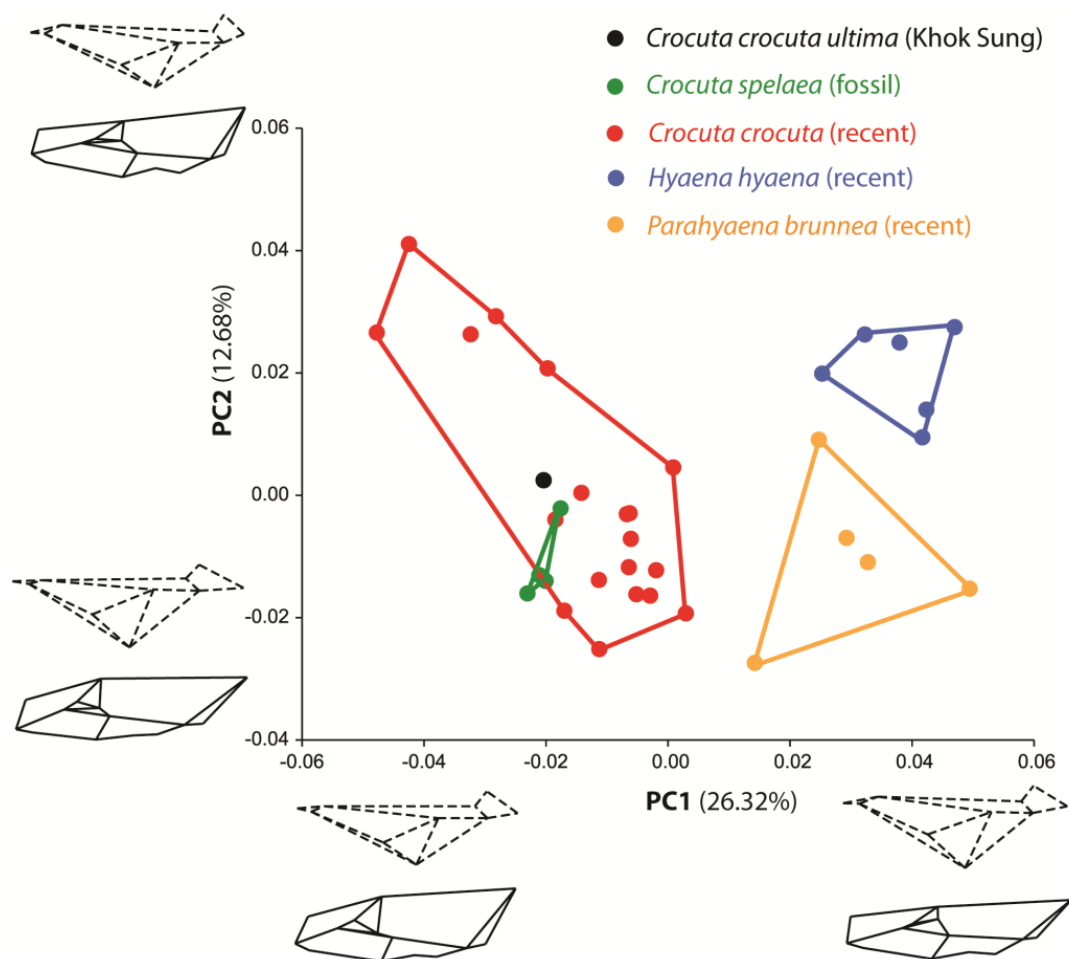


Figure 33. Principal components 1 and 2 with wireframes of cranial shapes represented by positive and negative extremities of each axis in dorsal (dash line) and lateral (solid line) views. The same color refers to the same species, as same as in Fig. 32.

The analysis of the first and second principal components of the complete crania shows a clear structuring of individual variation, with no overlap between three hyaenid genera (Fig. 33).

On PC1, *Hyaena hyaena* and *Parahyaena brunnea* score positively, while *Crocuta* runs more negatively. The sample of Khok Sung *C. c. ultima* falls within the range of variation of recent spotted hyaenas. Samples of *C. spelaea* mostly overlap with the recent spotted hyaenas. On PC2, *H. hyaena* scores more positively than *P. brunnea*, resulting in a clear separation between them. The morphological changes explained by PC1 include an elongation of the cranium, an anterior protrusion of the nasal bone, a relative decrease in the overall size of the orbit, a strengthening of the postorbital process, a shortening of supraoccipital and exoccipital regions, and a relative widening of the cranium in *Hyaena* and *Parahyaena*. These differences in morphological cranial features separate *Crocuta* from *Hyaena* and *Parahyaena*. Decreasing scores on PC2 indicate a weakening of the postorbital process, an increase in the angle of the slope of the nasal and frontal regions, a dorso-ventral constriction of the zygomatic arch, and a posterior elongation of the sagittal crest. These morphological differences distinguish *Hyaena* from *Parahyaena*.

Taxonomic remarks and comparisons

Fossils of spotted hyaenas have been variously identified as subspecies of *Crocuta crocuta* (*C. c. ultima*, *C. c. honanensis*, and *C. c. spelaea*) (e.g., Tseng and Chang, 2007; Diedrich, 2011) or as paleosubspecies of *C. ultima* (*C. ultima ultima* and *C. ultima ussurica*) (Baryshnikov, 2014), or treated as separate species (*C. ultima*, *C. honanensis*, and *C. spelaea*) (e.g., Baryshnikov, 1999; Werdelin and Lewis, 2008, 2012). According to Rohland et al. (2005), the modern spotted hyaenas from Africa and the Pleistocene spotted hyaenas from Eurasia are intermingled in phylogenetic analyses. This raises the question of the taxonomic delineation within the Pleistocene spotted hyaenas as either subspecies or even species that have diverged from a common ancestral spotted hyaena.

Tseng and Chang (2007) mentioned that the morphological variations observed among Eurasian fossils of *Crocuta crocuta* probably represent regional differences among populations (Colbert and Hooijer, 1953; Kurtén, 1956). For instance, *C. c. spelaea* is often regarded as the subspecies of the European or western Eurasian spotted hyaenas (Ehrenberg et al., 1938; Kurtén, 1956), whereas *C. c. ultima* is generally considered as the subspecies of the eastern Eurasian fossils (Tseng and Chang, 2007). Supporting the subspecies differentiation, the morphological distinction between *C. c. spelaea* and *C. c. ultima* is mainly supported by the skull and dentition, *C. c. ultima* displaying more robust cheek teeth and mandibles (compared to their skull sizes) and shorter limbs (Baryshnikov, 2014). Regarding these regional and morphological differences of Pleistocene spotted hyaenas, we thus follow the subspecies-level identification.

The subadult fossil of Khok Sung hyaena is referred to *C. c. ultima* because its dental characters, as well as its size, are comparable to Penghu specimens described by Tseng and Chang (2007). The parastyle of P4 is small but well-developed. The paracone and metastyle blade are more posteriorly elongated as observed in the Penghu material (Tab. 6). The protocone of P4 is situated very slightly more anterior than the parastyle (Fig. 31G), being even more anteriorly in other *C. c. ultima*. The accessory cusps of P3 and p3 are weakly developed or absent. The m1 is greatly reduced in size and displays a poorly developed metaconid and a unicuspid talonid. In addition, the Khok Sung spotted hyaena can be apparently distinguished from the Early Pleistocene *C. c. honanensis* by its larger size, relatively more robust upper premolars (see Fig. A1 for bivariate scatter diagrams of dental elements), and its less developed talonid on m1.

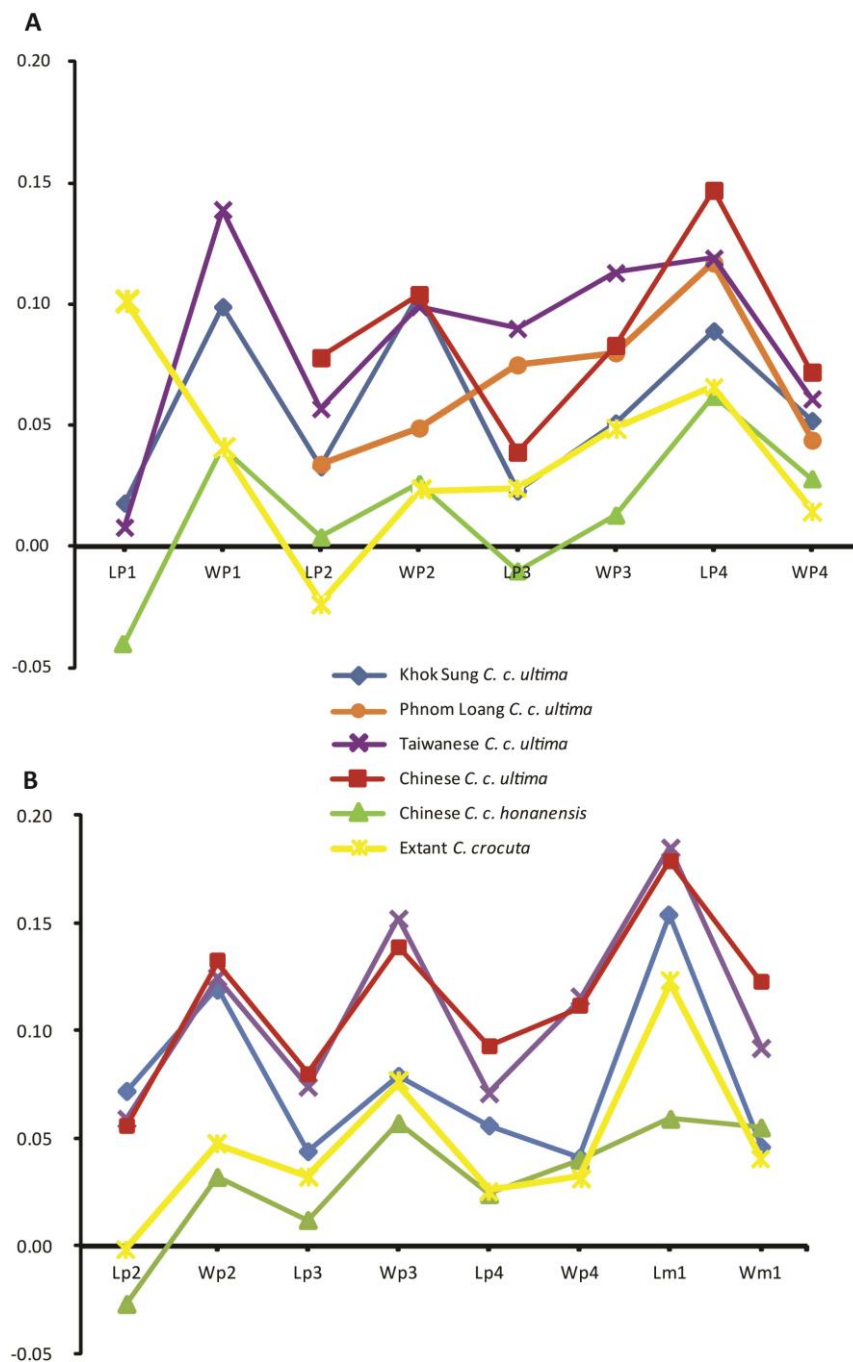


Figure 34. Log-ratio diagrams of fossil and extant representatives of *Crocuta crocuta* (measurements standardized to 6 individuals of *Hyaena hyaena*): **(A)** upper dentition and **(B)** lower dentition, comprising Khok Sung *C. c. ultima*, Phnom Loang *C. c. ultima*, Taiwanese *C. c. ultima* including specimens from the Penghu Channel (Ho et al., 1997; Tseng and Chang, 2007), Chinese *C. c. ultima* including specimens from Guanyindong, Xianrendong, Laochihe, Huainan (Tseng et al., 2008) and Zhoukoudian (Pei, 1940), Chinese *C. c. honanensis* including specimens from Henan (Zdansky, 1924), Yushe, Longdan, and Nihewan, and African extant spotted hyaenas (8 individuals). Dental measurements of fossil spotted hyaenas used here are given in Tab. A3.

As demonstrated by the log-ratio diagrams of cheek teeth (Fig. 34), the Khok Sung *C. c. ultima* displays an intermediate tooth size between *C. c. honanensis* (Yushe and Henan) and *C. c. ultima* from Taiwan and China. It is also larger than the African extant *C. crocuta*. The P1 of all fossil representatives is less elongated than that of the extant one. The P3 of the Khok Sung spotted hyaena is smaller than the P2, as for the Chinese *C. c. ultima* and *C. c. honanensis*. The tendency of the upper premolar sizes (P2, P3, and P4) of Cambodian *C. c. ultima* (Phnom Loang) is similar to that of extant spotted hyaenas, contrary to other fossils (Fig. 34A). The p3 of Thai *C. c. ultima* is relatively reduced in size, compared to those of other fossil and extant spotted hyaenas. The p4 of the Khok Sung spotted hyaena is more slender than that of other spotted hyaenas (Fig. 34B). According to well-documented fossils of spotted hyaenas from several Pleistocene Asian sites, *C. c. ultima* probably shows a high variation in size and proportion as observed among the recent spotted hyaena population (Fig. A1). We additionally suggest that the Khok Sung spotted hyaena is indistinguishable from the eastern Eurasian *C. c. ultima*, including Taiwanese, Chinese, and Southeast Asian (Thum Phedan (Fig. 1.3I-J), Thum Wiman Nakin (Fig. 31M), and Phnom Loang) population, in terms of morphology. All Pleistocene eastern Eurasian spotted hyaenas probably belong to the single subspecies *C. c. ultima*, corresponding to the postulation by Tseng and Chang (2007) and to the mtDNA evidences provided by Sheng et al. (2014).

According to our 3D geometric-morphometric analysis of fossil and recent hyaenid crania, differences in cranial morphology are a preliminary discrimination key to identify hyaenid taxa, with a considerable degree of confidence. The PCA analysis based on five hyaenid taxa reveals distinct patterns of cranial shapes for generic level identification (Fig. 33). *Crocuta* plotted at the negative values on PC1 reveals distinctive cranial morphologies characterized by a narrower but more robust cranium with a less-developed postorbital process on jugal and frontal bones and

with a short snout, compared to *Hyaena* and *Parahyaena*. On the basis of PC2, *Hyaena* differs from *Parahyaena* in having a narrower and shorter cranium with relatively flat nasal and frontal regions, a less dorso-ventrally constricted zygomatic arch, and more posterior extension of the nuchal crest. It is rather difficult to observe all these characters from those original crania. An application of the 3D geometric-morphometrics therefore provides greater resolution than the traditional observation, in case of hyaenid cranial morphology.

A single complete hyaenid cranium from Khok Sung, as well as that of *C. spelaea* from the Late Pleistocene European caves, is confirmed for its taxonomic identification as belonging to *Crocota* by the geometric-morphometric analysis. Although the principal component analysis of hyaenid crania shows the widest ranges of morphological variation for *Crocota*, there are possibly many important generic characters shared among members of *Hyaena* and *Parahyaena*. Due to the small number of individuals within the fossil spotted hyaena groups, our results should be treated as a first step until additional analyses are conducted with a larger sample size, in order to confirm relationships between these two fossil hyaenid species (*C. spelaea* and *C. c. ultima*) and other recent species.

In addition, the PCA results suggest that the cranial morphologies of *Hyaena* and *Parahyaena* appear distinguishable (Fig. 33). However, our 3D geometric-morphometric analysis has performed on the small number of samples (about 5–6 crania for *Hyaena* and *Parahyaena*) according to the scarcity of the complete skull. The additional samples of recent *Hyaena* and *Parahyaena* from other natural history museums need to be collected for the future analysis. This would confirm or strengthen our geometric-morphometric interpretation and allow performing more effectively statistical comparisons between samples.

Family CANIDAE Fischer de Waldheim, 1817**Genus *Cuon* Hodgson, 1838*****Cuon* sp.**

Referred material: a right ulna, DMR-KS-05-04-11-34; a right femur, DMR-KS-05-04-28-13

Material description

DMR-KS-05-04-11-34 is a half proximal ulna preserving complete parts from the olecranon to the midshaft (Fig. 30E, F). The olecranon tuber is well-developed. The upper margin of the olecranon is concave and possesses a slightly higher posterior part that extends laterally. The anconeal process is distinct. The medial and lateral coronoid processes diverge laterally (Fig. 30F). The trochlear notch is deep, forming nearly a semicircular surface for articulation (Fig. 30E).

The right femur preserves a complete proximal part and broken shaft (Fig. 30G, H). The greater trochanter is as high as the upper surface of the rounded femoral head. The intertrochanteric crest is straight and nearly oriented vertically (Fig. 30H). The upper border of the neck is flat. The lesser trochanter projects anteriorly and is situated at about 1.5 cm below the femoral head.

Taxonomic remarks and comparisons

The proximal ulna of canids is characterized by a bilobed and laterally compressed olecranon process, well-developed anconeal and lateral coronoid processes, and a laterally compressed shaft. The proximal crest of the olecranon is grooved anteriorly, but enlarged and rounded posteriorly (Tong et al., 2012). Pionnier-Capitan et al. (2011) suggest that in medial view the posteroproximal tuberosity of the olecranon of *Canis* is more proximally developed than in *Cuon*. The posteroproximal tuberosity of the Khok Sung ulna is as developed as that of *Cuon*. Furthermore, based on our comparisons with extant specimens, the Khok Sung canid ulna resembles that of *Cuon alpinus* because the olecranon bends more medially and the posterior

border of the olecranon is straighter than those observed in *Canis lupus*. The Khok Sung specimen is slightly smaller than the recent *Cuon alpinus* (Tab. 7). However, it is much smaller than recent and fossil *Canis lupus*, as well as the paleosubspecies *Cuon alpinus caucasicus* (Tab. 7).

Table 7. Measurements (in millimetres) of ulnae and femurs of Khok Sung and other extant and fossil canids. * indicates a subadult individual. Metrical data of fossil canids are from Baryshnikov (2012, 2015).

Ulna							
Specimen no.	Taxa	Age	Locality	LO	DPA	SDO	BPC
DMR-KS-05-04-11-34	<i>Cuon</i> sp.	late Middle Pleistocene	Khok Sung, northeastern Thailand	15.16	18.51	15.21	11.65
NMW 1531*	<i>Canis lupus</i>	Recent	Eastern India	29.91 29.29	24.11 24.43	18.38 18.43	15.65 15.33
ZIN 37274-27	<i>Canis lupus</i>	Late Pleistocene	Geographical Society Cave, Russia	–	32.30	27.80	–
NHMP R5387	<i>Canis lupus</i>	Late Pleistocene	Srbsko Chlum-Komin Cave, Czech Republic	–	34.80	27.60	–
NMW B5319	<i>Cuon alpinus</i>	Recent	Java, Indonesia	19.23 19.74	19.37 19.29	16.36 16.33	14.43 14.07
ZIN 36733-1	<i>Cuon alpinus caucasicus</i>	Late Pleistocene	Kudaro 1 Cave, Southern Ossetia, Caucasus	–	–	–	18.30
ZIN 36739	<i>Cuon alpinus caucasicus</i>	Late Pleistocene	Kudaro 1 Cave, Southern Ossetia, Caucasus	–	32.20	–	17.20
ZIN 36698-1	<i>Cuon alpinus caucasicus</i>	Late Pleistocene	Kudaro 3 Cave, Southern Ossetia, Caucasus	–	28.70	24.50	18.90
ZIN 36697-2	<i>Cuon alpinus caucasicus</i>	Late Pleistocene	Kudaro 3 Cave, Southern Ossetia, Caucasus	–	34.00	29.50	21.50
ZIN 36677-2	<i>Cuon alpinus caucasicus</i>	Late Pleistocene	Kudaro 3 Cave, Southern Ossetia, Caucasus	–	33.60	28.60	21.70
ZIN 31241-3	<i>Cuon alpinus caucasicus</i>	Late Pleistocene	Kudaro 3 Cave, Southern Ossetia, Caucasus	–	30.30	26.50	17.00
ZIN 36670	<i>Cuon alpinus caucasicus</i>	Late Pleistocene	Kudaro 3 Cave, Southern Ossetia, Caucasus	–	28.80	–	18.50

ZIN 36705-7	<i>Cuon alpinus</i> <i>caucasicus</i>	Late Pleistocene	Kudaro 3 Cave, Southern Ossetia, Caucasus	–	–	–	15.00
Femur							
Specimen no.	Taxa	Age	Locality	Bp	Dp	DC	SD
DMR-KS-05-04- 28-13	<i>Cuon</i> sp.	late Middle Pleistocene	Khok Sung, northeastern Thailand	35.69	17.90	16.58	11.34
NMW 1531*	<i>Canis lupus</i>	Recent	Eastern India	35.05 35.57	16.70 16.82	16.75 16.73	10.43 10.52
NMW B5319	<i>Cuon alpinus</i>	Recent	Java, Indonesia	31.03 31.58	15.95 16.08	16.62 16.38	11.66 11.79
ZIN 36692-2	<i>Cuon alpinus</i> <i>caucasicus</i>	Late Pleistocene	Kudaro 3 Cave, Southern Ossetia, Caucasus	48.70	–	22.70	–
ZIN 36700-2	<i>Cuon alpinus</i> <i>caucasicus</i>	Late Pleistocene	Kudaro 3 Cave, Southern Ossetia, Caucasus	–	–	21.70	15.20

Living canids generally show a typical morphology of the proximal femur, characterized by their relatively vertical intertrochanteric crests, prominent lesser trochanter with the sharp crest extending downward along the shaft, moderately-sized greater trochanter, and slender shaft (France, 2009; Tong et al., 2012). In *Canis lupus*, the lateral side of the caput femoris is obliquely prolonged towards the trochanteric fossa. The upper border of the neck is concave and shorter than those in *Cuon alpinus* (Ripoll et al., 2010). The femur DMR-KS-05-04-28-13 is canid-sized (Tab. 7) and is comparable in morphology to *Cuon alpinus*. For instance, the intertrochanteric crest is more oblique and straighter (nearly vertical and curved in *Canis lupus*), the caput femoris is round, and the upper border of the neck is long and flat (Ripoll et al., 2010).

Because the Khok Sung ulna and femur morphologically match better *Cuon alpinus* than *Canis lupus*, we identify these two postcranial specimens as belonging to *Cuon* sp.

Order PROBOSCIDEA Illiger, 1811

Family STEGODONTIDAE Osborn, 1918

Genus *Stegodon* Falconer and Cautley, 1857

Stegodon cf. orientalis Owen, 1870

Referred material: a right DP4 (posterior part), DMR-KS-05-03-28-14; a left DP4 (anterior part), DMR-KS-05-03-19-7; a left M2, DMR-KS-05-03-29-1 (posterior part); a right M3, DMR-KS-05-03-22-19 (posterior part); a fragmentary tusk, DMR-KS-05-03-15-2; a left dp3 (anterior part), DMR-KS-05-04-01-8; two mandibles with m3—DMR-KS-05-03-08-1 (right) and DMR-KS-05-03-08-2 (left); a right humerus fragment (proximal part), DMR-KS-05-03-10-5; a left humerus, DMR-KS-05-03-10-6; two ulna fragments (proximal parts)—DMR-KS-05-03-09-7 and DMR-KS-05-03-10-2; a femoral head fragment, DMR-KS-05-03-10-3; a right femur, DMR-KS-05-03-10-4; a right tibia fragment (distal part), DMR-KS-05-03-10-3; a right fibula, DMR-KS-05-03-00-124; two pelvis fragments—DMR-KS-05-03-10-11 (right) and DMR-KS-05-03-10-12 (left); five vertebrae—DMR-KS-05-03-17-11, DMR-KS-05-03-10-7, DMR-KS-05-03-09-18, DMR-KS-05-03-10-1, and DMR-KS-05-03-28-20; a sacrum fragment, DMR-KS-05-03-10-8; two ribs—DMR-KS-05-03-10-13 and DMR-KS-05-03-10-14; three rib fragments—DMR-KS-05-03-09-6 (body), DMR-KS-05-03-09-45 (body), DMR-KS-05-03-09-4 (head and neck)

Material description

Upper dentition: both fragments of DP4 (DMR-KS-05-03-28-14: fig. 35A, B) and DMR-KS-05-03-19-7: fig. 35C) are slightly worn and unworn respectively (for measurements, see Tab. 8). The former specimen lacks two or three anterior ridges, whereas the latter specimen preserves only the anterior cingulum and the first ridge. DMR-KS-05-03-28-14 has a rectangular outline in occlusal view, a convex crown base in lateral view, and a posterior cingulum. These characters indicate that this specimen belongs to a posterior lobe of DP4. The buccal and lingual surfaces of ridges display subvertically developed grooves. A median cleft is well-developed and runs from

anteriorly to posteriorly in the middle part of the tooth, starting from the halfway height of the crown. The second anterior ridge of DMR-KS-05-03-28-14 shows displacement between the pretrite and posttrite halves, a character sometimes present in deciduous molars of derived *Stegodon*. Each ridge bears ten to twelve mammillae.

DMR-KS-05-03-29-1 (M2) preserves three posterior ridges with a small cingulum (Fig. 35E, F and Tab. 8). Two anterior ridges bear slightly worn mammillae with stronger abrasion on the buccal side. The posterior-most ridge is unworn and reduced in width. The outline of the buccal side is concave in occlusal view and the base of the crown is nearly straight in lateral view. The median cleft is weakly developed. The number of the mammillae on each ridge ranges from eight to eleven.

DMR-KS-05-03-22-19 (M3) preserves only three posterior ridges with a cingulum (Fig. 35G, H and Tab. 8). The ridges are slightly worn with more abraded buccal surfaces. The general outline of this tooth is similar to that of M2, but is comparatively wider and displays a more developed posterior cingulum. The median cleft is poorly developed. Each ridge consists of eight to ten mammillae.

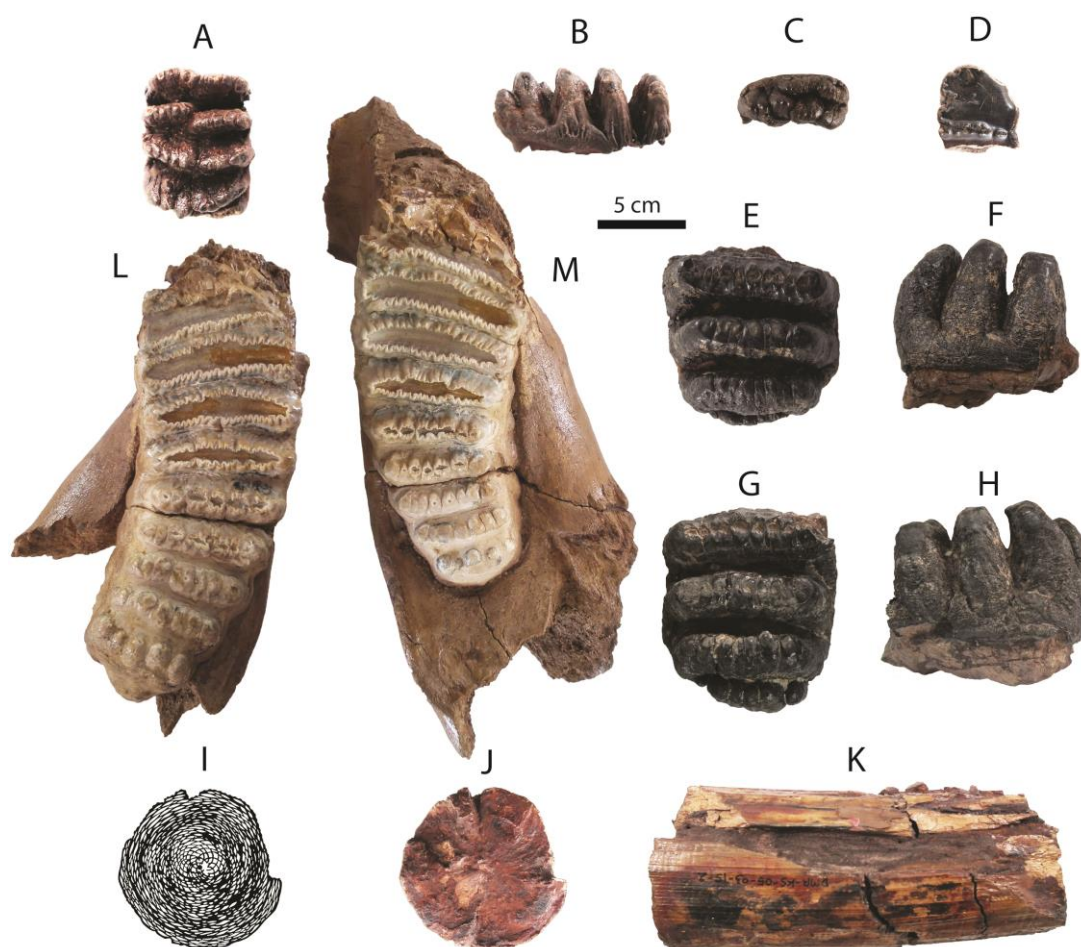


Figure 35. Dental remains of *Stegodon cf. orientalis* from Khok Sung: (A–B) DMR-KS-05-03-28-14, a right DP4 in occlusal (A) and buccal (B) views; (C) DMR-KS-05-03-19-7, an anterior lobe of DP4 in occlusal view; (D) DMR-KS-05-04-01-8, a left dp3 in occlusal view; (E–F) DMR-KS-05-03-29-1, a left posterior fragment of M2 in occlusal (E) and buccal (F) views; (G–H) DMR-KS-05-03-22-19, a right posterior fragment of M3 in occlusal (G) and buccal (H) views; (I–K) DMR-KS-05-03-15-2, a fragmentary upper tusk in proximal (I–J) and dorsal (K) views; (L) DMR-KS-05-03-08-1, a right mandible with m3 in occlusal view; (M) DMR-KS-05-03-08-2, a left mandible with m3 in occlusal view.

Table 8. Measurements (in millimeters) of cheek teeth of Khok Sung proboscideans, including a number of preserved ridges (NR), lengths (L), widths (W), heights (H), enamel thickness (ET), H/W indices ($100 \times H/W$), and laminar frequencies (LF). The laminar frequencies are expressed as the following formula: $LF = n \cdot 100 / d_l + n \cdot 100 / d_b / 2$, where “ d_l ” and “ d_b ” are referred to distances at the lingual and buccal side of the tooth, respectively, and “ n ” is equivalent to the number of ridges between two measuring points (van den Bergh, 1999). * indicates measurements of the maximum preservation according to incomplete specimens. The H/W index is calculated for each ridge. The laminar frequency is measured based on the maximum number of preserved ridges.

Specimen no.		NR	L	W	H	ET	H/W index	LF
<i>Stegodon cf. orientalis</i>								
DMR-KS-05-03-28-14	DP4	4	60.08	50.04	26.71	0.69–1.21	53.38–58.23	7.99
DMR-KS-05-03-19-7	DP4	1	18.65	49.89*	26.71	2.06	53.53	–
DMR-KS-05-03-29-1	M2	3	70.14*	78.83	55.18	1.62–3.06	70.00–73.34	4.61
DMR-KS-05-03-22-19	M3	3	90.43*	84.66	46.14	3.77–4.35	57.33–62.71	3.86
DMR-KS-05-04-01-8	dp3	3	26.68*	26.09	12.08	1.82	46.30–47.76	10.41
DMR-KS-05-03-08-1	m3	8	245.86*	95.66	41.50	3.41–6.87	43.38–51.77	3.91
DMR-KS-05-03-08-2	m3	8	247.78*	95.57	42.56	3.39–6.54	44.53–52.21	3.94
<i>Elephas sp.</i>								
DMR-KS-05-03-17-12	Lower molar	2	41.04*	66.77*	108.94	2.48–3.30	163.16–165.18	10.61

A fragmentary tusk (DMR-KS-05-03-15-2) displays dentine (outer and inner layers), cementum, and a pulp cavity (Fig. 35I–K). It is slightly curved upward and sub-rounded in cross section for both the proximal and the distal section. A median longitudinal groove is present on the dorsal surface. The Schreger pattern commonly developed in elephantoid tusks is visible on the inner dentine layer. The maximum length of DMR-KS-05-03-15-2 is 159.2 mm and the mediolateral and dorsoventral diameters of the proximal cross-section are 73.88 and 70.56 mm, respectively. The outline of the tusk (DMR-KS-05-03-15-2) resembles *S. trigonocephalus* in its more medial-laterally than the dorso-ventrally compressed cross section. The macroscopic

distinctive features in cross section are similar to *S. sompoensis* (van den Bergh 1999) but show the incremental lines more obviously.

Lower dentition: DMR-KS-05-04-01-8 (dp3) is heavily worn and comprises three preserved ridges and an anterior cingulum (Fig. 35D and Tab. 8). The buccal part of the third ridge is broken but it is presumably wider than the second ridge. The dp3 is subrectangular in outline or tapers towards the anterior part. The lateral sides between the first and second ridges are distinctly constricted.

Two hemi-mandibles of the same individual (DMR-KS-05-03-08-1 and DMR-KS-05-03-08-2) are moderately well-preserved (for measurements, see Tab. 8). The completely erupted m3 has eight ridges with small posterior cingulids (Fig. 35L, M). The symphysis and most of the ramus are broken away. The mandibular corpus is robust. We estimate the total number of ridges to be eleven based on the position on the corpus of the anterior root that supports two first lophs in *Stegodon* (Saegusa et al., 2005). The anteriormost preserved ridge is thus the third ridge, broken at its anterior and lateral parts in both specimens. The third to sixth ridges are strongly worn, whereas more posterior ridges are successively less damaged by abrasion. Valleys between the ridges are moderately filled with abundant cement. There is no median cleft. The m3 is much more elongated and contains five mammillae on the posteriormost ridge. The mammillae increase in size successively from the anterior to posterior ridge.

Postcranial remains: postcranial elements include two humeri (Fig. 36A, B), two ulnae, two femora (Fig. 36C, D), a tibia, a fibula (Fig. 36E), two pelvis girdles (Fig. 36F, G), five vertebrae, a sacrum (Fig. 36J), and five ribs (Fig. 36K, L) (for measurements, see Tab. A1). All postcranial bones excluding some vertebrae belong to a single individual because they were found together in association with two mandibles with the m3 (DMR-KS-05-03-08-1 and DMR-KS-05-03-08-2) and show fully fused epiphyses. This individual is a senior adult due to the heavy wear on the

anterior loph on the m3. Only two vertebrae (DMR-KS-05-03-09-18: fig. 36H and DMR-KS-05-03-10-7: fig. 36I) were found in association with that individual. The specimen DMR-KS-05-03-26-38 is a juvenile because the vertebral body is not fused.



Figure 36. Postcranial remains of *Stegodon* cf. *orientalis* from Khok Sung: (A–B) DMR-KS-05-03-10-6, a left distal humerus in anterior (A) and distal (B) views; (C–D) DMR-KS-05-03-10-4, a right femur posterior (C) and distal (D) views; (E) DMR-KS-05-03-00-124, a right fibula in posterior view; (F) DMR-KS-05-03-10-11, a right pelvis in dorsal view; (G) DMR-KS-05-03-10-12, a left pelvis in lateral view; (H) DMR-KS-05-03-09-18 and (I) DMR-KS-05-03-10-7, vertebrae in anterior view; (J) DMR-KS-05-03-10-8, a sacrum in ventral view; (K) DMR-KS-05-03-10-14 and (L) DMR-KS-05-03-10-13, ribs in anterior view.

Taxonomic remarks and comparisons

We assign the proboscidean cheek teeth from Khok Sung to *Stegodon* because there are more than five ridges or loph(id)s on molars, V-shaped valleys between ridges on molars, and step-like worn surface reliefs on the enamel layer (Saegusa, 1996; Saegusa et al., 2005). The Khok Sung material shows well-developed cheek tooth features of derived *Stegodon* (e.g., a greater number of ridges and mammillae, high filled cements between the ridges, and a high angled cliff on the enamel surfaces (step-like structure “type 3”, in Saegusa (1996)).

Table 9. Ridge dimensions (lengths and widths in millimeters) of upper fourth deciduous premolars between Khok Sung *Stegodon* and *Stegodon orientalis*.

DP4	Ridge (from anterior to posterior)					
	1st	2nd	3rd	4th	5th	6th
<i>Stegodon cf. orientalis</i> (Khok Sung)						
Length	15.7	–	>10.7	12.4	13.5	13.5
Width	49.9	–	49.9	50.0	49.7	48.4
Specimen measurements: DMR-KS-05-03-28-14 and DMR-KS-05-03-19-7						
<i>Stegodon orientalis</i> (x6x)						
N	3	3	3	3	3	3
Length	12.3–16.2	15.3–19.7	14.3–20.4	13.3–18.4	12.6–16.2	11.1–16.5
Mean	14.1	17.0	17.4	16.1	15.0	13.6
N	3	3	2	3	3	3
Width	43.7–54.1	49.2–63.1	51.8–63.3	51.2–60.2	50.0–57.2	45.8–52.2
Mean	49.0	54.6	57.5	54.4	53.0	48.9
Specimen measurements: IVPP V1869, IVPP V1870, IVPP V5215-38, and IVPP RV39068						

Table 10. Ridge dimensions (lengths and widths in millimeters) of lower third deciduous premolars between Khok Sung *Stegodon* and *Stegodon orientalis*.

dp3	Ridge (from anterior to posterior)					
	1st	2nd	3rd	4th	5th	6th
<i>Stegodon cf. orientalis</i> (Khok Sung)						
Length	9.3	–	–	–	–	–
Width	25.5	>26.1	–	–	–	–
<i>Stegodon orientalis</i> (x5x)						
N	7	7	7	7	7	–
Length	7.2–10.8	6.5–10.3	9.6–12.9	10.9–12.0	10.0–14.0	–
Mean	8.5	9.0	11.0	11.5	12.6	–
N	7	7	7	7	7	–
Width	19.5–32.3	24.8–27.9	27.3–31.9	32.6–37.8	36.2–42.3	–
Mean	25.0	26.6	29.9	34.9	39.2	–
Specimen measurements: IVPP V1798, IVPP V1800, IVPP V1804, IVPP V1807, IVPP V1808, IVPP V1812, and IVPP V1815						
<i>Stegodon orientalis</i> (x6x)						
N	5	5	5	5	5	5
Length	8.6–13.1	7.0–11.8	10.1–12.8	10.6–13.0	10.6–13.4	8.5–12.5
Mean	10.5	8.6	11.5	11.7	11.7	10.0
N	4	5	5	5	5	5
Width	23.7–31.1	26.8–32.1	29.1–34.7	33.1–41.1	36.7–47.3	36.0–52.4
Mean	27.3	28.9	31.5	36.8	41.3	40.4
Specimen measurements: IVPP1799, IVPP V1801, IVPP V1802, IVPP V1803, and IVPP V1816						

The morphologies and ridge sizes of upper molars from Khok Sung are congruent with Chinese *S. orientalis* (Tabs 9–11). However, we suggest that some comparative M3 of *S. orientalis* (e.g., IVPP V5216-9) represents a total ridge number of ten (excluding anterior and posterior halfridges), different from the ridge formula ($\times 11 \times$ for this species) given by van den Bergh et al. (2008: table. 3). The ridge formula of the M3 of *S. orientalis* therefore ranges from ten to eleven. The m3 of *S. orientalis* commonly has a total number of twelve ridges (excluding anterior and posterior halfridges). According to the fact that only a few comparative specimens of the m3 of *S. orientalis* are complete with the total ridge number of twelve, some of them (e.g., IVPP V1777 and IVPP V5216-16, based on our observations) display a total of 11 ridges (excluding anterior and posterior halfridges). In *S. orientalis*, the number of ridges on the m3 thus ranges from eleven to twelve. *S. insignis* has a total number of ridges ranging from eleven to thirteen (van den Bergh et al., 2008). The ridge formula of *Stegodon trigonocephalus trigonocephalus* is almost thirteen (excluding anterior and posterior halfridges) (van den Bergh, 1999). Another subspecies, *S. t. praecursor*, has a lower number of ridges ($\times 11 \times$, van den Bergh et al., 2008: table. 3). The m3 of the Khok Sung stegodontid share a similar ridge formula ($\times 11 \times$) with *S. orientalis* from South China and *S. insignis* from Punjab (Siwaliks). But it differs from *S. insignis* in having more delicately folded enamel, more pronounced curvature of the crown, and V-shaped valleys (between the two ridges) slightly less filled by cements. The ridge sizes of Khok Sung lower third molar are almost comparable to those of *S. orientalis* and *S. insignis*, but are distinctly larger than other derived *Stegodon* species from Indonesia (Tab. 12). We thus identify hereby all cheek teeth as belonging to *S. cf. orientalis*.

Table 11. Ridge dimensions (lengths and widths in millimeters) of upper second and third molars between Khok Sung *Stegodon* and *Stegodon orientalis*. The total ridge number of upper molars of Khok Sung stegodontids used for our comparisons follows that of *Stegodon orientalis*.

M2 and M3	Ridge (from anterior to posterior)										
	1st	2nd	3rd	4th	5th	6th	7th	8th	9th	10th	Posterior halfridge
<i>Stegodon cf. orientalis</i> (Khok Sung)											
DMPR-KS-05-03-29-1 (M2)											
Length	-	-	-	-	-	28.2	23.9	19.7	-	-	-
Width	-	-	-	-	-	78.8	76.9	63.3	-	-	-
DMPR-KS-05-03-22-19 (M3)											
Length	-	-	-	-	-	-	-	29.3	24.2	21.8	12.9
Width	-	-	-	-	-	-	-	80.5	77.6	70.1	49.7
<i>Stegodon orientalis</i> (M2) (x8x)											
N	1	1	1	1	1	2	2	2	-	-	-
Length	23.4	25.0	30.7	25.4	22.1	20.3-22.5	20.5-22.0	15.4-17.7	-	-	-
Mean	-	-	-	-	-	21.4	21.2	16.6	-	-	-
N	1	1	1	1	1	2	2	2	-	-	-
Width	77.8	80.4	83.1	83.0	81.6	76.4-78.4	73.0-73.8	63.2-69.1	-	-	-
Mean	-	-	-	-	-	77.4	73.4	66.1	-	-	-
Specimen measurements: IPPP V1821 and IPPP V5216-5											
<i>Stegodon orientalis</i> (M3) (x10x)											
N	3	3	3	2	1	1	1	2	2	2	2
Length	22.4-25.3	22.2-27.4	22.3-27.1	24.6-24.8	25.5	22.5	21.1	19.9-26.3	17.8-24.1	16.4-22.4	7.2-15.8
Mean	23.7	25.6	24.5	24.7	-	-	-	23.1	20.9	19.4	11.5
N	2	2	2	1	-	2	2	2	2	2	2
Width	85.4-91.5	88.3-96.7	84.9-101.3	100.4	-	81.4-87.1	83.3-85.7	75.0-87.9	65.4-89.5	57.4-81.8	38.6-54.6
Mean	88.4	92.5	93.1	-	-	84.3	84.5	81.4	77.5	69.6	46.6
Specimen measurements: IPPP V1772, IPPP V1775, IPPP V1763, and IPPP V5216-5											

Table 12. Ridge dimensions (lengths and widths in millimeters) of lower third molars of derived *Stegodon* in Southeast Asia. The ridge formula of each taxon follows van den Bergh et al. (2008: table. 3). The ridge number of *Stegodon insignis* is considered as representing a total of twelve.

Lower third molar	Ridge (from anterior to posterior)											
	1st	2nd	3rd	4th	5th	6th	7th	8th	9th	10th	11th	12th
<i>Stegodon cf. orientalis</i> (Khok Sung) ((x2)9x)												
N	-	-	-	2	2	2	2	2	2	2	2	2
Length	-	-	-	29.8-32.4	28.8-30.6	31.8-32.8	28.2-34.1	28.9-32.3	24.5-30.7	23.3-26.9	16.6-22.4	
Mean	-	-	-	31.1	29.7	32.3	31.2	30.6	27.6	25.1	19.5	
N	-	-	-	2	2	2	2	2	2	2	2	
Width	-	-	-	95.7-97.6	94.4-95.8	92.7-94.0	83.1-83.3	72.3-76.3	67.7-68.9	61.6-65.9	55.4-58.6	
Mean	-	-	-	96.7	95.1	93.4	83.2	74.3	68.3	63.8	57.0	
<i>Stegodon cf. orientalis</i> (x11x)												
N	-	2	2	2	2	2	2	2	2	2	2	2
Length	-	26.0-31.7	26.4-33.8	23.3-34.4	25.5-33.1	28.6-31.7	24.8-39.4	26.8-36.4	25.6-31.0	21.1-24.3	15.4-15.9	
Mean	-	28.9	30.1	28.9	29.3	30.2	32.1	31.6	31.3	22.7	15.7	
N	-	1	2	1	1	2	2	2	2	2	2	
Width	-	82.43	68.0-86.1	88.34	90.11	72.4-93.1	72.0-91.9	71.2-88.3	64.6-80.1	54.8-63.6	41.8-43.1	
Mean	-	-	77.1	-	-	82.8	82.0	79.8	72.4	59.2	42.5	
Specimen measurements: IVP V1777 and IVP5216-16												
<i>Stegodon insignis</i> (x12x)												
N	-	1	2	3	2	2	2	3	3	2	2	2
Length	-	27.7	26.4-29.2	20.7-23.7	24.2	21.6-23.8	20.9-22.8	23.0-25.6	23.4-30.9	22.5-25.3	21.5-23.5	19.5-23.7
Mean	-	-	27.8	22.1	24.2	22.7	21.9	24.6	26	23.9	22.5	21.6
N	-	1	3	3	2	2	2	3	2	2	2	2
Width	-	79.3	83.9-92.6	81.7-91.2	92.7-94.8	90.7-98.5	89.5-89.9	84.6-88.0	73.7-77.7	66.6-68.8	61.6-64.0	47.1-52.5
Mean	-	-	87.4	88.0	93.8	94.6	89.7	85.9	75.7	67.7	62.8	49.8
Specimen measurements: RMNH DUB 3049, RMNH DUB 3074, RMNH DUB 3072+3097, and RMNH DUB 3112												

Table 12 (continued). Ridge dimensions (lengths and widths in millimeters) of lower third molars of derived *Stegodon* in Southeast Asia. The ridge formula of each taxon follows van den Bergh et al. (2008: table. 3). The ridge number of *Stegodon insignis* is considered as representing a total of twelve.

<i>Stegodon orientalis</i> (x12x)													
	4	1	4	4	4	4	4	4	4	5	8	8	
N													
Length	17.4–25.1	20.4	25.5–31.7	25.9–33.8	23.3–34.42	25.5–35.0	28.6–35.3	24.8–39.4	26.8–36.4	25.6–37.0	16.2–31.5	13.4–22.6	
Mean	21.1	–	28.0	28.8	30.3	30.3	31.1	32.3	31.1	29.4	23.0	16.8	
N	4	1	2	3	3	3	4	4	4	6	8	8	
Width	71.6–81.0	75.7	81.2–82.4	68.0–86.1	85.6–88.3	84.9–90.1	72.4–93.1	72.0–91.9	71.2–88.3	64.6–82.7	54.8–78.3	28.7–59.1	
Mean	74.7	–	81.8	79.5	87.1	87.6	84.7	84.2	82.2	75.2	66.0	46.0	
Specimen measurements: IVP V0577, IVP V1770, IVP V1776, IVP V1817, IVP V1820, IVP V1826, IVP V1827, IVP V5216-13, and IVP V5216-15													
<i>Stegodon trigonocephalus trigonocephalus</i> (x13x)													
	1st	2nd	3rd	4th	5th	6th	7th	8th	9th	10th	11th	12th	13th
N	–	–	–	1	3	3	3	3	3	3	3	3	3
Length	–	–	–	16.8	20.4–25.0	22.1–26.0	24.4–26.0	23.7–24.9	21.4–24.5	21.1–24.0	16.6–24.2	18.4–19.4	18.0–21.1
Mean	–	–	–	–	23.4	24.0	25.3	24.1	22.9	22.5	21.1	19.0	19.3
N	–	–	–	1	3	3	3	3	3	3	3	3	3
Width	–	–	–	71.8	71.4–87.3	71.4–86.8	75.0–87.1	76.8–83.3	72.6–81.1	70.5–76.4	66.6–69.6	53.9–63.1	46.4–48.4
Mean	–	–	–	–	80.2	80.4	80.8	80.4	77.0	72.6	68.0	58.4	47.6
Specimen measurements: RMNH DUB 2895, RMNH DUB 3500, and RMNH DUB 4225													
<i>Stegodon florensis</i> (x13x)													
	1st	2nd	3rd	4th	5th	6th	7th	8th	9th	10th	11th	12th	13th
N	2	2	2	2	2	2	2	1	1	1	1	–	–
Length	23.1–25.8	20.2–20.9	19.2–21.6	18.4–23.8	17.6–22.7	18.9–20.9	18.3–20.3	21.16	21.83	26.48	26.97	–	–
Mean	24.5	20.6	20.4	21.1	20.2	19.9	19.3	–	–	–	–	–	–
N	1	2	2	2	2	2	2	1	1	1	1	–	–
Width	63.1	66.0	67.2–68.4	69.3–69.9	69.0–69.9	67.5–69.9	68.3–68.6	66.95	60.47	65.75	58.71	–	–
Mean	–	66.0	67.8	69.6	69.5	68.7	68.5	–	–	–	–	–	–
Specimen measurements: RGM.631600													

Family ELEPHANTIDAE Gray, 1821**Genus *Elephas* Linnaeus, 1758*****Elephas* sp.**

Referred material: a fragmentary tusk, DMR-KS-05-03-22-1; a posterior fragment of a right lower molar, DMR-KS-05-03-17-12

Material description

Upper tusk: DMR-KS-05-03-22-1 is a short fragmentary tusk. The dorsal side is partially broken away (Fig. 37A, B). This tusk curves slightly upward and is dorsoventrally compressed and probably obovoid or oval in cross section (Fig. 37B, C). The Schreger pattern in the dentine is poorly developed or absent. The fractures of the cross-section are developed, perpendicular to the outer surface (“radiate cracking or fracture pattern”) (van den Bergh, 1999) (Fig. 37C). The maximum length of the preserved tusk is 196.1 mm and the mediolateral and dorsoventral diameters measured on the proximal cross-section are 71.3 and 49.1 mm, respectively.

Lower molar: DMR-KS-05-03-17-12 preserves only two adjoining worn plates of a high-crowned molar, distinctly more hypsodont than that of *Stegodon* (Tab. 8). The plates are thin, anteroposteriorly compressed, and closely spaced (Fig. 37D, E). The occlusal enamel loops or folds are small and thin compared to *S. orientalis* molars, single-layered, and almost irregular. The grinding surface of the anterior plate is buccally inclined (Fig. 37F), indicating this is a right molar.

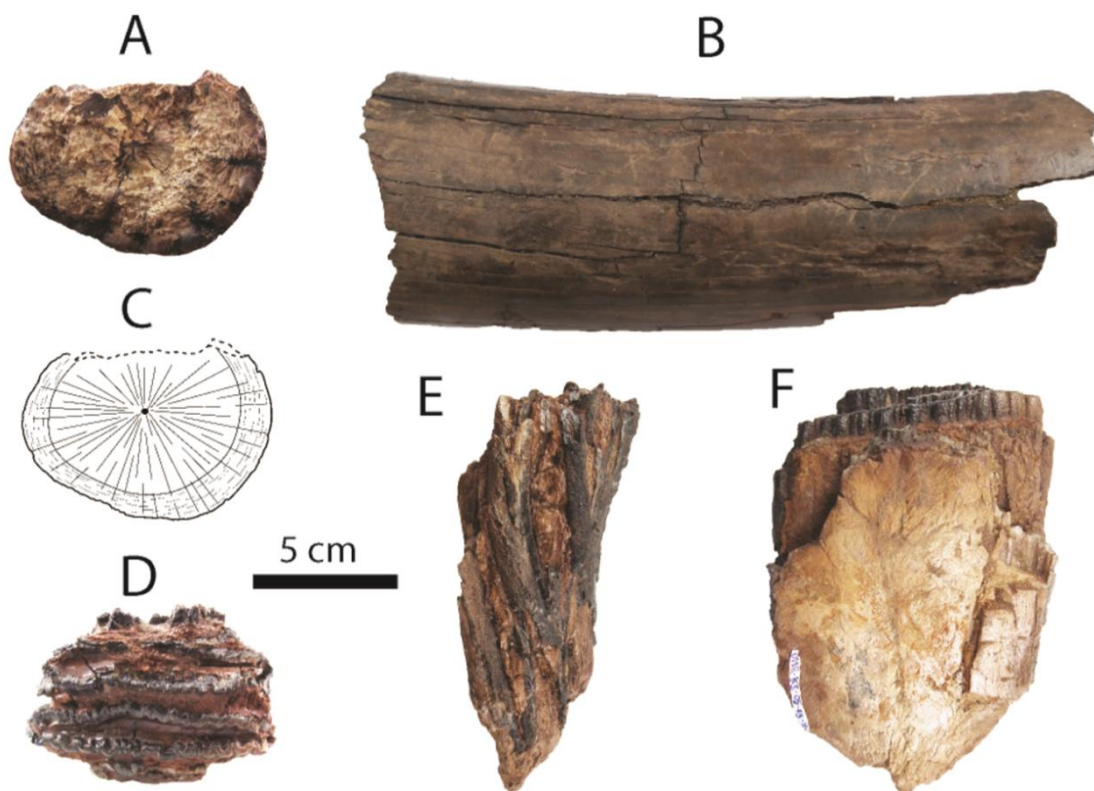


Figure 37. Dental remains of *Elephas* sp. from Khok Sung: (A–C) DMR-KS-05-03-22-1, a fragmentary upper tusk in proximal (A, C) and ventral (B) views; (D–F) DMR-KS-05-03-17-12, a posterior fragment of a right lower molar in occlusal (D), lingual (E), and anterior (F) views.

Taxonomic remarks and comparisons

The fragmentary tusk (DMR-KS-05-03-22-1) is distinguished from DMR-KS-05-03-15-2 (*S. orientalis*) by a more rounded cross-section, a larger diameter, and a radiate fracture pattern with the development of concentric incremental lines (Fig. 37C). The outline of DMR-KS-05-03-22-1 resembles *Elephas* (e.g., *E. maximus* (Palombo and Villa, 2001) and *E. celebensis* (van den Bergh, 1999)). The lower molar is also congruent morphologically with *Elephas* (Maglio, 1973; Zhou and Zhang, 1974), but differs from *P. namadicus* in its thinner and smoother enamel (Lydekker, 1880; Zhou and Zhang, 1974; Tshen, 2013). We therefore assign these two specimens (fragmentary tusk and molar) to *Elephas*.

Order PERISSODACTYLA Owen, 1848

Family RHINOCEROTIDAE Owen, 1840

Subfamily RHINOCEROTINAE Owen, 1845

Genus *Rhinoceros* Linnaeus, 1758

Rhinoceros sondaicus Desmarest, 1822

Referred material: a left P2, DMR-KS-05-03-00-128; a left P3, DMR-KS-05-03-22-17; a left M1, DMR-KS-05-03-00-129; a left M3, DMR-KS-05-03-00-127; a mandible with right (i2 and p2–m3) and left (p3–m3) tooth rows, DMR-KS-05-03-00-126; a partial mandible, DMR-KS-05-03-31-28; a fragmentary nasal bone, DMR-KS-05-03-00-56; a left scapula, DMR-KS-05-03-00-58; a left humerus, DMR-KS-05-03-31-3; a right metacarpus II, DMR-KS-05-03-28-29; a metacarpus III, DMR-KS-05-03-22-49; a right metacarpus IV, DMR-KS-05-04-05-15; a left tibia, DMR-KS-05-03-00-52; a right calcaneus, DMR-KS-05-04-27-19; a left astragalus, DMR-KS-05-03-26-23

Material description

Upper dentition: P2 (DMR-KS-05-03-00-128: fig. 38A), M1 (DMR-KS-05-03-00-129: fig. 38C), and M3 (DMR-KS-05-03-00-127: fig. 38D) are presumably from the same individual because they were found together at the same spot. The upper cheek teeth are lophodont (for measurements, see Tab. 13). Premolars are completely molarized (Fig. 38A, B) and molars exhibit well-preserved crochets. The M3 is triangular in occlusal outline and displays a well-developed parastyle, ectometaloph, medifossette, and hypocone, but a less developed parastyle fold (Fig. 38D).

Mandibles and lower dentition: a mandible (DMR-KS-05-03-00-126) preserves both sides of cheek tooth rows (right p2–m3 and left p3–m3), but most of its symphysis and entire ramus are broken off (Fig. 38E–G) (for measurements, see Tab. A4). The posterior edge of the mandibular symphysis ends nearly at the middle part of p3. The ventral margin of the mandible is convex in lateral view (Fig. 38E). The mental foramen is situated below the p3. In ventral view,

the small foramen is present at the central portion of the mandibular symphysis and the lingual mandibular outline is U-shaped (Fig. 38F, G). Only the basal part of a right tusk-like incisor is preserved in its socket. Another specimen DMR-KS-05-03-31-28 preserves a nearly complete mandibular symphysis and left p2 and p3 sockets (Fig. 38H, I). The left mandibular body behind the p3 is broken away. All lower cheek teeth are heavily worn and rectangular in occlusal outline (Fig. 38F) (for measurements, see Tab. 13).



Figure 38. Cranial, mandibular, dental remains of *Rhinoceros sondaicus* from Khok Sung: (A) DMR-05-03-00-128, a left P2 in occlusal view; (B) DMR-KS-05-03-22-17, a left P3 in occlusal view; (C) DMR-KS-05-03-00-129, a left M1 in occlusal view; (D) DMR-KS-05-03-00-127, a left M3 in occlusal view; (E–G) DMR-KS-05-03-00-126, a mandible in lateral (E), occlusal (F) and ventral (G) views; (H–I) DMR-KS-05-03-31-28, a fragmentary mandible in occlusal (H) and lateral (I) views; (J–K) DMR-KS-05-03-00-56, a nasal in dorsal (J) and lateral (K) views.

Table 13. Measurements (in millimeters) of cheek teeth of Khok Sung rhinoceroses, *Rhinoceros sondaicus* and *Rhinoceros unicornis*, compared to recent specimens (data from Guérin (1980)). “(i)” refers to an isolated tooth and “(m)” indicates a tooth attached to the mandible.

		<i>Rhinoceros sondaicus</i>			<i>Rhinoceros unicornis</i>		
		Khok Sung		Recent	Khok Sung		Recent
		Anterior	Posterior	Range	Anterior	Posterior	Range
Upper cheek teeth							
P2	L	35.57 (i)		30–38.5	–		37–45.5
	W	42.34 (i)	41.24 (i)	34.5–44	–		43–48
P3	L	42.00 (i)		36.5–50	–		43–50
	W	55.36 (i)	53.70 (i)	42–55	–		55.5–60.5
P4	L	–		41–47.5	–		42–51
	W	–		52–59	–		59–69.5
M1	L	51.38 (i)		46–51	47.95 (i)		48–58
	W	63.53 (i)	58.67 (i)	52.5–60	70.48 (i)	58.80 (i)	62–72.5
M2	L	–		44.5–55	–		53–62
	W	–		53–62.5	–		64.5–76
M3	L	55.65 (i)		44.5–61.5	–		59–65
	W	55.92 (i)		43.5–57	–		56–68.5
Lower cheek teeth							
p2	L	–		25–29.5	>30.80 (i)		31–32
	W	–		15.5–21	18.15 (i)	22.39 (i)	21.5–24.5
p3	L	42.83 (m)		33–39	40.24 (m)		38–42
	W	26.58 (m)	29.92 (m)	22–27.5	–		27–32
p4	L	43.03 (m)		36.5–42.5	48.13 (m)		41–46
	W	27.71 (m)	33.42 (m)	24–29	–		29–34
m1	L	41.45 (m)		41–46.5	42.57 (m)		46–48
	W	28.8–29.67 (m)	30.88 (m)	26–32	–		28–32.5
m2	L	44.83–48.87 (m)		40.5–51	50.74 (m)		52–56.5
	W	29.65 (m)	30.78–31.79 (m)	27–32.5	–		31–36
m3	L	54.90 (m)		41–53	55.48 (m)		49.5–60
	W	32.54 (m)	25.11* (m)	24.5–29.5	–		29–35
Lower tooth rows							
		DMR-KS-05-03-00-126		Recent	DMR-KS-05-03-17-13		Recent
Molar row length		133 (right)		126.5–147	158		147.5–161
Tooth row length		>238		211.5–257	–		242–276

Nasal: a nasal bone (DMR-KS-05-03-00-56) is short and robust, bending downward and narrowing anteriorly towards the tip (Fig. 38J). The anterior surface is nearly straight in lateral view (Fig. 38K), whereas its ventral surface is flattened at the central suture. This nasal bone is most similar to *Rhinoceros sondaicus* (e.g., specimen MNHN-ZMO-1985-159) because its anterior part is pointed rather than rounded (Colbert, 1942). In comparison, *R. unicornis* displays a convex anterior surface in lateral view and a well-developed horn protuberance of the nasal region. The maximum length and width of the nasal are 131.1 mm and 88.8 mm, respectively.

Postcranial remains: postcranial elements include a scapula (Fig. 39A, B), a humerus (Fig. 39C–E), three metacarpal bones (metacarpus II, III, and IV: fig. 39F–H), a tibia, a calcaneus (Fig. 39I), and an astragalus (Fig. 39J). All postcranial remains are comparable in size to the recent material (Guérin, 1980) (for measurements, see Tab. A1).



Figure 39. Postcranial remains of *Rhinoceros sondaicus* from Khok Sung: (A–B) DMR-KS-05-03-00-58, a left scapula in lateral (A) and distal (B) views; (C–E) DMR-KS-05-03-31-3, a left humerus in anterior (C), proximal (D), and distal (E) views; (F–H) DMR-KS-05-04-05-15, a right metacarpus IV in posterior (F), proximal (G), and distal (H) views; (I) DMR-KS-05-04-27-19, a right calcaneus in lateral view; (J) DMR-KS-05-03-26-23, a left astragalus in dorsal view.

Taxonomic remarks and comparisons

Four isolated cheek teeth (P2, P3, M1, and M3) assigned to *R. sondaicus* are characterized by the following morphological features: a presence of the moderately developed crochet, sinuosity of the ectoloph, distinct parastyle fold, and deeper median valley compared to the posterior valley, and the absences of an antecrochet, protocone fold, and metacone bulge on M3. All of these characters coincide with the upper molars of *R. sondaicus* (Pocock, 1945; Hooijer, 1946; Zin-Maung-Maung-Thein et al., 2006; Groves and Leslie Jr, 2011).

Large tusk-like incisors (i2) are notably typical of Asian rhinoceroses. The two small alveoli corresponding to the lost central incisors are autapomorphic of *Rhinoceros* (Groves and Leslie Jr, 2011). Our observations on the recent mandible iPHEP M05.5.001.B and MNHN-ZMO-1985-159 demonstrate that an alveolus extension of the lower incisors that reach posteriorly to the lingual side of the p2 is a characteristic of both living Javan (*R. sondaicus*) and Indian (*R. unicornis*) rhinoceroses (Tong and Guérin, 2009). This feature efficiently distinguishes *Rhinoceros* from the Sumatran rhinoceros, *Dicerorhinus sumatrensis*, where the alveoli of the lower incisors do not extend as far (Tong and Guérin, 2009). In the mandibles DMR-KS-05-03-00-126 and DMR-KS-05-03-31-28, the lower incisor alveoli extend posteriorly into the mandibular symphysis, ventral to the lingual side of the p2 (Fig. 38H, I). The latter specimen also shares similar mandibular dimensions (Tab. A4) and morphology with the former specimen.

Isolated lower molars of rhinoceroses from Khok Sung are difficult to assign to either *R. unicornis* or *R. sondaicus* due to heavy wear. In addition, there is a significant size overlap between these two species (Guérin, 1980). The lengths of lower cheek teeth and molar rows provide better distinction (little overlap in size) than those of isolated teeth. The lengths and widths of the cheek teeth on the mandible DMR-KS-05-03-00-126 fall almost within the range of *R. sondaicus*, with the exception of some specimens (p3, p4, and m3) that fit well with the larger-

sized *R. unicornis* (Tab. 13). However, the lengths of the mandibular cheek tooth and molar rows of this specimen fall within the ranges of *R. sondaicus* (211.5–257 mm and 126.5–147 mm, respectively) and outside of the ranges for *R. unicornis* (Guérin 1980: table. 6). We thus assign two mandibles, DMR-KS-05-03-00-126 and DMR-KS-05-03-31-28, to *R. sondaicus*.

***Rhinoceros unicornis* Linnaeus, 1758**

Referred material: a left mandible with p3–m3, DMR-KS-05-03-17-13; a left p2, DMR-KS-05-03-19-4; a right M1, KS-05-03-18-X; a left femur, DMR-KS-05-03-00-63; a left astragalus, DMR-KS-05-03-00-67

Material description

Upper dentition: a relatively worn M1 (DMR-KS-05-03-18-X) is nearly square in outline and displays a flattened ectoloph and a well-developed crochet, medifossette, and posterior fossette (Fig. 40A) (for measurements, see Tab. 13).

Mandible and lower dentition: a hemi-mandible (DMR-KS-05-03-17-13) is strongly compressed laterally and preserves a partial mandibular ramus and body with worn cheek teeth, except for the m3 which is unbroken (Fig. 40C–E) (for measurements, see Tab. A4). The lingual portion along the mandible is entirely broken. The mandibular depth below the m3 is higher than that of *R. sondaicus*. An isolated p2 is relatively worn and broken at its posterior part (Fig. 40B). At the lingual side of the p2, the anterior valley is slightly developed, whereas the posterior valley is prominent.

Postcranial remains: an isolated femur (Fig. 40F, G) and astragalus are comparable in size to *Rhinoceros unicornis*, but are larger than *Rhinoceros sondaicus* (Guérin, 1980) (for measurements, see Tab. A1).

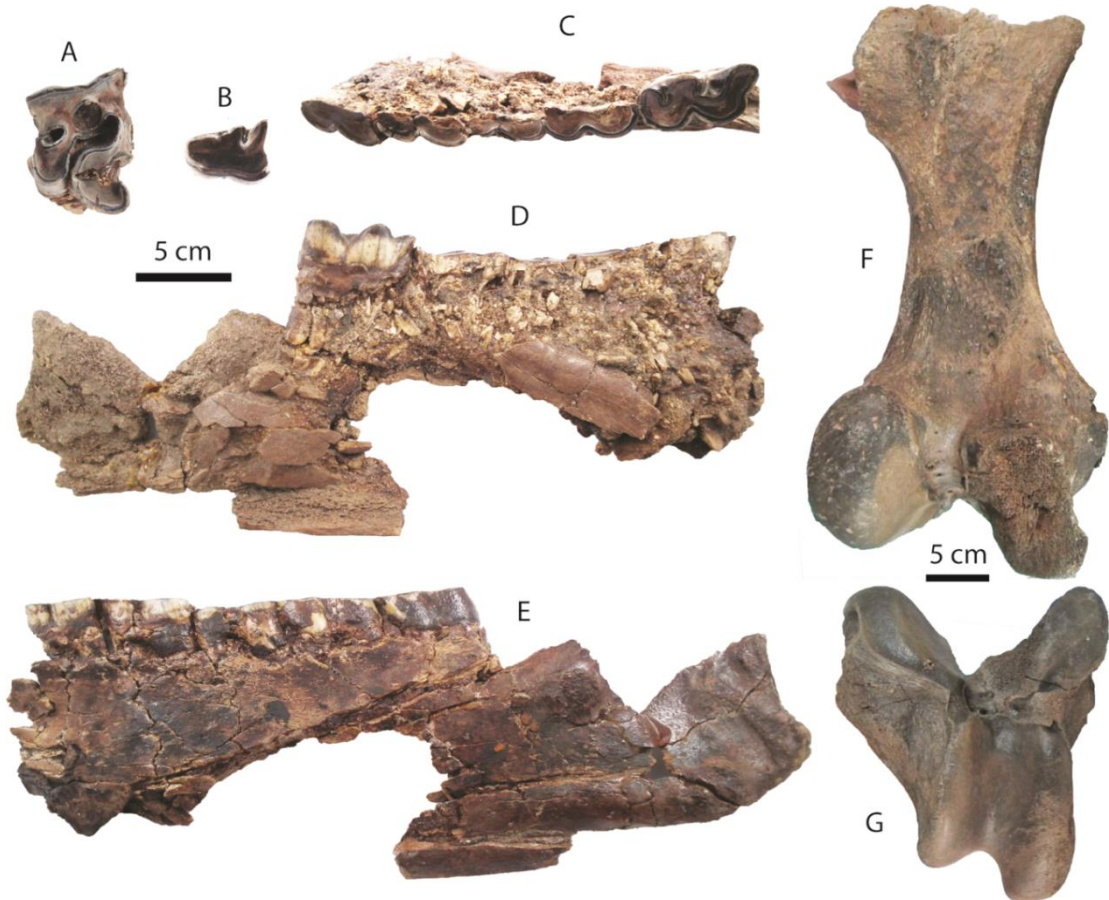


Figure 40. Remains of *Rhinoceros unicornis* from Khok Sung: (A) DMR-KS-05-03-18-X, a right M1 in occlusal view; (B) DMR-KS-05-03-19-4, a left p2 in occlusal view; (C–E) DMR-KS-05-03-17-13, a left mandible in occlusal (C), medial (D), and lateral (E) views; (F–G) DMR-KS-05-03-00-63, a left femur in posterior (F) and distal (G) views.

Taxonomic remarks and comparisons

We assign the M1 (DMR-KS-05-03-18-X) to *R. unicornis* according to the presence of the flattened ectoloph and enclosed medifossette (on a worn specimen), as well as its larger size than that of *R. sondaicus*. These upper molar features are characteristic of *R. unicornis* (Colbert, 1942). For the lower dentition, the size of the isolated p2 (DMR-KS-05-03-19-4) and the molar row length of the mandible DMR-KS-05-03-17-13 (Tab. 13) are comparable to those of recent *R. unicornis* (31–32 mm and 147.5–161 mm, respectively) (Guérin 1980: table. 6). We therefore identify another species of rhinoceroses, *R. unicornis*, at Khok Sung.

Order ARTIODACTYLA Owen, 1848

Family SUIDAE Gray, 1821

Genus *Sus* Linnaeus, 1758

Sus barbatus Müller, 1838

Referred material: a left maxillary fragment with P3–M2, DMR-KS-05-04-19-2; two left M2—DMR-KS-05-04-19-5 and DMR-KS-05-03-18-23 (posterior portion); two right M3—DMR-KS-05-04-03-4 and DMR-KS-05-04-19-4 (anterior portion); two mandible with two tooth rows—DMR-KS-05-03-15-1 (right: i1, i2, c1, p2, and p3 and left: i1, i2, c1, and p2–m2) and DMR-KS-05-04-19-1 (right: i1, i2, c1, and p1–m3 and left: i1, i2, c1, and p1–p4); a left posterior fragment of m3, DMR-KS-05-04-19-3; a right humerus, DMR-KS-05-03-26-8

Material description

Upper dentition: DMR-KS-05-04-19-2 is a maxillary tooth row preserving a slightly worn P3 to M2 (Fig. 41A). The P3 and P4 show *Sus*-like patterns with distinctly pre- and poststyles on the buccal side. On the P3, the paracone is well-developed and the postcrista projects posterobuccally. On the P4, three main cusps (protocone, paracone, and metacone) are distinct and the protofossa is present. Upper molars are unworn to slightly worn and exhibit distinct main (protocone, paracone, metacone, tetracone, and pentacone) and accessory (tetrapreconule, pentapreconule, and ectoconule) cusps. The posterior cingulum on the M2 is more developed than on the M1 (Fig. 41A–C). The M3 (DMR-KS-05-04-03-4: fig. 41D) is unworn and subtriangular in outline and has a distinct anterior cingulum, pentacone, and pentapreconule and bulky accessory cusps. Another M3 (DMR-KS-05-04-19-4) does not preserve a posterior part but has well-developed main cusps, anterior cingulum, median valley, tetrapreconule, and ectoconule (Fig. 41E). The cheek teeth of DMR-KS-05-04-19-4 are larger than those of DMR-KS-05-04-03-4.



Figure 41. Remains of *Sus barbatus* from Khok Sung: (A) DMR-KS-05-04-19-2, a left upper cheek tooth row in occlusal view; (B) DMR-KS-05-04-19-5, a left M2; (C) DMR-KS-05-03-18-23, a left fragmentary M2; (D) DMR-KS-05-04-03-4, a right M3; (E) DMR-KS-05-04-19-4, a right M3; (F–G) DMR-KS-05-03-15-1, a mandible in occlusal (F) and lateral (G) views; (H–I) DMR-KS-05-04-19-1, a mandible in occlusal (H) and lateral (I) views; (J) DMR-KS-05-04-19-3, a left fragmentary m3; (K–N) DMR-KS-05-03-26-8, a right humerus in proximal (K), posterior (L), anterior (M), and distal (N) views. Cross-sections of canines are given. All isolated teeth are shown in occlusal view.

Mandible and lower dentition: DMR-KS-05-03-15-1 is incomplete, lacking the body and ascending ramus, broken posterior to the right p3 and to the left m2 (Fig. 41F, G) (for measurements, see Tab. A5). The mandible is inflated. The small mental foramen is present below the diastema between p1 and p2. Only the i3 and p1 are missing. The left p2 is not aligned along the cheek tooth row due to the deformation. The specimen DMR-KS-05-04-19-1 preserves a complete symphysis and a right body with the tooth row. The ramus is broken away (Fig. 41H, I). The mandibular body is successively inflated. The mental foramina are situated below the diastema between p1 and p2. For the specimen DMR-KS-05-04-19-1, the teeth are complete and moderately to heavily worn but the third incisors are missing.

Lower incisors show a chisel-like appearance with long roots. The i2 is larger than the i1. Lower canines are slender and pointed, and curve backward. The lower canines of the mandible DMR-KS-05-03-15-1 belong to a male individual because of a more sharply triangular section (Hillson, 2005) (Fig. 41F). The mandible DMR-KS-05-04-19-1 possesses a female canine characterized by more rounded cross-sections and well-developed roots (Hillson, 2005) (Fig. 41H). The lower canines of the male specimen are more laterally inclined (about 30° from the cheek teeth) than those of the female individual (about 15°). The cross-section outlines of male canines (DMR-KS-05-03-15-1) are of the “verrucosic” type in which the posterior side is narrower than the labial one (Fig. 41F). All lower cheek teeth exhibit bunodont patterns with accessory tubercles, like in *Sus*. The lower cheek teeth increase in size from anteriorly to posteriorly (Tab. 14). Lower premolars are slightly to moderately worn. The p1 is unicuspid. Other premolars are tricuspid. All cuspids are sharp. The highest cuspid on the premolars is the metaconid. Lower molars are moderately to heavily worn and rectangular in outline (Fig. 41F–J). The lower molars show complex occlusal patterns with well-developed main cuspids (protoconid, metaconid, hypoconid, entoconid, and pentaconid) and a bulky median column (hypopreconulid). The m2 is

much larger and has a more developed posterior cingulid than the m1 (Fig. 41F, H). The m3 (DMR-KS-05-04-19-1) is elongated posteriorly (Fig. 41H). It has a well-developed talonid with bulky main and accessory cuspids (pentaconid, pentapreconulid, hexaconid, heptaconid). Another isolated posterior fragment (talonid) of the m3 (DMR-KS-05-04-19-3) is also elongated, as long as that of DMR-KS-05-04-19-1. This specimen exhibits smooth occlusal surfaces with wear and well developed main and accessory cuspids (Fig. 41J). The m3 is longer than the combination of m1 and m2 (Tab. 14).

Table 14. Measurements (lengths and widths in millimeters) of cheek teeth of Khok Sung *Sus barbatus* compared to the recent and fossil species. The number of specimens is given within the parentheses. The measured specimens of recent *Sus scrofa* include three subspecies: *S. s. scrofa*, *S. s. vittatus*, and *S. s. attila*.

		Khok Sung	Recent				Java (Pleistocene)	
		<i>Sus barbatus</i>	<i>Sus scrofa</i>	<i>Sus barbatus</i>	<i>Sus verrucosus</i>	<i>Sus celebensis</i>	<i>Sus brachygnathus</i>	<i>Sus macrognathus</i>
P3	L	16.75	12.33–14.41 (16)	13.17–14.98 (12)	11.87–13.77 (8)	9.37	11.09–12.29 (7)	12.47–13.86 (2)
	W	14.42	10.12–12.19 (16)	10.06–13.22 (12)	9.71–12.64 (8)	7.35	9.60–11.54 (7)	10.75–13.43 (2)
P4	L	15.06	11.41–14.61 (16)	12.56–14.81 (12)	11.85–13.97 (8)	8.96–9.44 (3)	10.35–11.61 (7)	11.89–12.39 (3)
	W	18.59	12.77–15.23 (16)	13.51–16.00 (12)	13.23–14.82 (8)	10.68–11.01 (3)	11.05–13.80 (7)	13.72–15.68 (3)
M1	L	20.68	14.01–17.88 (16)	16.71–19.24 (12)	14.36–16.13 (8)	13.44–13.76 (3)	13.89–14.94 (6)	13.62–17.17 (3)
	W	17.17	13.59–17.57 (16)	13.59–15.85 (12)	13.32–15.78 (8)	10.59–11.49 (3)	12.68–14.36 (6)	12.57–15.54 (3)
M2	L	29.35– 29.49 (2)	20.08–24.78 (16)	22.60–24.60 (12)	20.53–22.39 (8)	16.89–17.98 (4)	19.81–24.26 (7)	17.17–24.38 (4)
	W	21.37– 23.40 (3)	16.43–20.82 (16)	17.45–19.89 (12)	16.82–19.74 (8)	13.33–14.96 (4)	16.09–17.97 (7)	15.54–21.06 (4)
M3	L	37.36	29.09–39.01 (16)	30.31–36.50 (12)	31.75–37.13 (8)	21.59–24.81 (3)	27.27–33.26 (8)	31.44–40.89 (60)
	W	21.46– 24.97 (2)	19.68–23.76 (16)	17.44–24.94 (12)	18.73–20.59 (8)	14.88–16.18 (3)	18.08–20.37 (8)	19.95–24.30 (6)

p1	L	7.32– 7.71 (2)	7.03–9.13 (8)	7.25–9.51 (8)	5.42–7.81 (3)	?	6.32–9.98 (6)	?
	W	4.16– 4.35 (2)	3.56–4.17 (8)	3.33–4.09 (8)	3.22–3.88 (3)	?	3.50–5.15 (6)	?
p2	L	11.71– 13.17 (4)	10.42–13.21 (16)	12.10–14.80 (12)	10.77–11.89 (8)	?	9.96–12.02 (6)	?
	W	5.55– 6.66 (4)	4.48–6.49 (16)	4.78–6.61 (12)	5.84–6.43 (8)	?	4.87–5.46 (6)	?
p3	L	13.17– 14.31 (4)	13.09–15.75 (16)	14.01–16.07 (12)	12.91–14.85 (8)	10.31	11.94–14.59 (7)	12.14–13.84 (2)
	W	7.84– 8.60 (4)	6.32–9.10 (16)	6.51–8.53 (12)	6.49–7.80 (8)	6.57	6.56–7.38 (7)	7.44–7.46 (2)
p4	L	13.87– 15.01 (3)	13.40–16.05 (16)	14.57–17.29 (12)	14.44–16.10 (8)	10.11–10.22 (2)	12.75–14.30 (8)	15.41–15.75 (2)
	W	10.13– 11.68 (3)	8.78–11.44 (16)	9.18–10.60 (12)	8.79–11.28 (8)	7.46–8.34 (2)	8.84–10.60 (8)	9.56–10.48 (2)
m1	L	14.32– 18.47 (2)	14.64–18.75 (16)	15.94–19.60 (12)	12.90–14.95 (8)	12.34–12.61 (3)	13.77–14.83 (8)	15.81–17.94 (2)
	W	13.11– 13.8 (2)	11.55–13.94 (16)	10.84–13.22 (12)	11.04–13.56 (8)	8.55–9.92 (3)	10.80–12.07 (8)	11.79–12.11 (2)
m2	L	19.96– 23.38 (2)	19.66–24.24 (16)	21.84–23.97 (12)	19.88–21.22 (8)	15.35–16.01 (4)	17.19–20.84 (8)	21.31–25.00 (3)
	W	17.65– 18.06 (2)	14.61–17.39 (16)	14.61–16.56 (12)	14.14–15.95 (8)	10.77–13.25 (4)	12.96–14.45 (8)	14.15–16.30 (3)
m3	L	40.92	32.92–41.27 (16)	35.60–43.02 (12)	37.45–40.27 (8)	21.68–24.44 (3)	30.56–39.84 (7)	40.72–46.37 (4)
	W	19.89	16.71–19.32 (16)	16.24–19.74 (12)	15.92–17.84 (8)	12.16–13.38 (3)	16.06–21.44 (7)	15.84–18.15 (4)

Postcranial bone: DMR-KS-05-03-26-8 is a complete humerus (Fig. 41K–N), characterized by its prominent tubercle slightly overhanging the large bicipital groove (Fig. 41K), proximal part becoming wider than long (Fig. 41K), mesially flat and laterally compressed shaft, distinct deltoid ridge starting at the mid-shaft (Fig. 41L, M), relatively large supinator ridge (Fig. 41M), shallow musculo-spiral groove (Fig. 41N), and small deltoid tuberosity (Fig. 41N). The size and morphology of the humerus DMR-KS-05-03-26-8 resemble those of recent *Sus barbatus* (for measurements, see Tab. A1).

Taxonomic remarks and comparisons

We compare our material to some Pleistocene Southeast Asian suid species, although only two distinct suid species, *S. scrofa* and *S. barbatus*, are known from many Pleistocene localities of mainland Southeast Asia. The sizes of the Khok Sung material are obviously larger than those of Pleistocene and extant Indonesian suids (*S. brachygnathus*, *S. macrognathus*, *S. verrucosus*, and *S. celebensis*) (Tab. 14). The Khok Sung suid material is comparable in size to *S. scrofa* and *S. barbatus*. The two suid mandibles from Khok Sung also show some distinctive taxonomic characters of *S. scrofa* and *S. barbatus*. For example, the mandible is not laterally enlarged or swollen and the diastema from p1 to p2 is longer than from c1 to p1, which are only characteristics of some species of *Sus*: *S. scrofa*, *S. celebensis*, and *S. barbatus* (Groves, 1997). The lower premolar rows on the mandibles are aligned along the mandible, unlike *S. verrucosus* and *S. celebensis* in which the premolar rows diverge anteriorly (Groves, 1997).

However, it is difficult to distinguish *S. scrofa* from *S. barbatus* only based on the cheek teeth because both species overlap in size (Tab. 14) and show almost similar dental patterns. The main differential characters between *S. scrofa* and *S. barbatus* are defined on the basis of the shape of lower canines in male individuals, whether the outline of the cross section is of the “scrofic” (i.e. the posterior side is wider than the labial one (*S. scrofa*)) or “verrucosic” (*S. barbatus*) type (Badoux, 1959; Hardjasasmita, 1987). Similarly, this distinctive feature is demonstrated by the lower male canine index (the width of labial surface as a percentage of the width of posterior surface) (Groves, 1981, 1997). The canine index ranges from 61.5 to 109.1 for recent *S. scrofa* and from 105.6 to 144.4 for extant *S. barbatus* (Groves 1981: table. 1). The lower canines of the male mandible DMR-KS-05-03-15-1 show the verrucosic type with the canine index of *Sus barbatus* (for the detailed calculation see Tab. 15). We also provide the canine index of the female specimen DMR-KS-05-04-19-1 in Tab. 15. A minor distinctive character between *S.*

scrofa and *S. barbatus* is differences of the posterior accessory median cuspid (pentapreconulid) on the talonid. The pentapreconulid on the m3 is small or absent in *S. barbatus* (Badoux, 1959). For other molar characters, *S. barbatus* shows more complex patterns with accessory tubercles and more rugose enamel than in *S. scrofa* (Tougaard, 1998; Bacon et al., 2011). However, the latter character is useless to make a distinction between both suid species according to our observations on the recent material of *S. barbatus*. The enamel surfaces of the molars in *S. barbatus* are often smooth or even sometimes smoother than in *S. scrofa*.

Table 15. Measurements (in millimeters) of lower canines of *Sus barbatus* from Khok Sung. The canine index is expressed by the following formula: labial surface*100/posterior surface (Groves, 1981).

Specimen no.		Widths			Canine index
		anterolingual surface	posterior surface	labial surface	
DMR-KS-05-03-15-1 (male)	right c1	13.61	8.54	11.46	134.2
	left c1	13.88	9.05	11.57	127.8
DMR-KS-05-04-19-1 (female)	right c1	13.18	11.92	10.32	86.6
	left c1	13.30	12.21	10.54	86.3

We assign the female mandible (DMR-KS-05-04-19-1), as well as other isolated teeth, to *S. barbatus* according to those described features. We also suggest that Pleistocene *Sus barbatus* probably show evidence of sexual size dimorphism because the female specimen DMR-KS-05-04-19-1 is markedly smaller than the male specimen DMR-KS-05-03-15-1, as seen in their recent population.

Family CERVIDAE Gray, 1821

Genus *Axis* Hamilton-Smith, 1827

Axis axis (Erxleben, 1777)

Referred material: four crania—DMR-KS-05-04-18-50 (with two antlers) and DMR-KS-05-03-00-30 (with left partial and right broken antlers), DMR-KS-05-03-18-X9 (with pedicles), and DMR-KS-05-03-27-1 (with pedicles); three right complete antlers—DMR-KS-05-03-31-30 and DMR-KS-05-03-22-4; a nearly complete left antler, DMR-KS-05-04-4-1; five right fragmentary antlers—DMR-KS-05-03-18-21, DMR-KS-05-03-19-82, DMR-KS-05-03-28-22, DMR-KS-05-06-22-2, and DMR-KS-05-03-28-1; eight left fragmentary antlers—DMR-KS-05-03-00-12, DMR-KS-05-03-19-81, DMR-KS-05-03-22-2, DMR-KS-05-03-24-1, DMR-KS-05-04-09-1, DMR-KS-05-03-19-13, DMR-KS-05-03-26-21, and DMR-KS-05-03-08-17; two left fragmentary maxilla—DMR-KS-05-03-28-6 (with M1–M3) and DMR-KS-05-03-08-31 (with P3, P4, and M1 root); a right P4, DMR-KS-05-04-01-3; a left M1, DMR-KS-05-04-28-5; a left M2, DMR-KS-05-03-14-5; thirteen right mandibles—DMR-KS-05-03-14-2 (with m3), DMR-KS-05-03-20-1 (with p4–m3), DMR-KS-05-03-20-2 (with m2 and m3), DMR-KS-05-03-22-7 (with m2 and m3), DMR-KS-05-04-03-1 (with p2–m3), and DMR-KS-05-03-27-3 (with m2 and m3), DMR-KS-05-03-19-1 (with p2–m3), DMR-KS-05-03-22-8 (with m2 and m3), DMR-KS-05-04-01-1 (with p2–m3), DMR-KS-05-03-24-4 (with m2), DMR-KS-05-03-26-12 (with m2 and m3), DMR-KS-05-04-7-10 (with p3, m1, and m2), and DMR-KS-05-03-26-10 (with p2–m1); eight left mandibles—DMR-KS-05-03-18-22 (with p2), DMR-KS-05-03-22-6 (with m1–m3), DMR-KS-05-03-27-22 (with p3–m2 sockets and broken m3), and DMR-KS-05-04-09-2 (with p3, p4, m1 and m2 sockets, and m3), DMR-KS-05-03-00-102 (with p4 and m1), DMR-KS-05-03-19-2 (with m1–m3), DMR-KS-05-03-23-1 (with p2 and p3 roots and p4–m3), and DMR-KS-05-03-29-1 (with p2–m3); a left m1, DMR-KS-05-04-28-6; three m2, DMR-KS-05-03-25-4 (right), DMR-KS-05-03-00-104 (left), and DMR-KS-05-03-22-11 (left); four left m3—DMR-KS-05-04-9-4, DMR-KS-05-03-22-9, DMR-KS-05-04-01-2, and DMR-KS-05-03-08-33; three right fragmentary

humeri (distal part)—DMR-KS-05-03-13-4, DMR-KS-05-04-11-32, and DMR-KS-05-03-17-17; six metacarpi—DMR-KS-05-03-18-2 (right), DMR-KS-05-03-19-3 (right), DMR-KS-05-03-22-28 (right), DMR-KS-05-03-08-2 (right), DMR-KS-05-04-30-20 (right proximal fragment), and DMR-KS-05-03-19-37 (left); a right fragmentary femur, DMR-KS-05-03-27-4 (distal part); three metatarsus, DMR-KS-05-03-26-3 (right), DMR-KS-05-03-29-30 (left), and DMR-KS-05-03-15-14 (left)

Material description

Crania and upper dentition: four crania are almost complete, lacking only the anterior portions (e.g., nasal, jugal, palatine, and maxilla) (Fig. 42A–D). The specimen DMR-KS-05-04-18-50 shows nearly complete antlers, lacking only the left brow tine (Fig. 42A, B). The cranium DMR-KS-05-03-00-30 possesses a right antler portion preserving the complete brow tine but the broken main beam (Fig. 42C, D). The specimens DMR-KS-05-03-18-X9 (Fig. 42E) and DMR-KS-05-03-27-1 (Fig. 42F, G) preserve most of the rear part of the skull but lacks zygomatic arcs and antler portions. The specimen DMR-KS-05-03-27-1 preserves a deformed frontal area and broken pedicles (Fig. 42F). The basioccipital and basisphenoid are subtriangular in ventral view and show well-developed anterior and posterior tuberosities with a longitudinal groove running along the central part (Fig. 42B, D, G). The lateral edges of the basioccipital and basisphenoid are concave like in *Axis*. The foramina ovale are large and open ventrolaterally. The shed antlers are characterized by three main tines, smooth surfaces, a short pedicle and brow tine, a long and slender main beam, a high angle (about 100-120°) between the main beam and the brow tine, and a well-developed burr (Fig. 42A, C, H–L). A small ornamented tine (or knob) is sometimes present along the dorsal surface of the brow tine or at the main beam-brow tine junction (Fig. 42C, J–L). The main beam is oriented upward, laterally, and posteriorly, and consists of forked tines apically. At the antlered crown, the inner tine is much shorter than the outer one (Fig. 42A, H, I). The skull and antler exhibit a typical arrangement of recent *Axis axis* (e.g., the orientation of

the main beam and brow tine, the bifurcation at the apical crown tine, and the shape of the basioccipital and basisphenoid) (for measurements, see Tab. A6).



Figure 42. Cranial remains of *Axis axis* from Khok Sung: (A–B) DMR-KS-05-04-18-50, a cranium with nearly complete antlers in dorsal (A) and ventral (B) views; (C–D) DMR-KS-05-03-00-30, a cranium in lateral (C) and ventral (D) views; (E) DMR-KS-05-03-18-X9, a cranium in anterior view; (F–G) DMR-KS-05-03-27-1, a cranium in dorsal (F) and ventral (G) views; (H) DMR-KS-05-03-31-30, a right antler in anterior view; (I) DMR-KS-05-03-22-4, a right antler in lateral view; (J) DMR-KS-05-03-18-21, a left antler fragment in lateral view; (K) DMR-05-03-22-2, a left antler fragment in lateral view; (L) DMR-KS-05-03-19-81, a left antler fragment in medial view.

P3 and P4 are similar to recent *Axis*, characterized by well-developed styles, medial cristae (more distinct on the P4), and posterolingual fossettes (Fig. 43A) (for measurements, see Tab. 16). On the P4, the medial cristae join the postmetacrista and divide the fossa into two islands (Fig. 43A, C). Upper molars display distinct styles (particularly the mesostyle), entostyles, and anterior cingula (Fig. 43B, D, E). The metaconule fold is slightly developed. The M2 is slightly wider than the M3 (Tab. 16). The posterior lobe of the M3 is reduced in width (Fig. 43B).

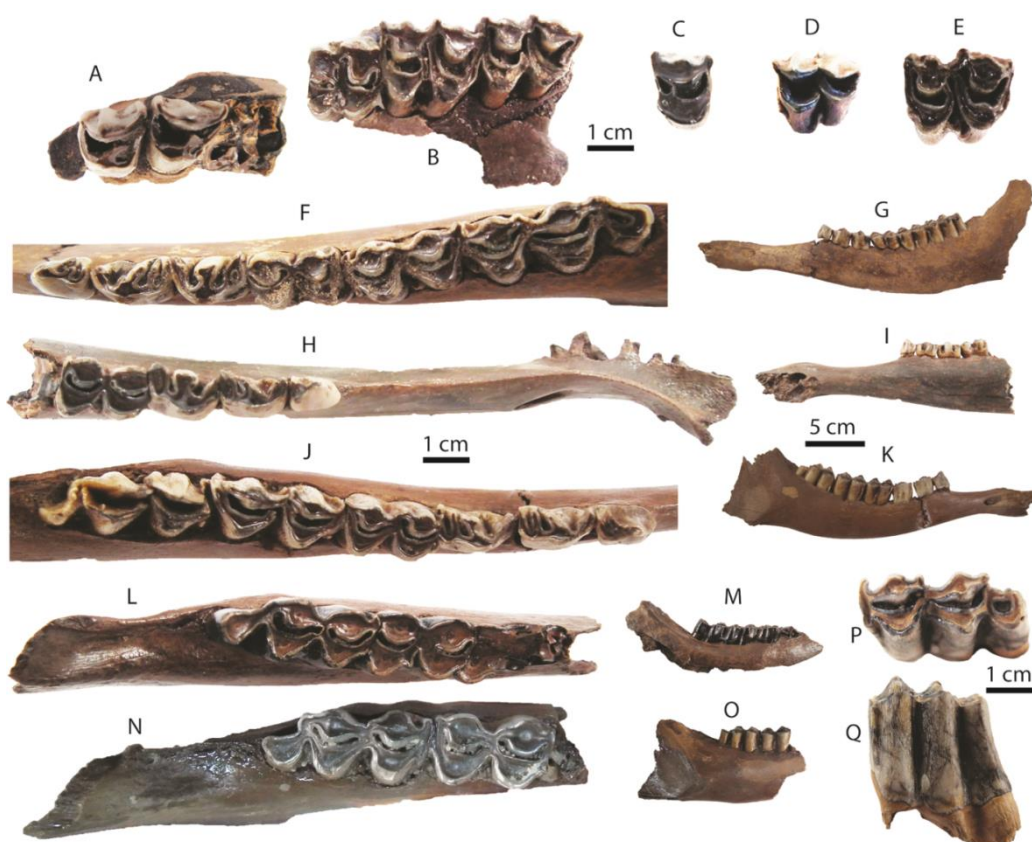


Figure 43. Dental remains of *Axis axis* from Khok Sung: **(A)** DMR-KS-05-03-08-31, an upper left P3 and P4 in occlusal view; **(B)** DMR-KS-05-03-28-6, a left upper molar row in occlusal view; **(C)** DMR-KS-05-04-01-3, a right P4 in occlusal view; **(D)** DMR-KS-05-04-28-5, a left M1 in occlusal view; **(E)** DMR-KS-05-03-14-5, a left M2 in occlusal view; **(F–G)** DMR-KS-05-03-29-1, a left mandible in occlusal **(F)** and lateral **(G)** views; **(H–I)** DMR-KS-05-03-26-10, a right mandibular fragment in occlusal **(H)** and medial **(I)** views; **(J–K)** DMR-KS-05-04-03-1, a right mandible in occlusal **(J)** and lateral **(K)** views; **(L–M)** DMR-KS-05-03-20-1, a right mandible in occlusal **(L)** and lateral **(M)** views; **(N–O)** DMR-KS-05-03-22-7, a right mandible in occlusal **(N)** and lateral **(O)** views; **(P–Q)** DMR-KS-05-03-08-33, a left m3 in occlusal **(P)** and buccal **(Q)** views.

Mandibles and lower dentition: twenty one mandibles range from fragmentary (preserving only the broken corpus) to nearly complete (lacking only the ascending ramus and coronoid process) individuals (Fig. 43F–O) (for measurements, see Tab. A7). The mandibular symphyses are almost complete, but all incisors are missing. The protoconulid of the p2 is poorly-developed or absent (Fig. 43F, H, J).

The p3 and p4 exhibit a well-developed metaconid which projects obliquely in occlusal view, posterior to the entoconid (Fig. 43F, H, J) (for measurements, see Tab. 16). The latter conid joins the posthypocristid, forming a back valley on moderately worn teeth. The metaconid is bifurcated (two separated flanges: pre- and postmetacristids) on the p4. All lower molars are morphologically characterized by their brachyodont crowns and well-developed stylids (parastylid, metastylid, and entostylid), ectostylids (basal pillars), and anterior cingulids (also called “goat fold”) (Fig. 43F–Q). On the m3, the posterior ectostylid is absent (Fig. 43F, G, J–Q). The third lobe is ring-shaped as it is present on the recent specimens (e.g., MNHN-ZMO-1901-547, MNHN-ZMO-1988-153, ZSM-1951-70, and ZSM-1961-3) (Fig. 43F, P). But the third lobe is sometimes small and poorly-developed, as observed from the recent specimen ZSM-1963-27 (Fig. 43J, L, N). The back fossa is present on unworn to slightly worn teeth (Fig. 43F, P), but absent on moderately to heavily worn ones (Fig. 43L, N). The posthypoconulidcristid is well-developed, a small crest protruding slightly more posterolingually (Fig. 43F).

Postcranial remains: postcranial bones include isolated humeri (Fig. 44A–B), metacarpi (Fig. 44C–H), a femur (Fig. 44I, J), and metatarsi (Fig. 44K–M). The humerus and femur are fragmentary. We identified here these fossil postcranial bones based on the size and proportion compared with the extant specimens (Tabs 17, A1, A9, A11–A12, and A14).

Table 16. Measurements (lengths and widths in millimeters) of cervid teeth from Khok Sung. N=number of specimens.

	Length			Width		
	N	Range	Mean	N	Range	Mean
<i>Axis axis</i>						
P3	1	12.40	–	1	13.60	–
P4	2	10.04–11.29	10.67	2	12.19–14.28	13.24
M1	2	13.32–15.19	14.26	2	15.60–15.93	15.77
M2	2	18.07–18.08	18.08	2	17.41–17.84	17.63
M3	1	17.53	–	1	16.42	–
p2	6	7.93–9.54	8.72	6	5.44–6.89	5.93
p3	7	9.17–12.11	10.67	7	6.53–7.14	6.88
p4	8	10.64–13.62	11.65	10	6.77–8.13	7.39
m1	9	11.81–18.20	14.2	13	8.27–10.29	9.59
m2	18	15.94–21.42	17.91	19	8.56–11.67	10.56
m3	18	21.69–25.78	24.1	20	8.87–11.89	10.74
<i>Panolia eldii</i>						
P2	1	11.09	–	1	13.97	–
M1	2	12.07–14.95	13.51	2	16.52–17.77	17.15
M2	5	16.67–20.48	19.35	6	17.85–19.35	18.56
M3	5	18.80–21.39	19.96	5	16.99–19.50	18.30
i1	1	12.86	–	1	6.31	–
p2	2	9.97–11.33	10.65	2	7.03–7.44	7.24
p3	2	13.04–13.67	13.36	2	8.33–8.56	8.45
p4	2	13.65–14.05	13.85	2	8.94–9.33	9.14
m1	2	14.67–15.67	15.17	2	11.23–12.25	11.74
m2	2	17.73–19.36	18.55	2	12.63–13.26	12.95
m3	1	23.61	–	1	12.84	–
<i>Rusa unicolor</i>						
M1	1	17.15	–	1	20.10	–
M2	2	20.67–22.88	21.78	2	23.06–27.07	25.07
M3	1	25.37	–	1	24.97	–
p3	1	17.29	–	1	9.26	–
p4	1	17.71	–	2	10.34–13.35	11.85
m1	2	18.64–20.84	19.74	2	14.39–14.59	14.49
m2	3	22.77–23.82	23.33	3	15.37–15.61	15.46
m3	3	30.78–34.57	32.67	3	15.49–17.85	16.79

Table 17. Proportional indices of postcranial remains of identified ruminant taxa from Khok Sung.

Scapula												
Specimen	Taxa	HS/Ld	DHA/Ld	Ld/SLC	LG/BG	GLP/LG	SLC/BG					
DMR-KS-05-03-26-2	<i>Bubalus arnee</i>	1.50	1.28	3.89	1.20	1.30	1.12					
DMR-KS-05-02-20-4	<i>Bubalus arnee</i>	1.39	1.42	4.09	1.23	1.26	0.96					
DMR-KS-05-06-24-4	<i>Panolia eldii</i>	1.95	1.90	4.62	1.10	1.27	0.74					
Humerus												
Specimen	Taxa	GL/Bp	GL/Dp	GL/Bd	GL/Dd	Bp/Bd	Dp/Dd	Bp/Dp	Bd/Dd	Bd/BT		
DMR-KS-05-03-20-2(1)	<i>Bos sauveli</i>	-	-	-	-	-	-	-	0.99	1.04		
DMR-KS-05-03-00-62	<i>Bos gaurus</i>	-	-	3.41	3.66	-	-	-	1.07	1.06		
DMR-KS-05-05-1-1	<i>Bos gaurus</i>	2.91	2.74	3.44	3.67	1.18	1.34	0.94	1.07	1.05		
DMR-KS-05-03-31-1	<i>Bubalus arnee</i>	3.57	3.25	4.30	4.77	1.21	1.47	0.91	1.11	1.05		
DMR-KS-05-03-31-8	<i>Bubalus arnee</i>	3.54	3.29	4.25	4.74	1.20	1.44	0.93	1.11	1.03		
DMR-KS-05-03-13-4	<i>Axis axis</i>	-	-	-	-	-	-	-	1.02	1.09		
DMR-KS-05-04-11-32	<i>Axis axis</i>	-	-	-	-	-	-	-	1.06	1.07		
DMR-KS-05-03-17-17	<i>Axis axis</i>	-	-	-	-	-	-	-	1.12	1.04		
DMR-KS-05-04-11-35	<i>Panolia eldii</i>	-	-	-	-	-	-	-	1.12	1.13		
DMR-KS-05-03-18-1	<i>Panolia eldii</i>	-	-	-	-	-	-	0.82	-	-		
DMR-KS-05-03-15-43	<i>Rusa unicorn</i>	-	-	-	-	-	-	-	1.14	1.12		
Ulna and radius												
Specimen	Taxa	PL/Bp	PL/Dp	PL/Bd	PL/Dd	Bp/Bd	Dd/Dp	Bp/Dp	Bd/Dd	Bp/BFp	Bd/BFd	GL/LO
DMR-KS-05-03-00-61	<i>Bubalus arnee</i>	2.87	5.76	3.04	4.63	1.06	1.24	2.00	1.52	1.15	1.11	3.86
DMR-KS-05-03-31-2	<i>Bubalus arnee</i>	3.15	5.85	3.25	4.61	1.03	1.27	1.86	1.42	1.09	1.12	3.48
DMR-KS-05-03-31-9	<i>Bubalus arnee</i>	3.09	5.88	3.24	4.55	1.05	1.29	1.90	1.40	1.10	1.12	3.45
DMR-KS-05-03-31-10	<i>Panolia eldii</i>	5.06	9.51	5.35	9.32	1.06	1.02	1.88	1.74	1.07	1.14	-
DMR-KS-05-04-11-3	<i>Panolia eldii</i>	4.83	9.09	5.54	8.70	1.15	1.04	1.88	1.57	1.11	1.06	-
DMR-KS-05-03-19-16	<i>Panolia eldii</i>	4.93	8.93	4.87	6.62	0.99	1.35	1.81	1.36	1.22	1.04	-

Table 17 (continued). Proportional indices of postcranial remains of identified ruminant taxa from Khok Sung.

Femur										
Specimen	Taxa	GL/Bp	GL/Dp	GL/Bd	GL/Dd	Bp/Bd	Dd/Dp	Bp/Dp	Dd/Bd	
DMR-KS-05-03-25-9	<i>Rusa unicolor</i>	-	-	-	-	-	-	1.90	-	1.03
DMR-KS-05-03-19-14	<i>Rusa unicolor</i>	-	-	-	-	-	-	1.70	-	1.04
DMR-KS-05-03-26-19	<i>Rusa unicolor</i>	-	-	-	-	-	-	-	1.34	1.05
Femur										
Specimen	Taxa	GL/Bp	GL/Dp	GL/Bd	GL/Dd	Bp/Bd	Dd/Dp	Bp/Dp	Dd/Bd	
DMR-KS-05-03-9-2	<i>Bos gaurus</i>	3.37	6.29	3.92	3.03	1.17	2.07	1.87	1.29	
DMR-KS-05-04-1-1	<i>Bubalus arnee</i>	2.79	5.54	3.48	2.85	1.25	1.95	1.99	1.22	
DMR-KS-05-04-1-2	<i>Bubalus arnee</i>	2.67	5.26	3.38	2.82	1.27	1.86	1.97	1.20	
DMR-KS-05-03-20-8	<i>Bubalus arnee</i>	-	-	-	-	-	-	-	1.46	
DMR-KS-05-03-27-4	<i>Axis axis</i>	-	-	-	-	-	-	-	1.37	
DMR-KS-05-03-27-11	<i>Panolia eldii</i>	-	-	-	-	1.26	2.23	2.11	1.33	
DMR-KS-05-03-17-36	<i>Panolia eldii</i>	-	-	-	-	1.21	2.06	1.93	1.29	
DMR-KS-05-03-28-20	<i>Panolia eldii</i>	-	-	-	-	-	-	-	1.34	
DMR-KS-05-04-05-38	<i>Panolia eldii</i>	-	-	-	-	-	-	1.92	-	
DMR-KS-05-03-00-119	<i>Panolia eldii</i>	-	-	-	-	-	-	-	1.38	
DMR-KS-05-03-19-2	<i>Panolia eldii</i>	-	-	-	-	-	-	-	1.41	
DMR-KS-05-08-16-1	<i>Panolia eldii</i>	-	-	-	-	-	-	1.84	-	
DMR-KS-05-04-11-2	<i>Rusa unicolor</i>	-	-	-	-	-	-	-	1.27	
DMR-KS-05-03-19-7	<i>Rusa unicolor</i>	-	-	-	-	-	-	1.51	-	
DMR-KS-05-03-12-2*	<i>Rusa unicolor</i>	-	-	-	-	-	-	1.52	-	
DMR-KS-05-04-30-9	<i>Rusa unicolor</i>	-	-	-	-	-	-	-	1.27	
DMR-KS-05-04-19-10	<i>Rusa unicolor</i>	-	-	-	-	-	-	-	1.11	
Tibia										
Specimen	Taxa	GL/Bp	GL/Dp	GL/Bd	GL/Dd	Bp/Bd	Dp/Dd	Bp/Dp	Bd/Dd	
DMR-KS-05-04-1-11	<i>Bubalus arnee</i>	3.24	3.43	4.82	6.03	1.49	1.76	1.06	1.25	
DMR-KS-05-04-1-3	<i>Bubalus arnee</i>	3.31	3.50	5.01	6.29	1.51	1.80	1.06	1.25	
DMR-KS-05-03-20-9	<i>Bubalus arnee</i>	3.21	3.83	4.60	6.29	1.43	1.64	1.19	1.37	

Table 17 (continued). Proportional indices of postcranial remains of identified ruminant taxa from Khok Sung.

DMR-KS-05-03-28-16	<i>Rusa unicorn</i>	4.00	4.38	6.68	8.48	1.67	1.94	1.10	1.27
Metacarpus									
Specimen	Taxa	GL/Bp	GL/Dp	GL/Bd	GL/Dd	Bp/Bd	Dp/Dd	Bp/Dp	Bd/Dd
DMR-KS-05-03-26-27	<i>Bos gaurus</i>	3.66	5.57	3.96	7.66	1.08	1.37	1.52	1.93
DMR-KS-05-03-26-3(1)	<i>Bubalus amee</i>	2.68	4.17	2.64	4.87	0.98	1.17	1.55	1.85
DMR-KS-05-03-18-2	<i>Axis axis</i>	6.50	9.99	6.69	10.55	1.03	1.06	1.54	1.58
DMR-KS-05-03-22-28	<i>Axis axis</i>	–	9.59	6.81	10.36	–	1.08	–	1.52
DMR-KS-05-03-08-2	<i>Axis axis</i>	6.36	8.79	6.18	10.18	0.97	1.16	1.38	1.65
DMR-KS-05-03-19-3	<i>Axis axis</i>	6.58	9.06	6.30	10.42	0.96	1.15	1.38	1.65
DMR-KS-05-03-19-37	<i>Axis axis</i>	7.14	11.05	6.84	10.75	0.96	0.97	1.55	1.57
DMR-KS-05-04-30-20	<i>Axis axis</i>	6.87	10.36	–	–	–	–	1.51	–
DMR-KS-05-03-24-2	<i>Panolia eldii</i>	6.39	8.99	6.57	10.41	1.03	1.16	1.41	1.58
DMR-KS-05-03-17-26	<i>Rusa unicorn</i>	5.97	7.57	6.06	9.10	1.02	1.20	1.27	1.50
Metatarsus									
Specimen	Taxa	GL/Bp	GL/Dp	GL/Bd	GL/Dd	Bp/Bd	Dp/Dd	Bp/Dp	Bd/Dd
DMR-KS-05-04-1-8	<i>Bubalus amee</i>	3.80	4.59	3.17	5.54	0.83	1.21	1.21	1.75
DMR-KS-05-04-1-6	<i>Bubalus amee</i>	3.88	4.39	3.11	5.67	0.80	1.29	1.13	1.82
DMR-KS-05-03-28-30	<i>Bubalus amee</i>	4.25	4.28	3.40	6.38	0.80	1.49	1.01	1.88
DMR-KS-05-03-26-3	<i>Axis axis</i>	7.21	6.91	6.99	9.16	0.97	1.33	0.96	1.31
DMR-KS-05-03-15-14	<i>Axis axis</i>	6.84	7.37	6.15	9.22	0.90	1.25	1.08	1.50
DMR-KS-05-03-29-30	<i>Axis axis</i>	6.91	6.82	6.52	8.58	0.94	1.26	0.99	1.32
DMR-KS-05-03-28-17	<i>Panolia eldii</i>	8.05	7.71	7.73	11.69	0.96	1.52	0.96	1.51
DMR-KS-05-03-25-8	<i>Panolia eldii</i>	7.81	7.47	7.22	11.57	0.92	1.55	0.96	1.60
DMR-KS-05-03-15-15	<i>Panolia eldii</i>	8.08	7.44	7.37	11.29	0.91	1.52	0.92	1.53
DMR-KS-05-03-19-11	<i>Rusa unicorn</i>	6.64	6.86	6.49	9.20	0.98	1.34	1.03	1.42



Figure 44. Postcranial remains of *Axis axis* from Khok Sung: (A–B) DMR-KS-05-04-11-32, a right distal humerus in anterior (A) and distal (B) views; (C–E) DMR-KS-05-03-18-2, a right metacarpus in proximal (C), anterior (D), and distal (E) views; (F–H) DMR-KS-05-03-19-37, a left metacarpus in proximal (F), anterior (G), and distal (H) views; (I–J) DMR-KS-05-03-27-4, a right distal femur in posterior (I) and distal (J) views; (K–M) DMR-KS-05-03-26-3, a right metatarsus in proximal (K), anterior (L), and distal (M) views.

Taxonomic remarks and comparisons

The antlers are useful to distinguish among the cervids, whereas the morphologies of lower cheek teeth are identical within *Axis*. The skulls, antlers, and teeth from Khok Sung are morphologically similar to those observed from recent *A. axis*. This suggests a morphological stasis in the evolution of antlers and teeth for this species.

Based on our observation on the extant comparative material of *A. axis* (e.g., the specimens MNHN-ZMO-1901-547, MNHN-ZMO-1988-153, ZSM-1951-70, and ZSM-1958-88), we thus demonstrate some dental morphological variation within species. The m3 of *A. axis* appears more morphologically variable than the other molars, such as the more or less developed posterior talonids and the presence/absence of back fossae. The cheek teeth of extant *A. axis* are relatively similar to those of *A. porcinus* (e.g., the extant specimens MNHN-ZMO-1904-60, MNHN-ZMO-1962-4188, ZSM-1968-493, and ZSM-1969-63). However, *A. axis* differs from *A. porcinus* in having less developed anterior cingulids on the lower molars and the presence of back fossae on the m3. Recent *A. axis* represents an intermediate size between *A. porcinus* and two large cervid species (*Panolia eldii* and *Rusa unicolor*) (Tab. 18). *A. axis* from Khok Sung also follows the size tendency of recent population (Figs 45 and 46).

Table 18. Body mass prediction of Khok Sung ruminants using second molar variables, compared to relative sizes of the recent population (Grzimek, 1975; Lekagul and McNeely, 1988; Nowak, 1999). The predictive equations follow Janis (1990: table. 16.8).

Body mass (kg)				
Cervidae		Khok Sung		Recent
Taxa	N	Range	Mean	Range
<i>Axis axis</i>	17	67.6–127.6	90.8	75–100
<i>Panolia eldii</i>	7	99.1–157.6	133.5	95–150
<i>Rusa unicolor</i>	5	215.6–332.3	255.4	100–350
Bovidae		Khok Sung		Recent
Taxa	N	Range	Mean	Range
<i>Bos sauveli</i>	3	660.8–756.0	720.5	700–900
<i>Bos gaurus</i>	3	808.5–940.8	873.2	700–1000
<i>Bubalus amee</i>	12	694.5–1243.0	944.7	700–1200

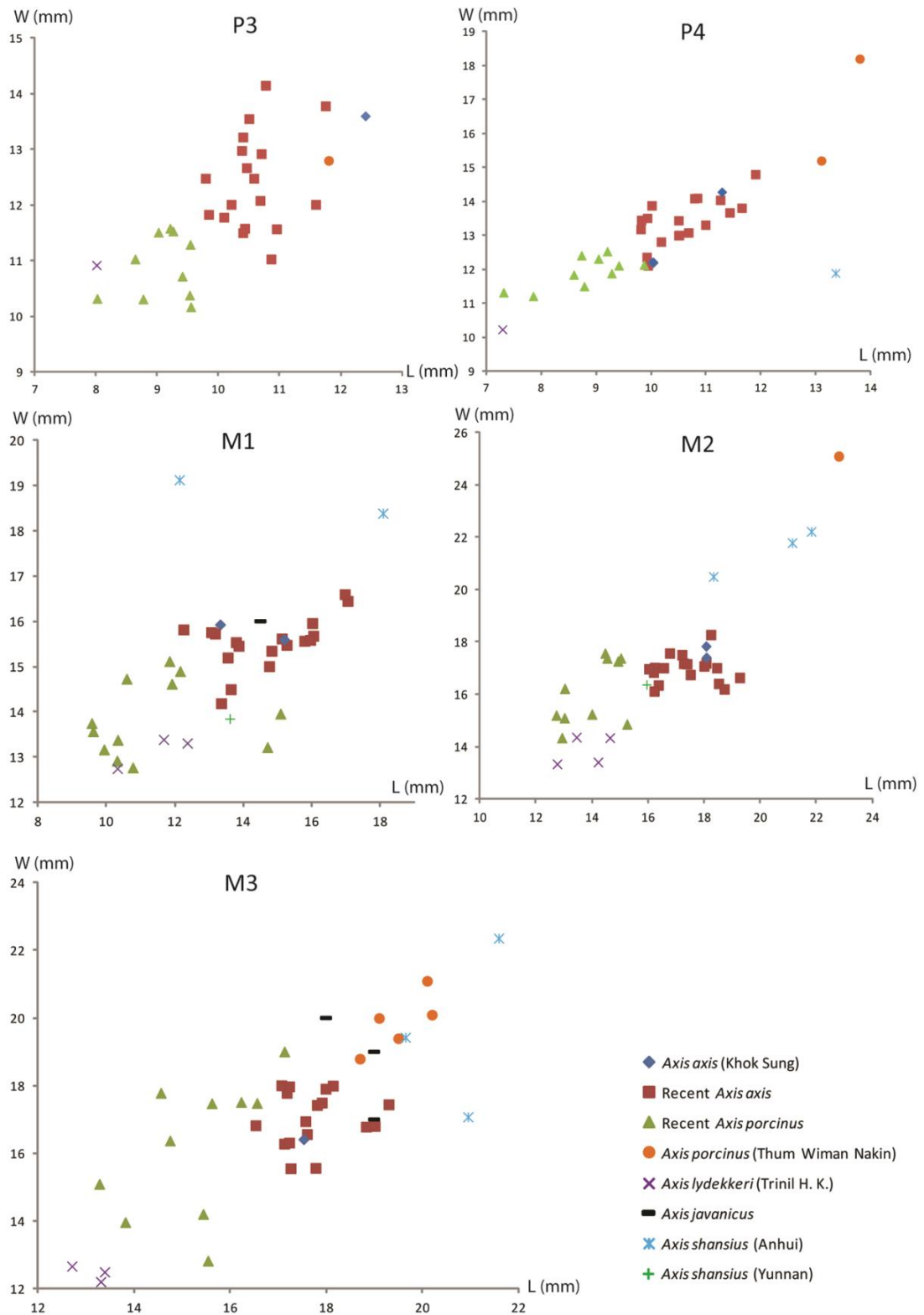


Figure 45. Scatter diagrams of upper cheek tooth (P3–M3) lengths and widths of recent and fossil *Axis*. Data of *Axis javanicus* (Trinil H. K.) and *Axis porcinus* (Thum Wiman Nakin) are from von Koenigswald (1933) and Tougard (1998), respectively.

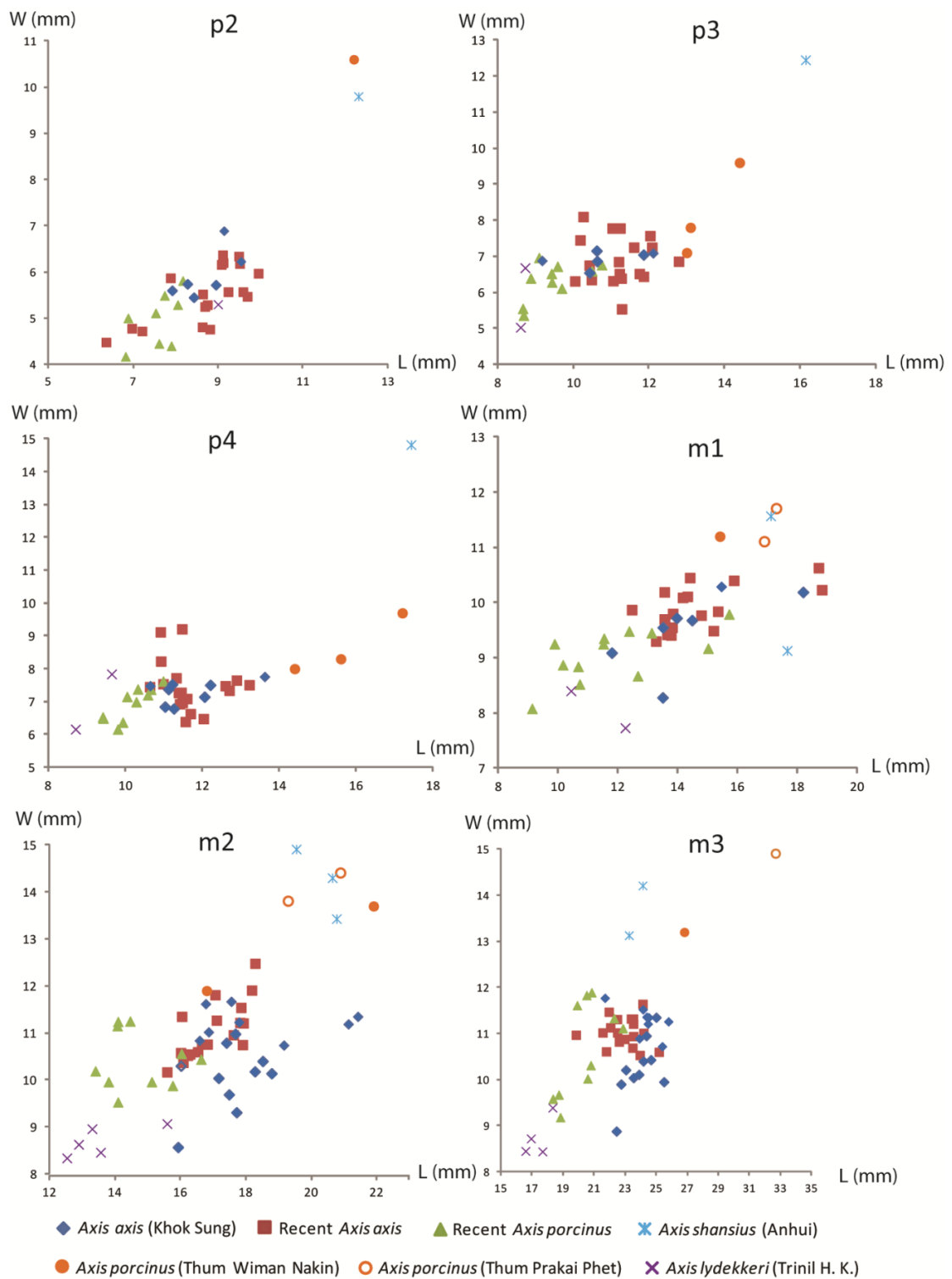


Figure 46. Scatter diagrams of lower cheek tooth (p2–m3) lengths and widths of recent and fossil *Axis*. Data of *Axis javanicus* (Trinil H. K.) and *Axis porcinus* (Thum Wiman Nakin and Thum Prakai Phet) are from von Koenigswald (1933), Tougard (1998), and Filoux et al. (2015), respectively.

Compared to other Pleistocene cervid species, the cheek teeth of *A. axis* from Khok Sung are smaller than those of *A. shansius* from Anhui and Yunnan (China) and of *A. javanicus* from Ngandong and Buitenzorg in Java and Carnul Cave in India, but are larger than those of *A. lydekkeri* from Trinil H. K. (Java) (Figs 45 and 46). Although, *A. javanicus* is closely related to or even synonymous with *A. axis* according to Meijaard and Groves (2004), it is considered as a valid species due to studies of the geometric morphometric analysis performed on the teeth (Gruwier et al., 2015). According to the scatter diagrams of the dental sizes (Figs 45 and 46), Thum Wiman Nakin and Thum Prakai Phet fossil teeth assigned to *A. porcinus* (Tougaard, 1998; Filoux et al., 2015) are much larger than their extant populations and those from Khok Sung. Although the Pleistocene hog deer probably show clinal variation in size (Bergmann's rule) in response to colder climates, the teeth attributed to *A. porcinus* from Thum Wiman Nakin and Thum Prakai Phet, identified by Tougaard (1998) and Filoux et al. (2015), possibly reveal a double size (or more) of the recent population. We suggest that these fossils likely belong to either other larger or new cervid species that lived during the Pleistocene across mainland Southeast Asia. We also cast doubt on the occurrence of *A. porcinus* in the Middle Pleistocene of Boh Dambang, Cambodia (Demeter et al., 2013). The existence of *A. porcinus* in Southeast Asia during the Middle Pleistocene is still doubtful.

Genus *Panolia* Gray, 1843

Panolia eldii (M'Clelland, 1842)

Referred material: a cranium with a right partial antler, DMR-KS-05-04-20-4; a right P2, DMR-KS-05-03-15-11; two left M1—DMR-KS-05-03-00-24 and DMR-KS-05-03-00-25; six M2—DMR-KS-05-03-00-23 (right), DMR-KS-05-03-30-5 (right), DMR-KS-05-04-3-4 (right), DMR-KS-05-03-30-6 (left posterior lobe), DMR-KS-05-03-27-7 (left), and DMR-KS-05-04-3-5 (left); five M3—DMR-KS-05-03-27-6 (right),

DMR-KS-05-04-9-1 (right), DMR-KS-05-04-8-3 (right), DMR-KS-05-03-00-22 (left), and DMR-KS-05-04-9-2 (left); two left mandibles—DMR-KS-05-03-27-2 (with p2–m3) and DMR-KS-05-04-9-5 (with p2–m2); a right i1, DMR-KS-05-03-29-2; a right scapula, DMR-KS-05-06-24-4; a left humerus, DMR-KS-05-04-11-35; a right fragmentary humerus, DMR-KS-05-03-18-1 (proximal part); three radii—DMR-KS-05-03-31-10 (right), DMR-KS-05-04-11-3 (right), and DMR-KS-05-03-19-16 (left); a right metacarpus, DMR-KS-05-03-24-2; two right femora—DMR-KS-05-03-27-11 and DMR-KS-05-03-17-36; five fragmentary femora—DMR-KS-05-04-05-38 (right proximal part), DMR-KS-05-03-28-20 (right distal part), DMR-KS-05-03-00-119 (right distal part), DMR-KS-05-03-19-2 (right distal part), and DMR-KS-05-08-16-1 (left proximal part); three left metatarsus—DMR-KS-05-03-25-8, DMR-KS-05-03-28-17, and DMR-KS-05-03-15-15

Material description

Cranium and upper dentition: DMR-KS-05-04-20-4 is an incomplete cranium, lacking the whole anterior parts (nasal, jugal, palatine, and maxilla) (Fig. 47A–C) (for measurements, see Tab. A6). This specimen is a juvenile individual according to the incompletely fused sutures. The basioccipital and basisphenoid are triangular in outline and have straight lateral edges (Fig. 47C), different from those of *Axis*, and as observed on the recent skull of *Panolia eldii* (e.g., MNHN-ZMO-1937-157, MNHN-ZMO-1944-307, MNHN-ZMO-2011-190, and NMW-2975). The foramina ovale of DMR-KS-05-04-20-4 are more circular and open more anteriorly than those of *Axis*. The right partial antler contains a half of the slender main beam, but lacks a brow tine entirely (Fig. 47A, B). The divergent angle between the main beam and the brow tine is of about 110° , similar to recent skulls of *P. eldii* (e.g., THNHM-M-125). The antler surface is smooth and the burr is poorly developed in relation to the ontogenetic stages. The preserved shed antler shows a typical character of *P. eldii*, whose main beams strongly project and curve laterally (Fig. 47A).

The P2 exhibits a prominent medial crista which divides the fossette into two islands (Fig. 47D). The separated anterior fossette is larger than the posterior one. On the upper molars, the buccal styles, anterior cingula, and entostyles are distinct (for measurements, see Tab. 16). The entostyle is bifurcated (Fig. 47E–H). The metaconule fold (spur) is poorly developed. The posterior lobe of the M3 is reduced in width (Fig. 47G, H). The buccal wall of the posterior lobe is oblique in occlusal view.

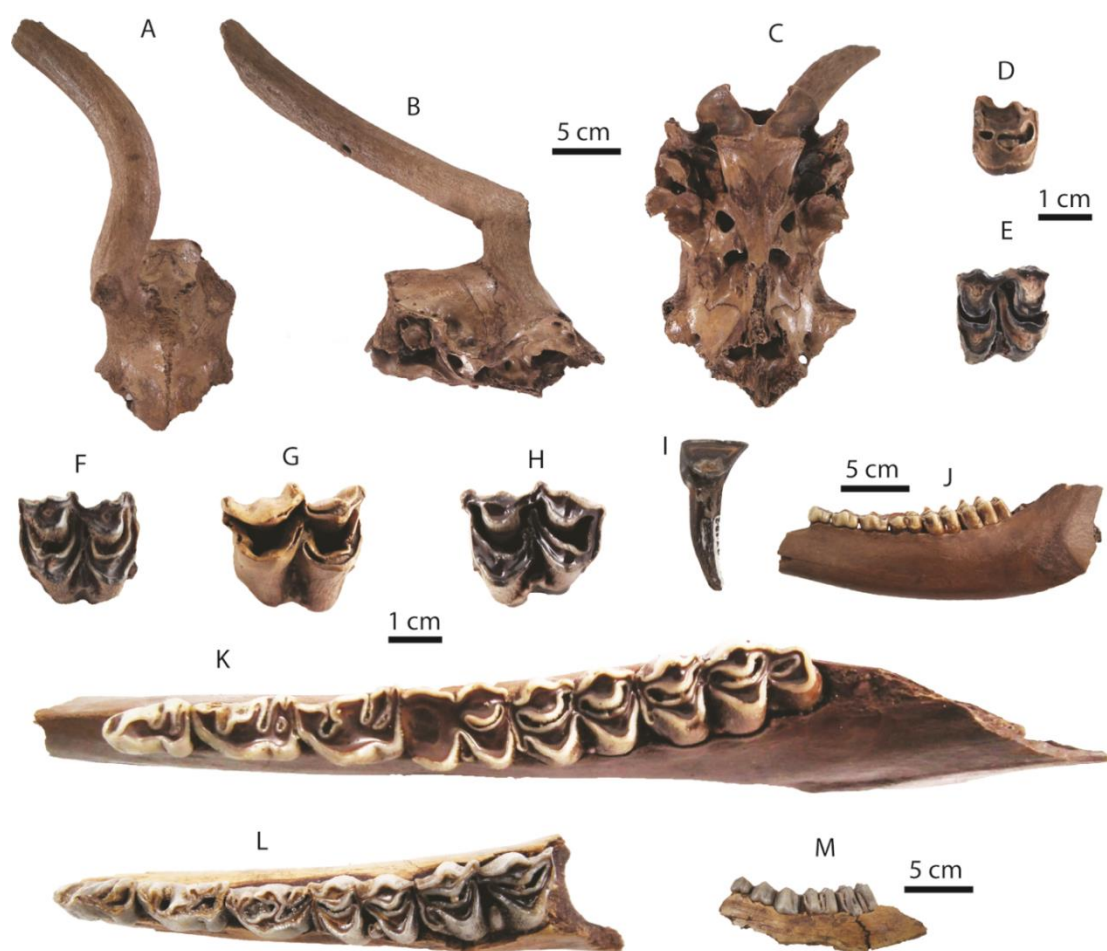


Figure 47. Remains of *Panolia eldii* from Khok Sung: (A–C) DMR-KS-05-04-20-4, a cranium in dorsal (A), lateral (B), and ventral (C) views; (D) DMR-KS-05-03-15-11, a right P2; (E) DMR-KS-05-03-00-24, a left M1; (F) DMR-KS-05-03-00-23, a right M2; (G) DMR-KS-05-03-27-6, a left M3; (H) DMR-KS-05-04-9-2, a left M3; (I) DMR-KS-05-03-29-2, a right i1 in lingual view; (J–K) DMR-KS-05-03-27-2, a left mandible in lateral (J) and occlusal (K) views; (L–M) DMR-KS-05-04-9-5, a left mandible in occlusal (L) and lateral (M) views. All teeth are shown in occlusal view.

Mandibles and lower dentition: Two mandibles (DMR-KS-05-03-27-2: fig. 47J, K and DMR-KS-05-04-9-5: fig. 47L, M) are nearly complete, preserving the bodies with cheek tooth rows (for measurements, see Tab. A7). The first specimen also preserves a partial ramus and is more complete than the second one in which the mandibular body is broken.

An isolated i1 is spatulate (Fig. 47I). Lower premolars show more complex patterns compared to *Axis* (e.g., the bifurcation of the metaconid on the p3, the irregular shape of the posterior valley, and the presence of more developed pre- and postprotoconulidcristids) (Fig. 47K, L). Lower molars display well-developed anterior cingulids and stylids (for measurements, see Tab. 16). The m3 is characterized by the presence of a posterior ectostylid (Fig. 47K). The shape of the posterior lobe of the m3 resembles that of *A. axis*.

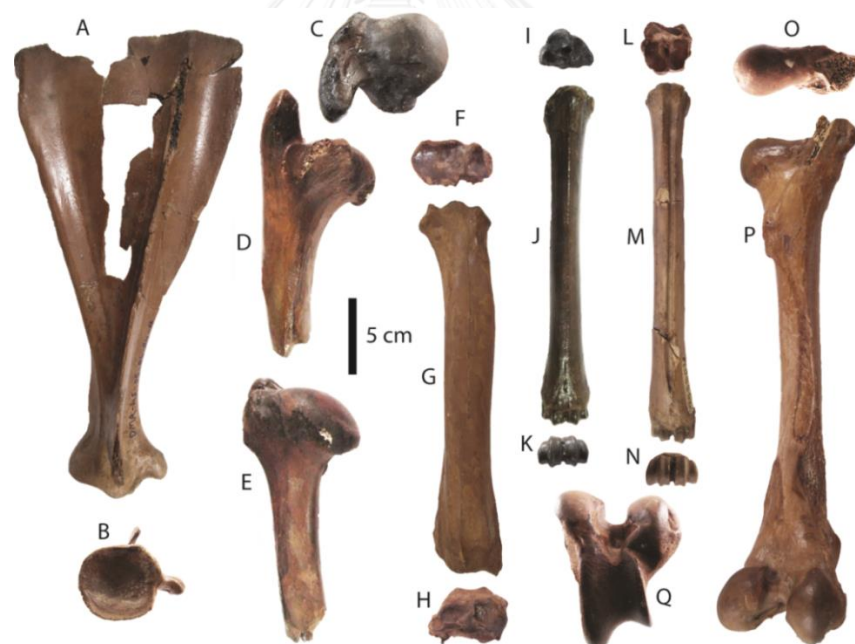


Figure 48. Postcranial remains of *Panolia eldii* from Khok Sung: (A–B) DMR-KS-05-06-24-4, a right scapula in lateral (A) and distal (B) views; (C–E) DMR-KS-05-03-18-1, a right proximal humerus in proximal (C), anterior (D), and posterior (E) views; (F–H) DMR-KS-05-03-31-10, a right radius in proximal (F), anterior (G), distal (H) views; (I–K) DMR-KS-05-03-24-2, a right metacarpus in proximal (I), anterior (J), and distal (K) views; (L–N) DMR-KS-05-03-25-8, a left metatarsus in proximal (L), anterior (M), distal (N) views; (O–Q) DMR-KS-05-03-17-36, a right femur in proximal (O), posterior (P), distal (Q) views.

Postcranial remains: postcranial bones include a scapula (Fig. 48A, B), humeri (Fig. 48C–E), radii, a metacarpus (Fig. 48I–K), femora (Fig. 48O–Q), and metatarsi (Fig. 48L–N). They are almost complete. We identify these postcranial bones based on the correlation of size and proportion with the extant specimens of *P. eldii* (Tabs 17, A1, A8–A12, and A14).

Taxonomic remarks and comparisons

Several authors consider Eld's deer as belonging to either the genus *Cervus* (e.g., Lekagul and McNeely, 1988; Tougard, 1998, 2001; Gruwier et al., 2015) or *Rucervus* (e.g., Grubb, 2005). However, Groves and Grubb (2011) suggested that placement of the Eld's deer in the genus *Panolia* is an acceptable alternative based on mtDNA analysis (Pitra et al., 2004).

The shed antler of the Eld's deer, *Panolia eldii*, is characterized by bow- or lyre-like shapes, long, noticeable, and laterally bending-main beams with a distal portion curving medially, and small ornamented branches of brow tines. The cheek teeth of *P. eldii* differ from those of *A. axis* in having a larger size, a more complex wear pattern of the mesolingual conids on the p3, more developed anterior cingulids on the lower molars, and a posterior ectostylid on the m3. The Khok Sung specimens assigned to *P. eldii* are similar in morphology to the extant specimens. As demonstrated by the body mass estimation (Tab. 18) and scatter diagrams (Figs 49 and 50), *P. eldii* from Khok Sung is also comparable in size to recent populations, to that from Thum Wiman Nakin, and to some fossil species (e.g., *Cervus kendengensis* from the Pleistocene of Bangle and Kali Gedeh in Java). Our identification thus confirms the existence of *P. eldii* in Thailand during the late Middle Pleistocene. However, we suggest that some isolated teeth of cervids, identified by Tougard (1998), from Thum Wiman Nakin reveal an improper taxonomic identification. The P2 (TF 3371 and TF 4570), p2 (TF 3938, TF 3313, TF 3358, and TF 3983), p3 (TF 3373), and m2 (TF 4025), attributed to *P. eldii*, may belong to other cervids (possibly *R. unicolor*) due to their larger sizes.

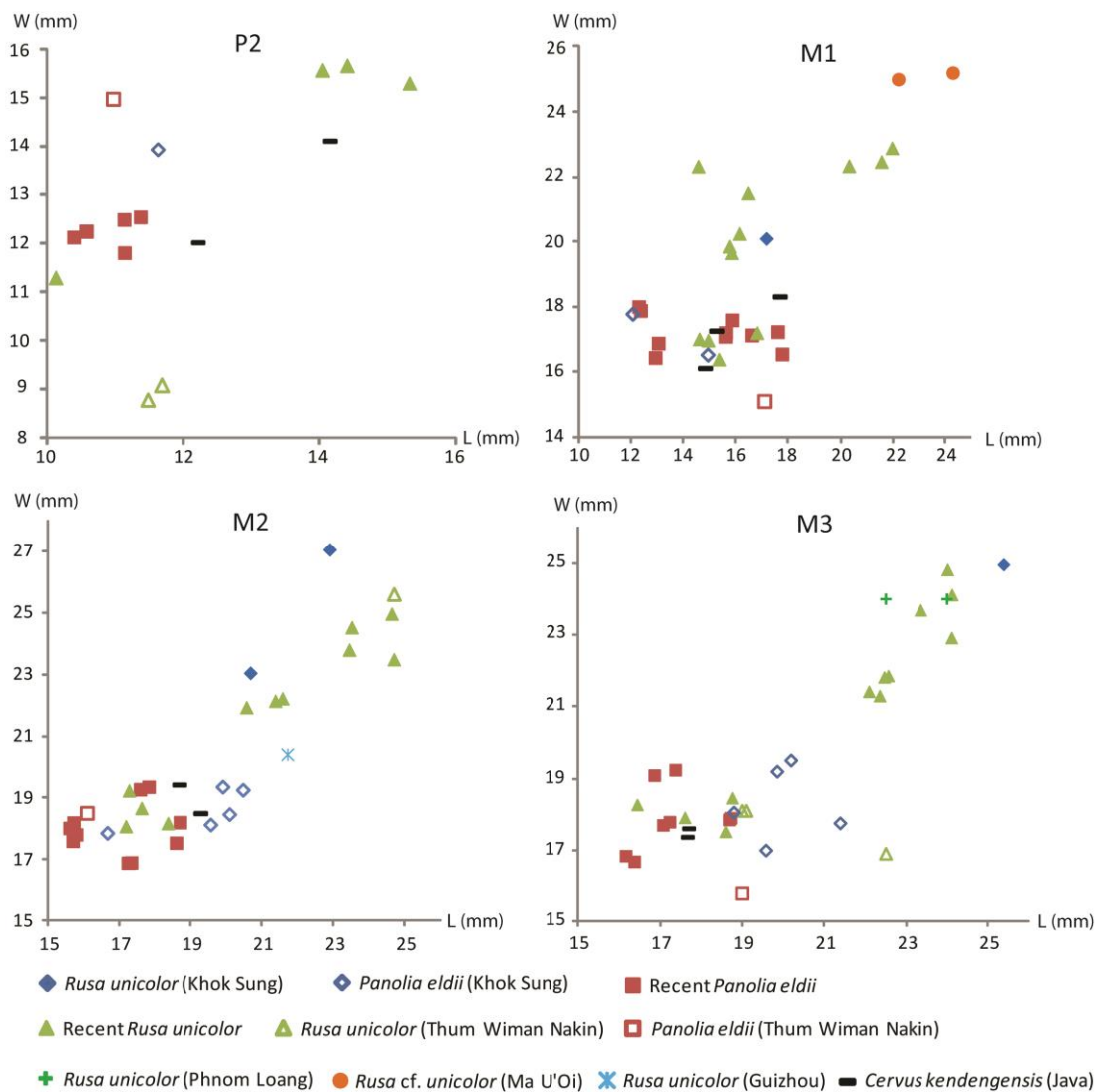


Figure 49. Scatter diagrams of upper cheek tooth (P2, M1, M2, and M3) lengths and widths of some recent and fossil large cervids. The measurements of fossil cervids from the caves of Phnom Loang, Thum Wiman Nakin, and Ma U'O'i are obtained from Beden and Guérin (1973), Tougard (1998), and Bacon et al. (2004), respectively.

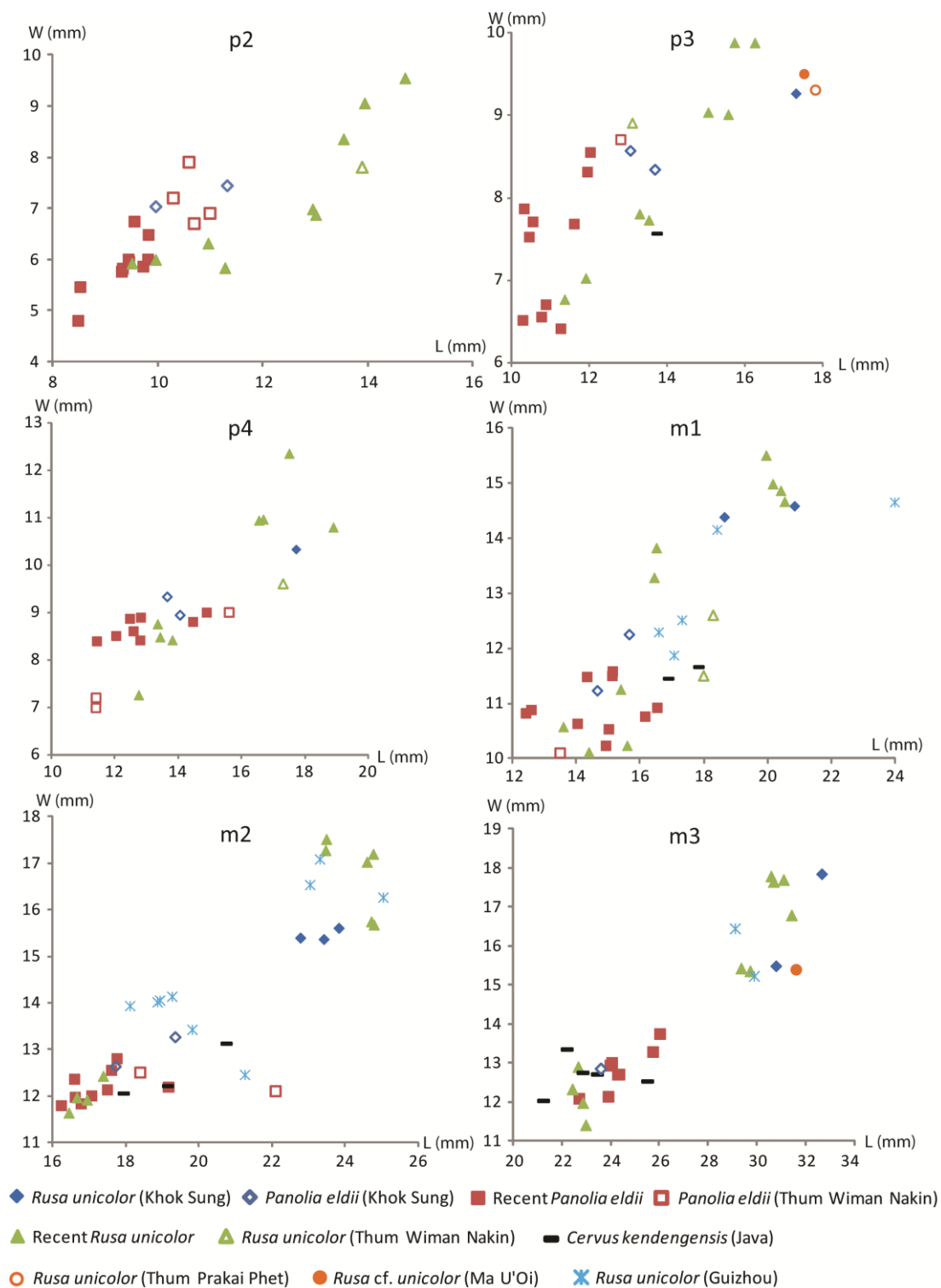


Figure 50. Scatter diagrams of lower cheek tooth (p2–m3) lengths and widths of some recent and fossil large cervids. The measurements of fossil cervids from the caves of Thum Wiman Nakin, Thum Prakai Phet, and Ma U’Oi are obtained from Tougard (1998), Filoux et al. (2015), and Bacon et al. (2004), respectively.

Genus *Rusa* Hamilton-Smith, 1827

Rusa unicolor (Kerr, 1792)

Referred material: three right antlers—DMR-KS-05-03-20-11 (nearly complete specimen), DMR-KS-05-03-26-2 (fragment), and DMR-KS-05-03-28-23 (fragment); a right M1, DMR-KS-05-03-22-10; two left M2—DMR-KS-05-04-9-3 and DMR-KS-05-04-3-3; a left M3, DMR-KS-05-03-31-1; two right mandibles—DMR-KS-05-03-31-2 (with m2) and DMR-KS-05-03-13 (with p4–m3); two left mandibles—DMR-KS-05-03-00-101 (with p3–m3) and DMR-KS-05-03-27-4 (with m3); a right m1, DMR-KS-05-03-00-5; a left fragmentary humerus—DMR-KS-05-03-15-43 (distal part); three right fragmentary radius—DMR-KS-05-03-25-9 (proximal part), DMR-KS-05-03-19-14 (proximal part), and DMR-KS-05-03-26-19 (distal part); a left metacarpus, DMR-KS-05-03-17-26; six fragmentary femora—DMR-KS-05-03-19-7 (right proximal part), DMR-KS-05-03-12-2 (right proximal part), DMR-KS-05-04-11-2 (right distal part), DMR-KS-05-03-26-5 (left proximal part), DMR-KS-05-04-30-9 (left distal part), and DMR-KS-05-04-19-10 (left distal part); a right tibia, DMR-KS-05-03-28-16; a right metatarsus, DMR-KS-05-03-19-11

Material description

Antlers: DMR-KS-05-03-20-11 is a nearly complete antler, slightly broken at the middle part of the main beam (Fig. 51A). The fragmentary antler DMR-KS-05-03-26-2 comprises a burr, a broken brow tine, and a half of the main beam (Fig. 51B). The specimen DMR-KS-05-03-28-23 preserves the broken brow tine and main beam (Fig. 51C). The antler surface is rough. The shed antlers are morphologically characterized by three main tines, a long and slender main beam, a forked construction at the tip, and a well-developed burr (Fig. 51A–C). On the apical bifurcation, the postero-internal tine is much shorter than the antero-external one. The main beam and brow tine are also much more robust, compared to the extant males of *A. porcinus* (e.g., the specimen MNHN-ZMO-1904-60 and NMW-2546). The divergent angle between the main beam and brow

tine ranges from 50° to 90° . The shed antlers of *Rusa unicorn* are different from those of *Axis axis* in having slightly rougher surfaces, more divergent insertion relative to the frontal orientation, a shorter main beam, and a smaller angle between the main beam and the brow tine, and in lacking small-ornamented tines or knobs on the brow tine (Fig. 51A–C). These characters match well the recent *R. unicorn*.

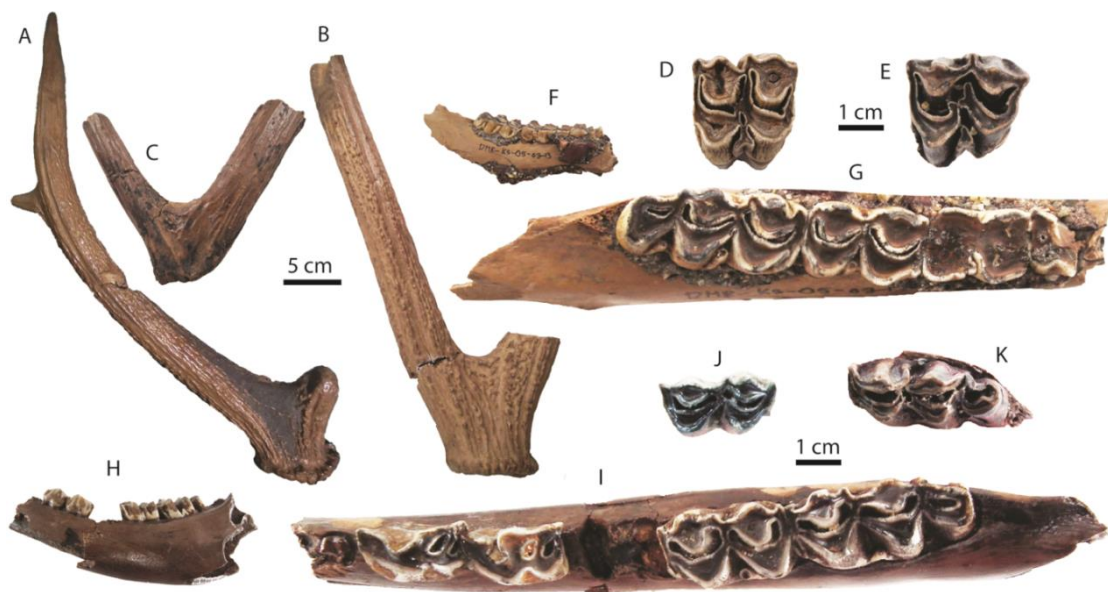


Figure 51. Remains of *Rusa unicorn* from Khok Sung: (A) DMR-KS-05-03-20-11, a right antler in lateral view; (B) DMR-KS-05-03-26-2, a right antler fragment in lateral view; (C) DMR-KS-05-03-28-23, a right antler fragment in medial view; (D) DMR-KS-05-04-9-3, a left M2; (E) DMR-KS-05-03-31-1, a left M3; (F–G) DMR-KS-05-03-13, a right mandible in lateral (F) and occlusal (G) views; (H–I) DMR-KS-05-03-00-101, a left mandible in lateral (H) and occlusal (I) views; (J) DMR-KS-05-03-00-5, a right m1; (K) DMR-KS-05-03-27-4, a left m3. All isolated teeth are shown in occlusal view.

Upper dentition: upper molars are robust (Tab. 16) and show well-developed styles (particularly the mesostyle), anterior cingula, and entostyles (Fig. 51D, E). The entostyle is bifurcated, like in *P. eldii*, in relation to the moderately to strongly worn teeth. The fossettes are present at least in the middle stage of wear. The metaconule fold is poorly developed or sometimes absent. On the M3, the anterior lobe is wider than the posterior one (Fig. 51E).

Mandibles and lower dentition: four mandibles are incomplete (for measurements, see Tab. A7). The specimens DMR-KS-05-03-13 (Fig. 51F, G) and DMR-KS-05-03-00-101 (Fig. 51H, I) preserve a partially broken mandibular body. The mandibles DMR-KS-05-03-31-2 and DMR-KS-05-03-27-4 are very fragmentary. All lower cheek teeth of *R. unicolor* are obviously larger than those of other Khok Sung cervids (Tab. 16). Lower molars display cervid-like patterns, such as well developed styles, anterior cingulids, and ectostylids (Fig. 51J, K). On the m3, the posterior lobe of the talonid in *R. unicolor* is more developed than those in *Axis*. Moreover, the posterior ectostylid is present (Fig. 51G, I, K), unlike in *Axis*.

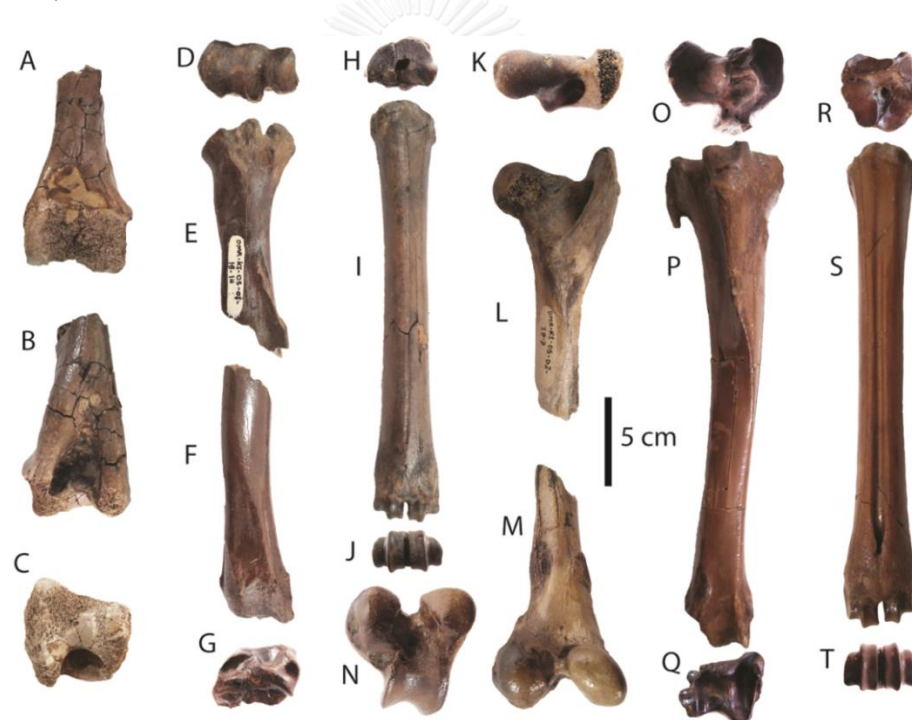


Figure 52. Postcranial remains of *Rusa unicolor* from Khok Sung: (A–C) DMR-KS-05-03-15-43, a left humerus in anterior (A), posterior (B), and distal (C) views; (D–E) DMR-KS-05-03-19-14, a right proximal radius in proximal (D) and anterior (E) views; (F–G) DMR-KS-05-03-26-19, a right distal radius in anterior (F) and distal (G) views; (H–J) DMR-KS-05-03-17-26, a left metacarpus in proximal (H), anterior (I), and distal (J) views; (K–L) DMR-KS-05-03-19-7, a right proximal femur in proximal (K) and anterior (L) views; (M–N) DMR-KS-05-04-30-9, a left distal femur in posterior (M) and distal (N) views; (O–Q) DMR-KS-05-03-28-16, a right tibia in proximal (O), anterior (P), and distal (Q) views; (R–T) DMR-KS-05-03-19-11, a right metatarsus in proximal (R), anterior (S), and distal (T) views.

Postcranial remains: postcranial elements include a humerus (Fig. 52A–C), radii (Fig. 52D–G), a metacarpus (Fig. 52H–J), femora (Fig. 52K–N), a tibia (Fig. 52O–Q), and a metatarsus (Fig. 52R–T). All radii and femora are fragmentary. We assign these postcranial bones to *R. unicolor* according to the sized and proportional correlation with the extant specimens (Tabs 17, A1, and A9–A14).

Taxonomic remarks and comparisons

According to Leslie (2011), we regard here *Rusa* as a separate genus within the family Cervidae. Four species are currently recognized: *R. unicolor* (sambar), *R. marianna* (Philippine deer), *R. timorensis* (rusa), and *R. alfredi* (Prince Alfred's deer).

Antlers of *R. unicolor* are characterized by its typical three tines and forked beams at the tip, similar in shape to those of *Axis porcinus* but much more robust. The sambar deer shares a similar dental morphology with the Eld's deer. But it differs from *P. eldii* as well as *A. axis* in being larger-sized and in having more developed anterior cingulids on lower molars. The sambar deer is much larger than *A. axis* (Figs 49 and 50). Based on the body mass estimated from the second molar sizes, Khok Sung large cervids fit well the size tendency of the modern populations of *R. unicolor* (Tab. 18). As demonstrated by the scatter diagrams (Figs 49 and 50), the recent sambar deer shows a wide range of size variation that sometimes overlaps with the Eld's deer. The cheek teeth of Khok Sung *Rusa unicolor* conform to the size variability of their recent population. They are also comparable in size and morphology to the fossil sambar deer from Thum Prakai Phet (Filoux et al., 2015), Phnom Loang (Beden and Guérin, 1973), and Ma U'Oi (Bacon et al., 2004) (Figs 49 and 50). As is the case for *P. eldii*, some cervid specimens described from Thum Wiman Nakin are improperly identified. For instance, the P2 (TF 3371 and TF 4570) probably do not belong to *Rusa unicolor* according to their smaller sizes. The taxonomic revision

of fossil cervids from Thum Wiman Nakin would lead to the recognition of either higher or lower diversity of cervids in Southeast Asia during the Middle Pleistocene.

Family BOVIDAE Gray, 1821

Genus *Bos* Linnaeus, 1758

***Bos sauveli* Urbain, 1937**

Referred material: a left DP3, DMR-KS-05-03-29-8; a left P3, DMR-KS-05-04-01-4; a left fragmentary M1 or M2 (posterior portion), DMR-KS-05-03-23-2; a right M3, DMR-KS-05-03-29-6; a right mandible with m1–m3, DMR-KS-05-03-9-1; two left mandibles—DMR-KS-05-04-9-1 (with p2, p4, and m1–m3) and DMR-KS-05-04-29-1 (with m3); a left i2, DMR-KS-05-03-15-12; a right i3, DMR-KS-05-03-23-4; a right p2, DMR-KS-05-04-01-6; a right m1, DMR-KS-05-03-15-10; a right m2, DMR-KS-05-03-29-7; two m3—DMR-KS-05-04-28-4 (right broken posterior lobe) and DMR-KS-05-03-24-5 (left); a left humerus, DMR-KS-05-03-20-2(1)

Material description

Upper dentition: DP3 (DMR-KS-05-03-29-8) is molariform and elongated, characterized by well-developed anterior and posterior cingula, buccal styles, and medial fossettes, a slightly developed entostyle, and a reduction of the anterior lobe width and height compared to the posterior lobe (Fig. 53A). The P3 (DMR-KS-05-04-01-4) has distinct styles (particularly the metastyle), protocone, and hypocone and an irregular fossette. (Fig. 53B). Upper molars have a rectangular outline and distinct styles, entostyles, and single medial fossettes with wear (Fig. 53C, E) (for measurements, see Tab. 19). The infundibula are X- or metacentric chromosome-shaped on the moderately worn molars (Fig. 53C, E). The entostyles (column) of DMR-KS-05-03-23-2 (M1 or M2: fig. 53C, D) and DMR-KS-05-03-29-6 (M3: fig. 53E) are often bifurcated and lingually flat in occlusal view. A distinct longitudinal groove runs along the lingual surface of the entostyle (Fig.

53D). The M3 is more rectangular in outline compared to other upper molars. The posterior lobe of the M3 is relatively reduced in width and the fossettes are large (Fig. 53E).

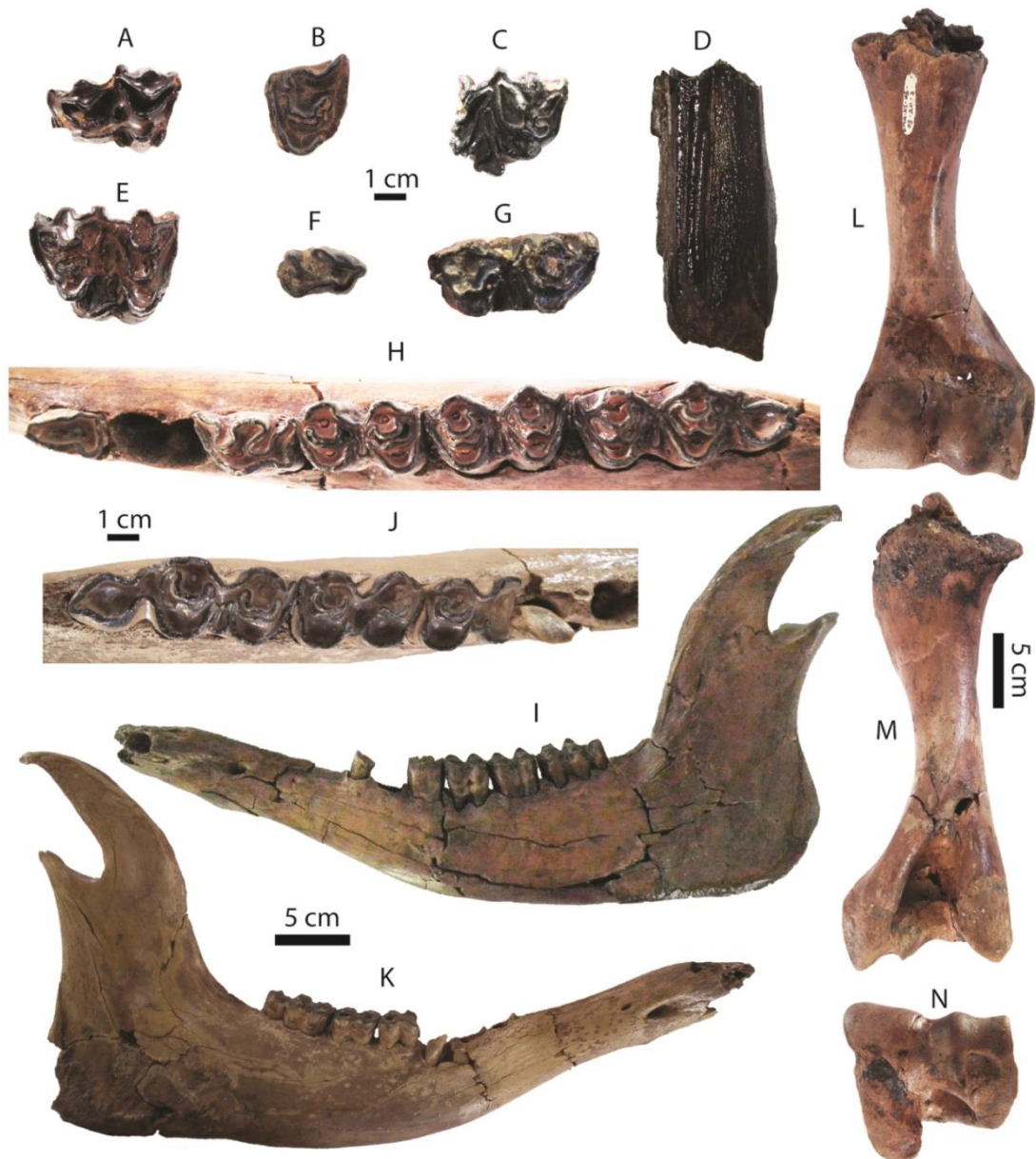


Figure 53. Remains of *Bos sauveli* from Khok Sung: (A) DMR-KS-05-03-29-8, a left DP3; (B) DMR-KS-05-04-01-4, a left P3; (C–D) DMR-KS-05-03-23-2, a left M1 or M2 in occlusal (C) and lingual (D) views; (E) DMR-KS-05-03-29-6, a right M3; (F) DMR-KS-05-04-01-6, a right p2; (G) DMR-KS-05-04-28-4, a broken right m3; (H–I) DMR-KS-05-04-9-1, a left mandible in occlusal (H) and lateral (I) views; (J–K) DMR-KS-05-03-9-1, a right mandible in occlusal (J) and lateral (K) views; (L–N) DMR-KS-05-03-20-2(1), a left humerus in anterior (L), posterior (M), and distal (N) views. All isolated teeth are shown in occlusal view.

Mandible and lower dentition: two mandibles, DMR-KS-05-03-9-1 (Fig. 53H, I) and DMR-KS-05-04-9-1 (Fig. 53J, K), are almost complete (for measurements, see Tab. A15). All incisors and premolars dropped out of the first specimen. The second specimen lacks all incisors and the p3. Another fragmentary mandible DMR-KS-05-04-29-1 preserves only a posterior lobe of the m3.

The i2 (DMR-KS-05-03-22-15) and i3 (DMR-KS-05-03-23-4) are spatulate and small, compared to other species of *Bos* (for measurements, see Tab. 19). The two p2 (DMR-KS-05-04-9-1: fig. 53H and DMR-KS-05-04-01-6: fig. 53F) is small and shows a protruding preprotoconulidcristid and a fusion between the postentocristid and the posthypocristid. The p4 display well-developed conids and cristids. The postprotocristid is large, compared to other *Bos* species. On the lower molars, the metastylid is poorly-developed, but becoming more prominent in m3 (Fig. 53H). The anterior and posterior fossettes is metacentric chromosome-shaped with wear (Fig. 53H, J). The posterior talonid of the m3 is well-developed (Fig. 53H, J). The posthyppoconulidcristid protrudes posteriorly and sometimes bifurcates into two flanges, as observed on the specimen DMR-KS-05-04-9-1 (fig. 53H). The entostylid slightly protrudes lingually in relation to heavy wear and the posterior ectostylid is usually absent.

Table 19. Measurements (lengths and widths in millimeters) of cheek teeth of large bovids from Khok Sung. N=number of specimens.

	Length			Width		
	N	Range	Mean	N	Range	Mean
<i>Bos sauveli</i>						
DP3	1	27.39	–	1	14.91	–
P3	1	17.57	–	1	19.71	–
M1 or M2	–	–	–	1	25.63	–
M3	1	35.46	–	1	23.55	–
i2	1	13.67	–	1	11.53	–
i3	1	13.68	–	1	8.68	–
p2	2	14.13–14.77	14.45	2	8.52–10.39	9.46
p4	1	23.39	–	1	12.91	–
m1	3	27.24–27.96	27.72	3	17.21–18.26	17.73

m2	3	29.70–32.47	30.11	3	17.87–18.79	18.29
m3	3	40.60–47.60	43.78	5	17.09–19.91	18.37
<i>Bos gaurus</i>						
DP2	1	22.28	–	1	10.67	–
P2	2	19.42–20.79	20.11	2	13.55–15.58	14.57
DP3	1	28.73	–	1	18.97	–
DP4	1	29.75	–	1	22.55	–
M1	1	26.33	–	1	29.95	–
M3	1	36.96	–	1	26.94	–
i1	1	20.30	–	1	11.35	–
p2	1	13.77	–	1	8.56	–
p3	1	21.58	–	1	11.92	–
p4	1	21.11	–	1	12.72	–
m1	2	25.29–28.67	26.98	2	18.25–19.28	18.77
m2	3	30.36–35.09	32.82	3	19.00–20.07	19.45
m3	2	42.56–46.23	44.40	2	18.72–18.79	18.76
<i>Bubalus arnee</i>						
P2	3	22.30–26.78	24.04	3	14.47–17.26	15.76
DP3	1	31.92	–	1	19.75	–
P3	7	17.85–25.03	21.58	7	15.56–21.93	20.32
DP4	1	31.60	–	1	23.36	–
P4	7	17.76–23.55	20.46	7	21.01–23.20	22.34
M1	9	25.73–33.16	28.61	8	26.01–29.79	27.30
M2	8	30.45–36.18	33.11	7	26.09–29.23	27.23
M3	6	33.74–37.40	36.07	6	25.26–27.30	26.29
i1	1	21.21	–	1	10.31	–
i2	1	16.17	–	1	11.94	–
i3	1	16.61	–	1	11.63	–
i4	1	15.82	–	1	8.80	–
p2	4	13.56–16.24	15.05	4	8.01–9.80	8.87
dp3	2	21.59–23.20	22.40	2	8.65–9.90	9.28
p3	3	21.88–23.09	22.30	3	10.23–13.09	11.80
dp4	3	37.25–42.59	40.74	3	13.34–15.24	14.39
p4	2	23.81–24.97	24.39	3	11.93–13.26	12.76
m1	9	30.49–36.77	32.66	6	17.67–20.36	18.94
m2	6	32.13–39.20	36.03	5	19.00–21.22	20.18
m3	3	46.52–48.33	47.29	4	17.64–20.72	19.66

Postcranial remains: a humerus, DMR-KS-05-03-20-2(1), preserves the shaft and distal part (Fig. L–N). We attribute this humerus to *B. sauveli* according to the proportional correlation with the extant specimens (Tabs 17 and A9). This specimen is also smaller than that of extant bantengs and gaurs (Tabs A1 and A9).

Taxonomic remarks and comparisons

Southeast Asian large bovids are accurately identified by differences in cranial features (especially horn cores), although they show sexual and ontogenetic variation in morphology. Lacking the cranial remains, it is difficult to make a distinction within the species of *Bos*. Due to the lack of cranial remains of koupreys (*B. sauveli*) collected from Khok Sung, we identify these fossils on the basis of dental features.

Based on our comparisons with some extant specimens (MNHN-ZMO-1940-51 and MNHN-ZMO-10801), the cheek teeth of koupreys are similar to those of other species of *Bos*, characterized by having hypsodont crowns, well-developed styles and stylids, a horse shoe-shaped infundibulum (anterior and posterior fossettes), and bifurcated or trifurcated entostyles depending on the wear stage. Among Southeast Asian large bovids, it differs from *B. javanicus* (banteng) and *B. gaurus* (gaur) in having a more developed postprotocristid on the p3 and p4, a metacentric chromosome-shaped molar in relation to the middle wear stage, a single large medial fossette on the upper molars, a flat lingual surface of the entostyle on the moderately to heavily worn molars. The M1 and M3 of *B. sauveli* are almost more square and rectangular in outline, respectively, compared to those of other *Bos* species. *B. sauveli* is usually smaller than *B. gaurus* and *Bubalus arnee* (wild water buffalo), but is often comparable in size to *B. javanicus* (Figs 54 and 55, and for the average of large bovid body mass, see Tab. 18).

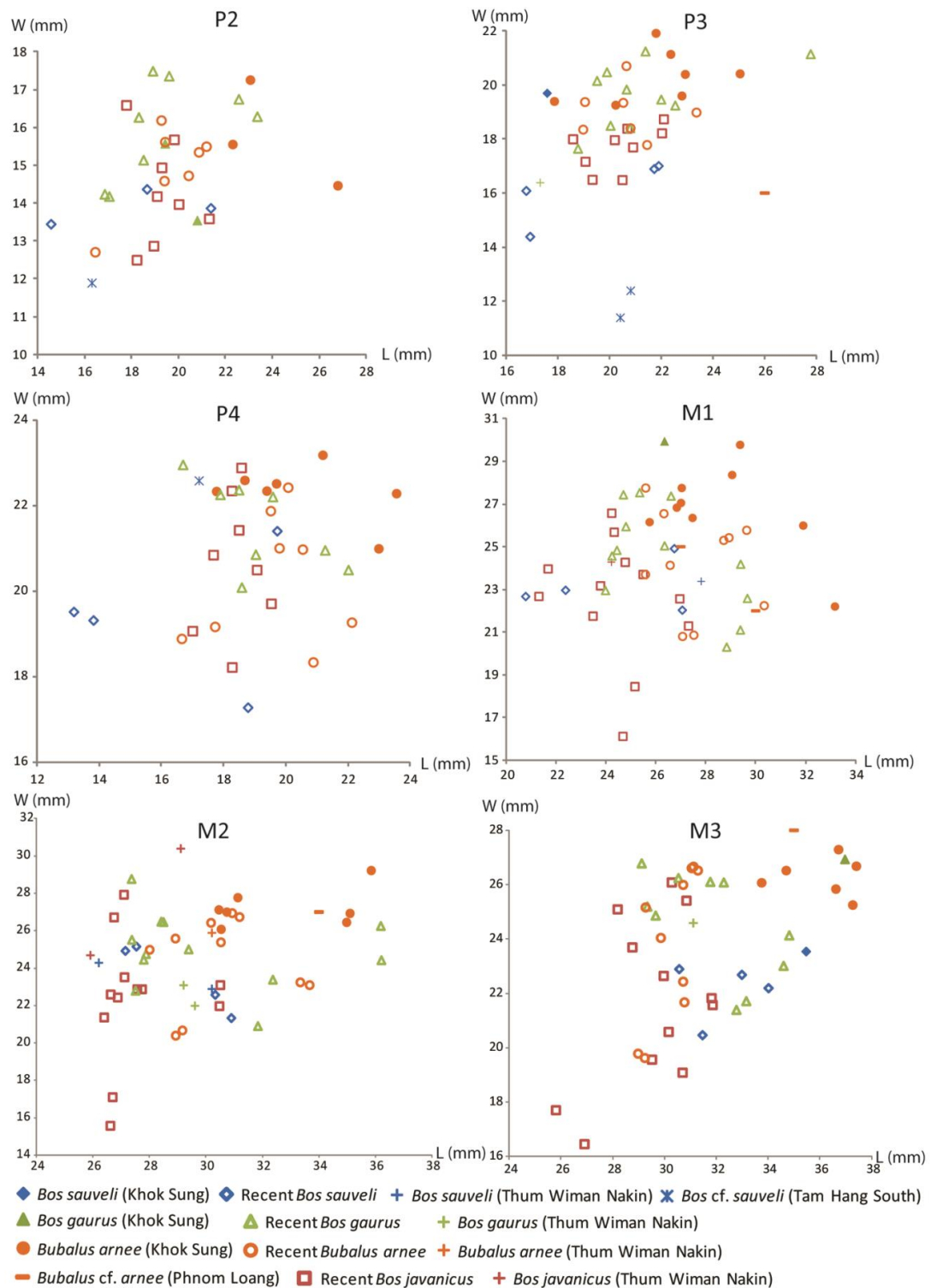


Figure 54. Scatter diagrams of upper cheek tooth (P2–M3) widths of recent and fossil large bovids. Fossil data from Phnom Loang, Lang Trang, Thum Wiman Nakin, and Tam Hang South are from Beden and Guérin (1973), de Vos and Long (1993), Tougard (1998), and Bacon et al. (2011), respectively.

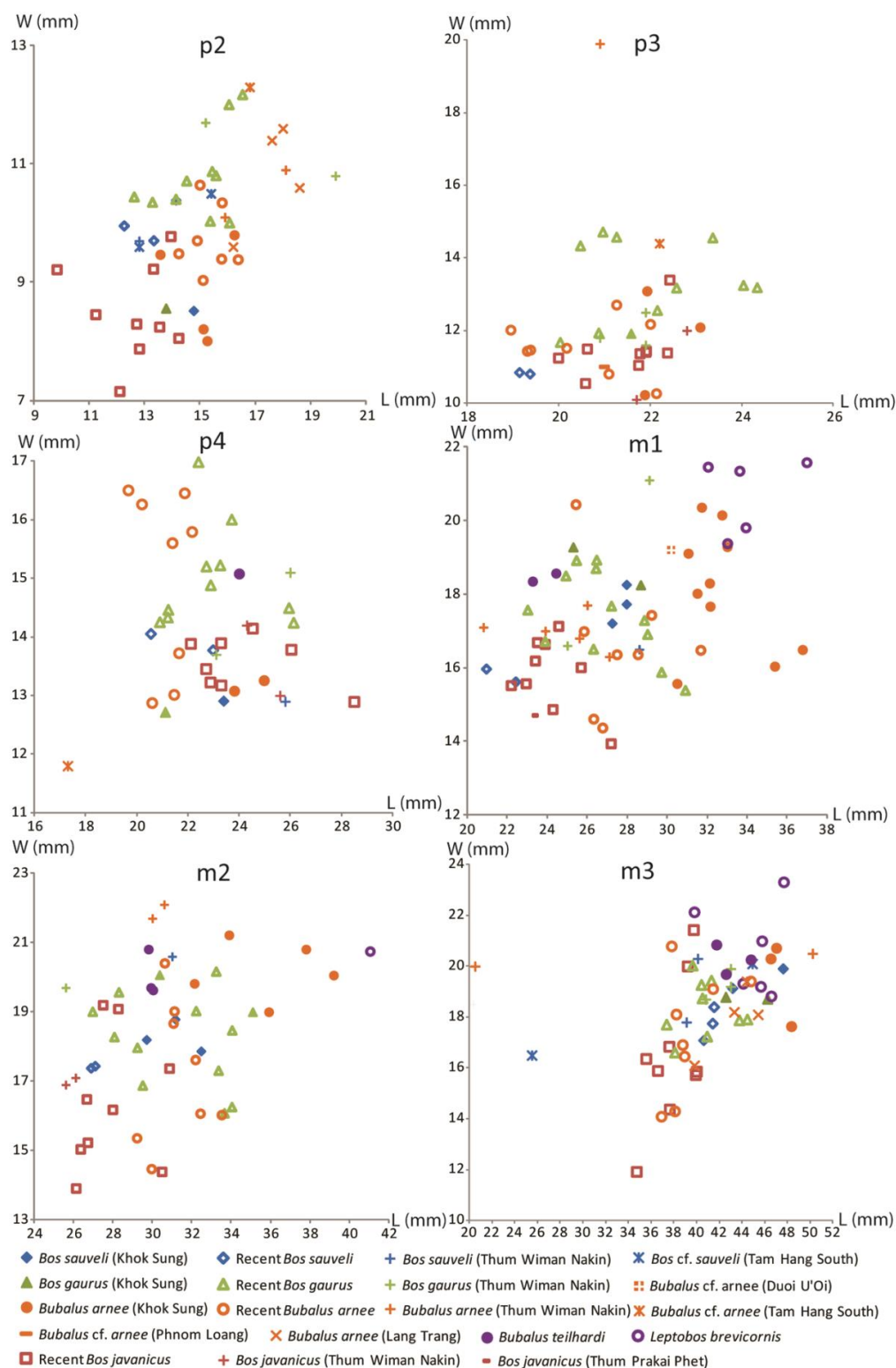


Figure 55. Scatter diagrams of lower cheek tooth (p2–m3) widths of recent and fossil large bovids. Fossil data from Phnom Loang, Lang Trang, Thum Wiman Nakin, Thum Prakai Phet, Duoi U’Oi, and Tam Hang South are from Beden and Guérin (1973), de Vos and Long (1993), Tougard (1998), Filoux et al. (2015), and Bacon et al. (2008b, 2011), respectively.

According to the molecular phylogenetic analyses, the kouprey may have been domesticated in Cambodia (Hassanin et al., 2006) and they are probably a feral animal derived from hybridization between *B. javanicus* and *B. taurus indicus* (zebu) (Galbreath et al., 2006). However, the latter statement is not recently supported by the molecular sequences available for koupreys, bantengs, and zebras (Hassanin and Ropiquet, 2007). These authors indicated that the mitochondrial sequences of Cambodian bantengs are divergent from those of Javan bantengs, but similar to those of koupreys. They also proposed that the mitochondrial genome of koupreys seems to have been transferred by natural hybridization into the ancestor of Cambodian bantengs. The taxonomic status of koupreys is currently under discussion and additional molecular analyses on Southeast Asian bantengs need to be examined in the future. However, our taxonomic identification of Khok Sung bovines suggests an existence of the Pleistocene kouprey in Thailand because of its high similarities in dental features with the type specimen MNHN-ZMO-1940-51 and the specimen MNHN-ZMO-10801.

***Bos gaurus* (Hamilton-Smith, 1827)**

Referred material: a left horn core, DMR-KS-05-03-26-22; a right DP2, DMR-KS-05-03-20-4; two right P2—DMR-KS-05-03-19-27 and DMR-KS-05-04-03-3; a right DP3, DMR-KS-05-03-20-3; a right DP4, DMR-KS-05-03-17-3; a right M1, DMR-KS-05-03-00-20; a right M3, DMR-KS-05-03-17-1; a right mandible with m1–m3, DMR-KS-05-03-00-1; a left mandible with p2–m3, DMR-KS-05-04-3-1; a left i1, DMR-KS-05-03-00-27; two left m2—DMR-KS-05-03-19-26 and DMR-KS-05-03-16-1; two humeri—DMR-KS-05-05-1-1 (right) and DMR-KS-05-03-00-62 (left); a right metacarpus, DMR-KS-05-03-26-27; two left femora—DMR-KS-05-03-9-2 and DMR-KS-05-04-30-1 (proximal part)

Material description

Horn core: a single horn core (DMR-KS-05-03-26-22) is small, curved upward (Fig. 56A, B) and slightly backward. The horn core base is oval in cross-section (Fig. 56A). A longitudinal ridge on the anterior surface of the horn core is present (Fig. 56B). This specimen belongs to a juvenile individual according to its very small size.

Upper dentition: DP2 (DMR-KS-05-03-20-4) is small and elongated, characterized by three main cones (anterior cone, paracone, and metacone) and a well-developed metastyle (Fig. 56C) (for measurements, see Tab. 19). The anterior and posterior fossettes fuse together. Two P2 (DMR-KS-05-03-19-27; fig. 56D and DMR-KS-05-04-03-3: fig. 56E) have a well developed paracone rib close to the parastyle and a nearly flat lingual wall. The fossettes are separated into two islands (larger for the anterior one) due to the heavy wear stage (Fig. 56D). The P2 also shows a nearly straight posterior wall and is wider than the DP2 (Fig. 56E). On the molarized DP3, the posterior lobe is broader than the anterior lobe (Fig. 56F). A small medial fossette is present. The entostyle is short and projects posteriorly. The molarized DP4 (DMR-KS-05-03-17-3) is slightly worn, characterized by a rectangular outline, well-developed buccal styles, an unfused entostyle, and two separated medial fossette (Fig. 56G–H). The entostyle is bifurcated and situated between the protocone and hypocone (Fig. 56G). Two parallel longitudinal grooves are present along the lingual surface of the entostyle, likely resulting in a trifurcated pattern in relation to the middle wear stage (Fig. 56H). The heavily worn M1 (DMR-KS-05-03-00-20) displays a subsquare outline and an unbifurcated entostyle positioned between the protocone and hypocone (Fig. 56I). The medial fossette is absent due to the heavy wear stage. The M3 (DMR-KS-05-03-17-1) exhibits well-developed buccal styles and large medial fossettes splitting into 2 islands with wear (Fig. 56J). The entostyle on the M3 is short, not bifurcated, and close to the hypocone.

Mandibles and lower dentition: DMR-KS-05-04-3-1 is complete, posterior to the p2, with the exception of a small part of the angular region (Fig. 56K, L) (for measurements, see Tab. A15). Another mandible (DMR-KS-05-03-00-1) preserves only a portion of the ramus with the complete molar row (Fig. 56M and Tab. A15).

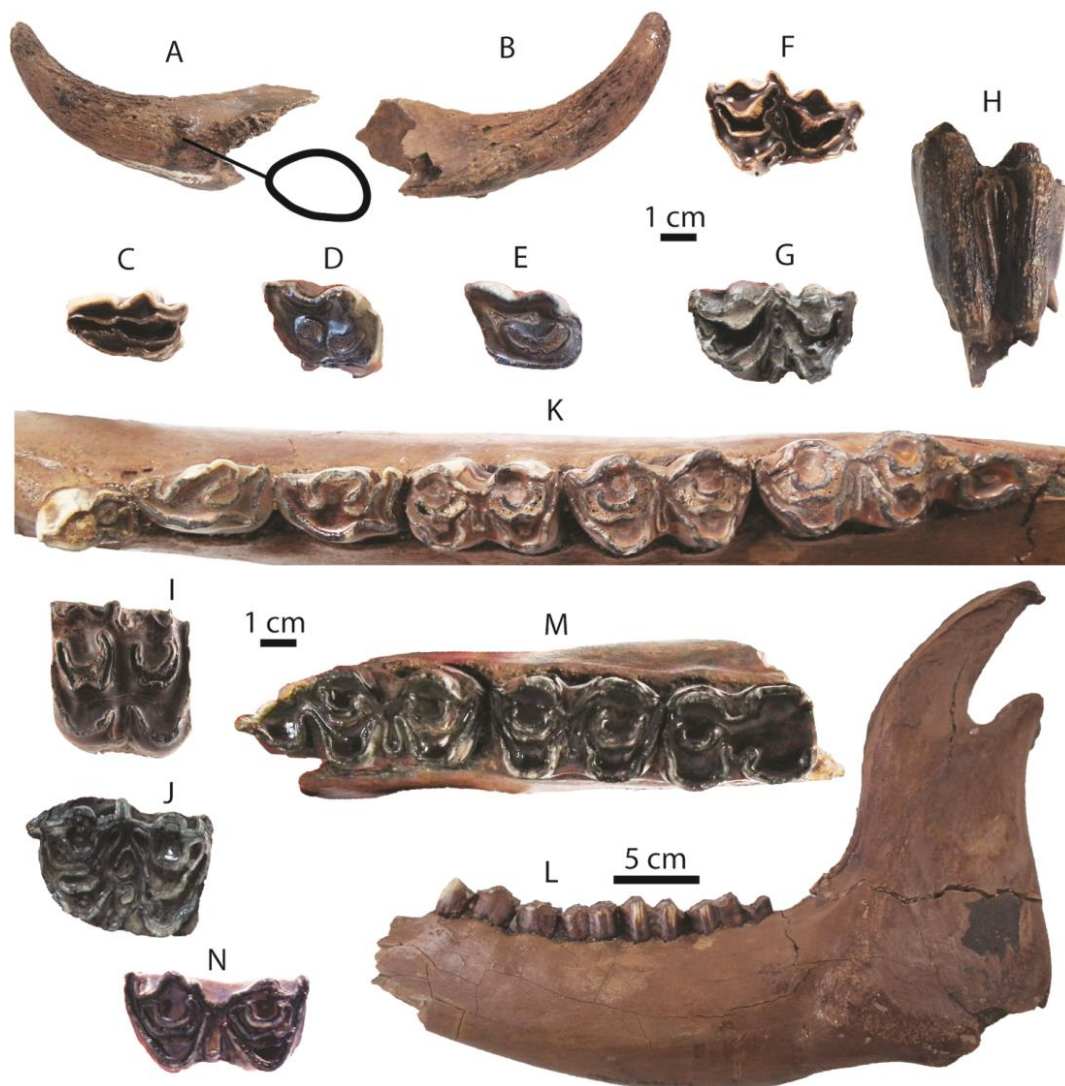


Figure 56. Remains of *Bos gaurus* from Khok Sung: (A–B) DMR-KS-05-03-26-22, a left horn core in posterior (A) and anterior (B) view; (C) DMR-KS-05-03-20-1, a right DP2; (D) DMR-KS-05-03-19-27, a right P2; (E) DMR-KS-05-04-03-03, a right P2; (F) DMR-KS-05-03-20-3, a right DP3; (G–H) DMR-05-03-17-3, a right DP4 in occlusal (G) and lingual (H) views; (I) DMR-05-03-17-1, a right M3; (J) DMR-05-03-19-26, a left m2; (K–L) DMR-KS-05-04-3-1, a left mandible in and occlusal (K) and lateral (L) views; (M) DMR-KS-05-03-00-1, a fragmentary mandible in occlusal view. All isolated teeth are shown in occlusal view.

The isolated i1 (DMR-KS-05-03-00-27) is heavily worn, spatulate, and robust. Lower premolars have well-developed main cuspids and cristids (Fig. 56K, M). On the p2, the protocone is the highest cuspid and the posterior fossette is present. The p3 is elongated as long as the p4. The premetacristid is poorly developed. The postprotocristid on the p3 is larger than that on the p4. On the p4, the postprotocristid is narrow and anteroposteriorly constricted. The metaconid is most developed, compared to *B. sauveli* and *B. javanicus* as well as *Bubalus arnee*. For all lower molars, the ectostylid is slightly developed and not bifurcated (Fig. 56K, M–N) (for measurements, see Tab. 19). In lingual view, the metastylid is absent at the medium wear stage (Fig. 56K, M). In occlusal view, the entostylid is straight and short. The buccal outline of the protoconid and hypoconid is U-shaped in relation to the strong wear (Fig. 56M). The posterior talonid on the m3 is well-developed. The posthypoconulidcristid protrudes posteriorly.



Figure 57. Postcranial remains of *Bos gaurus* from Khok Sung: (A–D) DMR-KS-05-05-1-1, a right humerus in proximal (A), posterior (B), anterior (C), and distal (D) views; (E–G) DMR-KS-05-03-26-27, a right metacarpus in proximal (E), anterior (F), and distal (G) views; (H–J) DMR-KS-05-03-9-2, a left femur in proximal (H), distal (I), and anterior (J) views.

Postcranial remains: postcranial elements include humeri (Fig. 57A–D), a metacarpus (Fig. 57E–G), and femora (Fig. 57H–J) (for measurements, see Tab. A1). The femur DMR-KS-05-04-30-1 lacks a distal portion. We assign these postcranial bones based on the proportional correlations with the recent specimens of *B. gaurus* (Tabs 17, A9, and A11–A14).

Taxonomic remarks and comparisons

According to IUCN (2015), the wild forms of gaurs are considered as *Bos gaurus*, while their domestic forms are recognized as *Bos frontalis* (Gentry et al., 2004). We consider here the Pleistocene fossil gaurs as belonging to wild forms in terms of taxonomic nomenclature.

We assign the juvenile horn core (DMR-KS-05-03-26-22) to *B. gaurus* because the horn cores of gaurs are different from all other *Bos* species. They grow outward and curve upward, similar to those of *Bubalus arnee*, but their apical portion curves inward and slightly forward (Lekagul and McNeely, 1988).

Mandibles and isolated teeth of *B. gaurus* are also observed. The cheek teeth of *B. gaurus* are distinguished from *B. sauveli* and *B. javanicus* by having two separate fossettes on the P2, more developed metaconids and more anteroposteriorly constricted postprotocristids on the p3 and p4, and more robust cheek teeth (Figs 54 and 55, and Tab. 19). The entostyles are usually bifurcated or sometimes trifurcated on the slightly to moderately worn upper molars (our observations on the comparative material of recent *B. gaurus*: e.g., ZSM-1972-5 and ZSM-1961-313), similar to those of *B. javanicus*. But the entostyle is not bifurcated, when the molar is extremely worn, as seen on the specimen DMR-KS-05-03-00-20 (Fig. 56l). This character is therefore morphologically variable through wear. On the m3, the entostylid and posterior talonid in *B. gaurus* is almost more developed than that in *B. javanicus*. The angle between the posthypocristid and prehypocristid is slightly more divergent in *B. sauveli* than in *B. gaurus*. The size of Khok Sung *B. gaurus* falls within the range of the recent population (Figs 54

and 55, and Tab. 18). We elucidate here the co-occurrence of two *Bos* species, *B. sauveli* and *B. gaurus* (larger), in Khok Sung.

Genus *Bubalus* Hamilton-Smith, 1827

Bubalus arnee (Kerr, 1792)

Referred material: a nearly complete cranium associated with a right mandible, DMR-KS-05-03-20-1; a cranium with a right tooth row (P3–M3), DMR-KS-05-03-21-1; a partial cranium with two tooth rows (P3–M1), DMR-KS-05-03-16-3; a partial cranium with a right tooth row (P3–M3), DMR-KS-05-03-11-1; three horn cores—DMR-KS-05-03-16-2 (right), DMR-KS-05-03-31-6 (right), and DMR-KS-05-03-19-28 (left); a left P2, DMR-KS-05-03-18-14; a left DP3, DMR-KS-05-03-00-103; two right P3—DMR-KS-05-03-22-14 and DMR-KS-05-04-05-3; a right DP4, DMR-KS-05-04-29-8 (broken anterior lobe); two P4—DMR-KS-05-03-18-13 (right) and DMR-KS-05-03-18-9 (left); four M1—DMR-KS-05-03-31-5 (right), DMR-KS-05-03-18-12 (right), DMR-KS-05-03-18-6 (left), and DMR-KS-05-03-22-13 (left); five M2—DMR-KS-05-03-00-2 (right), DMR-KS-05-03-25-21 (right), DMR-KS-05-03-18-5 (right), DMR-KS-05-03-16-2(1) (left), and DMR-KS-05-03-18-7 (left); four M3—DMR-KS-05-03-00-7 (right), DMR-KS-05-03-22-12 (left), DMR-KS-05-03-14-1 (left), and DMR-KS-05-03-18-10 (left); a right mandible with p2–m1, DMR-KS-05-03-20-2; three left mandibles—DMR-KS-05-03-10-3 (with p2–m3), DMR-KS-05-03-20-10 (with p2–m1), and DMR-KS-05-03-20-20 (with m1 and m2); a right i1, DMR-KS-05-03-18-8; a right i2, DMR-KS-05-03-22-15; a left i3, DMR-KS-05-03-00-106; a right i4, DMR-KS-05-03-16-3; a right p3, DMR-KS-05-03-14-4; a left dp4, DMR-KS-05-03-00-4; a right p4, DMR-KS-05-03-19-6; four m1—DMR-KS-05-03-25-3 (right), DMR-KS-05-03-18-18 (right), DMR-KS-05-03-00-105 (left), and DMR-KS-05-03-00-3 (left); two m2—DMR-KS-05-03-27-12 (right) and DMR-KS-05-03-25-2 (left); two m3—DMR-KS-05-03-18-11 and DMR-KS-05-04-29-2 (left posterior lobe); eleven thoracic vertebrae—DMR-KS-05-04-1-11 (T3), DMR-KS-05-04-1-26 (T4), DMR-KS-05-04-1-13 (T5), DMR-KS-05-04-1-14 (T6),

DMR-KS-05-04-1-15 (T7), DMR-KS-05-04-1-16 (T8), DMR-KS-05-04-1-12 (T9), DMR-KS-05-04-1-17 (T10), DMR-KS-05-04-1-18 (T11), DMR-KS-05-04-1-19 (T12), and DMR-KS-05-04-1-20 (T13); four lumbar vertebrae: DMR-KS-05-04-1-24 (L1), DMR-KS-05-04-1-23 (L2), DMR-KS-05-04-1-22 (L3), and DMR-KS-05-04-1-21 (L4); two humeri—DMR-KS-05-03-31-1 (right) and DMR-KS-05-03-31-8 (left); two scapulae—DMR-KS-05-03-26-2 (right) and DMR-KS-05-02-20-4 (left); three ulnae and radii—DMR-KS-05-03-00-61 (right), DMR-KS-05-03-31-2 (right) and DMR-KS-05-03-31-9 (left); a right metacarpus, DMR-KS-05-03-26-3(1); a pelvis, DMR-KS-05-04-1-25; two femora—DMR-KS-05-04-1-1 (right) and DMR-KS-05-04-1-2 (left); a right fragmentary femur, DMR-KS-05-03-20-8 (distal part); three tibiae—DMR-KS-05-4-1-11 (right), DMR-KS-05-04-1-3 (left), and DMR-KS-05-03-20-9 (left); two fourth tarsal bones—DMR-KS-05-04-1-7 (right) and DMR-KS-05-04-1-5 (left); three metatarsi—DMR-KS-05-04-1-8 (right), DMR-KS-05-04-1-6 (left), and DMR-KS-05-03-28-30 (left); a left astragalus, DMR-KS-05-04-1-4; a left phalanx I, DMR-KS-05-04-1-9; a left phalanx II, DMR-KS-05-04-1-10

Material description

Crania and upper dentition: DMR-KS-05-03-20-1 is undeformed and nearly complete (for measurements, see Tab. A16). Only the right maxilla, squamosals, and basicranium are damaged (Fig. 58A–C). The horn cores are broken at their middle portion. The cross-section of the horn core base is subtriangular and anteriorly flat (Fig. 58A). The frontals are narrow between the orbits and are flat or slightly convex at the region between horn core bases (Fig. 58A, C). The supraorbital foramina are large. The orbits face slightly forward (Fig. 58A, B), not laterally like *Leptobos brevicornis* and *Bubalus teilhardi* (Dong et al., 2014). The lateral margins of the premaxilla are concave (Fig. 58B).

DMR-KS-05-03-21-1, a juvenile cranium, is incomplete but slightly deformed. The posterior part of the skull is almost complete but the anterior part is broken (Fig. 58D, E). The cranium is likely elongated and laterally compressed (Fig. 58D). This specimen preserves two horn

cores (broken at the right one) and a right tooth row with the M1, the P3 and P4 roots, and the unerupted M2 and M3 (Fig. 58E). The horn cores of DMR-KS-05-03-21-1 are slender, straight, and inclined upward and backward, and bend outward (Fig. 58D), similar to that of recent *Bubalus arnee* (e.g., MNHN-ZMO-1863-65). The horn cores are subtriangular in cross section base, becoming subrounded toward the apex (Fig. 58D). The divergent angle between the horn cores is 105° . The frontals are short and narrow, forming an obtuse angle with the occipital plane. The parietals merged together. The occiput extends so far, posterior to the horn core bases. The basioccipital is laterally concave and triangular in outline (Fig. 58E).

DMR-KS-05-03-11-1 preserves the right zygomatic bone and the premaxilla and maxilla with a nearly complete tooth row (P3–M3) (Fig. 58F, G). Another specimen, DMR-KS-05-03-16-3, preserves the premaxilla and maxilla with P3–M1 (Fig. 58H, I). In dorsal and ventral views, the lateral margins of the premaxilla are concave, as expected for *Bubalus* (Fig. 58H).

Three isolated horn cores (DMR-KS-05-03-16-2: fig. 58J, DMR-KS-05-03-31-6, and DMR-KS-05-03-19-28) are incomplete. The apical portion is broken away on each specimen. All horn cores are robust, long, and curved backward. Their anterior and dorsal surfaces are flat and their cross-sections are subtriangular at the base (Fig. 58J).

Upper cheek teeth of *Bubalus arnee* are often filled by abundant cements and more robust, compared to those of *Bos*. P2 (DMR-KS-05-03-18-14: fig. 58K) is elongated. The parastyle on the P2 is less developed than that on the P3 and P4. The molarized DP3 (DMR-KS-05-03-00-103: fig. 58L) is characterized by a well-developed buccal styles, anterior cingulum, entostyle, and spur, and a larger posterior lobe. The P3 is subtriangular in outline and is marked by a distinct parastyle, paracone rib, and metastyle and a U-shaped fossette (Fig. 58G, I). The parastyle of the P3 often curves posteriorly. The DP4 (DMR-KS-05-04-29-8: fig. 58M) is also molarized with the broken protocone. This specimen has well-developed buccal styles and two separate medial

fossettes. The entostyle curves posteriorly in occlusal view and is positioned more lingually than the protocone and hypocone. The P4 is similar in morphology to the P3, but is more anteroposteriorly compressed.

Upper molars display *Bos*-like patterns (e.g., the degree of the hypsodonty and selenodonty and the presence of distinct styles) but are more robust than most species of *Bos* (e.g., *B. sauveli* and *B. javanicus*) (Tab. 19). However, the mesostyles of upper molars of *Bubalus arnee* are more developed than those of *Bos*. The medial fossette between the anterior and posterior fossettes (infundibula) is well-developed, often separating into two or three islands with wear (Fig. 58G, I, N). The infundibula are U-shaped but sometimes become metacentric chromosome-shaped due to strong wear, like in *B. sauveli* (Fig. 58G, N). In occlusal view, the entostyle is long and straight or curves posteriorly, depending on the stage of wear, but is never bifurcated (Fig. 58G, I, N). The small fossette is sometimes present within the entostyle in relation to strong wear (Fig. 58N).

Mandibles and lower dentition: five mandibles: DMR-KS-05-03-20-1 (Fig. 59A, B), DMR-KS-05-03-10-3 (Fig. 59C, D), DMR-KS-05-03-20-2 (Fig. 59E, F), DMR-KS-05-03-20-10 (Fig. 59G, H), and DMR-KS-05-03-20-20 (Fig. 59I), are almost complete (for measurements, see Tab. A15). The first specimen is associated with the cranium. The right specimen DMR-KS-05-03-20-2 and the left specimen DMR-KS-05-03-20-20 belong to the same individual, bearing p2, dp3, dp4, and an unerupted m2. The left one is very fragmentary. Another mandible DMR-KS-05-03-20-10 is nearly complete, preserving the mandibular symphysis and bearing an unerupted m2, but lacking all incisors. All incisors drop out of the mandibles. The isolated lower incisors are spatulate in shape (Fig. 59J–L). The i2 is similar in size to the i3 (Tab. 19).



Figure 58. Cranial and upper dental remains of *Bubalus amee* from Khok Sung: (A–C) DMR-KS-05-03-20-1, a cranium in dorsal (A), ventral (B), and lateral (C) views and (D–E) DMR-KS-05-03-21-1, a cranium in dorsal (D) and ventral (E) views; (F–G) DMR-KS-05-03-11-1, a right upper jaw in lateral (F) and occlusal (G) views; (H–I) DMR-KS-05-03-16-3, a partial cranium in ventral view (H) with a right tooth row (I); (J) DMR-KS-05-03-16-2, a right horn core in dorsal view; (K) DMR-KS-05-03-18-14, a left P2; (L) DMR-KS-05-03-00-103, a left DP3; (M) DMR-KS-05-04-29-8, a right DP4; (N) DMR-KS-05-03-00-7, a right M3. Cross-sections of basal horn cores are given. All isolated teeth are shown in occlusal view.

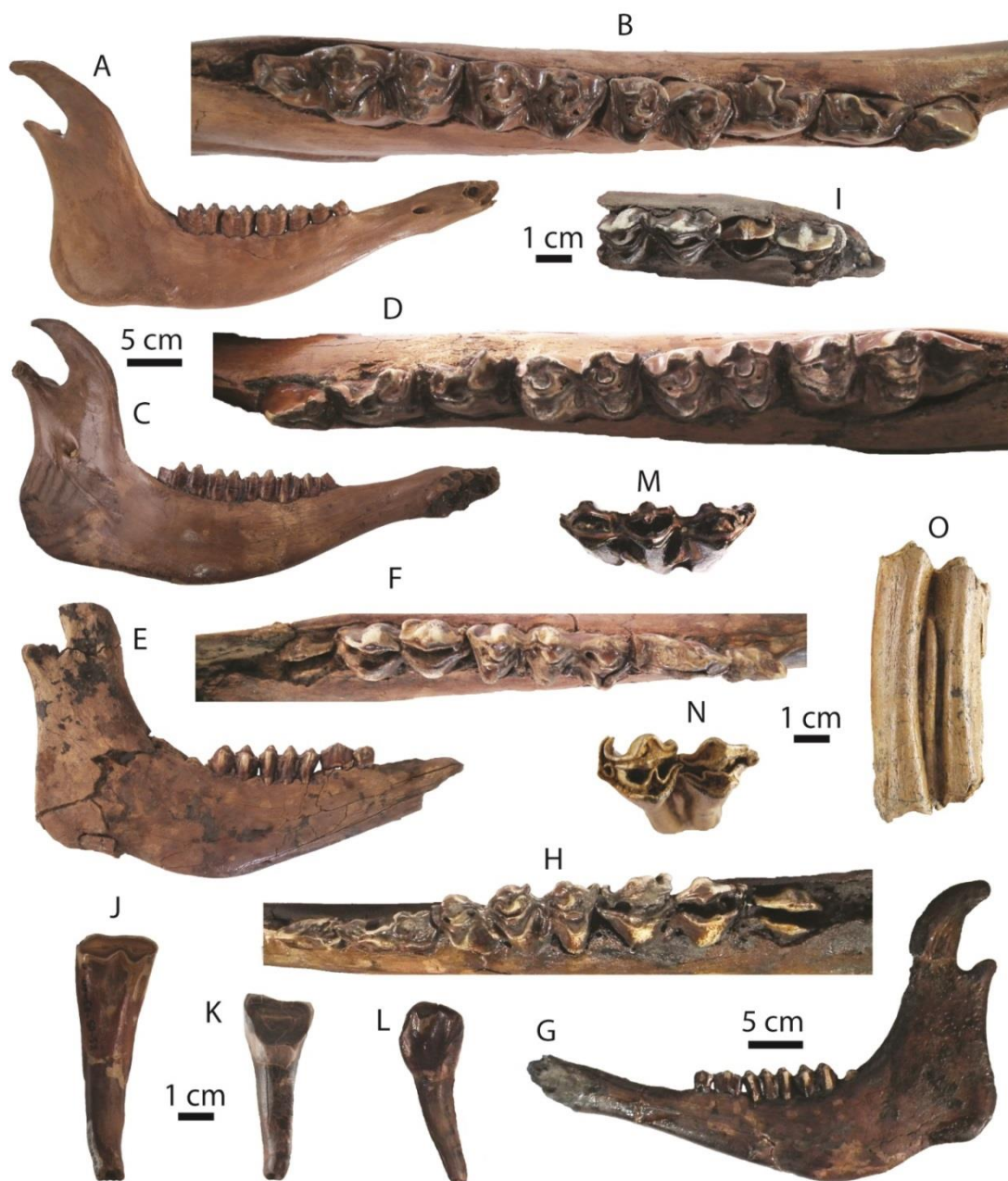


Figure 59. Mandibular and lower dental remains of *Bubalus arnee* from Khok Sung: (A–B) DMR-KS-05-03-20-1, a right mandible in lateral (A) and occlusal (B) views; (C–D) DMR-KS-05-03-10-3, a left mandible in mesial (C) and occlusal (D) views; (E–F) DMR-05-03-20-2, a right mandible in lateral (E) and occlusal (F) views; (G–H) DMR-05-03-20-10, a left mandible in lateral (G) and occlusal (H) views; (I) DMR-KS-05-03-20-20, a left fragmentary mandible with m1 and m2 in occlusal view; (J) DMR-KS-05-03-18-8, a right i1 in lingual view; (K) DMR-KS-05-03-00-106, a left i3 in lingual view; (L) DMR-KS-05-03-16-3, a right i4; (M) DMR-KS-05-03-00-4, a left dp4 in occlusal view; (N–O) DMR-KS-05-03-00-105, a left m1 in occlusal (N) and buccal (O) views.

All lower cheek teeth are almost filled by abundant cements. All lingual stylids are distinct. The p2 has a well-developed postentocristid and posthypocristid (Fig. 59B, D, F, H). The metaconid is positioned more lingually than all of lingual cristids. The dp3 is elongated (Fig. 59F, H). The postprotocristid is large and the metaconid is well-developed. A small anterior fossette is present with wear. The p3 displays a well-developed preprotoconulidcristid and a posteriorly bending metaconid (Fig. 59B, D). The isolated dp4 (DMR-KS-05-03-00-4: fig. 59M) is trilobed and elongated with a well-developed stylids (anterior and posterior ectostylid, parastylid, metastylid, and entostylid). On the dp4, the buccal outline of the protoconulid, protoconid, and hypoconid is V-shaped in occlusal view (Fig. 59F, H, M). The anterior ectostylid curves slightly posteriorly in contrast to the posterior ectostylid that bends anteriorly (Fig. 59M). A large fossette is present between the medial and posterior valley in relation to middle wear stage (Fig. 59M). On the p4, the metaconid is most lingually positioned (Fig. 59B, D). The premetacristid is more developed than the postmetacristids. The postprotocristid is very anteroposteriorly constricted. The postentocristid fuses with the posthypocristid beyond the middle stage of wear.

Lower molars have well-developed stylids and conids. The metastylid is most developed on the unworn to slightly worn specimens (Fig. 59F, H, I, N and Tab. 19). The metastylid is located closely to the metaconid. In occlusal view, the anterior and posterior fossettes are U-shaped, similar to that of *Bos*. The entostylid is well-developed and sometimes curves anteriorly (Fig. 59F, I). On the m3, the posterior ectostylid is absent. The posthypoconulidcristid protrudes posteriorly slightly and is sometimes bifurcated (Fig. 59B, D). The back fossette is sometimes present with wear.

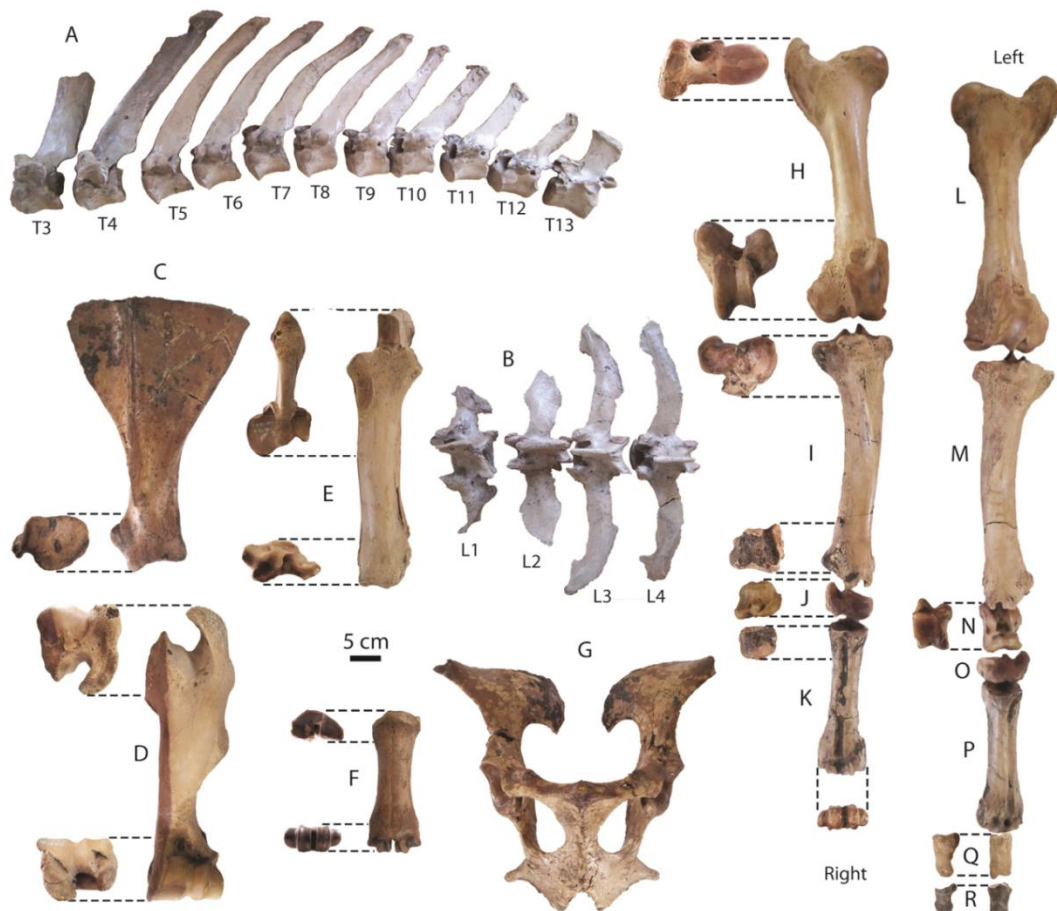


Figure 60. Articulated postcranial skeletons of *Bubalus arnee* from Khok Sung: **(A)** thoracic (abbreviated as “T”) vertebrae in lateral view: DMR-KS-05-04-1-11 (T3), DMR-KS-05-04-1-26 (T4), DMR-KS-05-04-1-13 (T5), DMR-KS-05-04-1-14 (T6), DMR-KS-05-04-1-15 (T7), DMR-KS-05-04-1-16 (T8), DMR-KS-05-04-1-12 (T9), DMR-KS-05-04-1-17 (T10), DMR-KS-05-04-1-18 (T11), DMR-KS-05-04-1-19 (T12), and DMR-KS-05-04-1-20, (T13); **(B)** lumbar (L) vertebrae in dorsal view: DMR-KS-05-04-1-24 (L1), DMR-KS-05-04-1-23 (L2), DMR-KS-05-04-1-22 (L3), and DMR-KS-05-04-1-21 (L4); **(C–E)** a left forelimb in anterior view: **(C)** DMR-KS-05-02-20-4, a scapula in lateral and distal views; **(D)** DMR-KS-05-03-31-8, a humerus in proximal and distal views; **(E)** DMR-KS-05-03-31-9, an ulna and a radius in proximal and distal views; **(F)** DMR-KS-05-03-26-3(1), a right metacarpus in proximal, anterior, and distal views; **(G)** DMR-KS-05-04-1-25, a pelvis in ventral view; **(H–R)** hindlimbs in anterior view: **(H)** DMR-KS-05-04-1-1, a right femur in proximal and distal views; **(I)** DMR-KS-05-4-1-11, a right tibia in proximal and distal views; **(J)** DMR-KS-05-04-1-7, a right 4th tarsal bone in dorsal view; **(K)** DMR-KS-05-04-1-8, a right metatarsus in proximal and distal views; **(L)** DMR-KS-05-04-1-2, a left femur; **(M)** DMR-KS-05-04-1-3, a left tibia; **(N)** DMR-KS-05-04-1-4, a left astragalus in plantar view; **(O)** DMR-KS-05-04-1-5, a left 4th tarsal bone; **(P)** DMR-KS-05-04-1-6, a left metatarsus; **(Q)** DMR-KS-05-04-1-9, a left phalanx I in lateral view; **(R)** DMR-KS-05-04-1-10, a left phalanx II in lateral view.

Postcranial remains: postcranial elements include scapulae (Fig. 60C), humeri (Fig. 60D), ulnae and radii (Fig. 60E), femora (Fig. 60H, L), tibiae (Fig. 60I, M), fourth tarsal bones (Fig. 60O), metacarpi (Fig. 60F), metatarsi (Fig. 60K, P), phalanges (Fig. 60Q, R), a pelvis (Fig. 60G), and thoracic and lumbar vertebrae (Fig. 60A, B). Most of postcranial remains belong to the same individual because they were found in connection. But some isolated specimens (scapula: DMR-KS-05-03-26-2, ulna and radius: DMR-KS-05-03-00-61, femur: DMR-KS-05-03-20-8, and metatarsus: DMR-KS-05-03-28-30) were found separately. The articulated skeletons show a typical character of *Bubalus arnee* whose postcranial bones are more massive and thicker than those of *Bos* (Fig. 60 and Tab. A1).

Taxonomic remarks and comparisons

According to IUCN (2015), the wild forms of water buffaloes are considered as *Bubalus arnee*, while their domestic forms are regarded as *Bubalus bubalis* (Gentry et al., 2004).

Although the cheek teeth of *Bos* and *Bubalus* are almost morphologically identical and often show highly variable occlusal morphologies in relation to the wear stages, they are distinguishable based on the dental morphology. Bacon et al. (2011) mentioned that *Bubalus arnee* is distinguished from *Bos* by several dental characters: more massive and voluminous cones, conids, and lingual stylids, more complex patterns of folded infundibula on the upper molars, U-shaped protoconids and hypoconids on the lower molars, and unilobed entostyles and ectostylids. However, the latter two characters are highly variable with wear, as observed on many extant specimens of *Bubalus arnee* from MNHN, ZSM, and THNHM. Among the modern large bovids in Southeast Asia, some lower premolar (p3 and p4) and third molar features are more informative for the species identification than others (Thein, 1974). Our comparisons suggest that the cheek teeth of *Bubalus arnee* differ from those of *Bos* in having more developed mesostyles, more complex shapes of the infundibulum at the similar stages of wear, less

developed or smaller metaconids and narrower postprotocristids on the p3 and p4, a presence of the small fossette within the entostyle and an absence of the longitudinal groove on the lingual surface of the entostyle on upper molars, more distinct entostylids on the m3, and a presence of the back fossette on the m3. For the incisors, it is difficult to make morphological distinction between *Bubalus* and *Bos*. However, we assign these isolated lower incisors to *Bubalus arnee* because they were found together with their molars at the same spot.

As demonstrated by the scatter diagrams (Figs 54 and 55), the cheek teeth of recent *Bos* and *Bubalus* populations are highly overlapping in size. The lower molar sizes of *Bubalus arnee* also overlap with some fossil species (*Bubalus teilhardi* and *Leptobos brevicornis*). However, tooth dimensions are informative to make an ongoing distinction among the Khok Sung large bovids. The largest bovid in this locality is *Bubalus arnee*, followed by *B. gaurus* and *B. sauveli*, respectively, similar to the size tendency of their recent population (Tab. 18).

Genus *Capricornis* Ogilby, 1836

Capricornis sumatraensis (Bechstein, 1799)

Referred material: a left M2, DMR-KS-05-03-18-16; three m3, DMR-KS-05-04-05-4 (right), DMR-KS-05-03-27-5 (left), and DMR-KS-05-03-28-10 (left posterior fragment)

Material description

Isolated teeth are almost complete (for measurements, see Tab. 20), with the exception of the specimen DMR-KS-05-03-28-10 that preserves only a posterior lobe (Fig. 61G). Molars show typical features of *Capricornis* characterized by hyposodont crowns, smooth enamel, and distinct styles and stylids, and an absence of the ectostylids (Fig. 61). The parastyle, mesostyle, and metastyle on the M2 are perpendicular to the buccal wall (Fig. 61A). On the m3, the mesostylid

is more developed than the other stylids and the posthypoconulid cristid protrudes posteriorly (Fig. 61C, E).

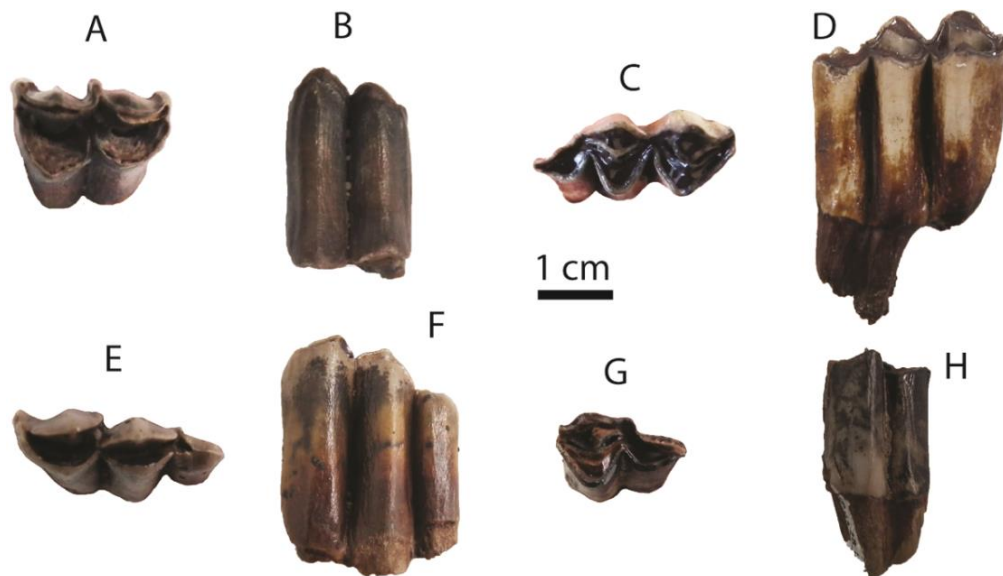


Figure 61. Dental remains of *Capricornis sumatraensis* from Khok Sung: (A–B) DMR-KS-05-03-18-16, a left M2 in occlusal (A) and lingual (B) views; (C–D) DMR-KS-05-04-05-4, a right m3 in occlusal (C) and buccal (D) views; (E–F) DMR-KS-05-03-27-5, a left m3 in occlusal (E) and buccal (F) views; (G–H) DMR-KS-05-03-28-10 in occlusal (G) and buccal (H) views.

Table 20. Measurements (lengths and widths in millimeters) of cheek teeth of Khok Sung *Capricornis sumatraensis*. N=number of specimens.

Specimen		Length	Width
DMR-KS-05-03-18-16	M2	17.02	15.62
DMR-KS-05-03-28-10	m3	–	10.72
DMR-KS-05-03-27-5	m3	23.94	9.94
DMR-KS-05-04-05-4	m3	21.99	9.52

Taxonomic remarks and comparisons

We assign these isolated teeth from Khok Sung to *Capricornis sumatraensis* (Sumatran serow) because they are comparable in size and morphology to the extant specimens (Fig. 62). Among congeneric species, *C. sumatraensis* is larger than *C. crispus* as well as two goral species (*Naemorhedus goral* and *Naemorhedus caudatus*), but is smaller than *C. milneedwardsi*. In addition, it differs from *C. crispus* in having more developed metastylid and entostylid and a presence of back fossettes on the slightly worn m3 and from *C. milneedwardsi* in having less developed metastylid and posthypoconulid cristid on the m3.

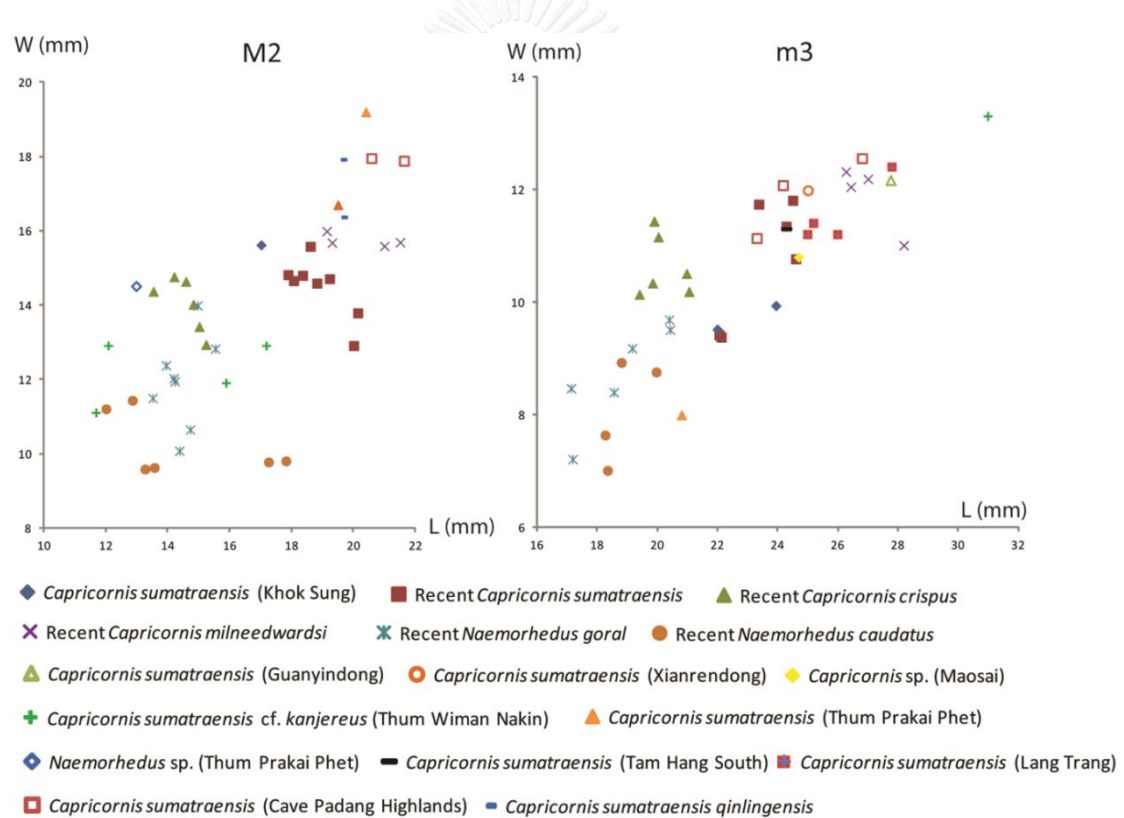
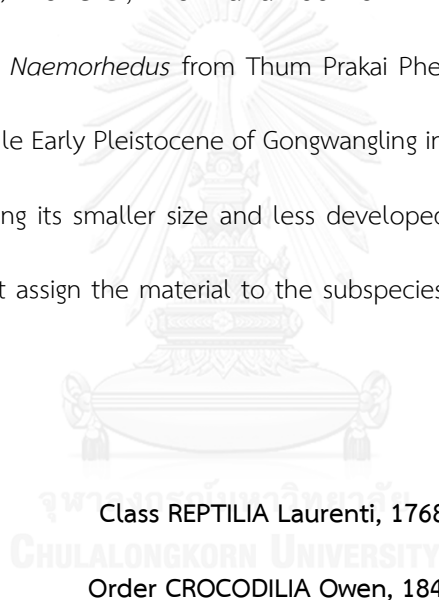


Figure 62. Scatter diagrams of M2 and m3 lengths and widths of recent and fossil serows and gorals. The measurements of fossil specimens from Lang Trang, Thum Wiman Nakin, Thum Prakai Phet, and Tam Hang South are from de Vos and Long (1993), Tougaard (1998), Filoux et al. (2015), and Bacon et al. (2011), respectively.

Compared to other fossil records, *C. sumatraensis* from Khok Sung is smaller than that from the Late Pleistocene of Lang Trang in Vietnam (de Vos and Long, 1993), Tam Hang South in Laos (Bacon et al., 2011), Padang Cave in Sumatra (Hooijer, 1958), and Xianrendong in China (Chen and Qi, 1978; Chen and Li, 1994) (Fig. 62) and from the late Middle Pleistocene of Guanyindong (Li and Wen, 1986) in China. The Khok Sung material also matches morphologically that of the subspecies *C. s. kanjereus* from the Middle Pleistocene of Yenchingkuo in China (Colbert and Hooijer, 1953) and from the late Middle Pleistocene of Thum Wiman Nakin in Thailand (Tougaard, 1998). However, *C. sumatraensis* from Khok Sung is larger than that from Thum Wiman Nakin and *Naemorhedus* from Thum Prakai Phet. It differs from *C. s. qinlingensis* described from the middle Early Pleistocene of Gongwangling in northern China (Hu and Qi, 1978; Zhu et al., 2015) in having its smaller size and less developed parastyle and metastyle on the M2. However, we do not assign the material to the subspecies level based on the few isolated teeth.



Class REPTILIA Laurenti, 1768

Order CROCODYLIA Owen, 1842

Family CROCODYLIDAE Laurenti, 1768

Genus *Crocodylus* Laurenti, 1768

Crocodylus cf. *siamensis* Schneider, 1801

Referred material: a fragmentary cranium, DMR-KS-05-03-30-30; a dentary fragment with one tooth, DMR-KS-05-03-21-1; five isolated teeth, DMR-KS-05-03-00-19, DMR-KS-05-03-14-3, DMR-KS-05-03-22-22, DMR-KS-05-04-06-3, and DMR-KS-05-04-29-10; three osteoderms—DMR-KS-05-03-29-57, DMR-KS-05-03-29-58, and DMR-KS-05-03-27-25

Material description

Skull and dentition: DMR-KS-05-03-30-30 is a slightly deformed skull preserving a nearly complete premaxilla, maxilla, nasal, and palatine process (Fig. 63A, B), and a partial palatine at the ventral part. The minimum length of the skull is 315 mm. The external naris is wide, dorsally directed, and presumably subcircular in outline (Fig. 63A). The nasal becomes narrower at the nearly premaxillary-maxillary suture and tapers into a point at the posterior rim of the naris. The premaxilla is broken anteriorly at the hole for the reception of the first dentary alveolus. The premaxilla contains at least four teeth on each side. The second one is the largest tooth in the premaxillary rows, regularly corresponding to the position of a large alveolar hole in dorsal view. A short premaxillary process extends to the second maxillary alveolus centrally or the first interalveolus laterally in ventral view (Fig. 63B). The premaxillary-maxillary suture is characterized by distinct notches. A maxilla comprises 14 alveoli, with the largest tooth crown (44.3 mm high) positioned at the fifth dentary alveolus. The width of the skull at the fifth maxillary tooth is 171.8 mm (the maximum width of the preserved skull). The width of the skull at the diastema between the last premaxillary tooth and the first maxillary tooth (the minimum width of the preserved skull) is 98.9 mm. Many small foramina in front of the alveoli are situated on both the premaxilla and the maxilla. Along the anterior to posterior maxillary rims, the tooth row is slightly convex until ending at the eighth or ninth alveolus. Teeth are characterized by their conical forms and striated surfaces. However, they are highly variable in shape and size, in relation to the position along the tooth row. The teeth of crocodyles are either slender and pointed or short and blunt (Fig. 63C) but much more massive than those of gharials. Asymmetrical surfaces of the tooth are divided by two prominent longitudinal ridges that are positioned anteriorly and posteriorly.

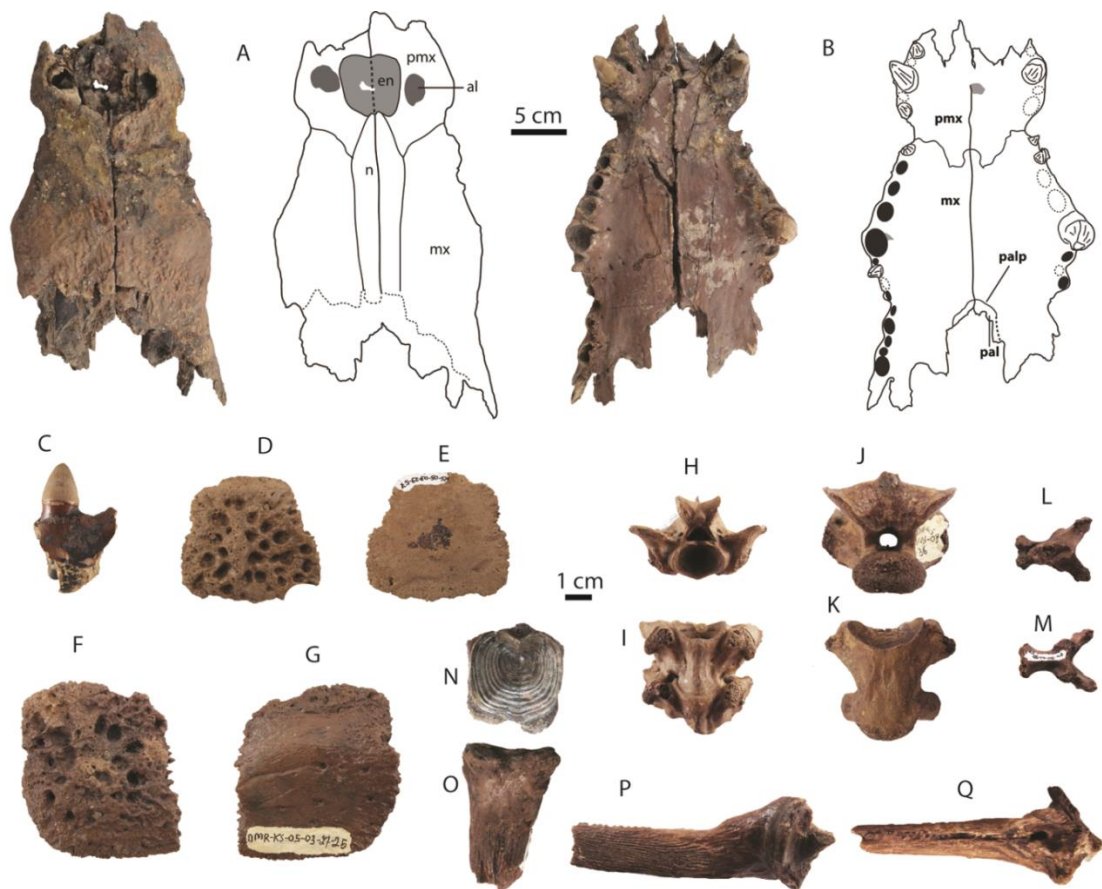


Figure 63. Remains of non-mammalian vertebrates from Khok Sung: *Crocodylus* cf. *siamensis*—(A–B) DMR-KS-05-03-30-30, a cranium in dorsal (A) and ventral (B) views; (C) DMR-KS-05-03-21-1, a tooth in lingual view; (D–E) DMR-KS-05-03-29-57 and (F–G) DMR-KS-05-03-27-25, osteoderms in dorsal (D, F) and ventral (E, G) views; *Python* sp.—(H–I) DMR-KS-05-03-00-16, a trunk vertebra in anterior (H) and ventral (I) views; *Varanus* sp.—(J–K) DMR-KS-05-03-08-36, a trunk vertebra in anterior (J) and ventral (K) views; Galliformes indet.—(L–M) DMR-KS-05-04-05-40, a cervical vertebra fragment in dorsal (L) and ventral (M) views; Siluridae indet.—(N–O) DMR-KS-05-03-22-76, a vertebra in anterior (N) and lateral (O) views; (P) DMR-KS-05-04-11-20, a pectoral spine in dorsal view; (Q) DMR-KS-05-04-05-25, a pectoral spine in medial view. Anatomical abbreviations: **al**, alveolus; **pmx**, premaxilla; **en**, external naris; **n**, nasal; **mx**, maxilla; **pal**, palatine; **palp**, palatine process.

Osteoderms: two nearly complete specimens (Fig. 63D–G) and one small fragment are characterized by rectangular shapes, wider than long (about 5–6 cm long and 7–8 cm width), and slightly flat to convex and irregular edges with small spiny outgrowths. A short median keel does not extend far anteriorly or posteriorly (Fig. 63D, F). The external surface has several large and

rounded to elliptical pits on the dorsal part and fewer small foramina and striae with surrounding fibrous patterns on the ventral part (Fig. 63E, G). These specimens differ from *Gavialis cf. bengawanicus* (Martin et al., 2012) in the same locality by their more ornamented pits and more irregular surfaces on the dorsal surface.

Taxonomic remarks and comparisons

The specimen DMR-KS-05-03-30-30 is a crocodylian cranium with a possible maximum length up to 50 cm. All morphological characters of the Khok Sung crocodiles are congruent with the extant fresh water crocodile, *Crocodylus siamensis*, as well as with its fossils recovered from the Early and Middle Pleistocene of Java (Trinil H. K., Kedung Brubus, and Kedung Lumbu) (Delfino and de Vos, 2010). However, the Khok Sung cranium preserves only the anterior midway portion of the skull and does not allow some morphological access to other important parts (e.g., lacrymals, jugals, pterygoids). We thus attribute this material to *C. cf. siamensis*.

Order SQUAMATA Opperl, 1811

Suborder SERPENTES Linnaeus, 1758

Family BOIDAE Gray, 1825

Genus *Python* Daudin, 1803

Python sp.

Referred material: four trunk vertebrae—DMR-KS-05-03-00-21, DMR-KS-05-03-00-16 (two attached vertebrae), and DMR-KS-05-04-28-12

Material description

Vertebrae are almost complete and represent a large-sized snake (for measurements, see Tab. 21). In anterior view, the cotyle is suboval in outline with the dorsoventral compression (Fig. 63H). The ventro-lateral margins of the cotyle are nearly straight. The neural spine is well-

developed and steep. The neural canal is narrow. The dorsal margin of the zygosphere is convex. The tubercle is located at the junction between the base of the zygosphere and the top of the neural canal. In posterior view, the neural arch is high and massive. The zygantra are wide and deep. In dorsal view, the median tubercle at the base of the zygosphere is distinct and the interzygapophyseal constriction is well-developed. In ventral view, the haemal keel is high (Fig. 63l) and the subcentral groove is poorly developed.

Table 21. Measurements (in millimeters) of vertebrae of *Python* and *Varanus* from Khok Sung. Abbreviations: **CL**, centrum length (measured at the ventral midline); **H**, maximum height (measured from the tip of the neural spine to the ventral rim of the cotyle); **WPP**, width between pre- and postzygapophyseal processes; **Wpre**, width across zygapophyseal processes; **Wpost**, width across postzygapophyseal processes; **Wcd**, width of the condyle; **Hcd**, height of the condyle (measured from the dorsal to ventral rim); **Wct**, width of the cotyle; **Hct**, height of the cotyle. ⁺ refers to the measurement of 2 attached vertebrae and * indicates an incomplete preservation.

	CL	H	WPP	Wpre	Wpost	Wcd	Hcd	Wcd	Hct
<i>Python</i> sp.									
DMR-KS-05-03-00-21	20.85	40.36	22.47	36.48	15.27	14.03	13.95	12.87	15.12
DMR-KS-05-03-00-16	28.75 ⁺	26.35*	23.82	35.23	13.73	–	12.04	–	16.44
DMR-KS-05-04-28-12	14.06	17.69*	17.18	20.46	23.64	6.50	6.80	6.62	7.82
<i>Varanus</i> sp.									
DMR-KS-05-03-29-36	24.98	25.39*	27.90	21.91	34.98	7.18	9.21	18.96	22.09
DMR-KS-05-03-08-36	31.73	28.56	34.11	36.21	35.60	7.82	12.68	18.27	21.91

Taxonomic remarks and comparisons

We attribute these four vertebrae to the family Boidae because of the following characters: a short, wide, and massive vertebral body (i.e., the widths of the centra are greater than the lengths (sensu Delfino et al., 2004)), a small prezygapophyseal process, paradiapophyses weakly subdivided into para- and diapophyseal surfaces, and an absence of spine-like hypapophyses on mid- and posterior-trunk vertebrae (replaced by haemal keels) (Szyndlar and

Böhme, 1996; Rage, 2001). Vertebrae of pythonines are commonly identified by many distinct characters: a straight and posteromedially angled zygapophyseal bridge, a triangular-shaped neural canal, a prominent zygosphenal tuberosity, a steep anterior border of the neural spine, a posterior border of the neural spine overhanging posteriorly, an absence of the paracotylar foramina, a haemal keel of mid- and posterior-trunk vertebrae delimited laterally by subcentral grooves that reach the cotylar rim, and a haemal keel projecting below the centrum (Scanlon and Mackness, 2001; Szyndlar and Rage, 2003). The Khok Sung snake vertebrae are identified based on overall similarities with extant taxa (from the original description by Hoffstetter (1964)): a relatively elongated centrum compared to the neural arch width and the vertebral height, a longitudinal ridge along the haemal keel, and a thick zygosphenal base. The Khok Sung specimens are comparable in size to recent (e.g., *Python molurus bivittatus*: the specimen NMW 17117) and fossil (e.g., *Python* sp.: the specimens RMNH DUB 5794, DUB 6951, and DUB 6952 recovered from Trinil H. K., Java) python vertebrae. According to the fact that the species-level distinction based on the vertebral morphology is poorly known, we therefore assign these vertebrae to *Python* sp.

จุฬาลงกรณ์มหาวิทยาลัย
CHULALONGKORN UNIVERSITY

Suborder LACERTILIA Günther, 1867

Family VARANIDAE Merrem, 1820

Genus *Varanus* Merrem, 1820

***Varanus* sp.**

Referred material: two trunk vertebrae—DMR-KS-05-03-08-36 and DMR-KS-05-03-29-36

Material description

The vertebra DMR-KS-05-03-08-36 is more complete than the specimen DMR-KS-05-03-29-36 (for measurements, see Tab. 21). The pre- and postzygapophyses are slightly broken at the

second specimen. In both specimens, the neural spines are unfortunately broken away. In anterior view, the cotyle is oval in outline, dorsoventrally compressed, and ventrally oriented (Fig. 63J). The prezygapophyses lack a part of the prezygapophyseal process and are dorsally inclined about 45° . The neural canal is narrow. The neural arch lacks a part of the zygosphenes. No paracotylar foramina are present. In posterior view, the condyle and the postzygapophyses show a mirrored morphology with the anterior part. No zygantrum is observed. In dorsal view, the prezygapophyseal facets are drop-shaped and project laterally. The interzygapophyseal constriction is also present. In ventral view, the synapophyses protrude laterally and the centrum is triangular in outline (Fig. 63K).

Taxonomic remarks and comparisons

We assign these two vertebrae to the the family Varanidae due to the following morphological characters: a centrum tapering posteriorly, a precondylar constriction, a ventrally facing cotyle, and a large and flared condyle (Romer, 1956; Averianov and Danilov, 1997). The Khok Sung vertebrae match well the genus *Varanus* because the condyle is much wider than the posterior end of the centrum and none of the articular surface is visible in ventral view. They are also similar in morphology to *Varanus* according to an amphicoelous centrum, condyles facing very dorsally (anterodorsal direction), an oval-shaped cotyle, a short neural spine, and an absence of the zygosphenes and zygantra (Lee, 2005). *Varanus* sp. is reported from the Middle Pleistocene of Phnom Loang (Beden and Guérin, 1973). Two varanid species, *V. cf. komodoensis* (larger) and *V. salvator*, are described from the Middle Pleistocene of Trinil H. K. (Hocknull et al., 2009). The Khok Sung specimens are comparable in size to the recent (e.g., *Varanus salvator*: NMW 39446/1) and fossil (e.g., *Varanus* sp.: RMNH DUB 3 and RMNH DUB 5792 recovered in Trinil H. K., Java) specimens. Identifying these vertebrae more precisely to the species-level, more detailed morphological comparisons need to be done in the future.

Faunal composition of Khok Sung vertebrate assemblage

Nine taxa: seven Testudines, an extinct gharial (*Gavialis bengawanicus*), and a spotted hyaena (*Crocuta crocuta ultima*), have been previously described from Khok Sung by Claude et al. (2011), Martin et al. (2012), and Suraprasit et al. (2015), respectively. In this paper, we studied other undescribed vertebrate fossils from Khok Sung. As a result, fourteen mammalian and three reptilian taxa are identified and added to the faunal list (Tab. 22). Overall, the Khok Sung fauna consists of at least 15 mammalian (13 genera) and 10 reptilian (9 genera) species. The mammalian assemblage comprises megaherbivores (>1000 kg) of about 19% of the species (including proboscideans, rhinoceroses, water buffaloes) and other large species of about 37% (including artiodactyls, primates, and carnivores) of the vertebrate fauna (Fig. 64). The most abundant mammal group of the locality is represented by the artiodactyls (9 species). The non-mammalian species consists of about 44% of the total vertebrate fauna. The order Testudines is the most diverse group of non-mammalian taxa in the locality (22% of the fauna). In addition, other vertebrates such as birds and fish are tentatively observed. A single fragmentary cervical vertebra of the bird order Galliformes is also present (Fig. 63L, M). Numerous fish remains including vertebrae (e.g., the specimen DMR-KS-05-03-22-76: fig. 63N) and pectoral spines (e.g., the specimen DMR-KS-05-04-11-20: fig. 63P and DMR-KS-05-04-05-25: fig. 63Q) are assigned to large silurids. Regarding our observations on the Khok Sung vertebrate collection, there are some complete reptile (e.g., carapaces of tortoises and soft-shelled turtles) and fish remains that have not been identified yet. The reptile and fish assemblages would probably indicate a higher diversity than those described from this study, if these undescribed specimens are taxonomically studied in the future. However, it is assumed that the identified mammal remains represent herein the whole mammalian fauna because we have already described almost all vertebrate fossils (especially skulls and teeth) recovered from the Khok Sung sand pit during the excavation.

Only few postcranial remains of mammals such as fragmentary or incomplete bones are unidentified according to the limitation of morphological accessibilities.

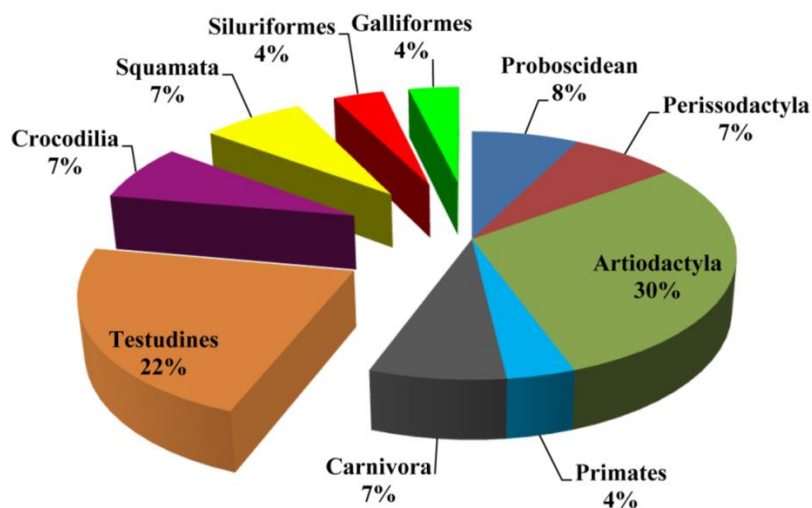


Figure 64. Pie chart showing the species richness of Khok Sung vertebrate fauna.

Table 22. Fauna list of Khok Sung vertebrate fauna.

Mammalia		
Primates	Cercopithecidae	<i>Macaca</i> sp.
Carnivora	Hyaenidae	<i>Crocuta crocuta ultima</i> (identified by Suraprasit et al. 2015)
	Canidae	<i>Cuon</i> sp.
Proboscidea	Stegodontidae	<i>Stegodon</i> cf. <i>orientalis</i>
	Elephantidae	<i>Elephas</i> sp.
Perissodactyla	Rhinocerotidae	<i>Rhinoceros sondaicus</i> <i>Rhinoceros unicornis</i>

Artiodactyla

Suidae

Sus barbatus

Cervidae

*Axis axis**Panolia eldii**Rusa unicolor*

Bovidae

*Bos sauveli**Bos gaurus**Bubalus arnee**Capricornis sumatraensis*

Reptilia

Testudines (identified by Claude et al. 2011)

Geoemydidae

*Batagur cf. trivittata**Heosemys annandalii**Heosemys cf. grandis**Malayemys sp.*

Trionychidae

*Chitra sp.**cf. Amyda sp.*

Crocodilia

Gavialidae

Gavialis cf. bengawanicus (identified by Martin et al. 2012)

Crocodylidae

Crocodylus cf. siamensis

Squamata

Varanidae

Varanus sp.

Boidae

Python sp.

Actinopterygii

Siluridae indet.

Aves

Galliformes indet.

According to the fact that Khok Sung yields only large mammals (> 8 kg), the absence of medium- and small-sized mammal remains is likely due to taphonomic conditions and/or fossil collecting methods. Similarly to most of the Middle and Late Pleistocene fossil sites in Southeast Asia, the biodiversity of Khok Sung large mammals is likely greater than that of present-day faunas (see Tabs 17–20 for the fossil and present-day fauna lists in South China and Southeast Asia). The Khok Sung fauna exhibits at least 15 large mammal species, whereas the Southeast Asia fossil and present-day faunas mostly yield an average of about 13 species per site (Tougaard and Montuire, 2006) and of less than 11 species per area, respectively (Lekagul and McNeely, 1988; Corbet and Hill, 1992). It is obvious that the Khok Sung mammalian assemblage is characterized by genera and/or species that are similar to the living population in the same area and surrounding regions. However, some mammalian (*Crocuta crocuta*, *Rhinoceros unicornis*, *Axis axis*, and *Sus barbatus*) and reptilian (*Batagur cf. trivittata*) species in the Khok Sung fauna are no longer present in the region but occur far away from Thailand or even from Southeast Asia. Moreover, two taxa, *Stegodon cf. orientalis* and *Gavialis cf. bengawanicus* were present in the locality but became globally extinct later. The Khok Sung vertebrate fauna totally contains 19 of 27 identified taxa that are currently present in Thailand (Tabs 22 and A20).

Individual species distribution patterns

We reveal past record and recent distribution patterns of large mammalian species present in Khok Sung. Paleontological sites in Southeast Asia as well as South China are examined for the Early, Middle, and Late Pleistocene, compared with the modern distribution patterns. We only focus on mammalian taxa assigned to the species-level, including *Stegodon orientalis* and their co-occurring species, *Rhinoceros sondaicus*, *Rhinoceros unicornis*, *Sus barbatus*, *Axis axis*,

Panolia eldii, *Rusa unicolor*, *Bos sauveli*, *Bos gaurus*, *Bubalus arnee*, and *Capricornis sumatraensis*.

Stegodontids and elephantids

The earliest records of derived *Stegodon* (e.g., *Stegodon orientalis* from Dayakou (Chen et al., 2013) and *Stegodon trigonocephalus* from Ci Saat (Sondaar, 1984; van den Bergh et al., 2001)) are likely from the Early Pleistocene. Fossils identified as *Stegodon orientalis* or *S. cf. orientalis* are recorded from South China (e.g., Daxin (Rink et al., 2008), Hejiang (Zhang et al., 2014), and Panxian Dadong (Han and Xu, 1985; Bekken et al., 2004; Schepartz et al., 2005)) and Vietnam (Tham Khuyen, Tham Hai, and Tham Om (Olsen and Ciochon, 1990)). Another species, *S. trigonocephalus*, is reported from Javanese localities (van den Bergh et al., 2001). During the Middle to Late Pleistocene, *Stegodon orientalis* co-occurred with *Elephas* sp. or *E. maximus* in many localities throughout the Indochinese province (Fig. 65). The two species are found together from Khok Sung and from the Late Pleistocene of the Cave of the Monk (Zeitoun et al., 2005, 2010) in Thailand, the early Late Pleistocene of Nam Lot and Tam Hang South (Bacon et al., 2008a, 2011, 2012, 2015) in Vietnam, and the Middle Pleistocene of Ganxian and Wuyun in South China (Chen et al., 2002; Rink et al., 2008; Wang et al., 2007, 2014). *Stegodon orientalis* is found in the Late Pleistocene of Luna (South China) and Keo Leng (northern Vietnam) caves (Olsen and Ciochon, 1990; Wang et al., 2014). Perhaps, this species survived until the Holocene in South China (Ma and Tang, 1992; Tong and Patou-Mathis, 2003; Tong and Liu, 2004). The number of species of *Stegodon* lessens from the Early to Late Pleistocene, based on the fossil records of South Chinese localities (Louys et al., 2007). Although *Stegodon orientalis* is likely to have had a less widespread distribution in the Late Pleistocene than in the Middle Pleistocene (Fig. 65), the Pleistocene geographical distribution of this species is only based on a limited number of localities.

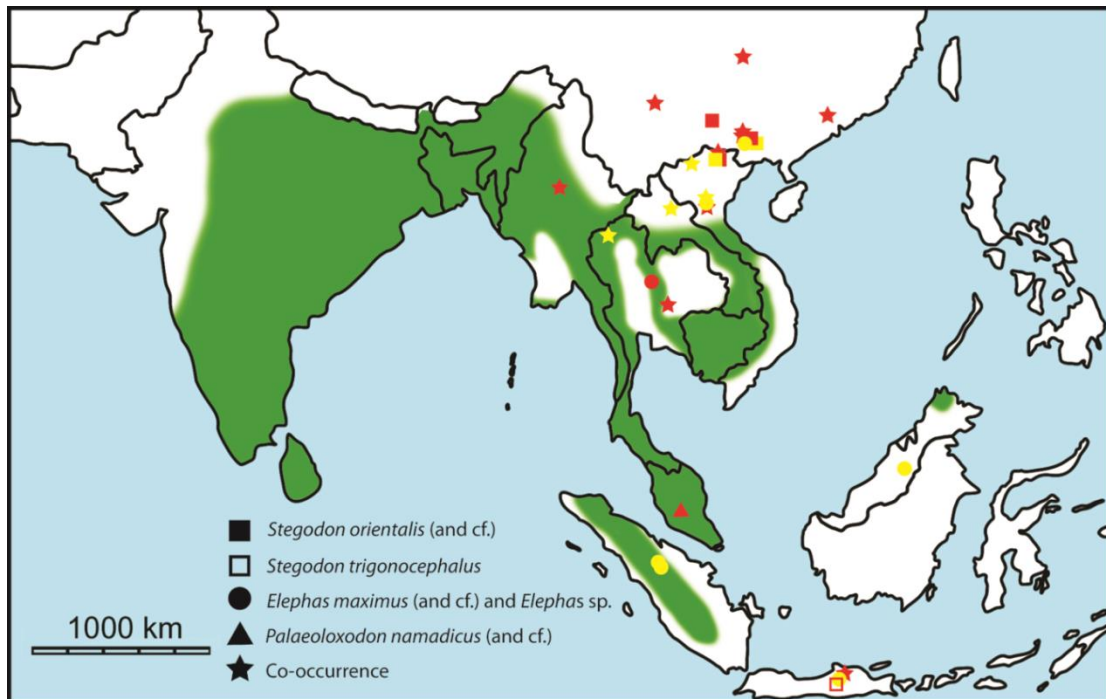


Figure 65. The Middle (red circle) and Late (yellow circle) Pleistocene records of stegodontids and relative fossil elephants, and the current distribution (green area) of *Elephas maximus* (Indian elephant). Stars indicate the co-occurrence of sympatric proboscideans. The current distribution of Indian elephants is compiled from Lekagul and McNeely (1988).

A fossil species of *Palaeoloxodon* is reported from several Middle Pleistocene localities in mainland Southeast Asia (Fig. 65), often co-occurring with *Stegodon orientalis* (e.g., the sites of Maba (Han and Xu, 1985; Wu et al., 2011) and Tham Khuyen (Olsen and Ciochon, 1990)). *Palaeoloxodon* is found in the Late Pleistocene fissure-filling deposits of Hum Hang, Lang Trang, and Ma U’Oi in northern Vietnam (Olsen and Ciochon, 1990; Long et al., 1996; Bacon et al., 2004, 2006), similar distribution to that of *Elephas*, but became extinct before the Holocene (Tong and Patou-Mathis, 2003; Louys et al., 2007). The cause of global and local extinction of *Stegodon orientalis* and *Palaeoloxodon* is unknown at this time.

Elephas maximus is known from the late Middle Pleistocene of Thum Wiman Nakin (northeastern Thailand) (Tougaard, 1998, 2001), and possibly reached the Indonesian islands of Sumatra, Borneo and Java during the late Pleistocene. *Elephas* is one of two living genera of

elephants. The Indian elephant, *E. maximus*, is the only extant species. It is distributed throughout mainland Asia (including India, Nepal, Bangladesh, Bhutan, Myanmar, Thailand, Malaysia, Sumatra, Laos, Cambodia, and Vietnam) (Lekagul and McNeely, 1988). The Indian elephant is not widespread throughout Southeast Asia as it is not found in central and northeastern Thailand and central southern Myanmar (Fig. 65). Those areas are mostly lowland or highland floodplains today, while Indian elephants prefer deep forest canopy (Lekagul and McNeely, 1988; Corbet and Hill, 1992). However, this preference for deep forests may be the result of humans encroaching and impacting their preferred habitats (Pushkina et al., 2010). It is possible that *E. maximus* became extinct locally in Java before 37 ka as it is absent from the locality of Wajak (dated to 37 ka, van den Brink (1982)). This local extinction is probably due to the drier and cooler climate beginning at 81 ka in Java (van der Kaars and Dam, 1995) and/or the loss of rainforest habitats (Storm et al., 2005).

Javan and Indian rhinoceroses

The Early Pleistocene records of Asian rhinoceroses are poorly documented in Southeast Asia. Only *R. sondaicus* is reported from the upper part of the Irrawaddy Formation, near Pauk Township in central Myanmar (Zin-Maung-Maung-Thein et al., 2006) and from Sangiran in Java (Hooijer, 1964) (Fig. 66).

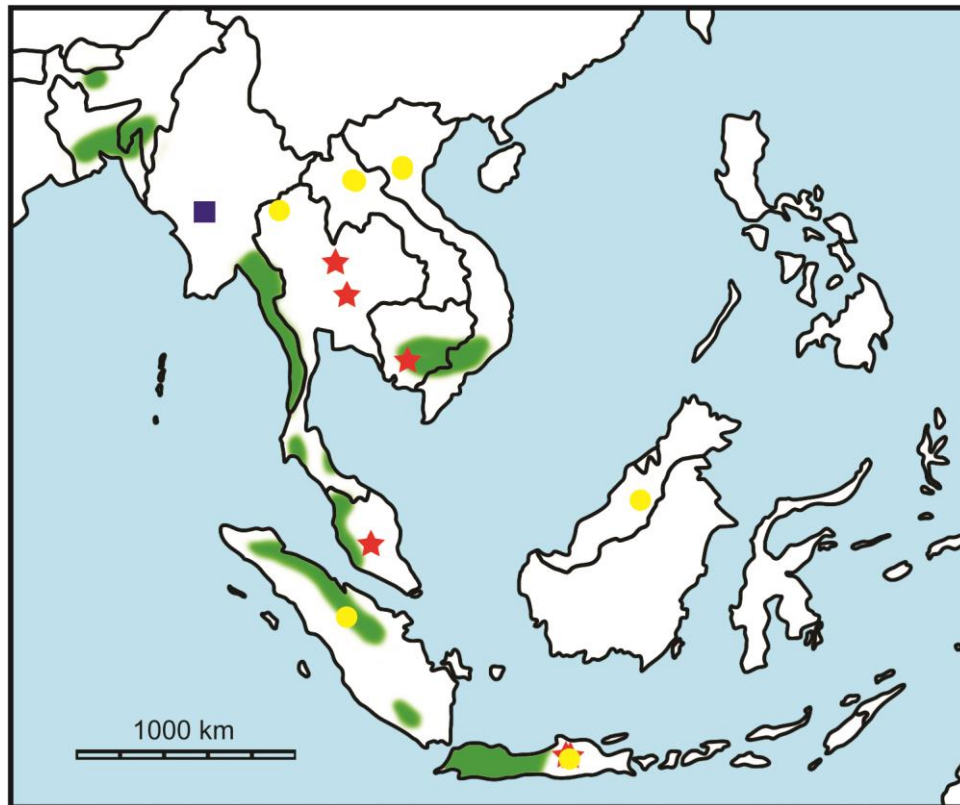


Figure 66. The Early (blue square), Middle (red star), and Late (yellow circle) Pleistocene records and the current distribution (green area) of *Rhinoceros sondaicus* (Javan rhinoceros). The current distribution of the species is compiled from Groves (1967), Rookmaker (1980), and Groves and Leslie Jr (2011).

The Middle Pleistocene record, especially the late Middle Pleistocene, includes numerous reports of Asian rhinoceroses (Figs 66 and 67). In the Indochinese subregion during the Middle Pleistocene, fossils of *R. unicornis* are found from Hsingan (Kahlke, 1961) and Maba (Wu et al., 2011) in South China, from Yenangyaung in Myanmar (sensu Antoine, 2012), from Tham Hai and Tham Om in northern Vietnam (sensu Antoine, 2012). During the late Middle Pleistocene, fossils of *R. unicornis* are known from Thum Prakai Phet (Tougard, 1998) in northeastern Thailand. Remains of *R. sondaicus* are recovered from the Middle Pleistocene of Phnom Loang (Beden and Guérin, 1973). The only co-occurrences of these two species are from the late Middle Pleistocene of Thum Wiman Nakin (Tougard, 1998, 2001) and from our discoveries at Khok Sung. In the Sundaic subregion, fossils of Indian rhinoceroses have been described from the Middle

Pleistocene of Tumbun (Malaysia) and Trinil H. K. (Java) (Hooijer, 1962; Medway, 1972; van den Bergh et al., 2001) and from the early Middle Pleistocene of Kedung Brubus where Javan rhinoceroses co-occurred (Hooijer, 1946). In other biogeographic regions, *R. unicornis* occurred in Yenchingkou (central eastern China) (sensu Antoine, 2012). According to original faunal descriptions, many Middle Pleistocene localities in China and Vietnam yielded fossil specimens of *R. sinensis*. This species was later synonymized with *R. unicornis* by Antoine (2012). However, *R. sinensis* is recently recognized as a valid species (Yan et al., 2014), so there remains some confusion about the presence of *R. unicornis* in many localities.

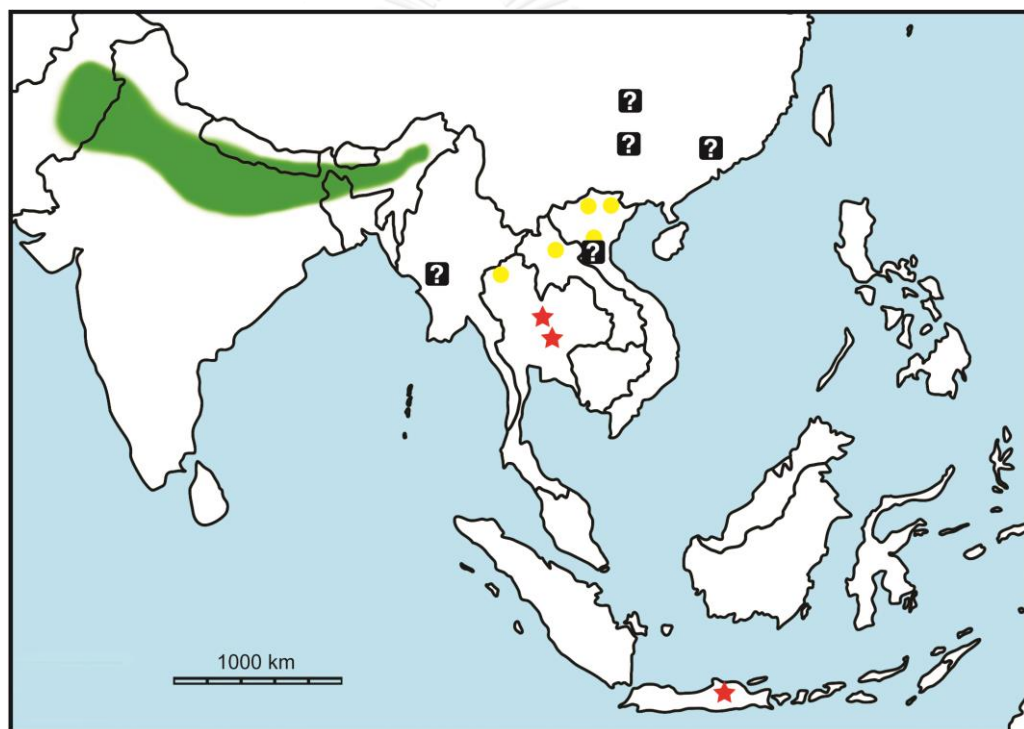


Figure 67. The Middle (red star) and Late (yellow circle) Pleistocene records and the current distribution (green area) of *Rhinoceros unicornis* (Indian rhinoceros). “?” indicates the possible record of *R. unicornis* according to Antoine (2012). The current distribution of the species is modified from Laurie et al. (1983).

During the late Pleistocene, Javan and Indian rhinoceroses were widespread in Indochinese subregion (Figs 66 and 67). They co-occurred in the Cave of the Monk (Ban Fa Suai, northern Thailand) (Zeitoun et al., 2005, 2010), in Nam Lot and Tam Hang South (northern Laos)

(Bacon et al., 2008a, 2011, 2012, 2015) , and in Duoi U’Oi and Ma U’Oi (northern Vietnam) (Bacon et al., 2004, 2006, 2008b) . Indian rhinoceros fossils were also found in the caves of Ham Hang and Keo Leng, northern Vietnam (Olsen and Ciochon, 1990), while Javan rhinoceroses were recovered from Niah caves (Borneo, Malaysia) (Medway, 1972; Harrison, 1996) and several Indonesian localities: Lida Ajer and Sibrambang in Sumatra (de Vos, 1983) and Punung, Gunung Dawung, and Wajak in Java (Badoux, 1959, van den Brink, 1982, Storm et al., 2005, 2013). Indian rhinoceroses seem to go extinct in Java after the middle Middle Pleistocene, as none are reported from Trinil H. K. (dated to ~540-430 ka, Joordens et al. (2015)) and early Late Pleistocene to Holocene sites.

Nowadays, the Indian rhinoceros is locally extinct from the Thai territory and several other countries in Southeast Asia. The species is restricted to Nepal and India and some parts of northernmost Myanmar (Laurie et al., 1983) (Fig. 67). The Javan rhinoceros survives across the Indochinese Peninsula and the Sundaic subregions (Groves and Leslie Jr, 2011) but became extinct in the island of Borneo during the Holocene (Medway, 1960; Cranbrook, 2000; Cranbrook et al., 2000; Cranbrook and Piper, 2007) (Fig. 66). The modern co-occurrences of the two species are restricted to a small area in eastern India (Antoine, 2012). In the Holocene, the Javan rhinoceros likely co-occurred with the Sumatran rhinoceros, *Dicerorhinus sumatrensis*, but they are not sympatric today almost certainly because of human induced habitat loss leading to reduction of their geographic range during the last century (Groves and Leslie Jr, 2011).

Bearded pigs

During the Middle Pleistocene, *Sus barbatus* (bearded pig) is known from the caves of Thum Wiman Nakin and Thum Prakai Phet (Tougaard, 1998, 2001) and the terrace deposit of Khok Sung (Fig. 68). Among these Thai localities, *S. barbatus* co-occurred with *S. scrofa* at least in Thum Wiman Nakin and Thum Prakai Phet.

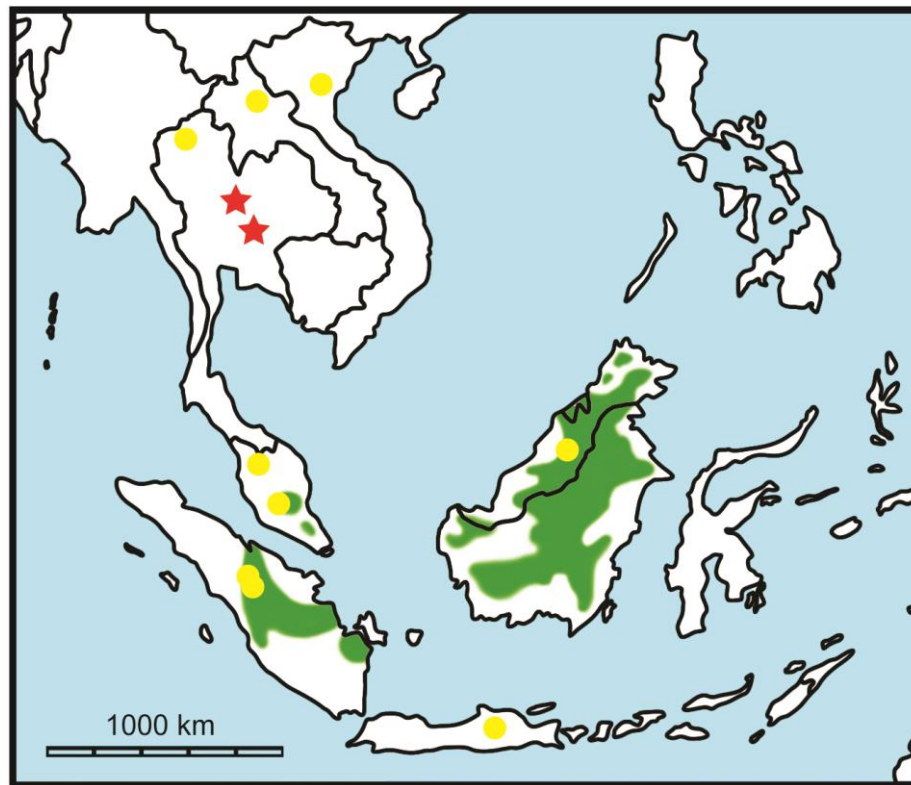


Figure 68. The Middle Pleistocene (red star) and Late Pleistocene to Holocene (yellow circle) records and the current distribution (green area) of *Sus barbatus* (bearded pig). The current distribution of the species is compiled from Corbet and Hill (1992).

In the late Pleistocene, *S. barbatus* is well-documented from many localities, extending its geographic distribution across Sumatra, Borneo, and Java. This species is likely more widespread in the late Pleistocene than the Middle Pleistocene (Fig. 68). In Indochinese and Sundaic subregions, the co-occurrence of *S. barbatus* and *S. scrofa* is known from the “Cave of the Monk” (Ban Fa Suai) in northern Thailand (Zeitoun et al. 2005, 2010), Tam Hang South in northern Laos (Bacon et al. 2008, 2011, 2015), Batu caves and Gua Cha (Holocene) in Peninsular Malaysia (Groves, 1985; Ibrahim et al., 2013), Lida Ajer and Sibrambang in Sumatra (de Vos, 1983), and Punung in Java (Badoux, 1959). Only fossils of bearded pigs are collected from the latest Pleistocene of Niah Cave, Borneo (Medway, 1972; Harrison, 1996).

Today *S. barbatus* is restricted to Peninsular Malaysia, Sumatra, and Borneo (Corbet and Hill, 1992) (Fig. 68), in contrast with its widespread distribution across the Indochinese subregion during the Middle to Late Pleistocene. This species dispersed to Indonesian islands by the Late Pleistocene, as it is recorded from Punung of Java (Badoux, 1959). After the land bridges submerged by rising sea level, some populations of *S. barbatus* were probably trapped on islands (Tougaard, 2001). Later on, *S. barbatus* went extinct in mainland Southeast Asia after the late Pleistocene. The cause of local extinction of *S. barbatus* in mainland Southeast Asia is unknown at this time. This taxon also became locally extinct later in Java as none is recorded from the Late Pleistocene of Wajak (van den Brink, 1982). The drier and cooler climates during the middle Middle Pleistocene or the reduction of rainforest habitats possibly explain the local extinction for bearded pigs in Java.

Chitals (Axis deer)

Fossils of *Axis axis* have never been previously recorded from Thailand but were present in mainland Southeast Asia, at least in Khok Sung, during the late Middle Pleistocene (Fig. 69). Only *Axis* cf. *porcinus* is reported from the Late Pleistocene of the Cave of the Monk (Zeitoun et al., 2005, 2010). Other species of *Axis* are also described in Asia. *A. shansius* and *A. rugosa* are reported from the Early Pleistocene of China (Han and Xu, 1985), whereas *A. lydekkeri* is recorded from the Early to Middle Pleistocene of Java (Gruwier et al., 2015). The Bawean deer, *A. kuhli*, is also reported in Java since the Holocene (van den Bergh et al., 2001; Moigne et al., 2004).

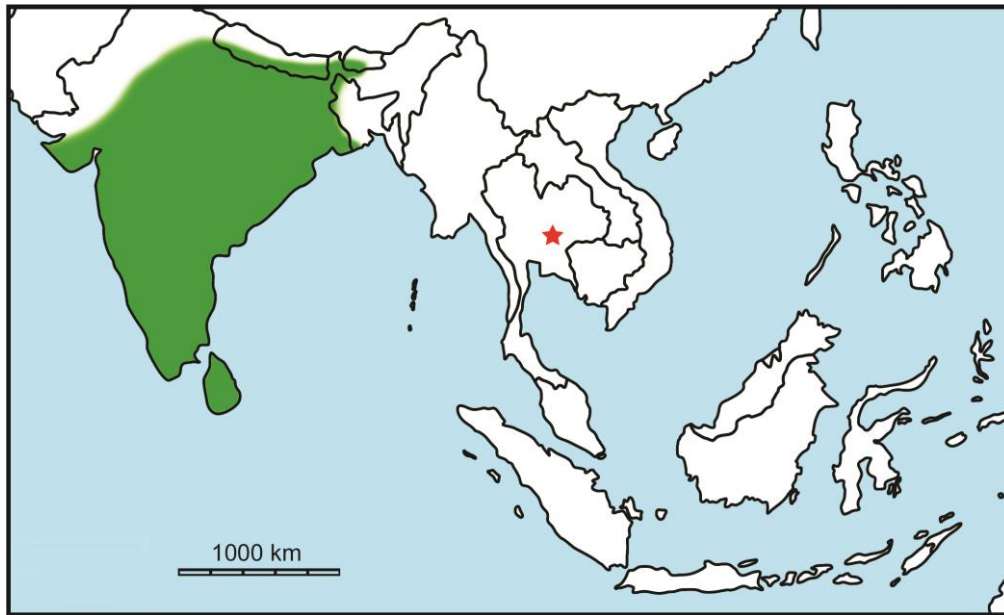


Figure 69. The Middle Pleistocene record (red star) and the current distribution (green area) of *Axis axis* (chital). The current distribution of the species is compiled from Duckworth et al. (2008a).

Nowadays *Axis axis* is restricted to the Indian subcontinent (India, Nepal, Sikkim, and Sri Lanka) (Fig. 69). Its habitat preferences are grasslands and open forests (Nowak, 1999). The Pleistocene chital has a different geographical distribution as it was present in Khok Sung. The distribution range of *A. axis* in the Pleistocene is probably wider than in the present day. Rainforests became more dominant across Southeast Asia during the Late Pleistocene (Heaney, 1991; Meijaard, 2003; Louys et al., 2007). The local extinction of the chital in Thailand is likely caused by the reduction of open grasslands. In the future, additional fossil records of *A. axis* in Southeast Asia would allow addressing some issues related to its local extinction, as well as its past distribution.

Eld's and sambar deer

The Eld's deer is known from the Middle Pleistocene of Thailand. Fossils of *P. eldii* are collected from the caves of Thum Wiman Nakin and Kao Pah Nam (Pope et al., 1981; Tougaard, 1998, 2001) and from the Khok Sung sand pit (Fig. 70). Fossils of sambar deer are widely recorded

from many Middle Pleistocene sites in mainland Southeast Asia: Hejiang, Panxian Dadong, and Maba in South China (Han and Xu, 1985; Bekken et al., 2004; Schepartz et al., 2005; Wu et al., 2011; Zhang et al., 2014), Thum Wiman Nakin (Tougaard, 1998, 2001), Thum Prakai Phet (Tougaard, 1998; Filoux et al., 2015), and Khok Sung in Thailand, Tham Khuyen, Tham Hai, and Tham Om in Vietnam (Olsen and Ciochon, 1990), Phnom Loang and Boh Dambang in Cambodia (Beden and Guérin, 1973; Demeter et al., 2013), and Badak Cave in Peninsular Malaysia (Ibrahim et al., 2013) (Fig. 71). Both taxa co-occurred in Thum Wiman Nakin and Khok Sung.

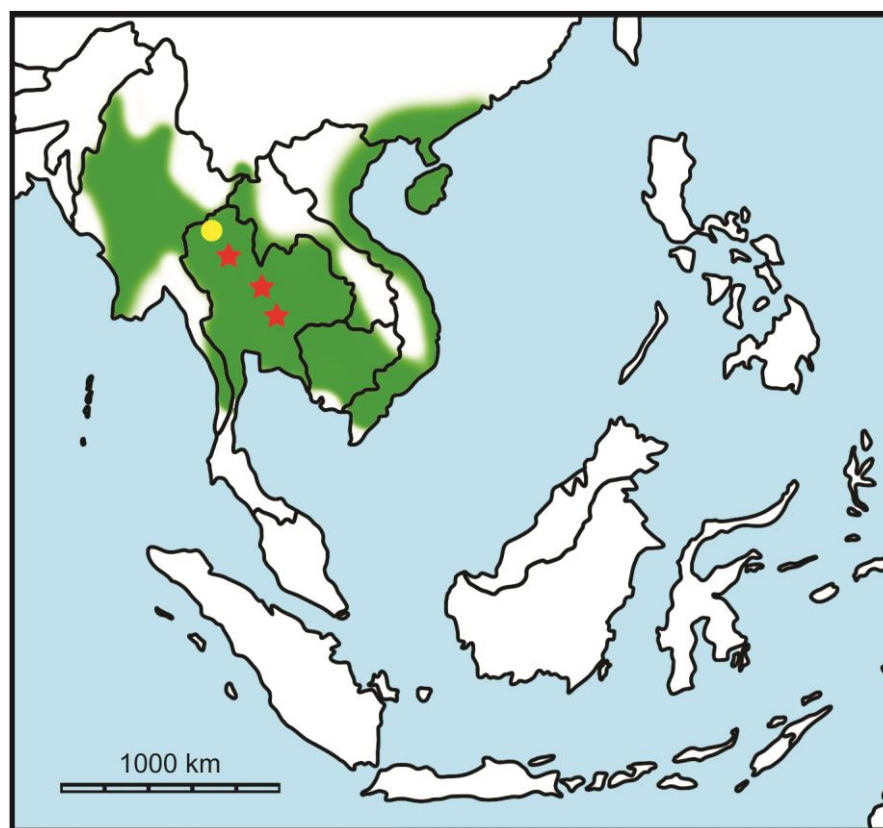


Figure 70. The Middle (red star) and Late (yellow circle) Pleistocene records and the current distribution (green area) of *Panolia eldii* (Eld's deer). The current distribution of the species is compiled from Lekagul and McNeely (1988).

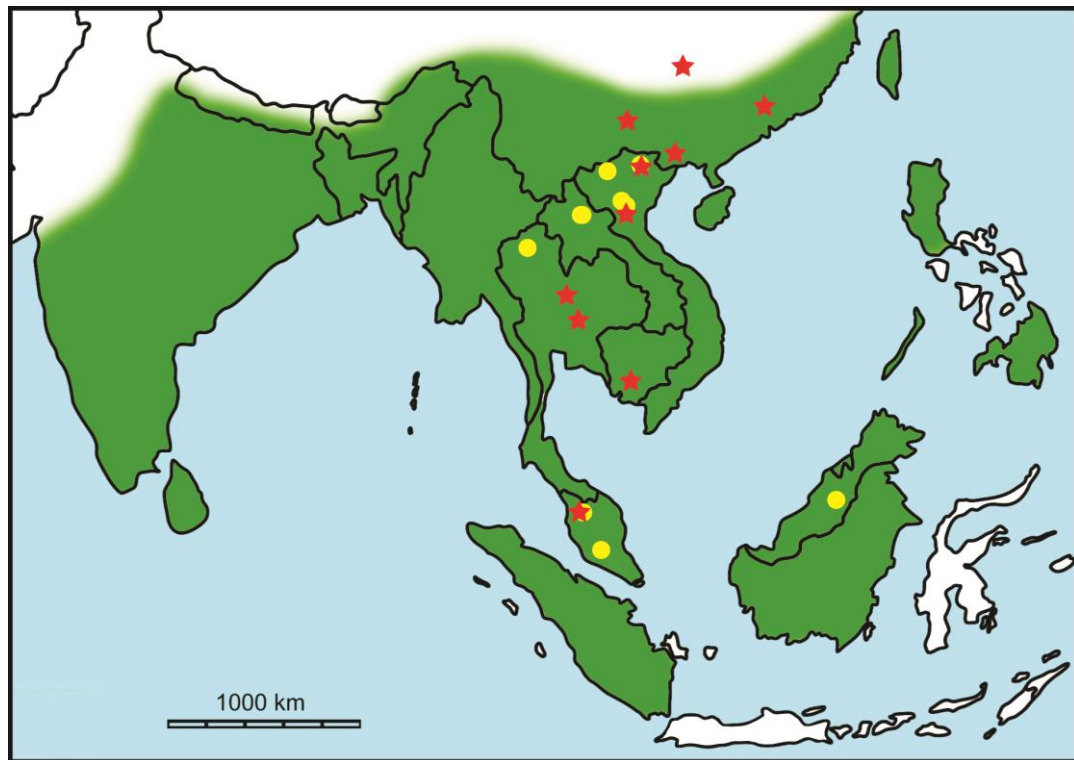


Figure 71. The Middle Pleistocene (red star) and Late Pleistocene to Holocene (yellow circle) records and the current distribution (green area) of *Rusa unicolor* (sambar deer). The current distribution of the species is compiled from Lekagul and McNeely (1988).

During the Late Pleistocene, the Eld's and sambar deer co-occurred in the Cave of the Monk (Ban Fa Suai), northern Thailand (Zeitoun et al., 2005, 2010). The sambar deer is widespread across Laos (Nam Lot and Tam Hang South (Bacon et al., 2008a, 2011, 2012, 2015)), Vietnam (Hang Hum, Keo Leng, Lang Trang, Duoi U'Oi, and Ma U'Oi (Olsen and Ciochon, 1990; Long et al., 1996; Bacon et al. 2004, 2006, 2008b)), Peninsular Malaysia (Batu Cave, Gua Gunung Runtuh, and Gua Cha (Holocene) (Groves, 1985; Davidson, 1994; Ibrahim et al., 2013)), and Borneo (Niah Cave (Medway, 1972; Harrison, 1996; Barker et al., 2007)). However, none are recorded in Sumatra and Java (Fig. 71).

Nowadays, *Panolia eldii* is restricted to the Indochinese province (Fig. 70). *Rusa unicolor* is a widespread species native to the Indian subcontinent, southern China, and Southeast Asia

(both Indochinese and Sundaic subregions with the exception of Java (Fig. 71)) (Lekagul and McNeely, 1988).

Koupreys, gaurs, and wild water buffaloes

Large bovids in Southeast Asia currently comprise four wild species: *Bos sauveli* (kouprey), *Bos javanicus* (banteng), *Bos gaurus* (gaur), and *Bubalus arnee* (wild water buffalo). Bantengs, gaurs, and koupreys presumably shared a common ancestor at 2.6 Ma (Plio-Pleistocene) and their lineages split in a short period of time (i.e., between 200 and 300 ka) based on the molecular estimations of divergence times (Hassanin and Ropiquet, 2004). These molecular estimations are congruent with the fossil records of bantengs and gaurs in Asia. Fossil remains attributed to these species have been recorded in Southeast Asia since the Middle Pleistocene. The co-occurrence of these Pleistocene large bovids is reported from Thum Wiman Nakin (Tougard, 1998, 2001) and Khok Sung in northeastern Thailand (Fig. 72–74). Fossil remains of gaurs are also reported from the Middle Pleistocene of Kao Pah Nam in northern Thailand (Pope et al., 1981), the middle Middle Pleistocene of Tham Khuyen and the late Middle Pleistocene of Tham Om in Vietnam (Olsen and Ciochon, 1990), and the Middle Pleistocene of Yenchingkou in central eastern China (Colbert and Hooijer, 1953) (Fig. 73). In addition, remains of fossil water buffaloes are described from the late Middle Pleistocene of Phnom Loang and Boh Dambang in Cambodia (Beden and Guérin, 1973; Demeter et al., 2013).

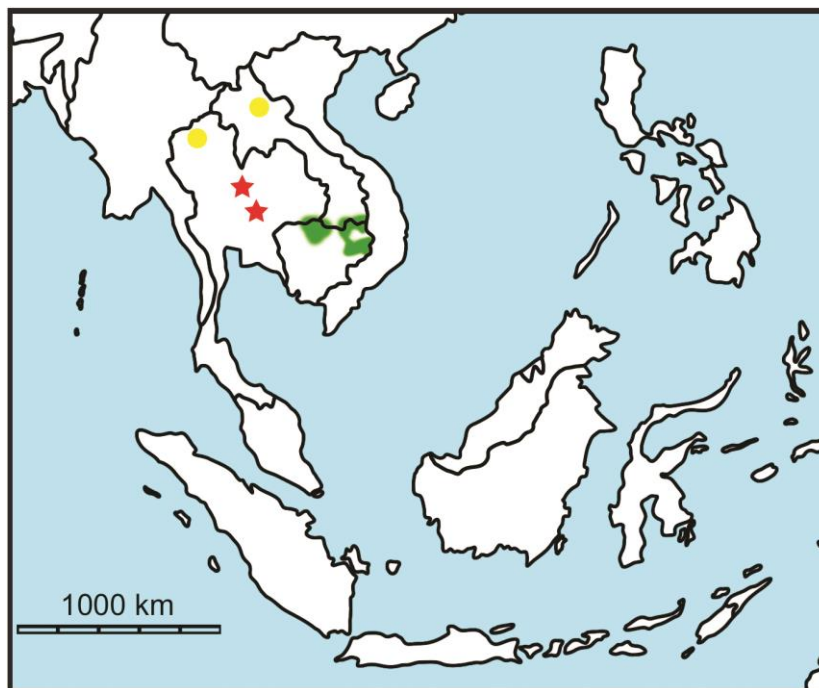


Figure 72. The Middle (red star) and Late (yellow circle) Pleistocene records and the current distribution (green area) of *Bos sauveli* (kouprey). The current distribution of the species is compiled from Lekagul and McNeely (1988) and Timmins et al. (2008).

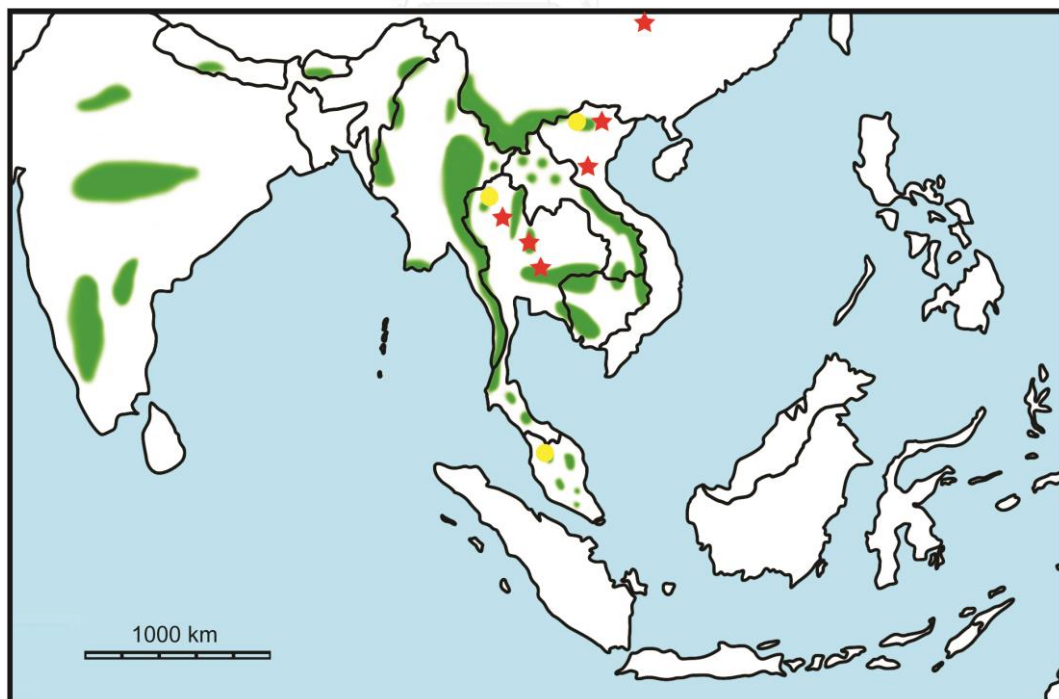


Figure 73. The Middle (red star) and Late (yellow circle) Pleistocene records and the current distribution (green area) of *Bos gaurus* (gaur). The current distribution of the species is compiled from Lekagul and McNeely (1988) and Duckworth et al. (2008b).

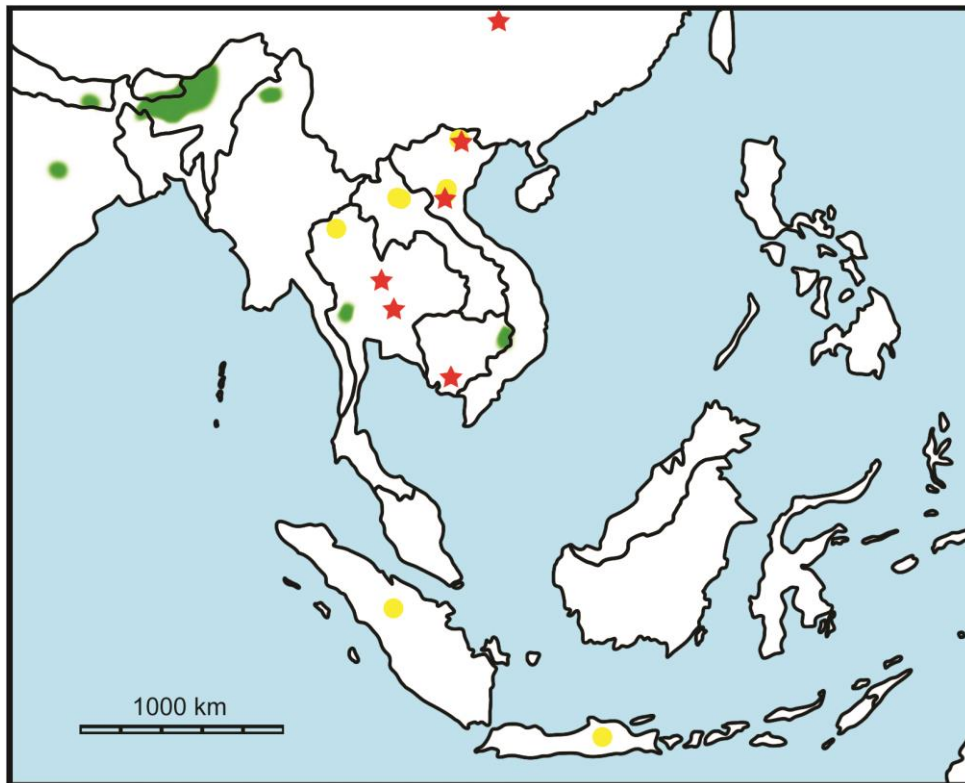


Figure 74. The Middle (red star) and Late (yellow circle) Pleistocene records and the current distribution (green area) of *Bubalus arnee* (wild water buffalo). The current distribution of the species is compiled from Lekagul and McNeely (1988) and Hedges et al. (2008).

During the Late Pleistocene, the locality of the Cave of the Monk (Ban Fa Suai) yielded remains of these bovid species (cf.) (Zeitoun et al., 2005, 2010). Other localities yielded either only one species of *Bos* or the co-occurrence of two *Bos* species and *Bubalus*. *Bubalus arnee* occurred not only in Sumatra but also in Java during the latest Middle/early Late Pleistocene according to their fossil records in Sibrambang and Punung (Badoux, 1959; de Vos, 1983; Storm and de Vos, 2006), respectively (Fig. 74). Both taxa disappeared subsequently in Sumatra either after the early Late Pleistocene or during the Holocene. Neither koupreys nor gaurs are identified in insular Southeast Asia, thus most likely restricted to mainland Southeast Asia (Figs 72 and 73).

The historical distribution of koupreys during the last century is restricted to Cambodia, southern Laos, southeastern Thailand, and western Vietnam (Lekagul and McNeely, 1988; Corbet and Hill, 1992). They become globally extinct today. Gaurs recently occur throughout mainland

South and Southeast Asia and Sri Lanka (Lekagul and McNeely, 1988; Duckworth et al., 2008b) (Fig. 73). Nowadays, they are also present in South China where their fossils have never been found. Wild water buffaloes are currently native to Bhutan, Cambodia, India, Myanmar, Nepal, and Thailand (Lekagul and McNeely, 1988; Hedges et al., 2008). They become locally extinct in Vietnam (likely), Laos, Indonesia, Sri Lanka, and Bangladesh (Fig. 74).

Overall, the Pleistocene large bovid species in Southeast Asia is more widespread than the modern population. The anthropogenic impacts on the environments and landscapes seem to have caused the reduction of large bovid population in several areas during the past decade. The koupreys is more widely distributed during the Pleistocene than today (Fig. 72). In addition to the human activity, the cause of reduction and extinction of koupreys is likely due to their high degrees of habitat specificity such as deciduous dipterocarp forests and especially in areas with extensive grasslands (Timmins et al., 2008), and/or according to high levels of niche competition with other large bovinds.

Sumatran serows

The possible earliest records of *Capricornis sumatraensis* are from the middle Early Pleistocene site of Gongwangling (Hu and Qi, 1978; Han and Xu, 1985), dated to 1.63 Ma (Zhu et al., 2015), in central mainland China and from the Early Pleistocene of the Upper Irrawaddy Formation (Colbert, 1938; Takai et al., 2006) in central Myanmar. *C. sumatraensis* during the Middle Pleistocene is widespread throughout mainland Asia and Southeast Asia (Fig. 75). It is known from the Middle Pleistocene of Yenchingkou in central eastern China (Colbert and Hooijer, 1953), Wuming, Panxian Dadong, and Wuyun in South China (Han and Xu, 1985; Chen et al., 2002; Bekken et al., 2004; Schepartz et al., 2005; Wang et al., 2007; Rink et al., 2008), Tham Om in Vietnam (Olsen and Ciochon, 1990), Thum Wiman Nakin, Thum Prakai Phet, and Khok Sung in Thailand (Tougaard, 1998, 2001; Filoux et al., 2015), Boh Dambang in Cambodia (Demeter et al.,

2013), and Badak Cave in Peninsular Malaysia (Ibrahim et al., 2013). Fossils of *C. sumatraensis* are also described from the latest Middle/early Late Pleistocene of Lida Ajer and Sibrambang in Sumatra and of Punung in Java (Badoux, 1959; de Vos, 1983; van den Bergh et al., 2001; Storm and de Vos, 2006). However, no serows are recorded from Borneo.

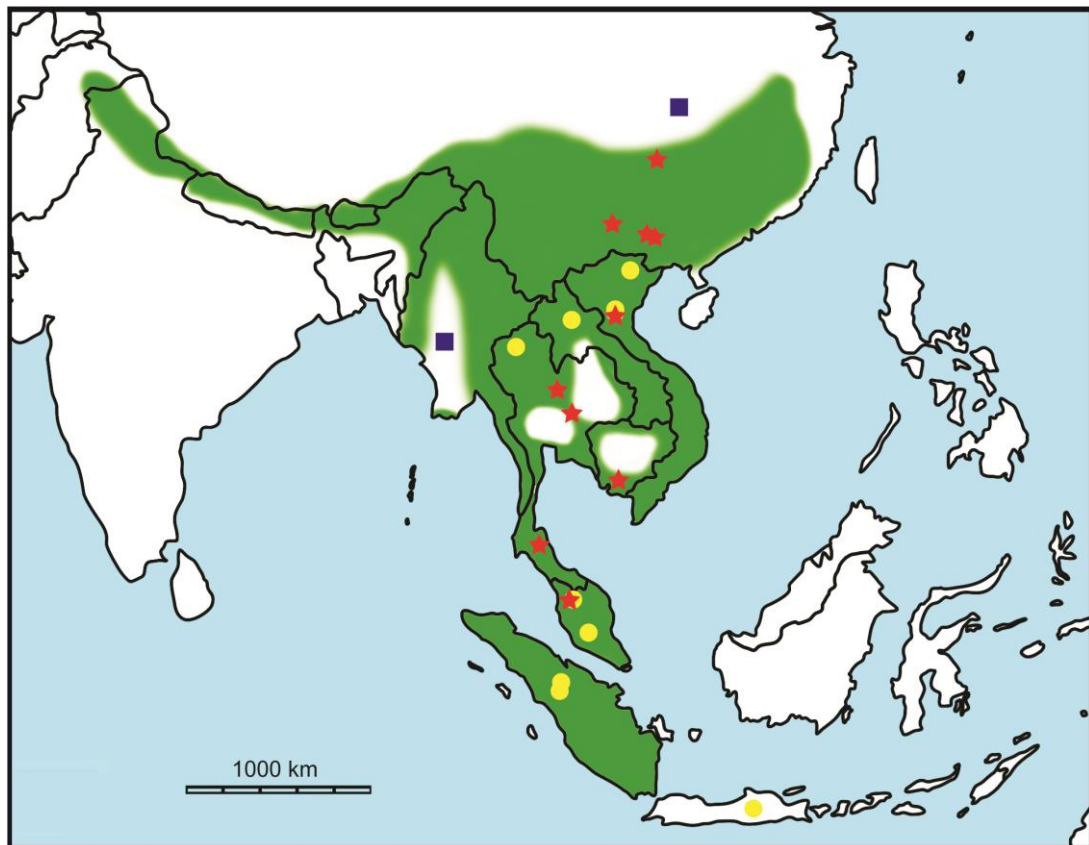


Figure 75. The Early Pleistocene (blue square), Middle Pleistocene (red star), and Late Pleistocene (yellow circle) records and the current distribution (green area) of *Capricornis sumatraensis* (Sumatran serow). The current distribution of the species is compiled from Lekagul and McNeely (1988).

The Sumatran serow is a widespread species, native to mountain forests on the Himalayan range (northern India, Sikkim, and Nepal) of the Indochinese subregion (Southern China, Myanmar, Thailand, Laos, Cambodia, Vietnam, and Peninsular Malaysia) and on the island of Sumatra (Lekagul and McNeely, 1988) (Fig. 75). *C. sumatraensis* became locally extinct in Java during the middle Late Pleistocene according to the lack of fossil records in Wajak (~37 ka). The

advocated cause for the local extinction of serows is possibly related to the unfavorable climatic conditions. The drier and cooler climate that occurred after 81 ka in Java (van der Kaars and Dam, 1995) probably affects significantly the niche preferences of forest-dwelling taxa.

Faunal comparisons of the assemblage with other penecontemporaneous assemblages

For the comparisons of vertebrate faunas between Khok Sung and other Pleistocene sites, we focus only on large mammals (for the mammalian fauna lists of the Middle to Late Pleistocene Southeast Asian sites, see Tabs A18 and A19). The identification of the family level referred to “indet.” and the species level designated “sp.” are herein excluded from our comparisons. The Khok Sung large mammalian assemblage yields most extant and some extinct taxa, which are characteristic of the *Ailuropoda-Stegodon* assemblage. Compared to other Thai Pleistocene faunas, the Khok Sung mammalian assemblage shares 10 species with Thum Wiman Nakin (Tougaard, 1998, 2001), 6 species with Thum Prakai Phet (Tougaard, 1998; Filoux et al., 2015), and 9 species with the Cave of the Monk (Zeitoun et al., 2005, 2010). However, most of the mammalian taxa from the Cave of the Monk are assigned to “cf.” (the open nomenclature) and the presence of fossil spotted hyaena, *Crocuta crocuta*, in this locality is still doubtful, i.e. only one fragmentary tooth is identified as belonging to Hyaenidae indet. by Zeitoun et al. (2005, 2010) (Tab. A19). Compared to the surrounding Pleistocene faunas, the Khok Sung mammalian assemblage has taxonomic similarities of 7 species with Nam Lot (Bacon et al., 2012, 2015) , 8 species with Tam Hang South (Bacon et al., 2008b, 2011, 2015) , 4 species with Tham Khuyen, 2 species with Tham Hai, 5 species with Tham Om, 4 species with Hang Ham, 5 species with Keo Leng (Olsen and Ciochon, 1990), 4 species with Lang Trang (Long et al., 1996), 3 species with Ma U’Oi (Bacon et al., 2004, 2006), 6 species with Duoi U’Oi (Bacon et al., 2008a), 4 species with Boh

Dambang (Demeter et al., 2013), and 4 species with Phnom Loang (Beden and Guérin, 1973) (Tabs A18 and A19). The Khok Sung assemblage is more different from other Pleistocene faunas, especially from the Indonesian islands, which mainly yield endemic forms. According to the number of shared taxa, the Khok Sung mammalian assemblage more nearly resembles diversified faunas from Thum Wiman Nakin, Thum Phra Khai Phet, Nam Lot, and Tam Hang South than the others.

The Khok Sung assemblage shares at least one similar archaic mammal taxon such as *Crocota crocota ultima* and *Stegodon orientalis*, with these faunas. *Crocota crocota* is also recorded from Thum Wiman Nakin, Thum Prakai Phet, and Nam Lot, whereas *Stegodon orientalis* is reported from two Laotian sites: Nam Lot and Tam Hang South. By the way, most of forest dwelling and carnivorous taxa that are representatives of Middle Pleistocene mammalian assemblages such as *Ailuropoda melanoleuca* (giant panda), *Ursus thibetanus* (Asiatic black bear), *Pongo pygmaeus* (orang-utan), *Muntiacus muntjak* (Southern red muntjac), and *Tapirus indicus* (Malayan tapir) are absent in Khok Sung. The absence of most of these taxa in Khok Sung is likely explained by the local environments that are unfavourable to those species. Although some forest-inhabiting taxa (e.g., *Elephas maximus* and *Capricornis sumatraensis*) are found in the locality, these fossils (rare, fragmentary, or represented by isolated teeth only) were transported from the surrounding upland forests by the river.

The degree of the faunal similarity also depends on the number of identified taxa for each site. We further analyse the relationships between the geographic regions and faunas in Southeast Asia, using the Simpson coefficient of faunal similarity (Tab. 23) performed with the multivariate clustering analysis. The final dataset analysed for the similarity comprises 18 localities and 85 taxa. The analysis is based on the presence/absence of mammalian taxa in the fauna lists compiled from literatures (Tabs A17 and A18).

Table 23. Similarity matrix based on the Simpson coefficients. Locality abbreviations: **YCK**, Yenchingkou; **KLS**, Koloshan; **DX**, Daxin; **HJ**, Hejiang; **GX**, Ganxian; **PXDD**, Panxian Dadong; **WY**, Wuyun; **MB**, Maba; **HST**, Hoshantung; **KS**, Khok Sung; **TWN**, Thum Wiman Nakin; **TPKP**, Thum Phra Khai Phet; **TK**, Tham Khuyen; **TO**, Tham Om; **BDB**, Boh Dambang; **KDBB**, Kedung Brubus; **TNHK**, Trinil Hauptknochenschicht; **ND**, Ngandong.

	YCK	KLS	DX	HJ	GX	PXDD	WY	MB	HST	KS	TWN	TPKP	TK	TO	BDB	KDBB	TNHK	ND
YCK	1.00																	
KLS	0.38	1.00																
DX	0.54	0.31	1.00															
HJ	0.55	0.27	0.45	1.00														
GX	0.50	0.20	0.40	0.40	1.00													
PXDD	0.53	0.46	0.46	0.55	0.30	1.00												
WY	0.53	0.23	0.38	0.45	0.70	0.33	1.00											
MB	0.94	0.38	0.62	0.55	0.50	0.44	0.47	1.00										
HST	0.50	0.30	0.20	0.30	0.20	0.40	0.40	0.50	1.00									
KS	0.50	0.00	0.08	0.18	0.10	0.25	0.17	0.25	0.10	1.00								
TWN	0.48	0.15	0.31	0.27	0.60	0.24	0.40	0.50	0.30	0.83	1.00							
TPKP	0.58	0.17	0.17	0.36	0.30	0.33	0.33	0.50	0.30	0.50	0.92	1.00						
TK	0.63	0.31	0.54	0.55	0.60	0.41	0.40	0.63	0.40	0.33	0.53	0.42	1.00					
TO	0.94	0.38	0.54	0.55	0.50	0.50	0.47	0.81	0.40	0.42	0.63	0.50	0.75	1.00				
BDB	0.80	0.10	0.20	0.20	0.30	0.40	0.50	0.60	0.20	0.40	0.80	0.60	0.60	0.60	1.00			
KDBB	0.11	0.08	0.00	0.09	0.00	0.06	0.07	0.13	0.10	0.17	0.22	0.17	0.06	0.13	0.10	1.00		
TNHK	0.21	0.08	0.08	0.09	0.00	0.14	0.14	0.21	0.10	0.08	0.14	0.17	0.07	0.14	0.30	0.64	1.00	
ND	0.10	0.10	0.00	0.10	0.00	0.10	0.10	0.10	0.10	0.00	0.10	0.00	0.00	0.10	0.00	0.90	0.60	1.00

As a result, the Middle Pleistocene Southeast Asian taxa reveal two distinct associations (Javanese and mainland Southeast Asian faunas) (Fig. 76). Within the mainland Southeast Asian assemblages, the cluster analysis resolves two different groups between the Thai, Cambodian, Vietnamese, and Chinese faunas (South China and Yenchingkou) and the central-eastern Chinese one (Koloshan) (Fig. 76). Among South Chinese localities, Hoshantung fauna is a distinct subcluster separated from other mainland Southeast Asian faunas. Hoshantung probably represents a different biochronological age from each other rather than high levels of endemism. The Thai and Cambodian faunas constitute a distinctive subgroup that is differentiated from the Vietnamese and Chinese assemblages. Within the Thai and Cambodian members, the Khok Sung fauna characterizes a distinct subcluster separated from three late Middle Pleistocene

assemblages: Thum Wiman Nakin, Thum Prakai Phet, and Boh Dambang (Fig. 76), although the fauna of Khok Sung is most similar in composition to that of Thum Wiman Nakin according to the Simpson's index (Tab. 23). This is likely due to the convention of the UPGMA method, which produces equal length branches from all nodes, and to the effects of higher faunal similarity between Thum Wiman Nakin and two other faunas.

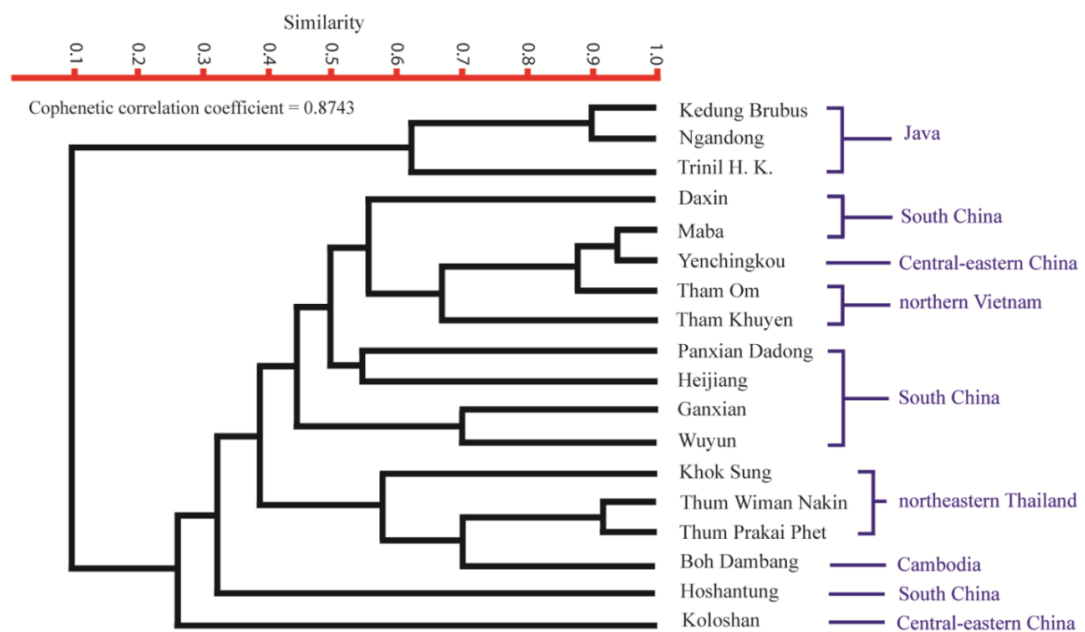


Figure 76. Cluster analysis of the Middle Pleistocene mammalian fossil records in Southeast Asian and some central-eastern and southern Chinese localities based on the Simpson coefficients.

Overall, this analysis suggests initially that the differences in species composition and distribution do not follow a trend of the latitudinal gradient north to south, but show spatial and time variability of large mammalian fauna in Southeast Asia. The main problems of mammalian fauna comparisons in Southeast Asia are likely due to the poorly-known species diversity and/or the imprecisely chronological determination in several localities.

Cenogram analysis

As demonstrated by a schematic representation of the cenogram (Fig. 77), an abundance of large mammals (body weight over 8 kg) is a characteristic of humid conditions (for body mass

estimation of each taxon, see Tab. A21), when compared to the diagram category of arid conditions that theoretically display a steeper slope (Legendre, 1989). Compared to schematic Thum Wiman Nakin cenogram (Tougaard and Montuire, 2006: fig. 4), our data represent a similar pattern of large mammal distribution (humid environments).

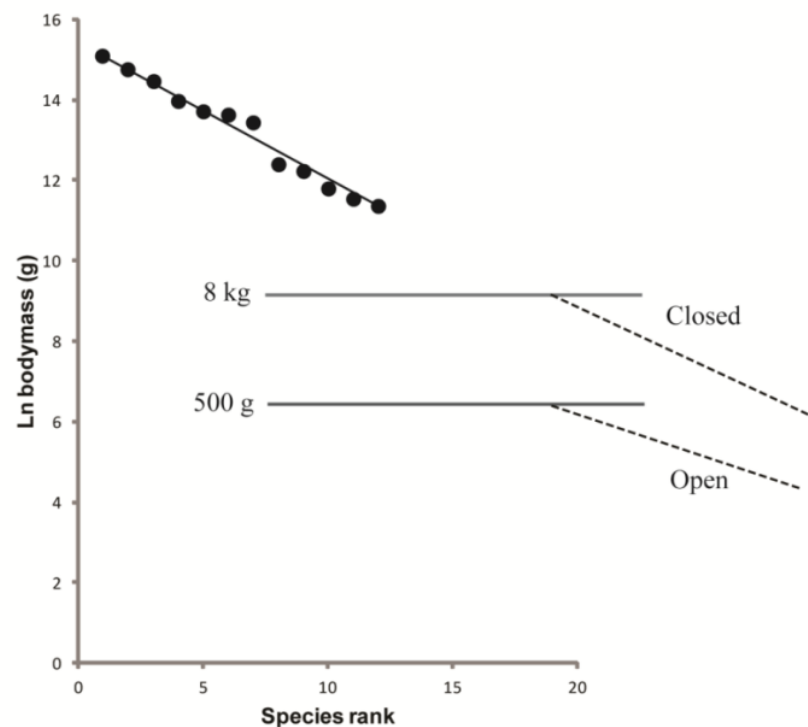


Figure 77. Illustration of the Khok Sung cenogram. Dash lines refer to missing data on the medium- (between 8 kg and 500 g) and small- (<500 g) sized mammals that indicate a characteristic of habitats (Legendre, 1989). The Y-axis represents the log-transformed mean body weight of a mammalian species in the community. The X-axis refers to a species rank, starting from large to small sizes in order descending.

Although this cenogram construction does not allow a full comparison according the lack of medium- to small-sized mammals, it could initially provide the information regarding the weight distribution of local large species in Khok Sung. The absence of medium and small mammals is likely due to longer distance transportation by the river where smaller fossils were deposited further away. As seen in other Pleistocene terrace deposits of Java (e.g., Kedung Brubus and Trinil H.K.), large-bodied animals were frequently found but the others are rare or absent.

CHAPTER 6

Discussion

Contribution to the age of Khok Sung

Crocota crocuta ultima is regarded as one of good biochronological indicators for a Middle to Late Pleistocene age. The first occurrence of *C. c. ultima* in Eastern part of Asia is dated between 500 and 400 ka (middle Middle Pleistocene). At lower latitudinal regions, such as Taiwan and South China, the records of *C. c. ultima* appear to be later, dated to late Middle Pleistocene. Shen and Jin (1991) proposed a maximum age of 240 ka for the southern Chinese *C. c. ultima*. The impacts of glaciations on environments may have played a decisive role in the dispersal of this species. Climatic cooling and low sea levels occurred cyclically during the late Middle Pleistocene (especially between 280 and 240 ka) (Zheng and Lei, 1999; Tougard, 2001; Tseng and Chang, 2007). During these periods, the northern Asian faunas extended their geographical range southwardly following the expansion of their biotopes (“dispersal events”), as demonstrated by several first occurrences of northern Asian mammals (including *C. c. ultima*) in the Indochinese and Sundaic provinces (Chaimanee, 1998; Tougard, 2001). *C. c. ultima* immigration to Thailand occurred probably via South China-Laos route. Therefore, its arrival in Thailand might have appeared contemporaneous with or slightly more recent than in the higher-latitudinal localities of eastern (Penghu Channel) and southern China. However, *C. crocuta* was found from the possible Early to Middle Pleistocene of Pha Bong, northern Thailand (Bocherens et al., in press). This latest discovery possibly extends the chronological range of the occurrence of spotted hyaenas in Thailand further back to the Middle Pleistocene. On the other hand, the study of ancient mtDNA of spotted hyaenas by Sheng et al. (2014) has indicated that extinct and

living spotted hyaenas originated from a widespread Eurasian population during the Middle Pleistocene. These authors also hypothesized that an ancestral Eurasian hyaena population dispersed across large steppe ecosystem but was fragmented by the changes of environmental conditions during the Middle Pleistocene. Due to these paleontological records and genetic data, the occurrence of *C. c. ultima* therefore suggests a Middle to Late Pleistocene age for the Khok Sung fauna.

According to the similarity analysis of the fauna, the mammalian fauna composition of Khok Sung is considerably different from the Early to early Middle Pleistocene assemblage of Java. This suggests an inconsistent age of the Early Pleistocene for Khok Sung. The Khok Sung assemblage is highly comparable in composition to three late Middle Pleistocene faunas: Thum Wiman Nakin (>169 ka, Esposito et al. (1998, 2002)), Thum Prakai Phet (Tougaard, 1998; Filoux et al., 2015), and Boh Dambang (Demeter et al., 2013). However, our faunal comparisons suggest that the biochronological age of Khok Sung is possibly different, slightly older or younger, from those three localities according to some of the compositional dissimilarity. Two early Late Pleistocene sites: Nam Lot (\approx 86-72 ka, Bacon et al. (2015)), and Tam Hang South (\approx 94-60 ka, Bacon et al. (2015)) possibly remains contemporaneous according to the occurrence of several taxa sharing with Khok Sung (>7 species).

In the light of this information, we suggest here tentatively that the short reverse polarity observed within the stratigraphic succession of the Khok Sung sand pit may be correlated to the “Iceland Basin” or to the “Pringle Falls” excursions, dated respectively of 188 ka and 213 ka. The short reversal event of the paleomagnetic field in Brunhes normal chron correlated to “Blake” excursion (dated to around 120 ka, Lund et al. (2001)) also remains a possibility. However, we suggest a late Middle Pleistocene age rather than a Middle/Late Pleistocene transition according

to the occurrence of several archaic taxa and to the closest faunal similarity with Thum Wiman Nakin.

Evolutionary and biogeographic affinities of Khok Sung fauna

Relationships of the Khok Sung vertebrate fauna for dispersal events from India to Java has been first proposed by Martin et al. (2012). *Gavialis bengawanicus* and *Crocodylus siamensis* as well as monitor lizards and pythons are known as typical taxa associated with the *Stegodon-Homo erectus* fauna, which presumably originated from the Miocene-Pliocene of Siwalik faunas in India and Pakistan (Head, 2005; de Vos, 2007; Hocknull et al., 2009; Delfino and de Vos, 2010; Martin et al., 2012). These taxa migrated from mainland Southeast Asia to Java, via the Siva-Malayan route, by the Early Pleistocene as they are first recorded from the Early Pleistocene of Java (von Koenigswald, 1935; de Vos, 1995; de Vos and Long, 2001; de Vos, 2007; Delfino and de Vos, 2010) (Fig. 78 and Tab. A18). According to the occurrence of *Gavialis cf. bengawanicus* in Khok Sung, Martin et al. (2012) hypothesized that this species reached Java through the fluvial drainages of Sunda shelf (rather than the dispersal by sea) during a low sea level event (with a minimum of about 170 m below the present day) of the Early-Middle Pleistocene transition (around 0.8 Ma) (Prentice and Denton, 1988; van den Bergh et al., 2001; van der Geer et al., 2010) (Fig. 78). In the light of this scenario, *G. bengawanicus* might have appeared either earlier than or during the Early Pleistocene in Thailand.

However, in terms of faunal age, this hypothesis is no longer consistent because the Khok Sung fauna is now attributed to a late Middle Pleistocene age (Suraprasit et al., 2015), younger than *Gavialis* and *Crocodylus*-bearing localities in Java. We propose that gharials and some other vertebrates (e.g., a freshwater crocodile, a large varanid, and a python) present in Khok Sung are possibly geographical remnants of the former Siva-Malayan fauna that survived

until the late Middle Pleistocene as they occurred earlier in Java. Otherwise, these vertebrates possibly appeared either firstly or repeatedly (if the local extinction of those taxa previously occurred) in Thailand during the late Middle Pleistocene. Several cyclic occurrences of high amplitude glacial periods (~50 times since the last 2.7 Ma, Woodruff (2010)), related to the sea level lowering, during the Early to Middle Pleistocene (Prentice and Denton, 1988; van der Kaars, 1991; Zheng and Lei, 1999) could provide high possibilities to facilitate faunal exchange between mainland and insular Southeast Asia (via the land bridges or the Sunda shelf). The faunal exchanges by corridor and/or filter bridge dispersal between Thailand and Java might have occurred habitually during the glacial events.

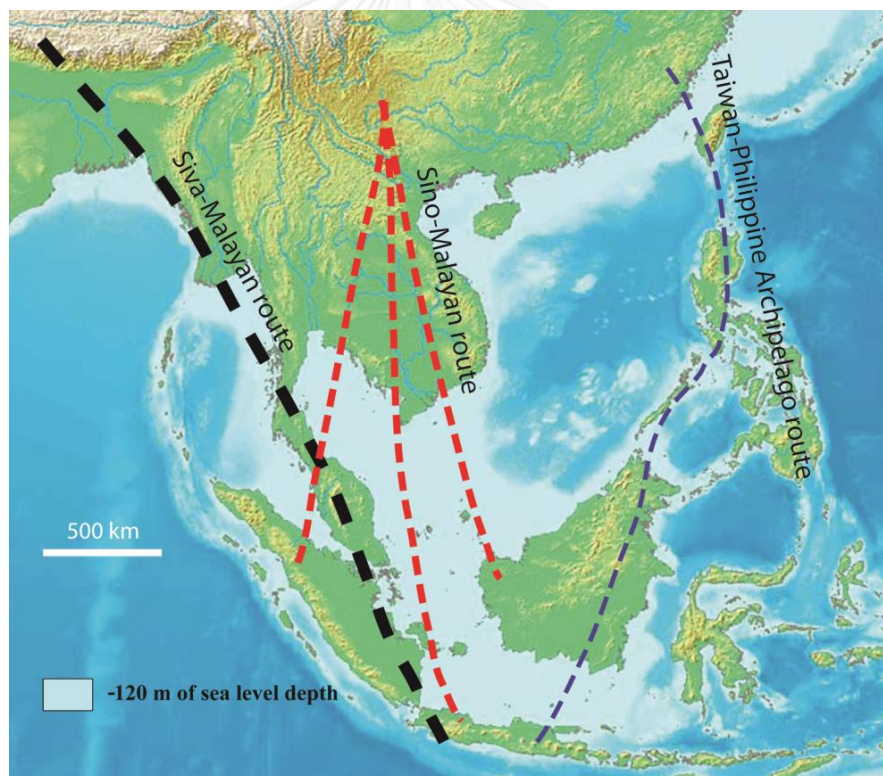


Figure 78. Map of Southeast Asia showing the Sundaland boundaries and the migration route hypothesis: Siva-Malayan route (black), Sino-Malayan route (red), and Taiwan-Philippine Archipelago route (blue). The boundaries of the Sunda shelf at the sea level of about 120 m lower than the present day are compiled from Voris (2000).

During the Middle Pleistocene, it has long been known that there were significant faunal exchanges that occurred between mainland Southeast Asia and Indonesian islands. Two migration routes, known as “Sino-Malayan”, are hypothesized (Fig. 78): an insular pathway via the Philippines proposed by von Koenigswald (1938–1939) and a continental pathway via Thailand, Myanmar, and Cambodia proposed by de Terra (1943). Recent studies on the paleogeographical affinities of Middle Pleistocene large mammals suggest that the latter route is most consistent (Tougaard, 2001; van den Bergh et al., 2001). The sea floor between Taiwan and the Philippine Archipelago was too deep for the emergence of a land bridge, and thus did not allow a dispersal route for large mammals during the Middle Pleistocene. This interpretation is also supported by a high number of endemic species that occur in Philippine Archipelago (Heaney, 1985; Corbet and Hill, 1992).

Based on the occurrence of mammalian taxa in Khok Sung, we suggest a biogeographic relevance of this fauna for the “Sino-malayan” dispersal events from mainland Southeast Asia to Java (Fig. 78). This evidence is supported by the faunal turnover that occurred in Punung (Java), around 128 to 118 ka dated by luminescence and U-series analysis performed on the breccias (Westaway et al., 2007). The modern rainforest assemblage, known as the *Pongo-Homo sapiens* or *Elephas-Homo sapiens* fauna, has replaced the former *Stegodon-Homo erectus* faunal association in Java during since latest Middle Pleistocene (Westaway et al., 2007). The new faunal elements include *Elephas maximus*, *Pongo pygmaeus*, *Symphalangus syndactylus* (siamang), *Macaca nemestrina* (pig-tailed macaque), *Panthera tigris* (tiger), *Dicerorhinus sumatrensis* (Sumatran rhinoceros), *Helarctos malayanus* (sun bear), *Capricornis sumatraensis*, *Bubalus arnee*, *Sus scrofa*, and *Sus barbatus* (Tab. A19). The Khok Sung mammalian assemblage consists of at least 4 of forest dwelling mammals: *Capricornis sumatraensis*, *Bubalus arnee*, *Sus barbatus*, and *Elephas* sp. (Tabs 22 and A18). These taxa presumably migrated from mainland Southeast Asia to

Java and some of them are living today in the mainland Southeast Asia (van den Bergh et al., 2001; van der Geer et al., 2010). The presence of exclusive tropical rainforest species in Punung indicates that their migration event could have occurred following the dry and open woodland environments of the penultimate glaciations at about 135 ka (de Vos, 1983; de Vos et al., 1994). These mammals migrated southward to the exposed Sunda shelf that occurred during the late Middle Pleistocene (between 135 to 125 ka), when the sea level dropped about 150 m (van der Kaars, 1991; Zheng and Lei, 1999). The Sundaland was then covered partly by a savannah corridor, stretching from Thailand to the Lesser Sunda Islands (Morley and Flenley, 1987; Heaney, 1991). This corridor served as a barrier to the dispersal of the rainforest-dependent species. However, the forest-dwelling mammals survived in rainforest refugia for a while before reaching Java (van den Bergh et al., 2001).

On the other hand, the Khok Sung fauna lacks any evidence of taxa originating from Java. But the possible presence of *Duboisia santeng* in Tambun site (Peninsular Malaysia) may indicate the faunal exchange from Indonesia to the mainland Southeast Asia (Hooijer, 1962; Medway, 1972; Tougaard, 2001). *D. santeng* is described from the early Middle Pleistocene of Kedung Brubus and the middle Middle Pleistocene of Trinil H. K. (Hooijer, 1958). This taxon presumably arrived on the island of Java via the Siva-Malayan route (von Koenigswald, 1935; Tougaard, 2001). The poor record or absence of the Indonesian taxa in mainland Southeast Asia is likely due to the disappearance of the land bridge during the interglacial phase. This acted as a sea barrier that did not facilitate insular mammals to migrate out of the islands.

The Khok Sung mammalian assemblage supports that Thailand was a biogeographic gateway of the Sino-Malayan migration event as the mainland forested faunal association replaced the earlier Siva-Malayan fauna (*Stegodon-Homo erectus* complex) subsequently in Java (von Koenigswald, 1938–1939; de Vos, 1995). The glacial episodes are likely a key factor of

southward onland dispersal of large mammals via the Sunda shelf. In addition, the occurrence of the Khok Sung reptiles is not truly representative of the early Siva-Malayan refugees but represents practically long-term survivors (e.g., *Crocodylus siamensis*, *Heosemys annandalii*, and *Heosemys grandis*) that evidently continued to exist up until today in Thailand.

Paleoecological, paleoenvironmental and paleoclimatic implications of Khok Sung

The Pleistocene spotted hyaena *Crocota crocuta ultima* was a predator that probably feed C4-plant consumers like bovids and cervids, as demonstrated by carbon isotopic results from roughly contemporaneous locality, Thum Wiman Nakin (Pushkina et al., 2010). The Khok Sung flood plain area was thus representing an attractive habitat for numerous and diversified herbivorous, providing easy preys for carnivores (Suraprasit et al., 2015). The unique terrestrial large mammalian predators of Khok Sung area were *C. c. ultima* and *Cuon*, while crocodiles and gharials were the major riverine predators. The other predators such as the tiger (*Panthera tigris*), the hog badger (*Arctonyx*), and the Asiatic black bear (*Ursus thibetanus*) were not present at Khok Sung, but were common in the late Middle Pleistocene sites of Southeast Asia (Tougaard, 2001; Louys et al., 2007). These carnivores were probably living nearby or hunting in forests around the caves where their fossils have been found. The absence of other mammalian predators discovered in Khok Sung might be explained by the specific differences of their paleoenvironmental and habitat preferences. Concerning the *in situ* Khok Sung fauna, relatively complete fossils including skulls of a spotted hyaena, cervids, bovids, and gharials, some articulated postcranial skeletons of a bovid (only skull missing for this individual) and an extinct proboscidean *Stegodon* (associated with its lower jaws), and carapaces and plastrons of turtles were recovered in the channel bar. It indicates that these fossils were transported on short

distances by the river. On the contrary, some specimens represent polished structures of reworking before deposition (Duangkrayom et al., 2014) and may have been transported on longer distances.

Based on the study of the Khok Sung flora by Grote (2007), the plant remains represent mixed tropical deciduous and dry evergreen forest paleoenvironments. However, some taxa (e.g., *Melia azedarach* and cf. *Cyperus*) can be recently found in Indian Himalayan Region (up to an elevation of 2000 m) (Board on Science and Technology for International Development, 1983) and in wetland environments at all altitudes (Cook, 1996), respectively. We therefore suggest that most of these plant remains have been transported by the river and rather correspond to the surrounding upland vegetation. In contrast to the paleobotanical interpretation of Grote (2007), several mammalian taxa recently inhabiting an open grassland landscape (e.g., *Crocota crocuta ultima*, *Rhinoceros unicornis*, *Bubalus amee*, *Axis axis*, and *Rusa unicolor*) were present at Khok Sung (Laurie et al., 1983; Lekagul and McNeely, 1988). Based on the occurrence of a great number of grassland-associated taxa and freshwater reptiles (turtles and soft-shelled turtles (Claude et al., 2011), gharials (Martin et al., 2012), and crocodiles) and on the sedimentary facies (Duangkrayom et al., 2014), the paleoenvironments therefore corresponded to an open habitat as floodplain near the river channel for Khok Sung. However, *Rhinoceros sondaicus* and *Sus barbatus* presently inhabiting rainforests were also found from Khok Sung (Grubb, 2005; Groves and Leslie Jr, 2011). These taxa may reinforce the paleoenvironmental attribution proposed for the upland surrounding area of Khok Sung, as open forest environments.

According to previous studies of the paleoclimates in Thailand, Chaimanee (1998) suggested wetter and cooler conditions than today for the late Middle Pleistocene of Thum Wiman Nakin based on the presence of some fossil rodent species. In addition, a cenogram analysis performed at this fauna has suggested slightly more temperate conditions and open

environments than today (Tougaard and Montuire, 2006). Paleoclimatic interpretation based on our cenogram analysis suggests a significantly humid condition for Khok Sung, similar to those observed for the late Middle Pleistocene cave deposit of Thum Wiman Nakin.



CHAPTER 7

Conclusion and perspectives

Since numerous vertebrate fossils were recovered from the Khok Sung sand pit, only a preliminary report on the fauna discovery and a few published works on the sedimentary facies and the taxonomy identification of reptiles have been done. Our research thus provides new information on the several aspects including the age, taxonomy, and paleobiogeographical affinities of the fauna and the paleoenvironments and paleoclimate of the locality.

Chronology

Without radiometric datings, the age of any Pleistocene Southeast Asian mammalian fauna is difficult to be precisely estimated due to the fact that the typical *Stegodon-Ailuropoda* faunal complex ranges from the Early to Late Pleistocene in age. We suggest here a late Middle Pleistocene age, possibly either around 188 or 213 ka, for the Khok Sung fauna based on the paleomagnetic data (correlated to the “Iceland Basin” and “Pringle Falls” excursions) coupled with the occurrence of *C. c. ultima* that represents a well-calibrated marker at least for its first appearance date in Asia. The ancient spotted hyaenas are supposed to have dispersed to mainland Southeast Asia during the late Middle Pleistocene. However, a Late Pleistocene age assigned for the Khok Sung fauna remains a possibility, since the spotted hyaenas continued to be documented up until the Late Pleistocene in Laos according to the latest chronological determination of Nam Lot (Bacon et al., 2015). In Thailand, the Late Pleistocene of the Cave of the Monk has yielded a single specimen of Hyaenidae indet. (Zeitoun et al., 2010), but this half fragmentary tooth is poorly preserved and is difficult to be more precisely identified. Remains of

C. crocuta are also reported from the cave of Pha Bong, where the age has been tentatively attributed to the Early to Middle Pleistocene according to the occurrence of *Gigantopithecus* (Bocherens et al., in press). This possibly suggests a wider chronological range for the appearance of spotted hyaenas in Thailand, probably before late Middle Pleistocene. The existence of spotted hyaenas until the Late Pleistocene of Thailand is still questionable. Based on the faunal correlations with other Southeast Asian sites, the biochronological age of Khok Sung is likely assigned to the late Middle Pleistocene according to the high similarity with the Thum Wiman Nakin (Snake cave) fauna.

Although the radiometric frameworks for the fissure-filling deposits of other localities in mainland Southeast Asia (e.g., Tam Pa Ling, Tam Hang South, Ma U'Oi, and Duoi U'Oi) have been well-documented based on various dating techniques (e.g., OSL, TL, U-series and ESR methods), these available methods have however their own disadvantages and sometimes make the obtained absolute ages rather unreliable. For instance, the main problems of the OSL dating rely on the incomplete bleaching of the material before deposition, which is a necessary condition for the measuring technique, leading to an overestimation of the age (Olley et al., 1998, 1999; Duller, 2004). Otherwise, several materials (in case of such as U-series or ESR datings) show evidence of departure from a closed-system behavior and also uranium uptake after burial or deposition (e.g., Grün et al., 1988; Rink, 1997; Esposito et al., 1998, 2002; Grün, 2000). Only some terrestrial materials (e.g., volcanic rocks and clean speleothems) are reliable for such techniques (Smart, 1991). The rareness of the available material for dating is one of the main problems in the Southeast Asian Pleistocene localities. Although the stratigraphic succession of the Khok Sung site does not show any evidence of the volcanic tuff or ash layer containing crystals for the better-calibrated procedure of radiometric datings (e.g., feldspar and zircon), other radiometric applications, such as U-series and ESR datings, can be also applied for the material such as teeth

and bones (e.g., Grün, 1989; Pike and Hedges, 2001; Grün et al., 2005). The new and recent developments of these techniques have been considerably improved for that material (Grün and Schwarcz, 2000; Grün, 2002, 2009; Hercman, 2014) and nowadays provide a relatively chronological reliability, but these absolute ages in several localities sometimes contrast with those obtained from biochronological information and/or even other radiometric applications. For this reason, the data regarding the fauna composition and the evolutionary frameworks (e.g., morphological evolution, speciation, and extinction) are also helpful and should be taken into account for the chronological determination of Khok Sung, as well as for other Pleistocene vertebrate faunas. We however realize that the Khok Sung locality should be radiometrically dated, for instance, using the U-series and/or ESR dating methods performed on the fossil teeth, in order to possibly restrict its wide chronological ranges, when combined with the biochronological and paleomagnetic data. This would possibly suggest a new age or more precise chronological constraint, which allows to establish more detailed information on the evolution of large mammals and on the paleoclimate of the region during the glacial-interglacial cycles.

Taxonomy and species composition

Overall, the Khok Sung vertebrate fauna comprises at least 15 large mammal species (13 genera) including a majority of modern and some extinct taxa. The modern species in Khok Sung are relatively similar to the present-day mammals in the area, but some globally (*Stegodon* cf. *orientalis*) and locally (*Axis axis*, *Sus barbatus*, *Rhinoceros unicornis*, *Crocuta crocuta*) extinct taxa were also present. A chital has been reported here for the first time in Southeast Asia. The most diverse group in the locality corresponds to artiodactyls (8 species), open-habitat grazers, whereas the forest associated taxa (e.g., Asian elephants and primates) are lower in diversity. Three reptilian taxa: *Crocodylus* cf. *siamensis*, *Varanus* sp. and *Python* sp. have been further identified

and added to the fauna list. The reptilian fauna represents a total of 10 species (9 genera). However, some complete fossils of reptiles, as well as a whole material of fishes, have not been identified in details yet, thus suggesting that the vertebrate fauna is probably greater in diversity.

The Khok Sung mammalian fauna yields a general characteristic of *Stegodon-Ailuropoda* complex, although some large carnivores (e.g., *Ursus thibetanus* and *Ailuropoda melanoleuca*) and primates (*Gigantopithecus blacki* and *Pongo pygmaeus*) are undocumented. The absence of these forest inhabiting taxa in Khok Sung is likely due to the unfavourable niche for those species. Otherwise, the rareness and poor preservation of forest dwelling fossils (e.g., a fragmentary molar of *Elephas* sp., three isolated m3 of *Capricornis sumatraensis*, and a single tibia of *Macaca* sp.) in Khok Sung suggest that these specimens have been probably transported from the surrounding upland forests by the river. Indeed, the faunal composition between Khok Sung and other Pleistocene sites could be fundamentally compared based on the presence/absence of taxa, but the taphonomic and paleoenvironmental conditions also need to be considered.

In another way, the main faunal comparisons of Pleistocene mammalian fossils in Southeast Asia are linked to the general practices in systematics of the scientific community. The major problem is likely due to the lack of stability in the systematics, particularly the use of different binomial nomenclature systems and the taxonomic attributions of species or subspecies in local scale. Numerous large- to middle-sized mammal species are only recorded from one site and the validity of some species known as “wastebasket taxa” remains questionable. These issues require a revision of the diagnosis because their hypodigms probably encompass at least two species or even more. Accordingly, the taxonomic study of the Khok Sung fauna is useful to develop standard references for the morphological comparisons of several fossil large mammals, especially for diverse ruminant species, recovered from other Southeast Asian localities because

this locality preserves obviously much more complete and numerous skull and postcranial bones than the others. The morphology and size of large mammals (cranial, mandibular, dental, and postcranial remains) in Khok Sung rather match well those of extant comparative specimens, suggesting conservative morphological evolution through the Pleistocene to today. However, the Khok Sung mammalian teeth are sometimes not congruent in morphology and/or in size with previously recorded fossils from some Southeast Asian localities (e.g., Thum Wiman Nakin). According to our observation on mammalian fossils from the nearby Thum Wiman Nakin cave fauna, which also represents one of the most diversified Pleistocene fauna in mainland Southeast Asia, we suggest a taxonomic revision of large mammals for this locality.

Paleobiogeography

Recent studies on the Middle and Late Pleistocene sites in Southeast Asia have revealed that some large mammals nowadays characterizing either the Indochinese or Sundaic subregion have been present in several localities. The Khok Sung fauna exhibits a more considerable amount of Indochinese large mammal taxa than those of the Sundaic species. Some species were locally extinct in mainland Southeast Asia, but their geographical distributions were obviously more widespread during the late Middle Pleistocene. The occurrence of *Crocota crocuta ultima* in Khok Sung is a successful example of distribution patterns of carnivores during the Pleistocene as it has been widely recorded from China to southern Thailand but is nowadays restricted to Sub-Saharan Africa. The extant Indian subcontinental taxa, *Rhinoceros unicornis* and *Axis axis*, were also present in Khok Sung. Moreover, the occurrence of *Sus barbatus* in the locality indicates that this species was common in mainland Southeast Asia during the late Middle Pleistocene before reaching Indonesian islands subsequently (Late Pleistocene). However, this taxon is no longer present in the Indochinese subregion. An extinct species of proboscideans,

Stegodon cf. orientalis, whose distribution was widespread in the Palearctic region and Indochinese subregion during the Pleistocene, is also present in the locality. This suggests the faunal dispersal events, both northward and southward migrations, did not involve only mainland Southeast Asia but also a larger territory including China and India in response to climatic fluctuations.

Similar to that of Thum Wiman Nakin, the discovery of the Khok Sung fauna provides supporting information on the migration routes of the dispersal events during the latest Middle Pleistocene, strengthening the continental dispersal hypothesis via the Sunda shelf ("Sino-Malayan" pathway). The faunal turnover has been obviously observed in Indonesian islands, mostly on Java, during the latest Middle Pleistocene/early Late Pleistocene, as exemplified by the differences in faunal composition between the late Middle Pleistocene of Ngandong and the latest Middle/early Late Pleistocene of Punung. The *Stegodon-Homo erectus* fauna was replaced by new tropical rainforest elements (the *Pongo-Homo sapiens* complex) that are supposed to have migrated from mainland Southeast Asia. However, evidence of the fauna turnover in mainland Southeast Asia is poorly documented. This is likely due to the scarcity of well-documented assemblages. Most of them have been known by an indecisive inventory of taxa, inaccurate taxonomic descriptions or comparisons, and by imprecise ages of the faunas. For this reason, the zoogeographical history of large mammal faunas is rather difficult to be reconstructed.

Previous studies on the distribution patterns of fossil rodents (Chaimanee, 1998) and large mammals (Tougaard, 1998, 2001) have suggested that the boundary between Indochinese and Sundaic subregions during the Pleistocene were different in location from the present-day limits, probably further south of the Kra Isthmus, in relation to the cooler climate during the glacial phase. Due to the latitudinal location of Khok Sung, the fauna is likely uninformative to

solve this issue. In Thailand, only few recovered Pleistocene sites (e.g., “Thum Phedan” (Nakhon Si Thammarat) and “Tham Le *Stegodon*” (Thung Wa, Satun) caves that are located further south of the Kra Isthmus have possibly potential to shed new light on the biogeographic boundaries between these two subregions during the Pleistocene. However, these faunas have never been taxonomically studied in details, only Thum Phedan having been preliminarily described by Yamee and Chaimanee (2005). Interestingly, *Crocota crocuta ultima* that was common in the Indochinese subregion and that has never been recorded in the Sundaic subregion is found from Thum Phedan. This provides therefore the first evidence of another Indochinese taxon (in addition to *Palaeoloxodon namadicus* and some rodents) that occurred further south of the Kra Isthmus during the Middle Pleistocene. We suggest that additional taxonomic descriptions of the mammalian faunas from Thum Phedan and Tham Le *Stegodon* caves may allow confirming the occurrence of present-day Indochinese taxa in the Sundaic subregion during the Middle Pleistocene, possibly supporting the fluctuating location of past boundaries between these two subregions.



Paleoenvironments and paleoclimate

The paleoenvironmental implications of mainland Southeast Asia during the Pleistocene are mostly inferred from the habitat preferences of large fossil mammals in relation to their relative living appearances in the region. In Khok Sung, the paleoenvironments corresponded to open environments as a floodplain near the river channel according to the sedimentary facies study (Duangkrayom et al., 2014) and the occurrence of numerous open-habitat grazers (e.g., large bovids and cervids). The occurrence of the spotted hyaena is also a paleoenvironmental indicator of savannah conditions. Moreover, the presence of fresh water reptiles (such as crocodiles, gharials, and soft-shelled turtles) is representatives of major riverine taxa. However,

several studies based on the stable carbon isotope analysis have shown that the ancient mammals could use more varied habitats or they might live in different landscapes from those of present day because their habitat preferences have been modified by human activities and/or natural events through time. In addition, since some Southeast Asian taxa found today appear to have been living in refugial areas, the periodic and numerous transitions between glacial and interglacial conditions altered environments, fractured landscapes, and acted to reduce and divide population by driving many species into refugia: rainforest species during the glacial periods and savannah species during the interglacial events. Accordingly, the Pleistocene mammals might have occupied the different habitats and environmental conditions from where they forage today.

With regards to other proxy data, plant macrofossils in Khok Sung have been previously studied (Grote, 2007), but they likely corresponded to the upland surrounding vegetation and have been transported by the river. Palynological records are widely known as indicators of past land vegetation and are hence useful for reconstructing the paleoenvironmental and paleoclimatic conditions. These proxy data have never been obtained from this locality. Regarding the plentiful petrified wood recovered from the Khok Sung sand pit, the interpretation of climatic proxy data from tree rings also becomes possible in the future. Otherwise, some applications such as mesowear and microwear analyses could be applied for the teeth of diversified ungulates in Khok Sung and would permit to examine both long and short term patterns in the paleodietary reconstruction of fossil mammals. In the future, the combination of our taxonomic information and other proxy data would therefore strengthen the understanding of the terrestrial paleoclimatic evolution of the region.

REFERENCES

- An, Z., Liu, T., Lu, Y., Porter, S.C., Kukla, G., Wu, X., and Hua, Y. 1990. The long-term paleomonsoon variation recorded by the loess-paleosol sequence in Central China. Quaternary International 7: 91-95.
- Antoine, P.-O. 2012. Pleistocene and Holocene rhinocerotids (Mammalia, Perissodactyla) from the Indochinese Peninsula. Comptes Rendus Palevol 11: 159-168.
- Appenzeller, T. 2012. Human migrations: Eastern odyssey. Nature 485: 24-26.
- Ashton, P.S. 1992. Plant conservation in the Malaysian region. in Proceedings of the International Conference on Conservation of Tropical Biodiversity. pp. 86-93. Kuala Lumpur. Malaysian Nature Society.
- Attwood, S.W., and Johnston, D.A. 2001. Nucleotide sequence differences reveal genetic variation in *Neotricula aperta* (Gastropoda: Pomatiopsidae), the snail host of schistosomiasis in the lower Mekong Basin. Biological Journal of the Linnean Society 73: 23-41.
- Averianov, A.O., and Danilov, I.G. 1997. A varanid lizard (Squamata: Varanidae) from the Early Eocene of Kirghizia. Russian Journal of Herpetology 4: 143-147.
- Ayob, M. 1970. Quaternary sediments at Sungei Besi, West Malaysia. Bulletin of the Geological Society of Malaysia 3: 53-61.
- Bacon, A.-M., Demeter, F., Düringer, P., Helm, C., Bano, M., Long, V.T., Thuy, N.T.K., Antoine, P.-O., Mai, B.T., Huong, N.T.M., Dodo, Y., Chabaux, F., and Rihs, S. 2008a. The Late Pleistocene Duoi U'Oi cave in northern Vietnam: palaeontology, sedimentology, taphonomy and palaeoenvironments. Quaternary Science Reviews 27: 1627-1654.
- Bacon, A.-M., Demeter, F., Düringer, P., Patole-Edoumba, E., Sayavongkhamdy, T., Coupey, A.-S., Shackelford, L., Westaway, K.E., Ponche, J.-L., Antoine, P.-O., and Sichanthongtip, P., eds. Les Sites de Tam Hang, Nam Lot et Tam Pà Ling au Nord du Laos. Des Gisements à Vertébrés du Pléistocène aux Origines des Hommes Modernes. 2012, CNRS Editions. 150 pp.
- Bacon, A.-M., Demeter, F., Roussé, S., Long, V.T., Düringer, P., Antoine, P.-O., Thuy, N.T.K., Mai, B.T., Huong, N.T.M., Dodo, Y., Matsumura, H., Schuster, M., and Anezaki, T. 2006. New palaeontological assemblage, sedimentological and chronological data from the Pleistocene Ma U'Oi cave (northern Vietnam). Palaeogeography, Palaeoclimatology, Palaeoecology 230: 280-298.
- Bacon, A.-M., Demeter, F., Schuster, M., Long, V.T., Thuy, N.T.K., Antoine, P.-O., Sen, S., Nga, H.H., and Huong, N.T.M. 2004. The Pleistocene Ma U'Oi cave, northern Vietnam: palaeontology, sedimentology and palaeoenvironments. Geobios 37: 305-314.

- Bacon, A.-M., Demeter, F., Tougard, C., de Vos, J., Sayavongkhamdy, T., Antoine, P.-O., Bouasisengpaseuth, B., and Sichanthongtip, P. 2008b. Redécouverte d'une faune pléistocène dans les remplissages karstiques de Tam Hang au Laos: Premiers résultats. Comptes Rendus Palevol 7: 277-288.
- Bacon, A.-M., Düringer, P., Antoine, P.-O., Demeter, F., Shackelford, L., Sayavongkhamdy, T., Sichanthongtip, P., Khamdalavong, P., Nokhamaomphu, S., Sysuphanh, V., Patole-Edoumba, E., Chabaux, F., and Pelt, E. 2011. The Middle Pleistocene mammalian fauna from Tam Hang karstic deposit, northern Laos: New data and evolutionary hypothesis. Quaternary International 245: 315-332.
- Bacon, A.-M., Westaway, K., Antoine, P.-O., Düringer, P., Blin, A., Demeter, F., Ponche, J.-L., Zhao, J.-X., Barnes, L.M., Sayavongkhamdy, T., Thuy, N.T.K., Long, V.T., Patole-Edoumba, E., and Shackelford, L. 2015. Late Pleistocene mammalian assemblages of Southeast Asia: New dating, mortality profiles and evolution of the predator-prey relationships in an environmental context. Palaeogeography, Palaeoclimatology, Palaeoecology 422: 101-127.
- Badoux, D.M. 1959. Fossil Mammals from Two Fissure Deposits at Punung (Java): with Some Remarks on Migration and Evolution of Mammals during the Quaternary in South East Asia. Ph.D thesis, Reijks Utrecht, Netherlands, Universiteit te Utrecht.
- Baker, W.J., Coode, M.J.E., Dransfield, J., Dransfield, S., Harley, M.M., Hoffmann, P., and Johns, R.J. 1998. Patterns of distribution of Malesian vascular plants. In Hall, R. and Holloway, J.D. (eds.), Biogeography and Geological Evolution of Southeast Asia, pp. 243-258. Leiden: Backhuys.
- Barker, G., Barton, H., Bird, M., Daly, P., Datan, I., Dykes, A., Farr, L., Gilbertson, D., Harrison, B., Hunt, C., Higham, T., Kealhofer, L., Krigbaum, J., Lewis, H., McLaren, S., Paz, V., Pike, A., Piper, P., Pyatt, B., Rabett, R., Reynolds, T., Rose, J., Rushworth, G., Stephens, M., Stringer, C., Thompson, J., and Turney, C. 2007. The 'human revolution' in lowland tropical Southeast Asia: the antiquity and behavior of anatomically modern humans at Niah Cave (Sarawak, Borneo). Journal of Human Evolution 52: 243-261.
- Bärmann, E.V., and Rössner, G.E. 2011. Dental nomenclature in Ruminantia: Towards a standard terminological framework. Mammalian Biology-Zeitschrift für Säugetierkunde 76: 762-768.
- Baryshnikov, G.F. 1999. Chronological and geographical variability of *Crocota spelaea* (Carnivora, Hyaenidae) from the Pleistocene of Russia. In Haynes, G., Klimowicz, J., and Reumer, J.W.F. (eds.), Mammoths and the Mammoth Fauna: Studies of an Extinct Ecosystem, pp. 155-174. Deinsea.

- Baryshnikov, G.F. 2012. Pleistocene Canidae (Mammalia, Carnivora) from the Paleolithic Kurado caves in the Caucasus. Russian Journal of Theriology 11: 77-120.
- Baryshnikov, G.F. 2014. Late Pleistocene hyena *Crocota ultima ussurica* (Mammalia: Carnivora: Hyenidae) from the Paleolithic site in Geographical Society Cave in the Russian far east. Proceedings of the Zoological Institute RAS 318: 197-225.
- Baryshnikov, G.F. 2015. Late Pleistocene Canidae remains from Geographical Society Cave in Russian Far East. Russian Journal of Theriology 14: 65-83.
- Batchelor, B.C. 1979. Discontinuously rising late Cainozoic sea-levels with special reference to Sundaland, Southeast Asia. Geologie en Mijnbouw 58: 1-10.
- Beden, M., and Guérin, C. 1973. Le Gisement de Vertébrés du Phnom Loang (Province de Kampot, Cambodge): Faune du Pléistocène Moyen Terminal (Loangien). Paris: O.R.S.T.O.M.
- Bekken, D., Schepartz, L.A., Miller-Antonio, S., Yamei, H., and Weiwen, H. 2004. Taxonomic Abundance at Panxian Dadong, a Middle Pleistocene Cave in South China. Asian Perspectives 43: 333-359.
- Bettis, E.A., Milius, A.K., Carpenter, S.J., Larick, R., Zaim, Y., Rizal, Y., Ciochon, R.L., Tassier-Surine, S.A., Murray, D., Suminto, and Bronto, S. 2009. Way out of Africa: Early Pleistocene paleoenvironments inhabited by *Homo erectus* in Sangiran, Java. Journal of Human Evolution 56: 11-24.
- Biasatti, D., Wang, Y., and Deng, T. 2010. Strengthening of the East Asian summer monsoon revealed by a shift in seasonal patterns in diet and climate after 2–3 Ma in northwest China. Palaeogeography, Palaeoclimatology, Palaeoecology 297: 12-25.
- Bien, M.N., and Chia, L.P. 1938. Cave rock-shelter deposits in Yunnan. Bulletin of the Geological Society of China 18: 325-348.
- Billups, K., and Schrag, D.P. 2003. Application of benthic foraminiferal Mg/Ca ratios to questions of Cenozoic climate change. Earth and Planetary Science Letters 209: 181-195.
- Bird, M.I., Taylor, D., and Hunt, C. 2005. Palaeoenvironments of insular Southeast Asia during the Last Glacial Period: a savanna corridor in Sundaland? Quaternary Science Reviews 24: 2228-2242.
- Board on Science and Technology for International Development. 1983. Firewood Crops: Shrub and Tree Species for Energy Production. Washington DC: National Academy Press.
- Bocherens, H., Schrenk, F., Chaimanee, Y., Kullmer, O., Mörike, D., Pushkina, D., and Jaeger, J.-J. in press. Flexibility of diet and habitat in Pleistocene South Asian mammals: Implications for the fate of the giant fossil ape *Gigantopithecus*. Quaternary International.

- Bookstein, F.L. 1982. Foundations of morphometrics. In Johnston, R.F., Frank, P.W., and Michener, C.D. (eds.), Annual Review of Ecology and Systematics, pp. 451-470. Palo Alto: Annual Reviews.
- Brasseur, B., Sémah, F., Sémah, A.-M., and Djubiantono, T. 2015. Pedo-sedimentary dynamics of the Sangiran dome hominid bearing layers (Early to Middle Pleistocene, central Java, Indonesia): A palaeopedological approach for reconstructing ‘*Pithecanthropus*’ (Javanese *Homo erectus*) palaeoenvironment. Quaternary International 376: 84-100.
- Brown, C.L., and Gustafson, C.E. 2000. A Key to Postcranial Skeletal Remains of Cattle/Bison, Elk, and Horse. 1st edition. Pullman: Washington State University.
- Bulbeck, F. 2003. Hunter-gatherer occupation of the Malay Peninsula from the ice age to the iron age. In Mercader, J. (ed.), Under the Canopy: The Archaeology of Tropical Rain Forests, pp. 119-160. New Brunswick: Rutgers University Press.
- Bulbeck, F. 2014. The chronometric Holocene archaeological record of the southern Thai-Malay Peninsula. International Journal of Asia Pacific Studies 10: 111-162.
- Chaimanee, Y. 1998. Plio-Pleistocene rodents of Thailand. Thai Studies in Biodiversity 3: 1-303.
- Chaimanee, Y. 2013. VERTEBRATE RECORDS | Late Pleistocene of Southeast Asia. In Mock, C.J. (ed.), Encyclopedia of Quaternary Science, pp. 693-699. Amsterdam: Elsevier.
- Chaimanee, Y., and Jaeger, J.-J. 1993. Pleistocene mammals of Thailand and their use in the reconstruction of the palaeoenvironments of Southeast Asia. SPAFA Journal 3: 4-10.
- Chaimanee, Y., and Jaeger, J.-J. 2000. Evolution of *Rattus* (Mammalia, Rodentia) during the Plio-Pleistocene in Thailand. Historical Biology 15: 181-191.
- Chaimanee, Y., Suteethorn, V., Jintasakul, P., Vidthayanon, C., Marandat, B., and Jaeger, J.-J. 2004. A new orang-utan relative from the Late Miocene of Thailand. Nature 427: 439-441.
- Chaimanee, Y., Yamee, C., Tian, P., and Khaowiset, K. 2005. Fossils and Their Managements at Ban Khok Sung, Muang District, Nakhon Ratchasima Province, NE Thailand. Bangkok, Thailand: Department of Mineral Resources.
- Channell, J.E.T. 2006. Late Brunhes polarity excursions (Mono Lake, Laschamp, Iceland Basin and Pringle Falls) recorded at ODP Site 919 (Irringer Basin). Earth and Planetary Science Letters 244: 378-393.
- Charusiri, P., Daorerk, V., Krowchan, V., Klongsara, N., Kosuwan, S., Srirattanachatchawan, V., and Santatiwongchat, U. 2002. Quaternary tektites and their sediment hosts at Ban Thachang sand pit, Chaloeprakiat, Nakhon Ratchasima, NE Thailand: stratigraphy and its ages. in Proceedings of the Symposium on Geology of Thailand. pp. 1-9. Bangkok. Department of Mineral Resources.

- Chasen, F.W. 1940. A handlist of Malaysian mammals: a systematic list of the mammals of the Malay Peninsula, Sumatra, Borneo and Java, including adjacent small islands. Bulletin of the Raffles Museum 15: 1-209.
- Chen, D., and Qi, G. 1978. Fossil human and associated mammalian fauna from Xizhou, Yunnan. Vertebrata Palasiatica 16: 33-46.
- Chen, G.J., Wang, W., Mo, J.Y., Huang, Z.T., Tian, F., and Huang, W.W. 2002. Pleistocene vertebrate fauna from Wuyun Cave of Tiandong County, Guangxi. Vertebrata Palasiatica 40: 42-51.
- Chen, Q., and Li, Q. 1994. A brief report on Xianrendong cave site, Jilin province. Acta Anthropologica Sinica 13: 12-19.
- Chen, S.K., Pang, L.B., He, C.D., Wei, G.B., Huang, W.B., Yue, Z.Y., Zhang, H., and Qin, L. 2013. New discoveries from the classic Quaternary mammalian fossil area of Yanjinggou, Chingqing, and their chronological explanations. Chinese Science Bulletin 58: 3780-3787.
- Ciochon, R.L. 2009. The mystery ape of Pleistocene Asia. Nature 459: 910-911.
- Ciochon, R.L., Long, V.T., Larick, R., González, L., Grün, R., de Vos, J., Yonge, C., Taylor, L., Yoshida, H., and Reagan, M. 1996. Dated co-occurrence of *Homo erectus* and *Gigantopithecus* from Tham Khuyen Cave, Vietnam. Proceedings of the National Academy of Sciences 93: 3016-3020.
- Claude, J., Naksri, W., Boonchai, N., Buffetaut, E., Duangkrayom, J., Laojumpon, C., Jintasakul, P., Lauprasert, K., Martin, J., Suteethorn, V., and Tong, H. 2011. Neogene reptiles of northeastern Thailand and their paleogeographical significance. Annales de Paléontologie 97: 113-131.
- Colbert, E.H. 1938. Fossil mammals from Burma in the American Museum of Natural History. Bulletin of the American Museum of Natural History 74: 255-436.
- Colbert, E.H. 1942. Notes on the lesser one-horned rhinoceros, *Rhinoceros sondaicus*: 2. the position of the *Rhinoceros sondaicus* in the phylogeny of the genus *Rhinoceros*. American Museum Novitates 1207: 1-6.
- Colbert, E.H. 1943. Pleistocene vertebrates collected in Burma by the American Southeast Asiatic expedition. Transactions of the American Philosophical Society 32: 395-429.
- Colbert, E.H., and Hooijer, D.A. 1953. Pleistocene mammals from the limestone fissures of Szechwan, China. Bulletin of the American Museum of Natural History 102: 1-134.
- Cook, C.D.K. 1996. Aquatic and Wetland Plants of India. New York, USA: Oxford University Press.
- Corbet, A.S., and M., P.H. 1992. The Butterflies of the Malay Peninsula. 4th edition. Kuala Lumpur: Malay Nature Society.
- Corbet, G.B., and Hill, J.E. 1992. Mammals of the Indomalayan Region: a Systematic Review. Oxford: Oxford University Press.

- Cranbrook, E.O. 1988. Mammals: distribution and ecology. In Treherne, J.E. (ed.), Key Environments, pp. 146-166. Oxford: Malaysia Pergamon.
- Cranbrook, E.O. 2000. Northern Borneo environments of the past 40,000 years: archaeozoological evidence. The Sarawak Museum Journal 55: 61-109.
- Cranbrook, E.O., Carrant, A.P., and Davison, G.W. 2000. Quaternary mammal fossils from Borneo: *Stegodon* and *Hippopotamus*. The Sarawak Museum Journal 55: 215-233.
- Cranbrook, E.O., and Piper, P.J. 2007. The Javan rhinoceros *Rhinoceros sondaicus* in Borneo. The Raffles Bulletin of Zoology 55: 217-220.
- Croft, D.A. 2001. Cenozoic environmental change in South America as indicated by mammalian body size distributions (cenograms). Diversity and Distributions 7: 271-287.
- Cuong, N.L. 1971. After the excavations of Hang Hum, Tham Kuyen and Keo Leng caves. Archaeology (Hanoi) 11-12: 7-11.
- Cuong, N.L. 1985. Fossile Menschenfunde aus Nordvietnam. In Herrmann, J. and Ullrich, H. (eds.), Menschwerdung-Biotischer und Gesellschaftlicher Entwicklungsprozess, pp. 96-102. Berlin: Akademie Verlag.
- Damuth, J. 1990. Problems in estimating body masses of archaic ungulates using dental measurements. In Damuth, J. and MacFadden, B.J. (eds.), Body Size in Mammalian Paleobiology: Estimation and Biological Implications, pp. 229-253. Cambridge: Cambridge University Press.
- Davidson, G.W.H. 1994. Some remarks on vertebrate remains from the excavation of Gua Gunung Runtuh, Perak. In Zuraina, M. (ed.), The Excavation of Gua Gunung Runtuh, pp. 141-148. Department of Museums and Antiquity.
- de Terra, H. 1938. Preliminary Report on Recent Geological and Archaeological Discoveries Relating to Early Man in Southeast Asia. Proceedings of the National Academy of Sciences of the United States of America 24: 407-413.
- de Terra, H. 1943. Pleistocene geology and early man in Java. Transactions of the American Philosophical Society 32: 437-464.
- de Vos, J. 1983. The *Pongo* faunas from Java and Sumatra and their significance for biostratigraphical and paleoecological interpretations. Proceedings of the Koninklijke Nederlandse Akadademie van Wetenschappen, Serie B 86: 417-425.
- de Vos, J. 1984. Reconsideration of Pleistocene cave faunas from South China and their relation to the faunas from Java. Courier Forschungsinstitut Senckenberg 69: 259-266.
- de Vos, J. 1995. The migration of *Homo erectus* and *Homo sapiens* in South East Asia and the Indonesian Archipelago. In Bower, J.R.F. and Sartono, S. (eds.), Human Evolution on the

- Ecological Context: Evolution and Ecology of *Homo erectus*, pp. 239-260. Netherlands: *Pithecanthropus* Centennial Foundation, Leiden University.
- de Vos, J. 2007. VERTEBRATE RECORDS | Mid-Pleistocene of Southern Asia In Elias, S.A. (ed.), Encyclopedia of Quaternary Science, pp. 3232-3249. Oxford: Elsevier.
- de Vos, J., and Long, V.T. 1993. Systematic discussion of the Lang Trang fauna. Unpublished report.
- de Vos, J., and Long, V.T. 2001. First settlements: relations between continental and insular Southeast Asia. In Sémah, F., et al. (eds.), Origine des Peuplements et Chronologie des Cultures Paléolithiques dans le Sud-Est Asiatique Semenanjung-Artcom, pp. 225-249. Paris: Semenanjung.
- de Vos, J., Sondaar, P.Y., van den Bergh, G.D., and Aziz, F. 1994. The *Homo*-bearing deposits of Java and its ecological context. Courier Forschungs-Institut Senckenberg 171: 129-140.
- Delfino, M., and de Vos, J. 2010. A Revision of the Dubois Crocodylians, *Gavialis bengawanicus* and *Crocodylus ossifragus*, from the Pleistocene *Homo erectus* Beds of Java. Journal of Vertebrate Paleontology 30: 427-441.
- Delfino, M., Segid, A., Yosief, D., Shoshani, J., Rook, L., and Libsekal, Y. 2004. Fossil reptiles from the Pleistocene *Homo*-bearing locality of Buia (Eritrea, Northern Danakil Depression). Rivista Italiana di Paleontologia e Stratigrafia (Research In Paleontology and Stratigraphy) 110: 51-60.
- Demeter, F., Bacon, A.-M., and Sytha, P. 2013. État des connaissances actuelles sur le Cambodge. In Patole-Edoumba, E., Durringer, P., and Pottier, C. (eds.), Premiers Peuplements d'Asie du Sud-Est, pp. 1-74. Phnom Penh: UNESCO.
- Demeter, F., Bacon, A.-M., Thuy, N.T.K., Long, V.T., Durringer, P., Roussé, S., Coppens, Y., Matsumura, H., Dodo, Y., Huong, N.T.M., and Tomoko, A. 2005. Discovery of a second human molar and cranium fragment in the late Middle to Late Pleistocene cave of Ma U'Oi (Northern Vietnam). Journal of Human Evolution 48: 393-402.
- Demeter, F., Bacon, A.-M., Thuy, N.T.K., Long, V.T., Matsumura, H., Nga, H.H., Schuster, M., Huong, N.T.M., and Coppens, Y. 2004. An Archaic *Homo* Molar from Northern Vietnam. Current Anthropology 45: 535-541.
- Demeter, F., Shackelford, L., Westaway, K., Durringer, P., Bacon, A.-M., Ponche, J.-L., Wu, X., Sayavongkhamdy, T., Zhao, J.-X., Barnes, L., Boyon, M., Sichanthongtip, P., Sénégas, F., Karpoff, A.-M., Patole-Edoumba, E., Coppens, Y., and Braga, J. 2015. Early Modern Humans and Morphological Variation in Southeast Asia: Fossil Evidence from Tam Pa Ling, Laos. PLoS ONE 10: e0121193.

- Demeter, F., Shackelford, L.L., Bacon, A.-M., Durringer, P., Westaway, K., Sayavongkhamdy, T., Braga, J., Sichanthongtip, P., Khamdalavong, P., Ponche, J.-L., Wang, H., Lundstrom, C., Patole-Edoumba, E., and Karpoff, A.-M. 2012. Anatomically modern human in Southeast Asia (Laos) by 46 ka. Proceedings of the National Academy of Sciences 109: 14375-14380.
- DeNinno, L.H., Cronin, T.M., Rodriguez-Lazaro, J., and Brenner, A. 2015. An early to mid-Pleistocene deep Arctic Ocean ostracode fauna with North Atlantic affinities. Palaeogeography, Palaeoclimatology, Palaeoecology 419: 90-99.
- Department of Mineral Resources. 2007. Geological map of Nakhon Ratchasima Province. [Online]. Available from: <http://www.dmr.go.th>
- Dheeradolok, P., and Kaewyana, W. 1986. On the Quaternary Deposits of Thailand. Bulletin of the Geological Society of Malaysia 19: 515-532.
- Diedrich, C.G. 2011. Periodical use of the Balve Cave (NW Germany) as a Late Pleistocene *Crocota crocuta spelaea* (Goldfuss 1823) den: Hyena occupations and bone accumulations vs. human Middle Palaeolithic activity. Quaternary International 233: 171-184.
- Dong, W., Liu, J.-y., Zhang, L.-m., and Xu, Q.-q. 2014. The Early Pleistocene water buffalo associated with *Gigantopithecus* from Chongzuo in southern China. Quaternary International 354: 86-93.
- Duangkrayom, J., Ratanasthien, B., Jintasakul, P., and Carling, P.A. 2014. Sedimentary facies and paleoenvironment of a Pleistocene fossil site in Nakhon Ratchasima province, northeastern Thailand. Quaternary International 325: 220-238.
- Dubois, E. 1894. *Pithecanthropus erectus*: Eine Menschenähnliche Übergangsform aus Java. Batavia: Landesdruckerei.
- Duckworth, J.W., Kumar, N.S., Anwarul Islam, M., Hem Sagar Baral, and Timmins, R.J. 2008a. *Axis axis*. [Online]. Version 2015.2. Available from: www.iucnredlist.org
- Duckworth, J.W., Steinmetz, R., Timmins, R.J., Pattanavibool, A., Than Zaw, Do Tuoc, and Hedges, S. 2008b. *Bos gaurus*. [Online]. Version 2015.2. Available from: www.iucnredlist.org
- Duller, G.A.T. 2004. Luminescence dating of quaternary sediments: recent advances. Journal of Quaternary Science 19: 183-192.
- Ehrenberg, K., Sickenberg, O., and Stiff-Gottlieb, A. 1938. Die Fuchs-oder Teufelslucken bei Eggenburg, Niederdonau. Wien: Verlag der Zoologisch-Botanischen Gesellschaft.
- Esposito, M., Chaimanee, Y., Jaeger, J.-J., and Reyss, J.-L. 1998. Datation des concrétions carbonatées de la « Grotte du Serpent » (Thaïlande) par la méthode Th/U. Comptes Rendus de l'Académie des Sciences, Series IIA: Earth and Planetary Science 326: 603-608.
- Esposito, M., Reyss, J.-L., Chaimanee, Y., and Jaeger, J.-J. 2002. U-series Dating of Fossil Teeth and Carbonates from Snake Cave, Thailand. Journal of Archaeological Science 29: 341-349.

- Fabre, A.C., Cornette, R., Slater, G., Argot, C., Peigné, S., Goswami, A., and Pouydebat, E. 2013. Getting a grip on the evolution of grasping in musteloid carnivorans: a three-dimensional analysis of forelimb shape. Journal of Evolutionary Biology 26: 1521-1535.
- Ferreira, F., Frontalini, F., Leão, C.J., and Leipnitz, I.I. 2014. Changes in the water column structure and paleoproductivity in the western South Atlantic Ocean since the middle Pleistocene: Evidence from benthic and planktonic foraminifera. Quaternary International 352: 111-123.
- Filoux, A., Wattanapitaksakul, A., Lespes, C., and Thongcharoenchaikit, C. 2015. A Pleistocene mammal assemblage containing *Ailuropoda* and *Pongo* from Tham Prakai Phet cave, Chaiyaphum Province, Thailand. Geobios 48: 341-349.
- France, D. 2009. Human and Nonhuman Bone Identification: A Color Atlas. Boca Raton: CRC Press.
- Francis, C.M. 2001. A Photographic Guide to Mammals of South-East Asia. London: New Holland.
- Francis, C.M. 2008. A Field Guide to the Mammals of Thailand and South-East Asia. Bangkok: Asia Books.
- Fromaget, J. 1936. Sur la stratigraphie des formations récentes de la Chaîne annamitique septentrionale et sur l'existence de l'Homme dans le Quaternaire inférieur de cette partie de l'Indochine. Comptes Rendus de l'Académie des Sciences. Series IIA: Earth and Planetary Science 203: 738-741.
- Gaboardi, M., Deng, T., and Wang, Y. 2005. Middle Pleistocene climate and habitat change at Zhoukoudian, China, from the carbon and oxygen isotopic record from herbivore tooth enamel. Quaternary Research 63: 329-338.
- Galbreath, G.J., Mordacq, J.C., and Weiler, F.H. 2006. Genetically solving a zoological mystery: was the kouprey (*Bos sauveli*) a feral hybrid? Journal of Zoology 270: 561-564.
- Gatinsky, Y.G., and Hutchison, C.S. 1987. Cathaysia, Gondwanaland and the Palaeotethys in the evolution of continental Southeast Asia. Geological Society of Malaysia Bulletin 20: 179-199.
- Gentner, W., Storzer, D., and Wagner, G.A. 1969. New fission track ages of tektites and related glasses. Geochimica et Cosmochimica Acta 33: 1075-1081.
- Gentry, A., Clutton-Brock, J., and Groves, C.P. 2004. The naming of wild animal species and their domestic derivatives. Journal of Archaeological Science 31: 645-651.
- Gentry, A.W., Rössner, G.E., and Heizmann, E.P.J. 1999. Suborder Ruminantia. In Rössner, G.E. and Heissig, K. (eds.), The Miocene Land Mammals of Europe, pp. 225-258. München Verlag Dr. Friedrich Pfeil.
- Ginsburg, L., Ingavat, R., and Sen, S. 1982. A Middle Pleistocene (Loangian) cave fauna in northern Thailand. Comptes Rendus de l'Académie des Sciences. Série III 294: 295-297.

- Glaubrecht, M., and Köhler, F. 2004. Radiating in a river: systematics, molecular genetics and morphological differentiation of viviparous freshwater gastropods endemic to the Kaek River, central Thailand (Cerithioidea, Pachychilidae). Biological Journal of the Linnean Society 82: 275-311.
- Gorog, A.J., Sinaga, M.H., and Engstrom, M.D. 2004. Vicariance or dispersal? Historical biogeography of three Sunda shelf murine rodents (*Maxomys surifer*, *Leopoldamys sabanus* and *Maxomys whiteheadi*). Biological Journal of the Linnean Society 81: 91-109.
- Granger, W. 1938. Medicine bones. Natural History 42: 264-271.
- Gray, D., Piprell, C., and Graham, M. 1994. National Parks of Thailand. Bangkok: Thai Wattana Panish.
- Grossman, A., Liutkus-Pierce, C., Kyongo, B., and M'Kirera, F. 2014. New Fauna from Loperot Contributes to the Understanding of Early Miocene Catarrhine Communities. International Journal of Primatology 35: 1253-1274.
- Grote, P. 2007. Studies of fruits and seeds from the Pleistocene of northeastern Thailand. Courier Forschungsinstitut Senckenberg 258: 171-181.
- Groves, C.P. 1967. On the rhinoceroses of south-east Asia. Säugetierkundliche Mitteilungen 15: 221-237.
- Groves, C.P. 1981. Ancestors for the Pigs: Taxonomy and Phylogeny of the Genus *Sus*. Canberra: Department of Prehistory, Research School of Pacific Studies, Australian National University.
- Groves, C.P. 1985. Plio-Pleistocene mammals in Island Southeast Asia. Modern Quaternary Research SE Asia 9: 43-54.
- Groves, C.P. 1997. Taxonomy of wild pigs (*Sus*) of the Philippines. Zoological Journal of the Linnean Society 120: 163-191.
- Groves, C.P., and Grubb, P. 2011. Ungulate Taxonomy. Baltimore, Maryland: Johns Hopkins University Press.
- Groves, C.P., and Leslie Jr, D.M. 2011. *Rhinoceros sondaicus* (Perissodactyla: Rhinocerotidae). Mammalian Species 43: 190-208.
- Grubb, P. 2005. Artiodactyla. In Wilson, D.E. and Reeder, D.M. (eds.), Mammal Species of the World: A Taxonomic and Geographic Reference, pp. 637-722. Baltimore: Johns Hopkins University Press.
- Grün, R. 1989. Electron spin resonance (ESR) dating. Quaternary International 1: 65-109.
- Grün, R. 2000. An alternative for model for open system U-series/ESR age calculations: (closed system U-series)-ESR, CSUS-ESR. Ancient TL 18: 1-4.

- Grün, R. 2002. ESR dose estimation on fossil tooth enamel by fitting the natural spectrum into the irradiated spectra. Radiation Measurements 35: 87-93.
- Grün, R. 2009. The DATA program for the calculation of ESR age estimates on tooth enamel. Quaternary Geochronology 4: 231-232.
- Grün, R., and Schwarcz, H.P. 2000. Revised open system U-series/ESR age calculations for teeth from Stratum C at the Hoxnian Interglacial type locality, England. Quaternary Science Reviews 19: 1151-1154.
- Grün, R., Schwarcz, H.P., and Chadam, J. 1988. ESR dating of tooth enamel: Coupled correction for U-uptake and U-series disequilibrium. International Journal of Radiation Applications and Instrumentation. Part D. Nuclear Tracks and Radiation Measurements 14: 237-241.
- Grün, R., Stringer, C., McDermott, F., Nathan, R., Porat, N., Robertson, S., Taylor, L., Mortimer, G., Eggins, S., and McCulloch, M. 2005. U-series and ESR analyses of bones and teeth relating to the human burials from Skhul. Journal of Human Evolution 49: 316-334.
- Gruwier, B., de Vos, J., and Kovarovic, K. 2015. Exploration of the taxonomy of some Pleistocene Cervini (Mammalia, Artiodactyla, Cervidae) from Java and Sumatra (Indonesia): a geometric- and linear morphometric approach. Quaternary Science Reviews 119: 35-53.
- Grzimek, B. 1975. Grzimek's Animal Life Encyclopedia: Mammals II. Germany: Van Nostrand Reinhold Company.
- Guérin, C. 1980. Les Rhinocéros (Mammalia, Perissodactyla) du Miocène Terminal au Pléistocène Supérieur en Europe Occidentale. Lyon, France: Laboratoires de Géologie de Lyon.
- Gunz, P., and Harvati, K. 2007. The Neanderthal "chignon": Variation, integration, and homology. Journal of Human Evolution 52: 262-274.
- Haines, P.W., Howard, K.T., Ali, J.R., Burrett, C.F., and Bunopas, S. 2004. Flood deposits penecontemporaneous with ~0.8 Ma tektite fall in NE Thailand: impact-induced environmental effects? Earth and Planetary Science Letters 225: 19-28.
- Hall, R., and Holloway, J.D. 1998. Biogeography and Geological Evolution of Southeast Asia. Leiden: Backhuys.
- Hammer, Ø., Harper, D.A.T., and Ryan, P.D. 2001. PAST: Paleontological statistics software package for education and data analysis. Palaeontologia Electronica 4, 1-9.
- Han, D., and Xu, C. 1985. Pleistocene mammalian faunas of China. In Wu, R. and Olsen, J. (eds.), Palaeoanthropology and Palaeolithic Archaeology in the People's Republic of China, pp. 267-289. Orlando: Academic Press.
- Hardjasmita, H.S. 1987. Taxonomy and phylogeny of the Suidae (Mammalia) in Indonesia. Scripta geologica 85: 1-68.

- Harrison, S.P., and Prentice, C.I. 2003. Climate and CO₂ controls on global vegetation distribution at the last glacial maximum: analysis based on palaeovegetation data, biome modelling and palaeoclimate simulations. Global Change Biology 9: 983-1004.
- Harrison, T. 1996. The palaeoecological context at Niah Cave, Sarawak: evidence from the primate fauna. Indo-Pacific Prehistory Association Bulletin 14: 90-100.
- Harrison, T., Jin, C., Zhang, Y., Wang, Y., and Zhu, M. 2014. Fossil *Pongo* from the Early Pleistocene *Gigantopithecus* fauna of Chongzuo, Guangxi, southern China. Quaternary International 354: 59-67.
- Hassanin, A., and Ropiquet, A. 2004. Molecular phylogeny of the tribe Bovini (Bovidae, Bovinae) and the taxonomic status of the Kouprey, *Bos sauveli* Urbain 1937. Molecular Phylogenetics and Evolution 33: 896-907.
- Hassanin, A., and Ropiquet, A. 2007. What is the taxonomic status of the Cambodian banteng and does it have close genetic links with the kouprey? Journal of Zoology 271: 246-252.
- Hassanin, A., Ropiquet, A., Cornette, R., Tranier, M., Pfeffer, P., Candegabe, P., and Lemaire, M. 2006. Has the kouprey (*Bos sauveli* Urbain, 1937) been domesticated in Cambodia? Comptes Rendus Biologies 329: 124-135.
- Head, J.J. 2005. Snakes of the Siwalik Group (Miocene of Pakistan): systematics and relationship to environmental change. Palaeontologia Electronica. 8, 1-33.
- Heaney, L.R. 1985. Zoogeographic evidence for middle and late Pleistocene land bridges to the Philippine Islands. Modern Quaternary Research in Southeast Asia 9: 127-144.
- Heaney, L.R. 1991. A synopsis of climatic and vegetational change in Southeast Asia. Climatic Change 19: 53-61.
- Hedges, S., Sagar Baral, H., Timmins, R.J., and Duckworth, J.W. 2008. *Bubalus arnee*. [Online]. Version 2015.2. Available from: www.iucnredlist.org
- Heintz, E. 1970. Les Cervidés villafranchiens de France et d'Espagne. Muséum. Paris.
- Hercman, H. 2014. U-series dating of collagen – A step toward direct U-series dating of fossil bone? Quaternary International 339–340: 4-10.
- Hillson, S. 2005. Teeth. 2nd edition. Cambridge: Cambridge University Press.
- Ho, C.K., Qi, G.Q., and Chang, C.H. 1997. A preliminary study of late Pleistocene carnivore fossils from the Penghu Channel, Taiwan. Annual of Taiwan Museum 40: 195-224.
- Hocknull, S.A., Piper, P.J., van den Bergh, G.D., Due, R.A., Morwood, M.J., and Kurniawan, I. 2009. Dragon's Paradise Lost: Palaeobiogeography, Evolution and Extinction of the Largest-Ever Terrestrial Lizards (Varanidae). PLoS ONE 4: e7241.
- Hoffstetter, R. 1964. Les serpents du Néogène du Pakistan (couches des Siwaliks). Bulletin de la Société Géologique de France, Série 7 6: 467-474.

- Hooijer, D.A. 1946. Prehistoric and fossil rhinoceros from the Malay Archipelago and India. Zoologische Mededeelingen 26: 1-138.
- Hooijer, D.A. 1950. The fossil Hippopotamidae of Asia, with notes on the recent species. Zoologische Verhandelingen 8: 1-123.
- Hooijer, D.A. 1958. Fossil Bovidae from the Malay Archipelago and the Punjab. Zoologische Verhandelingen 38: 1-112.
- Hooijer, D.A. 1962. Report upon a collection of Pleistocene mammals from Tin-bearing deposits in a limestone cave near Ipoh, Kinta Valley, Perak. Federation Museum Journal 7: 1-5.
- Hooijer, D.A. 1964. New records of mammals from the Middle Pleistocene of Sangiran, Central Java. Zoologische Mededeelingen 40: 73-87.
- Hu, C.K., and Qi, T. 1978. Gongwangling Pleistocene mammalian fauna of Lantian, Shaanxi. Palaeontologica Sinica 155: 1-64.
- Hughes, J.B., Round, P.D., and Woodruff, D.S. 2003. The Indochinese–Sundaic faunal transition at the Isthmus of Kra: an analysis of resident forest bird species distributions. Journal of Biogeography 30: 569-580.
- Hutchison, C.S. 1989. Geological Evolution of South-East Asia. Oxford: Clarendon Press.
- Hutchison, C.S. 2005. The geological framework. In Gupta, A. (ed.), The Physical Geography of Southeast Asia, pp. 3-23. Oxford: Oxford University Press.
- Huybers, P. 2007. Glacial variability over the last two million years: an extended depth-derived agetmodel, continuous obliquity pacing, and the Pleistocene progression. Quaternary Science Reviews 26: 37-55.
- Ibrahim, Y.K., Tshen, L.T., Westaway, K.E., Cranbrook, E.o., Humphrey, L., Muhammad, R.F., Zhao, J.-x., and Peng, L.C. 2013. First discovery of Pleistocene orangutan (*Pongo* sp.) fossils in Peninsular Malaysia: Biogeographic and paleoenvironmental implications. Journal of Human Evolution 65: 770-797.
- Indriati, E., Swisher, C.C., III, Lepre, C., Quinn, R.L., Suriyanto, R.A., Hascaryo, A.T., Grün, R., Feibel, C.S., Pobiner, B.L., Aubert, M., Lees, W., and Antón, S.C. 2011. The Age of the 20 Meter Solo River Terrace, Java, Indonesia and the Survival of *Homo erectus* in Asia. PLoS ONE 6: e21562.
- Inger, R.F. 1999. Distribution of amphibians in Southern Asia and adjacent islands. In Duellman, W.E. (ed.), Patterns of Distribution of Amphibians, pp. 445-482. Baltimore: Johns Hopkins University Press.
- IUCN. 2015. The IUCN Red List of Threatened Species. [Online]. Version 2015.1. Available from: www.iucnredlist.org
- Jackson, J.E. 1991. A User's Guide to Principal Components. New York: John Wiley and Sons.

- Jahn, B., Donner, B., Müller, P.J., Röhl, U., Schneider, R.R., and Wefer, G. 2003. Pleistocene variations in dust input and marine productivity in the northern Benguela Current: Evidence of evolution of global glacial–interglacial cycles. Palaeogeography, Palaeoclimatology, Palaeoecology 193: 515-533.
- Janis, C.M. 1990. Correlation of cranial and dental variables with body size in ungulates and macropodoids. In Damuth, J. and MacFadden, B.J. (eds.), Body Size in Mammalian Paleobiology: Estimation and Biological Implications, pp. 255-299. Cambridge: Cambridge University Press.
- Janssen, R., Joordens, J.C.A., Koutamanis, D.S., Puspaningrum, M.R., de Vos, J., van der Lubbe, J.H.J.L., Reijmer, J.J.G., Hampe, O., and Vonhof, H.B. 2016. Tooth enamel stable isotopes of Holocene and Pleistocene fossil fauna reveal glacial and interglacial paleoenvironments of hominins in Indonesia. Quaternary Science Reviews 144: 145-154.
- Joordens, J.C.A., d'Errico, F., Wesselingh, F.P., Munro, S., de Vos, J., Wallinga, J., Ankjaergaard, C., Reimann, T., Wijbrans, J.R., Kuiper, K.F., Mucher, H.J., Coqueugnot, H., Prie, V., Joosten, I., van Os, B., Schulp, A.S., Panuel, M., van der Haas, V., Lustenhouwer, W., Reijmer, J.J.G., and Roebroeks, W. 2015. *Homo erectus* at Trinil on Java used shells for tool production and engraving. Nature 518: 228-231.
- Kahlke, H.D. 1961. On the complex of the Stegodon-Ailuropoda fauna of Southern China and the chronological position of *Gigantopithecus blacki* V. Koenigswald. Vertebrata Palasiatica 6: 83-108.
- Kamaludin, b.H., Nakamura, T., Price, D.M., Woodroffe, C.D., and Fujii, S. 1993. Radiocarbon and thermoluminescence dating of the Old Alluvium from a coastal site in Perak, Malaysia. Sedimentary Geology 83: 199-210.
- Kamaludin, H., and Azmi, H.Y. 1997. Interstadial records of the last glacial period at Pantai Remis, Malaysia. Journal of Quaternary Science 12: 419-434.
- Kha, L.T. 1976. First remarks on the Quaternary fossil fauna of northern Vietnam. Vietnamese Studies 46: 107-126.
- Kha, L.T., and Bao, T.V. 1967. Forschungsbericht über die Fossile Fauna des Späten Oberen Pleistozän au Keo Leng (Lang Son). Hanoi: Archäologischen Instituts Vietnams
- Kirschvink, J.L. 1980. The least-square line and plane and the analysis of palaeomagnetic data. Geophysical Journal of the Royal Astronomical Society 62: 699-718.
- Klingenberg, C.P. 2011. MorphoJ: an integrated software package for geometric morphometrics. Molecular Ecology Resources 11: 353-357.
- Kurtén, B. 1956. The status and affinities of *Hyaena sinensis* Owen and *Hyaena ultima* Matsumoto. American Museum Novitates 1764: 1-48.

- Laurie, W.A., Lang, E.M., and Grove, C.P. 1983. *Rhinoceros unicornis*. Mammalian Species 211: 1-6.
- Lee-Thorp, J.A., Sponheimer, M., and Luyt, J. 2007. Tracking changing environments using stable carbon isotopes in fossil tooth enamel: an example from the South African hominin sites. Journal of Human Evolution 53: 595-601.
- Lee, M.S.Y. 2005. Squamate phylogeny, taxon sampling, and data congruence. Organisms Diversity & Evolution 5: 25-45.
- Legendre, S. 1986. Analysis of mammalian communities from the late Eocene and Oligocene of southern France. Palaeovertebrata 16: 191-212.
- Legendre, S. 1989. Les communautés de mammifères du Paléogène (Eocène et Oligocène) d'Europe occidentale: structures, milieu et évolution. Münchner Geowissenschaftliche Abhandlungen 16: 1-110.
- Lekagul, B., and McNeely, J.A. 1988. Mammals of Thailand. Association for the Conservation of Wildlife. Bangkok: Darnsutha Press.
- Lekagul, B., and Round, P.D. 1991. A Guide to the Birds of Thailand. 1st. Bangkok: Saha Karn Bhaet Co.
- Leslie, D.M. 2011. *Rusa unicolor* (Artiodactyla: Cervidae). Mammalian Species 1-30.
- Lézine, A.-M., Duplessy, J.-C., and Cazet, J.-P. 2005. West African monsoon variability during the last deglaciation and the Holocene: Evidence from fresh water algae, pollen and isotope data from core KW31, Gulf of Guinea. Palaeogeography, Palaeoclimatology, Palaeoecology 219: 225-237.
- Li, Y., and Wen, B. 1986. Guanyindong: A Lower Paleolithic Site at Qianxi County, Guizhou Province. Beijing: Cultural Relics Publishing House.
- Licht, A., van Cappelle, M., Abels, H.A., Ladant, J.B., Trabucho-Alexandre, J., France-Lanord, C., Donnadiou, Y., Vandenberghe, J., Rigaudier, T., Lecuyer, C., Terry Jr, D., Adriaens, R., Boura, A., Guo, Z., Soe, A.N., Quade, J., Dupont-Nivet, G., and Jaeger, J.J. 2014. Asian monsoons in a late Eocene greenhouse world. Nature 513: 501-506.
- Löffler, E., Thompson, W.P., and Liengsakul, M. 1983. Geomorphological Development of the Thung Kula Ronghai. in Proceedings of the 1st Symposium on Geomorphology and Quaternary Geology of Thailand. pp. 123-130.
- Löffler, E., Thompson, W.P., and Liengsakul, M. 1984. Quaternary geomorphological development of the lower Mun River Basin, North East Thailand. CATENA 11: 321-330.
- Long, V.T., de Vos, J., and Ciochon, R.S. 1996. The fossil mammal fauna of the Lang Trang caves, Vietnam, compared with Southeast Asian fossil and recent mammal faunas: the geographical implications. Bulletin of the Indo-Pacific Prehistory Association 14: 101-109.

- Long, V.T., and Du, H.V. 1981. Zoological species belonging to the Pleistocene and the geochronology of sediments containing them in caves and grottos in Northern Viet Nam. Khao Co Hoc 1: 16-19.
- Louys, J., Curnoe, D., and Tong, H. 2007. Characteristics of Pleistocene megafauna extinctions in Southeast Asia. Palaeogeography, Palaeoclimatology, Palaeoecology 243: 152-173.
- Louys, J., and Meijaard, E. 2010. Palaeoecology of Southeast Asian megafauna-bearing sites from the Pleistocene and a review of environmental changes in the region. Journal of Biogeography 37: 1432-1449.
- Lund, S.P., Williams, T., Acton, G., Clement, B., and Okada, M. 2001. Brunhes Chron magnetic field excursions recovered from Leg 172 sediments. in Proceedings of the Ocean Drilling Program-Scientific Results. pp. 1-18.
- Lydekker, R. 1880. Indian Tertiary and Post-Tertiary Vertebrata-Sivaliks and Narbada Proboscidea. Palaeontologia Indica, Series 10 1: 182-294.
- Ma, A., and Tang, H. 1992. On discovery and significance of a Holocene *Ailuropoda-Stegodon* fauna from Jinhua, Zhejiang. Vertebrata Palasiatica 30: 295-312.
- Maglio, V.J. 1973. Origin and evolution of the Elephantidae. Transactions of the American Philosophical Society, New Series 63: 1-149.
- Martin, J.E., Buffetaut, E., Naksri, W., Lauprasert, K., and Claude, J. 2012. *Gavialis* from the Pleistocene of Thailand and Its Relevance for Drainage Connections from India to Java. PLoS ONE 7: e44541.
- Martin, R. 1988. Anthropologie. In Knußmann, R. (ed.), Handbuch der Vergleichenden Biologie des Menschen, pp. 444-480. Stuttgart: Gustav Fischer.
- Marwick, B., Shoocongdej, R., Thongcharoenchaikit, C., Chaisuwan, B., Khawkhiew, C., and Kwak, S. 2013. Hierarchies of engagement and understanding: Community engagement during archaeological excavations at Khao Toh Chong rockshelter, Krabi, Thailand. In O'Connor, S. (ed.), Transcending the Culture-Nature Divide in Cultural Heritage: Views from the Asia-Pacific Region, pp. 129-140. Canberra: ANU E Press.
- Matthew, W., and Granger, W. 1923. New fossil mammals from the Pliocene of Szechuan, China. Bulletin, American Museum of Natural History 48: 563-598.
- Medway, L. 1960. The Malay Tapir in late Quaternary Borneo. The Sarawak Museum Journal 9: 356-360.
- Medway, L. 1972. The Quaternary era in Malesia. In S., A.P. and M., A. (eds.), Miscellaneous Series, Aberdeen, Scotland, pp. 63-83. Hull: University of Hull.
- Medway, L. 1983. The Wild Mammals of Malaya (Peninsular Malaysia and Singapore). Kuala Lumpur: Oxford University Press.

- Meijaard, E. 2003. Mammals of South-East Asian Islands and Their Late Pleistocene Environments. Journal of Biogeography 30: 1245-1257.
- Meijaard, E., and Groves, C.P. 2004. Morphometrical relationships between South-east Asian deer (Cervidae, tribe Cervini): evolutionary and biogeographic implications. Journal of Zoology 263: 179-196.
- Meijaard, E., and Groves, C.P. 2006. The Geography of Mammals and Rivers in Mainland Southeast Asia. In Primate Biogeography: Progress and Prospects, pp. 305-329. Boston, MA: Springer US.
- Mitteroecker, P., and Gunz, P. 2009. Advances in Geometric Morphometrics. Evolutionary Biology 36: 235-247.
- Moigne, A.-M., Awe, R.D., Sémah, F., and Sémah, A.M. 2004. The cervids from the Ngebung site ('Kabuh' series, Sangiran Dome, Central Java) and their biostratigraphical significance. In Keates, S.G. and Pasveer, J.M. (eds.), Quaternary Research in Indonesia, pp. 45-62. Leiden: Balkema.
- Molengraaff, G.A.F. 1922. De Geologie der Zeeën Van de Nederlandsch Oost-Indie Archipel. Amsterdam: Nederlandsch Aardrijkskundig Genootschap.
- Montuire, S., and Marcolini, F. 2002. Palaeoenvironmental significance of the mammalian faunas of Italy since the Pliocene. Journal of Quaternary Science 17: 87-96.
- Morley, R.J. 1982. A Palaeoecological Interpretation of a 10,000 Year Pollen Record from Danau Padang, Central Sumatra, Indonesia. Journal of Biogeography 9: 151-190.
- Morley, R.J. 1998. Palynological evidence for Tertiary plant dispersals in the SE Asian region in relation to plate tectonics and climate. In Hall, R. and Holloway, J.D. (eds.), Biogeography and Geological Evolution of Southeast Asia, pp. 211-234. Leiden: Backhuys.
- Morley, R.J. 2000. Origin and evolution of tropical rain forests. Chichester: John Wiley and Sons.
- Morley, R.J. 2007. Cretaceous and Tertiary climate change and the past distribution of megathermal rainforests. In Bush, M.B., Flenley, J.R., and Gosling, W.D. (eds.), Tropical Rainforest Responses to Climatic Change, pp. 1-31. Berlin: Springer Berlin Heidelberg.
- Morley, R.J. 2012. A review of the Cenozoic palaeoclimate history of Southeast Asia. In Gower, D., et al. (eds.), Biotic Evolution and Environmental Change in Southeast Asia, pp. 79-114. Cambridge: Cambridge University Press.
- Morley, R.J., and Flenley, J.R. 1987. Late Cainozoic vegetational and environmental changes in the Malay archipelago. In Whitmore, T.C. (ed.), Biogeographical Evolution of the Malay Archipelago, pp. 50-59. Oxford: Clarendon Press.

- Murray-Wallace, C.V., Jones, B.G., Nghi, T., Price, D.M., Van Vinh, V., Nguyen Tinh, T., and Nanson, G.C. 2002. Thermoluminescence ages for a reworked coastal barrier, southeastern Vietnam: a preliminary report. Journal of Asian Earth Sciences 20: 535-548.
- Musser, G.G., and Newcomb, C. 1983. Malaysian murids and the giant rat of Sumatra. Bulletin of the American Museum of Natural History 174: 329-598.
- Nowak, R.M. 1999. Walker's Mammals of the World. 6th edition. London: John Hopkins University Press.
- Olley, J.M., Caitcheon, G.G., and Murray, A. 1998. The distribution of apparent dose as determined by Optically Stimulated Luminescence in small aliquots of fluvial quartz: Implications for dating young sediments. Quaternary Science Reviews 17: 1033-1040.
- Olley, J.M., Caitcheon, G.G., and Roberts, R.G. 1999. The origin of dose distributions in fluvial sediments, and the prospect of dating single grains from fluvial deposits using optically stimulated luminescence. Radiation Measurements 30: 207-217.
- Olsen, J.W., and Ciochon, R.L. 1990. A review of evidence for postulated Middle Pleistocene occupations in Viet Nam. Journal of Human Evolution 19: 761-788.
- Osborn, H.F. 1942. Stegodontoidea and Elephantoidea. New York: American Museum of Natural History.
- Palombo, M.R., and Villa, P. 2001. Schreger lines as support in the Elephantinae identification. In Cavaretta, G., et al. (eds.), The World of Elephants, pp. 656-660. Roma: Consiglio Nazionale Ricerche.
- Passey, B.H., Ayliffe, L.K., Kaakinen, A., Zhang, Z., Eronen, J.T., Zhu, Y., Zhou, L., Cerling, T.E., and Fortelius, M. 2009. Strengthened East Asian summer monsoons during a period of high-latitude warmth? Isotopic evidence from Mio-Pliocene fossil mammals and soil carbonates from northern China. Earth and Planetary Science Letters 277: 443-452.
- Patte, E. 1928. Comparaison des faunes de mammifères de Langson (Tonkin) et du SE Tchouen. Bulletin de la Société Géologique Française 28: 55-63.
- Pei, W.C. 1935. Fossil mammals from the Kwangsi caves. Bulletin of the Geological Society of China 14: 413-425.
- Pei, W.C. 1940. The Upper Cave fauna of Choukoutien. Palaeontologia Sinica New Series C 10: 1-100.
- Pei, W.C. 1957. The zoogeographical divisions of Quaternary mammalian faunas in China. Vertebrata Palasiatica 1: 9-24.
- Peng, S., Ge, J., Li, C., Liu, Z., Qi, L., Tan, Y., Cheng, Y., Deng, C., and Qiao, Y. 2015. Pronounced changes in atmospheric circulation and dust source area during the mid-Pleistocene as

- indicated by the Caotan loess-soil sequence in North China. Quaternary International 372: 97-107.
- Penny, D. 2001. A 40,000 year palynological record from north-east Thailand; implications for biogeography and palaeo-environmental reconstruction. Palaeogeography, Palaeoclimatology, Palaeoecology 171: 97-128.
- Pike, A.W.G., and Hedges, R.E.M. 2001. Sample geometry and U uptake in archaeological teeth: implications for U-series and ESR dating. Quaternary Science Reviews 20: 1021-1025.
- Pionnier-Capitan, M., Bemilli, C., Bodu, P., Célérier, G., Ferrié, J.-G., Fosse, P., Garcià, M., and Vigne, J.-D. 2011. New evidence for Upper Palaeolithic small domestic dogs in South-Western Europe. Journal of Archaeological Science 38: 2123-2140.
- Pitra, C., Fickel, J., Meijaard, E., and Groves, C. 2004. Evolution and phylogeny of old world deer. Molecular Phylogenetics and Evolution 33: 880-895.
- Pocock, R.I. 1945. Some Cranial and Dental Characters of the existing species of Asiatic Rhinoceroses. Proceedings of the Zoological Society of London 114: 437-450.
- Pope, G.G., Frayer, D.W., Liangchareon, M., Kulasing, P., and Nakabanlang, S. 1981. Palaeoanthropological investigations of the Thai-American expeditions in Northern Thailand (1978-1980): an interim report. Asian Perspectives 21: 147-163.
- Pramankij, S., and Subhavan, V. 2001a. Preliminary report on the discovery of evidence of the oldest hominids (2 million to 200000 years old) in Thailand. Silpa Wattanatham 23: 38-47.
- Pramankij, S., and Subhavan, V. 2001b. Report on Fossils from Hat Pu Dai, Northern Thailand. Unpublished report.
- Prentice, M.L., and Denton, G.H. 1988. The deep-sea oxygen isotope record, the global ice sheet system, and hominid evolution. In Grine, F.E. (ed.), The Evolutionary History of the Robust Australopithecines, pp. 383-403. New York: Aldine de Gruyter.
- Pushkina, D., Bocherens, H., Chaimanee, Y., and Jaeger, J.-J. 2010. Stable carbon isotope reconstructions of diet and paleoenvironment from the late Middle Pleistocene Snake Cave in Northeastern Thailand. Naturwissenschaften 97: 299-309.
- Raes, N., Cannon, C.H., Hijmans, R.J., Piessens, T., Saw, L.G., van Welzen, P.C., and Slik, J.W.F. 2014. Historical distribution of Sundaland's Dipterocarp rainforests at Quaternary glacial maxima. Proceedings of the National Academy of Sciences 111: 16790-16795.
- Rage, J.-C. 2001. Fossil snakes from the Paleocene of São José de Itaboraí, Brazil. Part II. Boidae. Palaeovertebrata 30: 111-150.
- Rink, W.J. 1997. Electron spin resonance (ESR) dating and ESR applications in quaternary science and archaeometry. Radiation Measurements 27: 975-1025.

- Rink, W.J., Wei, W., Bekken, D., and Jones, H.L. 2008. Geochronology of *Ailuropoda*–*Stegodon* fauna and *Gigantopithecus* in Guangxi Province, southern China. Quaternary Research 69: 377-387.
- Ripoll, M.P., Morales Pérez, J.V., Sanchis Serra, A., Aura Tortosa, J.E., and Montañana, I.S. 2010. Presence of the genus *Cuon* in upper Pleistocene and initial Holocene sites of the Iberian Peninsula: new remains identified in archaeological contexts of the Mediterranean region. Journal of Archaeological Science 37: 437-450.
- Rohland, N., Pollack, J.L., Nagel, D., Beauval, C., Airvaux, J., Pääbo, S., and Hofreiter, M. 2005. The Population History of Extant and Extinct Hyenas. Molecular Biology and Evolution 22: 2435-2443.
- Romer, A.S. 1956. Osteology of the Reptiles. Chicago: University of Chicago Press.
- Rookmaker, L.C. 1980. The distribution of the rhinoceroes in eastern India, Bangladesh, China, and the Indo-Chinese region. Zoologischer Anzeiger 205: 253-268.
- Roth, V.L. 1990. Insular dwarf elephants: a case study in body mass estimation and ecological inference. In Damuth, J. and MacFadden, B.J. (eds.), Body Size in Mammalian Paleobiology: Estimation and Biological Implications, pp. 151-179. Cambridge: Cambridge University Press.
- Round, P.D., Hughes, J.B., and Woodruff, D.S. 2003. Latitudinal range limits of resident forest birds in Thailand and the Indochinese–Sundaic zoogeographic transition. Natural History Bulletin of the Siam Society 51: 69-96.
- Ruddiman, W.F., and Kutzbach, J.E. 1989. Forcing of late Cenozoic northern hemisphere climate by plateau uplift in southern Asia and the American west. Journal of Geophysical Research: Atmospheres 94: 18409-18427.
- Ruddiman, W.F., and Kutzbach, J.E. 1990. Late Cenozoic plateau uplift and climate change. Earth and Environmental Science Transactions of the Royal Society of Edinburgh 81: 301-314.
- Saegusa, H. 1996. Stegodontidae: Evolutionary relationships. In Shoshani, J. and Tassy, P. (eds.), The Proboscidea: Evolution and Palaeoecology of Elephants and Their Relatives, pp. 178-192. Oxford: Oxford University Press.
- Saegusa, H., Thasod, Y., and Ratanasthien, B. 2005. Notes on Asian stegodontids. Quaternary International 126–128: 31-48.
- Santa Luca, A.P. 1980. The Ngandong Fossil Hominids. Yale University Publications in Anthropology 78: 1-175.
- Sattayarak, N. 1985. Review of the continental Mesozoic stratigraphy of Thailand. in Proceedings of the Workshop on Stratigraphic Correlation of Thailand and Malaysia. pp. 127-140.

- Sattayarak, N., Chaisiboon, B., Srikulwong, S., Charusirisawat, R., Mahattanachai, T., and Chantong, W. 1998. Tectonic evolution and basin development of the Northeast, Thailand. Seminar on the Mesozoic Redbeds in Northeastern Thailand, Bangkok. 1-20.
- Scanlon, J.D., and Mackness, B.S. 2001. A new giant python from the Pliocene Bluff Downs Local Fauna of northeastern Queensland. Alcheringa: An Australasian Journal of Palaeontology 25: 425-437.
- Schepartz, L.A., Stoutamire, S., and Bekken, D.A. 2005. *Stegodon orientalis* from Panxian Dadong, a Middle Pleistocene archaeological site in Guizhou, South China: taphonomy, population structure and evidence for human interactions. Quaternary International 126-128: 271-282.
- Sémah, A.-M., Sémah, F., Djubiantono, T., and Brasseur, B. 2010. Landscapes and Hominids' environments: Changes between the Lower and the Early Middle Pleistocene in Java (Indonesia). Quaternary International 223-224: 451-454.
- Shen, G., and Jin, L. 1991. U-series age of Yanhui Cave, the site of Tongzi Man. Acta Anthropologica Sinica 10: 65-72.
- Shen, G., Tu, H., Xiao, D., Qiu, L., Feng, Y.-x., and Zhao, J.-x. 2014. Age of Maba hominin site in southern China: Evidence from U-series dating of Southern Branch Cave. Quaternary Geochronology 23: 56-62.
- Sheng, G.-L., Soubrier, J., Liu, J.-Y., Werdelin, L., Llamas, B., Thomson, V.A., Tuke, J., Wu, L.-J., Hou, X.-D., Chen, Q.-J., Lai, X.-L., and Cooper, A. 2014. Pleistocene Chinese cave hyenas and the recent Eurasian history of the spotted hyena, *Crocuta crocuta*. Molecular Ecology 23: 522-533.
- Shoocongdej, R. 2006. Late Pleistocene Activities at Tham Lod Rockshelter in Highland Pang Mapha, Mae Hong Son Province, Northwestern Thailand. The 10th International Conference of the European Association of Southeast Asian Archaeologists: Uncovering Southeast Asia's Past, 22-37.
- Simpson, G.G. 1943. Mammals and the nature of continents. American Journal of Science 241: 1-31.
- Simpson, G.G. 1960. Notes on the measurement of faunal resemblance. American Journal of Science 258A: 300-311.
- Singer, B.S., Guillou, H., Zhang, X., Schnepf, E., and Hoffman, K.A. 2006. Multiple Brunhes chron excursions in the Eifel volcanic field. AGU Fall Meeting, San Francisco.
- Singer, B.S., Hoffman, K.A., Coe, R.S., Brown, L.L., Jicha, B.R., Pringle, M.S., and Chauvin, A. 2005. Structural and temporal requirements for geomagnetic field reversal deduced from lava flows. Nature 434: 633-636.

- Singer, B.S., Jicha, B.R., Kirby, B.T., Geissman, J.W., and Herrero-Bervera, E. 2008. 40Ar/39Ar dating links Albuquerque Volcanoes to the Pringle Falls excursion and the Geomagnetic Instability Time Scale. Earth and Planetary Science Letters 267: 584-595.
- Smart, P.L. 1991. Uranium series dating. In Smart, P.L. and Frances, P.D. (eds.), Quaternary Dating Methods: A Users Guide: Technical Guide No.4, pp. 45-83. Cambridge: Quaternary Research Association.
- Smith, J.R., Giegengack, R., and Schwarcz, H.P. 2004. Constraints on Pleistocene pluvial climates through stable-isotope analysis of fossil-spring tufas and associated gastropods, Kharga Oasis, Egypt. Palaeogeography, Palaeoclimatology, Palaeoecology 206: 157-175.
- Sondaar, P.Y. 1984. Faunal evolution and the mammalian biostratigraphy of Java. Courier Forschungsinstitut Senckenberg 69: 219-235.
- Southeast Asian Mammal Databank. 2006. Ecological data set and GIS based models: a tool for biodiversity based conservation in Southeast Asia. [Online]. Available from: www.ieaitaly.org/samd [January 2008]
- Sreekumar, K.P., and Nirmalan, G. 1989. Estimation of body weight in Indian elephants (*Elephas maximus indicus*). Veterinary Research Communications 13: 3-9.
- Stamp, L.D. 1922. An outline of the Tertiary Geology of Burma. Geological Magazine 59: 481-501.
- Sterling, E.J., Hurley, M.M., and Minh, L.D. 2006. Vietnam: A natural history. New Haven: Yale University Press.
- Storm, P., Aziz, F., de Vos, J., Kosasih, D., Baskoro, S., Ngaliman, and van den Hoek Ostende, L.W. 2005. Late Pleistocene *Homo sapiens* in a tropical rainforest fauna in East Java. Journal of Human Evolution 49: 536-545.
- Storm, P., and de Vos, J. 2006. Rediscovery of the Late Pleistocene Punung hominin sites and the discovery of a new site Gunung Dawung in East Java. Senckenbergiana Lethaea 86: 271-281.
- Storm, P., Wood, R., Stringer, C., Bartsiakas, A., de Vos, J., Aubert, M., Kinsley, L., and Grün, R. 2013. U-series and radiocarbon analyses of human and faunal remains from Wajak, Indonesia. Journal of Human Evolution 64: 356-365.
- Sun, X., Li, X., and Luo, Y. 2002. Vegetation and climate on the sunda shelf of the South China Sea during the last Glactiation—Pollen results from station 17962. Acta Botanica Sinica 44: 746-752.
- Sun, X., Li, X., Luo, Y., and Chen, X. 2000. The vegetation and climate at the last glaciation on the emerged continental shelf of the South China Sea. Palaeogeography, Palaeoclimatology, Palaeoecology 160: 301-316.

- Sun, X., Luo, Y., Huang, F., Tian, J., and Wang, P. 2003. Deep-sea pollen from the South China Sea: Pleistocene indicators of East Asian monsoon. Marine Geology 201: 97-118.
- Sun, Y., Lu, H., and An, Z. 2006. Grain size of loess, palaeosol and Red Clay deposits on the Chinese Loess Plateau: Significance for understanding pedogenic alteration and palaeomonsoon evolution. Palaeogeography, Palaeoclimatology, Palaeoecology 241: 129-138.
- Suraprasit, K., Jaeger, J.-J., Chaimanee, Y., Benammi, M., Chavasseau, O., Yamee, C., Tian, P., and Panha, S. 2015. A complete skull of *Crocota crocota ultima* indicates a late Middle Pleistocene age for the Khok Sung (northeastern Thailand) vertebrate fauna. Quaternary International 374: 34-45.
- Szyndlar, Z., and Böhme, W. 1996. Redescription of *Tropidonotus atavus* von Meyer, 1855 from the upper Oligocene of Rott (Germany) and its allocation to *Rottophis* gen. nov. (Serpentes, Boidae). Palaeontographica Abteilungen A 240: 145-161.
- Szyndlar, Z., and Rage, J.C. 2003. Non-Erycine Booidea from the Oligocene and Miocene of Europe. Kraków: Institute of Systematics and Evolution of Animals, Polish Academy of Sciences Kraków.
- Takai, M., Saegusa, H., Thaug-Htike, and Zin-Maung-Maung-Thein. 2006. Neogene mammalian fauna in Myanmar. Asian paleoprimateology 4: 143-172.
- Takaya, Y. 1967. Observations on some Pleistocene outcrops in Cambodia. The center of Southeast Asian Studies, Kyoto University 5: 556-571.
- Tallman, M., Almécija, S., Reber, S.L., Alba, D.M., and Moyà-Solà, S. 2013. The distal tibia of *Hispanopithecus laietanus*: More evidence for mosaic evolution in Miocene apes. Journal of Human Evolution 64: 319-327.
- Teeuw, R.M., Rhodes, E.J., and Perkins, N.K. 1999. Dating of Quaternary sediments from Western Borneo, using optically stimulated luminescence. Singapore Journal of Tropical Geography 20: 181-192.
- Teilhard de Chardin, P. 1935. Les récents progrès de la préhistoire en Chine. L'Anthropologie 45: 735-740.
- Thein, T. 1974. La Faune Néolithique du Phnom Loang (Cambodge) (Ruminants). Ph.D thesis, Doctorat de 3ème cycle Université Paris VI.
- Thiramongkol, N. 1986. Neotectonism and rate of uplift in the eastern margin of the lower central plain of Thailand. in Proceedings of the Workshop on Economic Geology, Tectonics, Sedimentary Processes and Environment of the Quaternary in Southeast Asia. pp. 35-44. 3-7 February. Hat Yai. Department of Geology, Chulalongkorn University, Bangkok, Thailand,.

- Timmins, R.J., Hedges, S., and Duckworth., J.W. 2008. *Bos sauveli*. [Online]. Version 2015.2. Available from: www.iucnredlist.org
- Tobias, P.V. 2002. The Pleistocene dispersal of humanity and the place of Thailand. *Siriraj Hospital Gazette* 55: 42-54.
- Tong, H.-w., and Guérin, C. 2009. Early Pleistocene *Dicerorhinus sumatrensis* remains from the Liucheng *Gigantopithecus* Cave, Guangxi, China. *Geobios* 42: 525-539.
- Tong, H., Hu, N., and Wang, X.M. 2012. New remains of *Canis chiliensis* (Mammalia, Carnivora) from Shanshenmiaozui, a Lower Pleistocene site in Yangyuan, Hebei. *Vertebrata PalAsiatica* 50: 335-360.
- Tong, H., and Liu, J. 2004. The Pleistocene–Holocene extinctions of mammals in China. in *Proceedings of the Ninth Annual Symposium of the Chinese Society of Vertebrate Paleontology*. pp. 111-119. Beijing. China Ocean Press.
- Tong, H., and Patou-Mathis, M. 2003. Mammoth and other proboscideans in China during the Late Pleistocene. *Deinsea* 9: 421-428.
- Tougaard, C. 1998. *Les Faunes de Grands Mammifères du Pléistocène Moyen Terminal de Thaïlande dans leur Cadre Phylogénétique, Paléoécologique et Biochronologique*. Ph.D thesis, University of Montpellier II.
- Tougaard, C. 2001. Biogeography and migration routes of large mammal faunas in South–East Asia during the Late Middle Pleistocene: focus on the fossil and extant faunas from Thailand. *Palaeogeography, Palaeoclimatology, Palaeoecology* 168: 337-358.
- Tougaard, C., Chaimanee, Y., Suteethorn, V., Triamwichanon, S., and Jaeger, J.-J. 1996. Extension of the geographic distribution of the giant panda (*Ailuropoda*) and search for the reasons for its progressive disappearance in Southeast Asia during the Latest Middle Pleistocene. *Comptes rendus de l'Académie des sciences, Série IIA: Sciences de la terre et des planètes* 323: 973-979.
- Tougaard, C., and Ducrocq, S. 1999. Abnormal fossil upper molar of *Pongo* from Thailand: Quaternary climatic changes in Southeast Asia as a possible cause. *International Journal of Primatology* 20: 599-607.
- Tougaard, C., Jaeger, J.-J., Chaimanee, Y., Suteethorn, V., and Triamwichanon, S. 1998. Discovery of a *Homo* sp. tooth associated with a mammalian cave fauna of Late Middle Pleistocene age, Northern Thailand. *Journal of Human Evolution* 35: 47-54.
- Tougaard, C., and Montuire, S. 2006. Pleistocene paleoenvironmental reconstructions and mammalian evolution in South-East Asia: focus on fossil faunas from Thailand. *Quaternary Science Reviews* 25: 126-141.

- Travouillon, K.J., Archer, M., Hand, S.J., and Godthelp, H. 2006. Multivariate analyses of Cenozoic mammalian faunas from Riversleigh, northwestern Queensland. Alcheringa: An Australian Journal of Palaeontology 30: 323-349.
- Travouillon, K.J., and Legendre, S. 2009. Using cenograms to investigate gaps in mammalian body mass distributions in Australian mammals. Palaeogeography, Palaeoclimatology, Palaeoecology 272: 69-84.
- Tseng, Z.J., and Chang, C.H. 2007. A study of New Material of *Crocuta crocuta ultima* Carnivora: Hyaenidae) from the Quaternary of Taiwan. Collection and Research 20: 9-19.
- Tseng, Z.J., Jin, C.Z., Liu, J.Y., Zheng, L.T., and Sun, C.K. 2008. Fossil Hyaenidae (Mammalia: Carnivora) from Huainan, Anhui Province, China. Vertebrata Palasiatica 46: 133-146.
- Tshen, L.T. 2013. Quaternary *Elephas* fossils from Peninsular Malaysia: historical overview and new material. The Raffles Bulletin of Zoology 29: 139-153.
- Tsubamoto, T., Takai, M., and Egi, N. 2004. Quantitative analyses of biogeography and faunal evolution of middle to late Eocene mammals in East Asia. Journal of Vertebrate Paleontology 24: 657-667.
- Turley, K., Guthrie, E.H., and Frost, S.R. 2011. Geometric Morphometric Analysis of Tibial Shape and Presentation Among Catarrhine Taxa. The Anatomical Record: Advances in Integrative Anatomy and Evolutionary Biology 294: 217-230.
- Udvardy, M.D.F. 1975. A classification of the biogeographical provinces of the world. IUCN Occasional Paper 18: 1-48.
- van Bemmelen, R.W. 1949. The Geology of Indonesia. Nijhoff: Government Printing Office.
- van den Bergh, G.D. 1999. The late Neogene elephantoid-bearing faunas of Indonesia and their palaeozoogeographic implications: a study of the terrestrial faunal succession of Sulawesi, Flores and Java, including evidence for early hominid dispersal east of Wallace's Line. Scripta Geologica 117: 1-419.
- van den Bergh, G.D., Awe, R.D., Morwood, M.J., Sutikna, T., Jatmiko, and Wahyu Saptomo, E. 2008. The youngest *stegodon* remains in Southeast Asia from the Late Pleistocene archaeological site Liang Bua, Flores, Indonesia. Quaternary International 182: 16-48.
- van den Bergh, G.D., de Vos, J., and Sondaar, P.Y. 2001. The Late Quaternary palaeogeography of mammal evolution in the Indonesian Archipelago. Palaeogeography, Palaeoclimatology, Palaeoecology 171: 385-408.
- van den Brink, L.M. 1982. On the mammal fauna of the Wajak Cave, Java (Indonesia). Modern Quaternary Research Southeast Asia 7: 177-193.
- van der Geer, A., Lyras, G., de Vos, J., and Dermitzakis, M. 2010. Evolution of Island Mammals: Adaptation and Extinction of Placental Mammals on Islands. Oxford: Wiley Blackwell.

- van der Kaars, S. 1998. Marine and terrestrial pollen records of the last glacial cycle from the Indonesian region: Bandung Basin and Banda Sea. Palaeoclimates 3: 209-219.
- van der Kaars, S., and Dam, R. 1997. Vegetation and climate change in West-Java, Indonesia during the last 135,000 years. Quaternary International 37: 67-71.
- van der Kaars, W.A. 1991. Palynology of eastern Indonesian marine piston-cores: a Late Quaternary vegetational and climatic record for Australasia. Palaeogeography, Palaeoclimatology, Palaeoecology 85: 239-302.
- van der Kaars, W.A., and Dam, M.A.C. 1995. A 135,000-year record of vegetational and climatic change from the Bandung area, West-Java, Indonesia. Palaeogeography, Palaeoclimatology, Palaeoecology 117: 55-72.
- van der Made, J. 1996. Listriodontinae (Suidae, Mammalia), their evolution, systematic, and distribution in time and space. Contributions to Tertiary and Quaternary Geology 33: 3-254.
- Versteegh, G.J.M. 1997. The onset of major Northern Hemisphere glaciations and their impact on dinoflagellate cysts and acritarchs from the Singa section, Calabria (southern Italy) and DSDP Holes 607/607A (North Atlantic). Marine Micropaleontology 30: 319-343.
- von den Driesch, A. 1976. A Guide to the Measurement of Animal Bones from Archaeological Sites. Cambridge: Peabody Museum of Archaeology and Ethnology, Harvard University.
- von Koenigswald, G.H.R. 1933. Beitrag zur Kenntnis der fossilen Wirbeltiere Javas, I. Teil. Wetenschappelijke Mededeelingen (Dienst van den Mijnbouw in Nederlandsch Indië) 23: 1-185.
- von Koenigswald, G.H.R. 1935. Die fossilen Saugertier Fauna Javas. Proceeding Koninklijke Nederlandsche Akademie van Wetenschappen 38: 188-198.
- von Koenigswald, G.H.R. 1938–1939. The relationship between the fossil mammalian faunae of Java and China, with special reference to early man. Peking Natural History Bulletin 13: 293–298.
- Voris, H.K. 2000. Maps of Pleistocene sea levels in Southeast Asia: shorelines, river systems and time durations. Journal of Biogeography 27: 1153-1167.
- Wallace, A.R. 1869. The Malay Archipelago. London: Macmillan.
- Wallace, A.R. 1876. The Geographical Distribution of Animals. London: Macmillan.
- Wang, W., Liao, W., Li, D., and Tian, F. 2014. Early Pleistocene large-mammal fauna associated with *Gigantopithecus* at Mohui Cave, Bubing Basin, South China. Quaternary International 354: 122-130.

- Wang, W., Potts, R., Baoyin, Y., Huang, W., Cheng, H., Edwards, R.L., and Ditchfield, P. 2007. Sequence of mammalian fossils, including hominoid teeth, from the Bubing Basin caves, South China. Journal of Human Evolution 52: 370-379.
- Werdelin, L., and Lewis, M.E. 2008. New species of *Crocota* from the early Pliocene of Kenya, with an overview of early Pliocene hyenas of eastern Africa. Journal of Vertebrate Paleontology 28: 1162-1170.
- Werdelin, L., and Lewis, M.E. 2012. The taxonomic identity of the type specimen of *Crocota sivalensis* (Falconer, 1867). Journal of Vertebrate Paleontology 32: 1453-1456.
- Werdelin, L., and Solounias, N. 1991. The Hyaenidae: taxonomy, systematics and evolution. Fossils and Strata 30: 1-104.
- Westaway, K.E., Morwood, M.J., Roberts, R.G., Rokus, A.D., Zhao, J.x., Storm, P., Aziz, F., van den Bergh, G., Hadi, P., Jatmiko, and de Vos, J. 2007. Age and biostratigraphic significance of the Punung Rainforest Fauna, East Java, Indonesia, and implications for *Pongo* and *Homo*. Journal of Human Evolution 53: 709-717.
- White, J.C., Penny, D., Kealhofer, L., and Maloney, B. 2004. Vegetation changes from the late Pleistocene through the Holocene from three areas of archaeological significance in Thailand. Quaternary International 113: 111-132.
- Whitmore, T.C. 1984. Tropical Rainforests of the Far East. 2nd edition. Oxford: Oxford University Press.
- Whitmore, T.C. 1987. Biogeographical Evolution of the Malay Archipelago. Oxford: Clarendon Press.
- Whitmore, T.C. 1998. An Introduction to Tropical Rain Forests. Oxford: Oxford University Press.
- Whittow, J. 1984. Dictionary of Physical Geography. London: Penguin Books.
- Wiley, D.F., Amenta, N., Alcantara, D.A., Ghosh, D., Kil, Y.J., Delson, E., Harcourt-Smith, W., Rohlf, F.J., St John, K., and Hamann, B. 2005. Evolutionary morphing. in VIS 05. IEEE Visualization, 2005. pp. 431-438. 23-28 Oct. 2005.
- Woodruff, D.S. 2003. Neogene marine transgressions, palaeogeography and biogeographic transitions on the Thai–Malay Peninsula. Journal of Biogeography 30: 551-567.
- Woodruff, D.S. 2010. Biogeography and conservation in Southeast Asia: how 2.7 million years of repeated environmental fluctuations affect today's patterns and the future of the remaining refugial-phase biodiversity. Biodiversity and Conservation 19: 919-941.
- Woodruff, D.S., and Turner, L.M. 2009. The Indochinese–Sundaic zoogeographic transition: a description and analysis of terrestrial mammal species distributions. Journal of Biogeography 36: 803-821.

- World Conservation Monitoring Centre. 1992. Global Biodiversity: Status of the Earth's Living Resources. London: Chapman and Hall.
- Wu, X.-J., Schepartz, L.A., Liu, W., and Trinkaus, E. 2011. Antemortem trauma and survival in the late Middle Pleistocene human cranium from Maba, South China. Proceedings of the National Academy of Sciences 108: 19558-19562.
- Yamee, C., and Chaimanee, Y. 2005. Fossils of a Hyaenid (*Crocota crocuta*) and its Associated Fauna from Thum Phedan, Thung Yai District, Nakhon Sri Thammarat. Bangkok, Thailand: Department of Mineral Resources.
- Yan, Y., Wang, Y., Jin, C., and Mead, J.I. 2014. New remains of *Rhinoceros* (Rhinocerotidae, Perissodactyla, Mammalia) associated with *Gigantopithecus blacki* from the Early Pleistocene Yanliang Cave, Fusui, South China. Quaternary International 354: 110-121.
- Young, C.C. 1932. On some fossil mammals from Yunnan. Bulletin of the Geological Society of China 11: 383-394.
- Zdansky, O. 1924. Jungtertiäre Carnivoren Chinas. Palaeontologia Sinica New Series C 2: 1-149.
- Zeitoun, V., Lenoble, A., Laudet, F., Thompson, J., Rink, W.J., Mallye, J.-B., and Winayalai, C. 2010. The Cave of the Monk (Ban Fa Suai, Chiang Dao wildlife sanctuary, northern Thailand). Quaternary International 220: 160-173.
- Zeitoun, V., Seveau, A., Forestier, H., Thomas, H., Lenoble, A., Laudet, F., Antoine, P.-O., Debruyne, R., Ginsburg, L., Mein, P., Winayalai, C., Chumdee, N., Doyasa, T., Kijngam, A., and Nakbunlung, S. 2005. Découverte d'un assemblage faunique à *Stegodon-Ailuropoda* dans une grotte du Nord de la Thaïlande (Ban Fa Suai, Chiang Dao). Comptes Rendus Palevol 4: 255-264.
- Zelditch, M.L., Donald, L., Swiderski, H., Sheets, D., and Fink, W.L. 2004. Geometric Morphometrics for Biologists: a Primer. New York and London: Elsevier Academic Press.
- Zhang, Y., Jin, C., Cai, Y., Kono, R., Wang, W., Wang, Y., Zhu, M., and Yan, Y. 2014. New 400–320 ka *Gigantopithecus blacki* remains from Hejiang Cave, Chongzuo City, Guangxi, South China. Quaternary International 354: 35-45.
- Zheng, Z., and Lei, Z.Q. 1999. A 400,000 year record of vegetational and climatic changes from a volcanic basin, Leizhou Peninsula, southern China. Palaeogeography, Palaeoclimatology, Palaeoecology 145: 339-362.
- Zhou, M.Z., and Zhang, Y.P. 1974. Fossil Elephants of China. Beijing: Science Press.
- Zhu, Z.-Y., Dennell, R., Huang, W.-W., Wu, Y., Rao, Z.-G., Qiu, S.-F., Xie, J.-B., Liu, W., Fu, S.-Q., Han, J.-W., Zhou, H.-Y., Ou Yang, T.-P., and Li, H.-M. 2015. New dating of the *Homo erectus* cranium from Lantian (Gongwangling), China. Journal of Human Evolution 78: 144-157.

Zijderveld, J.D.A. 1967. AC demagnetization of rocks: analysis of results. In Collinson, D.W. and Creer, K.M. (eds.), Methods in Paleomagnetism, pp. 254-286. Amsterdam: Elsevier.

Zin-Maung-Maung-Thein, Thaung-Htike, Tsubamoto, T., Takai, M., Egi, N., and Maung-Maung. 2006. Early Pleistocene Javan rhinoceros from the Irrawaddy Formation, Myanmar. Asian Paleoprimatology 4: 197-204.





APPENDIX

จุฬาลงกรณ์มหาวิทยาลัย
CHULALONGKORN UNIVERSITY

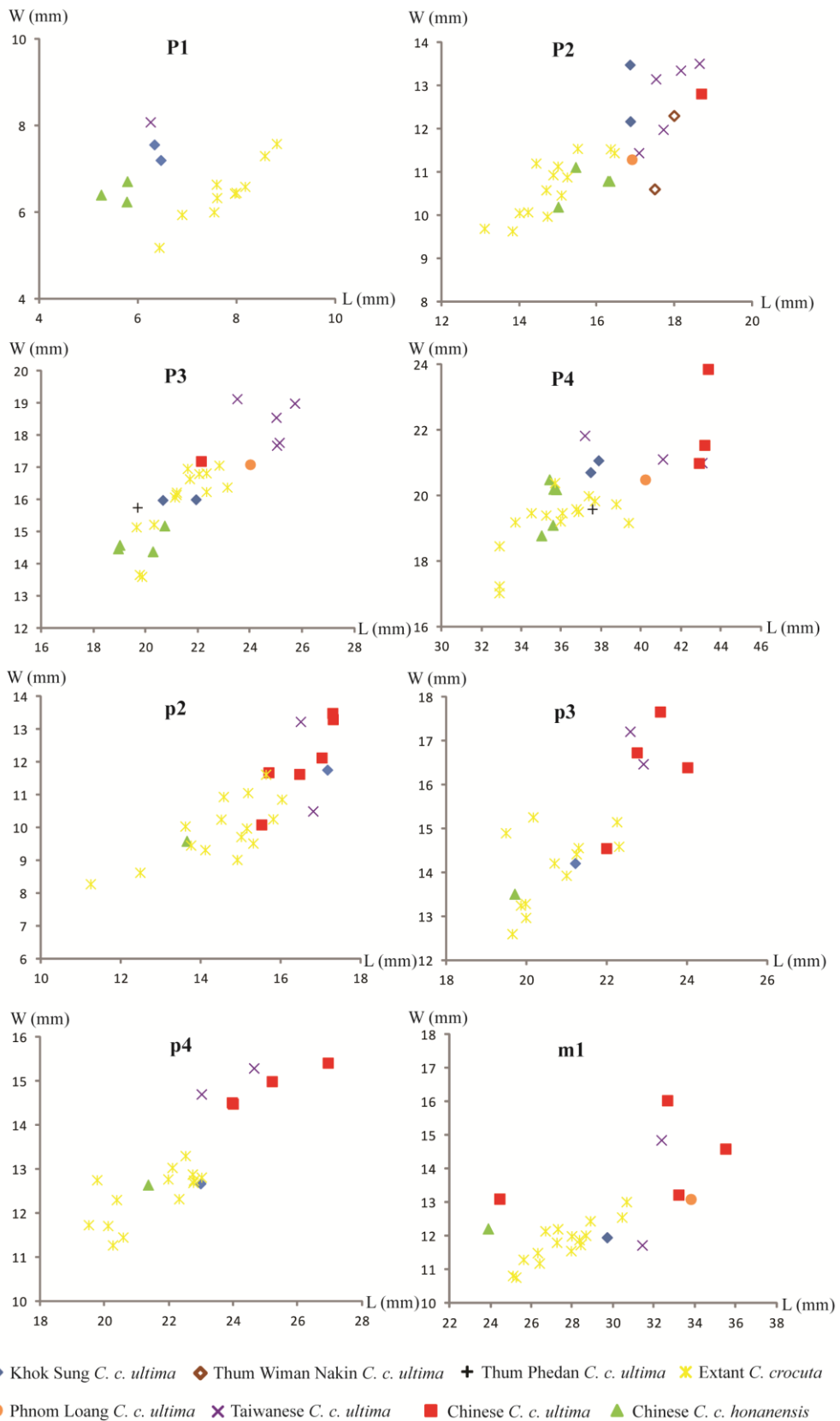


Figure A1. Bivariate diagrams of lengths (L)/widths (W) of upper and lower cheek teeth of Asian fossil and African extant spotted hyaenas.

Table A1. Measurements (in millimeters) of postcranial remains of identified mammal taxa from Khok Sung. * indicates a juvenile individual.

Scapula															
Specimen	Taxa	GLP	LG	SLC	BG	Ld	DHA	HS	GLC	GLI	GL	SD	Dd		
DMR-KS-05-03-00-58	<i>Rhinoceros sondaicus</i>	87.49	78.81	62.97	55.33	144.77	–	325.57	–	–	–	–	–		
DMR-KS-05-03-26-2	<i>Bubalus amee</i>	106.72	81.99	76.45	68.40	297.28	381.27	445.28	377.04	422.18	437.23	66.09	–		
DMR-KS-05-02-20-4	<i>Bubalus amee</i>	84.00	66.89	52.13	54.50	213.22	301.79	296.17	224.71	236.13	238.28	20.72	–		
DMR-KS-05-06-24-4	<i>Panolia eldii</i>	44.00	34.56	23.41	31.54	108.17	206.05	211.37	–	–	–	38.86	–		
DMR-KS-05-03-00-62	<i>Bos gaurus</i>	>99.45	>98.85	103.69	98.14	96.59	50.36	328.18	328.18	347.28	353.87	56.37	–		
DMR-KS-05-05-1-1	<i>Bos gaurus</i>	122.37	130.12	103.54	98.77	97.16	56.37	317.26	317.26	354.28	356.28	52.29	–		
DMR-KS-05-03-31-1	<i>Bubalus amee</i>	125.53	135.07	104.40	101.70	93.72	52.29	343.74	343.74	413.22	444.12	52.29	–		
DMR-KS-05-03-31-8	<i>Bubalus amee</i>	125.79	138.19	104.38	99.09	94.07	52.92	347.41	347.41	424.77	449.11	52.92	–		
DMR-KS-05-03-13-4	<i>Axis axis</i>	–	–	34.75	31.96	34.12	<17.02	–	–	–	–	<17.02	–		
DMR-KS-05-04-11-32	<i>Axis axis</i>	–	–	35.98	33.77	34.05	17.37	–	–	–	–	17.37	–		
DMR-KS-05-03-17-17	<i>Axis axis</i>	–	–	36.86	35.57	32.77	16.10	–	–	–	–	16.10	–		
DMR-KS-05-04-11-35	<i>Panolia eldii</i>	–	>59.10	46.10	40.85	41.18	23.3	187.53	–	–	–	23.3	–		
DMR-KS-05-03-18-1	<i>Panolia eldii</i>	53.34	65.34	–	–	–	21.45	–	–	–	–	21.45	–		
DMR-KS-05-03-15-43	<i>Rusa unicorn</i>	–	–	54.89	49.04	48.30	<27.70	–	–	–	–	<27.70	–		
Ulna and radius															
Specimen	Taxa	Bp/BPC	BFP	Dp	Bd	BFD	Dd	LO	DPA	SDO	SD	PL	LI	GLL	GL
DMR-KS-05-03-00-61	<i>Bubalus amee</i>	106.16	92.17	52.99	100.36	90.17	65.85	125.53	93.64	72.61	55.54	305.18	308.75	476.61	484.72
DMR-KS-05-03-31-2	<i>Bubalus amee</i>	108.45	98.91	57.03	103.37	92.25	73.75	131.15	98.37	76.03	50.74	335.29	343.51	427.78	452.17
DMR-KS-05-03-31-9	<i>Bubalus amee</i>	106.69	97.99	57.44	103.49	92.06	72.92	128.89	99.00	76.54	47.66	335.93	344.77	424.77	449.11
DMR-KS-05-03-31-10	<i>Panolia eldii</i>	39.40	36.72	20.95	37.22	32.67	21.37	–	–	–	22.52	199.23	198.21	–	197.52

Table A1 (continued). Measurements (in millimeters) of postcranial remains of identified mammal taxa from Khok Sung. * indicates a juvenile individual.

Specimen	Taxa	GL	LA	LS	SH	SB	SC	LFO	GBTc	GBA	GBTI	SBI	
DMR-KS-05-04-11-3	<i>Panolia eldii</i>	42.30	38.22	22.47	36.84	34.64	23.46	-	-	-	22.61	204.18	215.70
DMR-KS-05-03-19-16	<i>Panolia eldii</i>	40.16	33.03	22.16	40.62	39.21	29.89	-	-	-	23.58	197.89	204.53
DMR-KS-05-03-25-9	<i>Rusa unicolor</i>	55.06	53.58	28.92	-	-	-	-	-	-	-	-	-
DMR-KS-05-03-19-14	<i>Rusa unicolor</i>	52.37	50.16	30.83	-	-	-	-	-	-	28.12	-	-
DMR-KS-05-03-26-19	<i>Rusa unicolor</i>	-	-	-	43.12	41.08	32.20	-	-	-	24.83	-	-
Pelvis													
Specimen	Taxa	GL	LA	LS	SH	SB	SC	LFO	GBTc	GBA	GBTI	SBI	
DMR-KS-05-03-10-11	<i>Stegodon orientalis</i>	>855.79	148.93	-	139.18	66.29	399.46	206.77	-	-	-	-	-
DMR-KS-05-03-10-12	<i>Stegodon orientalis</i>	>496.75	140.75	-	145.17	59.60	389.92	201.25	-	-	-	-	-
DMR-KS-05-04-1-25	<i>Bubalus arnee</i>	494.85	96.57	149.23	70.55	35.81	256.67	103.24	517.48	303.98	319.25	204.37	-
Femur													
Specimen	Taxa	Bp	Dp	DC	Bd	Dd	SD	GLC	GL				
DMR-KS-05-03-10-4	<i>Stegodon orientalis</i>	-	-	125.14	178.16	211.72	126.18	-	-				
DMR-KS-05-03-00-63	<i>Rhinoceros unicornis</i>	-	-	-	140.58	183.17	46.21	-	-				
DMR-KS-05-03-9-2	<i>Bos gaurus</i>	124.57	66.64	52.31	106.89	138.24	46.15	405.57	419.28				
DMR-KS-05-04-30-1	<i>Bos gaurus</i>	150.06	>65.51	59.63	-	-	-	-	-				
DMR-KS-05-04-1-1	<i>Bubalus arnee</i>	160.51	80.69	66.76	128.54	156.98	54.05	420.18	447.15				
DMR-KS-05-04-1-2	<i>Bubalus arnee</i>	165.98	84.20	67.30	130.92	156.78	55.12	425.66	442.68				
DMR-KS-05-03-20-8	<i>Bubalus arnee</i>	-	-	-	124.57	181.53	-	-	-				
DMR-KS-05-03-27-4	<i>Axis axis</i>	-	-	-	50.49	69.42	-	-	-				
DMR-KS-05-03-27-11	<i>Panolia eldii</i>	66.29	31.42	28.4	52.67	70.12	21.97	-	-				
DMR-KS-05-03-17-36	<i>Panolia eldii</i>	68.57	35.49	28.73	56.56	73.06	21.97	251.58	-				
DMR-KS-05-03-28-20	<i>Panolia eldii</i>	-	-	-	53.72	72.00	-	-	-				
DMR-KS-05-04-05-38	<i>Panolia eldii</i>	67.59	35.21	27.74	-	-	-	-	-				
DMR-KS-05-03-00-119	<i>Panolia eldii</i>	-	-	-	51.60	71.30	<22.94	-	-				
DMR-KS-05-03-19-2	<i>Panolia eldii</i>	-	-	-	51.85	73.23	<26.51	-	-				
DMR-KS-05-08-16-1	<i>Panolia eldii</i>	59.40	32.32	26.14	-	-	-	-	-				
DMR-KS-05-04-11-2	<i>Rusa unicolor</i>	-	-	-	55.20	69.90	22.54	-	-				

Table A1 (continued). Measurements (in millimeters) of postcranial remains of identified mammal taxa from Khok Sung. * indicates a juvenile individual.

Specimen	Taxa	Bp	Dp	Bd	Dd	SD	LI	GL		
DMR-KS-05-03-19-7	<i>Rusa unicorn</i>	67.01	44.50	28.58	-	-	21.72	-		
DMR-KS-05-03-12-2*	<i>Rusa unicorn</i>	48.57	31.96	-	-	-	18.91	-		
DMR-KS-05-03-26-5	<i>Rusa unicorn</i>	>77.29	42.06	37.82	-	-	30.98	-		
DMR-KS-05-04-30-9	<i>Rusa unicorn</i>	-	-	-	54.46	69.12	21.85	-		
DMR-KS-05-04-19-10	<i>Rusa unicorn</i>	-	-	-	48.39	53.48	23.49	-		
Tibia										
Specimen	Taxa	Bp	Dp	Bd	Dd	SD	LI	GL		
DMR-KS-05-03-00-52	<i>Rhinoceros sondaicus</i>	-	-	94.95	>74.11	-	-	-		
DMR-KS-05-04-1-11	<i>Bubalus arnee</i>	132.04	125.08	87.26	69.54	55.84	363.36	437.17		
DMR-KS-05-04-1-3	<i>Bubalus arnee</i>	128.45	121.16	86.15	68.95	52.64	385.14	415.56		
DMR-KS-05-03-20-9	<i>Bubalus arnee</i>	126.74	106.22	88.37	64.62	53.42	354.45	406.77		
DMR-KS-05-03-28-16	<i>Rusa unicorn</i>	79.37	72.45	47.53	37.44	30.61	300.01	317.52		
DMR-KS-05-04-04-1	<i>Macaca sp.</i>	27.50	21.46	18.12	12.95	8.77	158.71	167.57		
Fibula										
Specimen	Taxa	GL								
DMR-KS-05-03-00-124	<i>Stegodon orientalis</i>	>354.56								
Metacarpus										
Specimen	Taxa	Bp	Dp	Bd	Dd	DD	SD	LI	GLI	GL
DMR-KS-05-03-28-29	<i>Rhinoceros sondaicus</i>	53.45	42.75	48.53	39.70	-	40.32	-	-	152.50
DMR-KS-05-03-22-49	<i>Rhinoceros sondaicus</i>	-	-	51.80	34.10	22.26	-	-	-	-
DMR-KS-05-04-05-15	<i>Rhinoceros sondaicus</i>	49.18	41.15	37.64	36.51	25.58	31.19	136.96	138.35	141.26
DMR-KS-05-03-26-27	<i>Bos gaurus</i>	70.18	46.08	64.78	33.53	30.97	43.42	247.28	252.75	256.78
DMR-KS-05-03-26-3(1)	<i>Bubalus arnee</i>	77.07	49.58	78.33	42.45	30.17	52.02	189.78	197.23	206.75
DMR-KS-05-03-18-2	<i>Axis axis</i>	25.80	16.79	25.06	15.89	11.69	14.50	160.18	162.37	167.66
DMR-KS-05-03-22-28	<i>Axis axis</i>	-	19.82	27.91	18.35	14.76	17.61	186.70	187.90	190.10
DMR-KS-05-03-08-2	<i>Axis axis</i>	29.68	21.47	30.56	18.54	16.46	16.38	186.68	187.11	188.81
DMR-KS-05-03-19-3	<i>Axis axis</i>	29.27	21.25	30.59	18.49	15.60	19.37	188.77	191.11	192.58
DMR-KS-05-03-19-37	<i>Axis axis</i>	23.45	15.14	24.46	15.56	12.74	12.03	163.43	165.54	167.32

Table A1 (continued). Measurements (in millimeters) of postcranial remains of identified mammal taxa from Khok Sung. * indicates a juvenile individual.

DMR-KS-05-04-30-20	Axis axis	28.80	19.11	-	-	14.22	195.55	196.17	197.89	
DMR-KS-05-03-24-2	<i>Panolia eldii</i>	30.95	22.01	30.11	19.01	14.96	192.33	194.14	197.83	
DMR-KS-05-03-17-26	<i>Rusa unicolor</i>	37.58	29.64	37.00	24.64	19.31	216.98	217.35	224.25	
Metatarsus										
Specimen	Taxa	Bp	Dp	Bd	Dd	DD	SD	LI	GLI	GL
DMR-KS-05-04-1-8	<i>Bubalus arnee</i>	66.22	54.89	79.59	45.49	38.42	44.58	237.44	241.11	251.92
DMR-KS-05-04-1-6	<i>Bubalus arnee</i>	65.79	58.19	82.22	45.07	38.88	44.44	239.66	241.52	255.33
DMR-KS-05-03-28-30	<i>Bubalus arnee</i>	55.89	55.48	69.85	37.24	35.40	39.31	225.71	229.18	237.54
DMR-KS-05-03-26-3	<i>Axis axis</i>	25.54	26.65	26.37	20.11	16.67	15.61	176.37	180.01	184.21
DMR-KS-05-03-15-14	<i>Axis axis</i>	32.87	30.52	36.54	24.38	20.48	21.48	219.75	220.21	224.81
DMR-KS-05-03-29-30	<i>Axis axis</i>	27.10	27.45	28.73	21.81	16.14	16.88	183.77	184.96	187.21
DMR-KS-05-03-28-17	<i>Panolia eldii</i>	27.78	29.00	28.93	19.12	17.32	17.75	217.28	219.89	223.54
DMR-KS-05-03-25-8	<i>Panolia eldii</i>	28.90	30.23	31.26	19.51	18.51	20.04	221.45	224.13	225.71
DMR-KS-05-03-15-15	<i>Panolia eldii</i>	28.12	30.52	30.82	20.11	17.01	17.80	218.79	221.74	227.14
DMR-KS-05-03-19-11	<i>Rusa unicolor</i>	36.89	35.69	37.75	26.63	22.36	24.08	233.75	238.89	244.97

Table A2. Measurements of the cranium and mandible of Khok Sung *C. c. ultima*. * indicates the maximum length of the fossil preservation. ** represents the estimated length of the reconstructed parts. The measurements follow the methods demonstrated in Fig. 10.

Metrical parameters	(mm)
Cranium	
1—Total length	255.1*
2—Basicranial axis (= intersphenoid suture)	72.4
3—Upper neurocranium length	153.0
4—Facial length	113.0**
5—Greatest length of the nasals	45.0**
6—Length of the horizontal part of the palatine	52.1
7—Length of the tooth row, P2 - M1	80.9 (left) 80.8 (right)
8—Length of the premolar row	44.3 (left) 44.2 (right)
9—Greatest diameter of the auditory bulla	36.3
10—Greatest mastoid breadth	98.1
11—Breadth dorsal to the external auditory meatus	97.2
12—Greatest breadth of the occipital condyles	53.4
13—Greatest breadth of the bases of the paraoccipital processes	83.9
14—Greatest breadth of the foramen magnum	26.7
15—Height of the foramen magnum	17.7
16—Greatest neurocranium breadth	83.6
17—Zygomatic breadth	173.8
18—Least breadth of the skull	40.9
19—Frontal breadth	73.6
20—Least breadth between the orbits	55.6
21—Least palatal breadth	64.7
22—Breadth at the canine alveoli	64.4
23—Greatest inner height of the orbits	44.0

24—Skull height	100.8
25—Skull height without the sagittal crest	95.9
26—Height of the occipital triangle	68.4

Mandible

27—Total length	177.5
28—Length: the angular process to infradentale	184.6*
29—Length from the indentation between the condyle process and the angular process - infradentale	174.3
30—Length: the condyle process - aboral border of the canine alveolus	156.1
31—Length from the indentation between the condyle process and the angular process - aboral border of the canine alveolus	153.5
32—Length: the angular process - aboral border of the canine alveolus	158.3*
33—Length: the aboral border of the alveolus of m1 - aboral border of the canine alveolus	89.6
34—Length of the tooth row, p2 - m1	84.0
35—Length of the premolar row, p2 -p4, measured along the alveoli	56.9
36—Length of the carnassial alveolus	27.9
37—Height of the vertical ramus: basal point of the angular process - coronion	86.2
38—Height of the mandible behind m1, measured on the lingual side and at right angles to the basal border	46.3
39—Height of the mandible between p2 and p3, measured on the lingual side and at right angles to the basal border	33.8

Table A3. Dental measurements of fossil spotted hyaenas used for log-ratio diagrams. Some measurements are provided by the literatures.

Upper dentition						
Specimen	Taxon	Locality		L	W	References
IVPP V05198.2	<i>C. c. ultima</i>	Guanyindong, Qianxi, Guizhou province	P2 (right)	18.69	12.82	
IVPP V05198.3	<i>C. c. ultima</i>		P4 (right)	43.35	23.87	
IVPP V15164.2	<i>C. c. ultima</i>	Xiliexi, Huainan, Anhui province	P3 (left)	22.12	17.20	Tseng et al. (2008)
			P4 (left)	-	21.16	
Unnumbered	<i>C. c. ultima</i>	Upper cave of Zhoukoudian, Beijing	P4 (left)	42.90	21.00	Pei (1940)
IVPP V05234.19	<i>C. c. ultima</i>	Xianrendong, Xichou, Yunnan province	P4 (left)	43.17	21.55	
UPM M1975	<i>C. c. honanensis</i>	Hsinanhsien, Henan province	P4 (left)	35.40	20.50	Zdansky (1924)
IVPP V13535	<i>C. c. honanensis</i>	Longdan (Nalesi Town), Dongxiang, Gansu province	P1 (right)	5.25	6.41	
			P2 (right)	16.28	10.80	
			P3 (right)	18.94	14.48	
			P4 (right)	35.74	20.20	
			P1 (left)	5.77	6.25	
			P2 (left)	16.33	10.80	
			P3 (left)	19.00	14.59	
			P4 (left)	35.61	20.21	
IVPP V07294	<i>C. c. honanensis</i>	Nihewan, Yuxian, Hebei province	P1 (left)	5.78	6.72	
			P2 (left)	15.00	10.20	
			P3 (left)	20.27	14.39	
			P4 (left)	35.57	19.11	
			P2 (right)	15.45	11.12	
			P3 (right)	20.72	15.19	
			P4 (right)	35.00	18.79	
CJ-0013	<i>C. c. ultima</i>	Penghu channel, Taiwan Strait between the Penghu Archipelago and the main island of Taiwan	P2 (right)	18.16	13.36	Tseng and Chang (2007)
			P3 (right)	25.00	18.56	
			P2 (left)	17.52	13.16	
			P3 (left)	23.50	19.14	

CJ-0038	<i>C. c. ultima</i>		P2 (left)	18.64	13.52	Tseng and Chang (2007)
			P3 (left)	25.12	17.78	
			P4 (left)	41.08	21.12	
CJ-0032	<i>C. c. ultima</i>		P2 (left)	17.71	11.99	Ho et al. (1997)
			P3 (left)	25.02	17.69	
			P4 (left)	37.17	21.84	
HL-0001	<i>C. c. ultima</i>		P1 (left)	6.25	8.09	Ho et al. (1997)
			P2 (left)	17.08	11.45	
			P3 (left)	25.71	19.00	
			P4 (left)	43.05	21.01	
PNL 176	<i>C. c. ultima</i>	Phnom Loang, Kampot, Cambodia	P2 (right)	16.90	11.30	Beden and Guérin (1973)
PNL 178	<i>C. c. ultima</i>		P3 (right)	24.00	17.10	Beden and Guérin (1973)
PNL 179	<i>C. c. ultima</i>		P4 (right)	40.20	20.50	Beden and Guérin (1973)
Lower dentition						
Specimen	Taxon	Locality		L	W	References
IVPP V15164.3-4	<i>C. c. ultima</i>	Xiliexi, Huainan, Anhui province	p2 (left)	15.52	10.10	Tseng et al. (2008)
			m1(left)	24.44	13.11	
IVPP V15160	<i>C. c. ultima</i>	Dadingshan, Huainan, Anhui province	p2 (left)	16.47	11.64	Tseng et al. (2008)
			p3 (left)	22.75	16.74	
			p4 (left)	23.99	14.49	
IVPP V15163	<i>C. c. ultima</i>	Xiliexi, Huainan, Anhui province	p2 (left)	15.70	11.69	Tseng et al. (2008)
			p3 (left)	21.99	14.56	
			p4 (left)	23.96	14.52	
Unnumbered	<i>C. c. ultima</i>	Upper cave of Zhoukoudian, Beijing	p2 (left)	17.30	13.50	Pei (1940)
			p3 (left)	24.01	16.40	
			p4 (left)	25.20	15.00	
			m1(left)	35.50	14.60	
IVPP V07296	<i>C. c. honanensis</i>	Baihaicun, Yushe, Shanxi province	p2 (left)	13.65	9.60	
			p3 (left)	19.70	13.52	
			p4 (left)	21.35	12.65	
			m1(left)	23.88	12.22	
IVPP	<i>C. c. ultima</i>	Guanyindong, Qianxi,	p3 (right)	23.33	17.67	

V05198.6		Guizhou province	p4 (right)	26.94	15.42	
IVPP V05198.1	<i>C. c. ultima</i>		p2 (right)	17.03	12.14	
IVPP V03084	<i>C. c. ultima</i>	Laochihe, Lantian, Shaanxi province	m1 (right)	33.20	13.23	
IVPP V00151a	<i>C. c. ultima</i>	Xianrendong, Xichou, Yunnan province	p2 (right)	17.31	13.31	
IVPP V00151b	<i>C. c. ultima</i>		m1 (left)	32.65	16.04	
CJ-0039	<i>C. c. ultima</i>	Penghu channel, Taiwan Strait between the Penghu	p2 (left)	16.50	13.24	Tseng and Chang (2007)
			p3 (left)	22.58	17.22	
			p4 (left)	24.64	15.30	
			m1(left)	32.36	14.86	
HL-0002	<i>C. c. ultima</i>	Archipelago and the main island of Taiwan	p2 (left)	16.81	10.51	Ho et al. (1997)
			p3 (left)	22.91	16.48	
			p4 (left)	23.01	14.71	
			m1(left)	31.42	11.73	
PNL 182	<i>C. c. ultima</i>	Phnom Loang, Kampot, Cambodia	m1 (left)	33.80	13.10	Beden and Guérin (1973)

Table A4. Measurements (in millimeters) of mandibles of rhinoceroses from Khok Sung.

Taxon	<i>Rhinoceros sondaicus</i>		<i>Rhinoceros unicornis</i>
Mandible no.	DMR-KS-05-03-00-126	DMR-KS-05-03-31-28	DMR-KS-05-03-17-13
Metrical parameters (mm)			
Length of the mandible	>311.0	>198.3	>404.1
Length of the mandibular symphysis	>108.1	124.2	–
Width of the mandibular symphysis	–	59.5	–
Length of the diastema	–	50.5	–
Height of the mandibular corpus below the p2	51.7 (right)	44.5 (right)	–
	–	41.0 (left)	–
Height of the mandibular corpus below the p3	56.1 (right)	–	–
	50.1 (left)	46.8 (left)	–
Height of the mandibular corpus below the p4	76.2 (right)	–	–
	74.5 (left)	–	–
Height of the mandibular corpus below the m1	80.7 (right)	–	–
	84.2 (left)	–	–
Height of the mandibular corpus below the m2	94.0 (right)	–	–
	91.9 (left)	–	–
Height of the mandibular corpus below the m3	97.6 (right)	–	–
	92.4 (left)	–	126.6 (left)
Width of the mandibular corpus below the m1	55.3 (right)	–	–
	54.2 (left)	–	–
Width of the mandibular corpus below the m2	57.7 (right)	–	–
	57.5 (left)	–	–
Width of the mandibular corpus below the m3	57.3 (right)	–	–
	56.4 (left)	–	–

Table A5. Measurements (in millimeters) of mandible of *Sus barbatus* from Khok Sung. Numbers within the parentheses refer to the numbers used in von den Driesch's metrical methods (1976: fig. 22b).

Taxon	<i>Sus barbatus</i>	
Mandible no.	DMR-KS-05-03-15-1	DMR-KS-05-04-19-1
Metrical parameters (mm)	male	female
Minimum length of the mandible	189.0	207.0
Diastema between c1 and p1	8.6	5.8
Diastema between p1 and p2	13.9	6.5
(9) Length of the premolar row, p1–p4	58.2 (left)	53.4 (right) 60.1 (left)
(9a) Length of the premolar row, p2–p4	41.4 (left)	38.4 (right) 39.0 (left)
(8) Length of the molar row	–	75.3 (right)
(7a) Length of the cheek tooth row, p2–m3	–	112.4 (right)
(7) Length of the cheek tooth row, p1–m3	–	126.3 (right)
(4) Length of the horizontal ramus: aboral border of the alveolus of m3 to infradentale	–	163.4 (right)
(6) Length: aboral border of the alveolus of m3 to aboral border of the canine alveolus	–	133.2 (right)
(11) Length: oral border of the alveolus of p2 to aboral border of the alveolus of i3	45.1 (right) 45.9 (left)	39.4 (right) 39.2 (left)
(12) Length of the median section of the body of mandible: from the mental prominence to infradentale	64.9 (right) 64.7 (left)	58.8 (right)
(16c) Height of the mandible in front of p2	50.9 (right) 50.4 (left)	41.5 (right)
(16b) Height of the mandible in front of m1	48.5 (left)	43.3 (right)
(16a) Height of the mandible in front of m3	–	45.1 (right)

Table A6. Measurements (in millimeters) of crania of cervids from Khok Sung. Numbers within the parentheses refer to the numbers used in von den Driesch's metrical methods (1976: fig.11). * indicates measurements of the maximum length of the preservation according to incomplete specimens. "es" refers to an estimated value of the full length due to incomplete specimens.

Taxon	Axis axis				Panolia eldii
	DMR-KS-05-03-00-30	DMR-KS-05-04-18-50	DMR-KS-05-03-18-X9	DMR-KS-05-03-27-1	
Cranium no.					DMR-KS-05-04-20-4
Metrical parameters (mm)					
(6) Basicranial axis: Basion-Synsphenion	68.11	76.94	70.95	58.65*	93.34
(8) Neurocranium length: Basion-Nasion	-	-	-	143.64*	-
(10) Median frontal length: Akrokranium-Nasion	-	-	-	148.51*	-
(23) Greatest inner length of the orbit: Ectorbitale-Entorbitale	-	-	48.76 (right)	47.26 (left)	-
(25) Greatest mastoid breadth: Otion-Otion	100.94	92.35	93.29	96.29	98.28
(26) Greatest breadth of the occipital condyles	55.28	50.66	51.42	52.35	57.13
(27) Greatest breadth at the bases of the paraoccipital processes	83.89	78.94	80.24	88.51*	83.49
(28) Greatest breadth of the foramen magnum	22.53	25.15	22.65	24.83	26.20
(31) Least frontal breadth = least breadth of the forehead aboral of the orbits	88.42	99.22	-	99.06	81.08
(32) Greatest breadth across the orbits = greatest frontal breadth = nearly greatest breadth of skull: Ectorbitale-Ectorbitale	-	-	-	124.03*	-
(38) Basion-the highest point of the superior nuchal crest	62.62	61.91	62.65	63.52	66.97
(40) Proximal circumference of the burr = circumference of the distal end of the pedicle	116.2 (right) 114.50 (left)	104.56 (right) 104.81 (left)	111.87 (right) 103.59 (left)	100 (es) (right and left)	85.13 (right)
(41) Distal circumference of the burr	129.80 (left)	146.53 (right) 144.53 (left)	-	-	88.51* (right)

Table A7. Measurements (in millimeters) of mandibles of cervids from Khok Sung. Numbers within the parentheses refer to the numbers used in von den Driesch's metrical methods (1976: fig. 21).

Taxon	Axis axis										Panolia eldii	
	DMR-KS-05-03-19-2	DMR-KS-05-03-19-1	DMR-KS-05-03-22-8	DMR-KS-05-04-01-1	DMR-KS-05-03-23-1	DMR-KS-05-03-29-1	DMR-KS-05-04-7-10	DMR-KS-05-03-26-10	DMR-KS-05-03-27-2	DMR-KS-05-04-9-5		
Mandible no.												
Metrical parameters (mm)								Juvenile				
(3) Length: Gonion caudale-aboral border of the alveolus of m3	-	59.47	-	-	-	-	-	-	-	-	-	-
(5) Length: Gonion caudale-oral border of the alveolus of p2	-	149.42	-	-	-	-	-	-	-	-	-	-
(7) Length of the cheek tooth row, measured along the alveoli on the buccal side	-	-	-	80.53	88.11	84.49	-	-	89.82	-	-	-
(8) Length of the molar row, measured along the alveoli on the buccal side	-	56.09	-	54.29	54.22	54.20	-	-	54.83	-	-	-
(9) Length of the premolar row, measured along the alveoli on the buccal side	-	31.24	-	28.59	34.18	30.34	-	28.85	34.91	39.01	-	-
(11) Length of the diastema: oral border of the alveolus of p2-aboral border of the alveolus of i4	-	-	-	-	58.40	60.02	-	68.60	-	-	-	-
(12) Aboral height of the vertical ramus: Gonion ventrale-highest point of the condyle process	-	85.87	-	-	-	-	-	-	-	-	-	-
(13) Middle height of the vertical ramus: Gonion ventrale-deepest point of the mandibular notch	-	79.22	-	-	-	-	-	-	-	-	-	-
(15a) Height of the mandible behind m3 from the most aboral point of the alveolus on the buccal side	31.99	33.60	34.35	29.03	36.02	35.60	31.14	-	38.84	-	-	-
(15b) Height of the mandible in front of m1	-	26.72	-	-	29.74	26.01	-	28.85	31.13	-	-	-
(15c) Height of the mandible in front of p2	-	22.13	-	24.11	21.43	21.57	16.28	23.02	27.10	-	-	-

Table A7 (continued). Measurements (in millimeters) of mandibles of cervids from Khok Sung. Numbers within the parentheses refer to the numbers used in von den Driesch's metrical methods (1976: fig. 21).

Taxon	Axis axis								Rusa unicorn	
	DMR-KS-05-03-18-22	DMR-KS-05-03-20-1	DMR-KS-05-03-22-7	DMR-KS-05-03-22-6	DMR-KS-05-04-03-1	DMR-KS-05-03-27-22	DMR-KS-05-03-27-3	DMR-KS-05-04-09-2	DMR-KS-03-00-101	DMR-KS-05-03-13
Mandible no.										
(3) Length: Gonion caudale-aboral border of the alveolus of m3	-	-	-	-	-	-	-	59.53	-	-
(7) Length of the cheek tooth row, measured along the alveoli on the buccal side	-	-	-	-	95.21	-	-	-	-	-
(8) Length of the molar row, measured along the alveoli on the buccal side	-	53.17	-	-	61.52	-	-	51.78	68.51	78.11
(9) Length of the premolar row, measured along the alveoli on the buccal side	-	-	-	-	35.88	-	-	-	-	-
(11) Length of the diastema: oral border of the alveolus of p2-aboral border of the alveolus of i4	-	-	-	-	58.91	-	-	-	-	-
(12) Aboral height of the vertical ramus: Gonion ventrale-highest point of the condyle process	-	-	-	-	-	-	-	88.50	-	-
(13) Middle height of the vertical ramus: Gonion ventrale-deepest point of the mandibular notch	-	-	-	-	-	-	-	84.79	-	-
(14) Oral height of the vertical ramus: Gonion ventrale-Coronion	-	-	-	-	-	-	-	125.12	-	-
(15a) Height of the mandible behind m3 from the most aboral point of the alveolus on the buccal side	-	-	36.92	-	38.71	36.22	38.50	37.30	51.76	-
(15b) Height of the mandible in front of m1	-	-	-	28.58	24.35	32.29	-	31.76	-	-
(15c) Height of the mandible in front of p2	23.21	-	-	-	19.72	-	-	-	-	-

Table A8. Measurements (in millimeters) of scapulae of extant ruminants from Southeast Asia.

	HS	DHA	Ld	SLC	GLP	LG	BG	HS/Ld	DHA/Ld	Ld/SLC	LG/BG	GLP/LG	SLC/BG
Axis axis (N=6)													
Max	176.10	164.20	98.30	21.42	38.84	30.11	25.46	1.82	1.72	4.70	1.25	1.42	0.85
Min	157.80	152.10	91.20	19.39	34.32	25.50	23.66	1.73	1.58	4.51	1.02	1.19	0.82
Mean	168.62	157.47	95.18	20.75	36.60	27.83	24.69	1.77	1.65	4.59	1.13	1.32	0.84
Axis porcinus (N=2)													
Max	145.40	134.10	80.90	17.73	31.45	23.58	23.82	1.80	1.66	4.61	1.05	1.35	0.79
Min	143.60	133.20	80.80	17.54	30.20	22.41	22.55	1.78	1.65	4.56	0.94	1.33	0.74
Mean	144.50	133.65	80.85	17.64	30.83	23.00	23.19	1.79	1.65	4.58	0.99	1.34	0.76
Panolia eldii (N=4)													
Max	228.90	210.10	118.50	28.07	42.45	34.93	32.25	1.93	1.77	4.86	1.15	1.28	0.87
Min	200.20	178.90	109.31	22.63	39.75	31.07	27.75	1.82	1.63	4.22	1.07	1.22	0.82
Mean	214.65	194.53	114.04	25.38	41.16	33.07	29.99	1.88	1.70	4.53	1.10	1.25	0.84
Rusa unicolor (N=4)													
Max	269.40	274.70	167.40	38.43	61.87	47.23	45.60	1.62	1.66	4.43	1.08	1.32	0.93
Min	233.10	235.10	152.70	34.69	52.37	40.50	37.66	1.52	1.54	4.36	1.01	1.29	0.83
Mean	250.93	254.73	159.78	36.38	56.94	43.64	41.50	1.57	1.59	4.39	1.05	1.30	0.88
Bos sauveli (N=4)													
Max	389.00	359.70	216.50	66.42	73.22	62.72	56.78	2.25	2.12	3.28	1.13	1.17	1.18
Min	381.20	357.80	169.60	52.38	65.48	56.54	50.25	1.80	1.65	3.23	1.10	1.15	1.03
Mean	385.08	358.85	193.08	59.31	69.41	59.59	53.55	2.02	1.89	3.25	1.11	1.16	1.10

Table A8 (continued). Measurements (in millimeters) of scapulae of extant ruminants from Southeast Asia.

<i>Bos javanicus</i> (N=6)													
Max	441.90	381.60	226.80	62.95	77.54	65.88	61.83	1.95	1.71	3.69	1.18	1.19	1.03
Min	384.30	339.10	198.20	53.91	71.11	61.66	52.24	1.83	1.65	3.60	1.07	1.15	1.01
Mean	403.53	355.58	211.47	57.94	74.20	63.41	56.79	1.91	1.68	3.65	1.12	1.17	1.02
<i>Bos gaurus</i> (N=6)													
Max	536.10	491.20	258.70	71.23	90.16	80.07	70.45	2.07	1.90	3.72	1.19	1.20	1.20
Min	393.70	356.70	191.30	54.34	79.07	66.08	55.65	1.87	1.86	3.52	1.14	1.13	0.91
Mean	462.95	434.45	230.78	63.76	83.68	72.37	62.47	2.01	1.88	3.61	1.16	1.16	1.02
<i>Bubalus arnee</i> (N=6)													
Max	374.00	362.80	238.10	71.55	81.72	65.77	55.71	1.66	1.52	4.29	1.39	1.31	1.50
Min	320.90	303.70	207.60	53.11	74.22	62.38	45.02	1.41	1.34	3.07	1.17	1.16	1.04
Mean	346.50	327.02	223.60	64.02	79.49	64.20	50.60	1.55	1.46	3.55	1.28	1.24	1.27

Table A9. Measurements (in millimeters) of humeri of extant ruminants from Southeast Asia.

	Bp	Dp	Bd	Dd	SD	GL	BT	GLC	GLI	GL/Bp	GL/Dp	GL/Bd	GL/Dd	Bp/Bd	Dp/Dd	Bp/Dp	Bd/Dd	Bd/BT
<i>Axis axis</i> (N=8)																		
Max	48.01	55.42	41.82	36.58	18.48	200.30	36.44	177.10	196.80	4.20	3.77	5.13	5.67	1.30	1.68	0.91	1.23	1.17
Min	42.12	47.92	33.98	30.63	15.21	172.40	31.87	153.10	167.30	3.84	3.16	4.59	5.16	1.11	1.46	0.80	1.04	1.07
Mean	48.16	44.50	35.57	24.98	98.52	107.03	98.24	169.66	90.14	3.77	4.16	5.10	3.29	1.37	1.20	1.00	1.12	1.12
<i>Axis porcinus</i> (N=2)																		
Max	35.42	51.11	32.42	27.11	14.67	153.20	27.65	125.10	142.30	4.40	3.02	4.87	5.78	1.12	1.91	0.69	1.23	1.19
Min	34.74	50.53	31.49	26.43	14.55	152.80	27.34	124.30	141.80	4.33	3.00	4.71	5.65	1.07	1.89	0.69	1.16	1.14
Mean	35.08	50.82	31.96	26.77	14.61	153.00	27.50	124.70	142.05	4.36	3.01	4.79	5.72	1.10	1.90	0.69	1.19	1.16
<i>Panolia eldii</i> (N=4)																		
Max	54.56	62.98	43.48	38.15	20.40	211.70	36.81	185.80	206.30	4.08	3.40	4.87	5.57	1.26	1.66	0.87	1.19	1.19
Min	47.17	56.65	42.52	35.75	18.52	192.30	36.02	171.30	190.40	3.88	3.35	4.51	5.35	1.11	1.57	0.83	1.14	1.16
Mean	50.94	59.78	43.06	36.97	19.46	202.00	36.53	178.53	198.45	3.97	3.38	4.69	5.46	1.18	1.62	0.85	1.17	1.18
<i>Rusa unicorn</i> (N=4)																		
Max	73.14	85.10	66.12	46.33	27.62	277.80	61.23	252.40	267.90	3.98	3.54	4.81	6.22	1.21	1.91	0.89	1.48	1.14
Min	64.44	72.40	53.35	44.66	24.82	256.40	47.29	224.10	254.30	3.80	3.26	4.19	5.54	1.10	1.56	0.86	1.16	1.08
Mean	68.75	78.66	59.81	45.61	26.06	266.83	54.21	238.05	261.23	3.89	3.40	4.49	5.85	1.15	1.73	0.88	1.31	1.11
<i>Bos sauveli</i> (N=4)																		
Max	105.62	104.67	90.28	84.60	43.08	338.10	86.30	306.10	333.70	3.28	3.23	3.86	4.17	1.18	1.41	1.01	1.08	1.07
Min	90.62	100.44	76.98	71.24	32.67	296.80	71.78	276.10	291.20	3.19	2.94	3.74	3.99	1.17	1.23	0.90	1.07	1.05
Mean	98.12	102.63	83.64	77.67	37.89	317.35	79.09	290.95	312.63	3.24	3.09	3.80	4.09	1.17	1.33	0.95	1.08	1.06

Table A9 (continued). Measurements (in millimeters) of humeri of extant ruminants from Southeast Asia

<i>Bos javanicus</i> (N=6)																		
Max	111.54	137.34	102.41	79.42	43.75	354.40	83.12	291.30	318.40	3.48	3.00	3.82	4.48	1.12	1.74	0.95	1.29	1.23
Min	94.97	109.87	86.67	76.08	40.06	326.10	77.15	278.80	302.50	3.13	2.58	3.46	4.25	1.08	1.43	0.80	1.14	1.12
Mean	103.36	119.39	94.08	77.42	42.71	337.57	79.41	285.97	312.97	3.27	2.85	3.60	4.36	1.10	1.54	0.87	1.21	1.18
<i>Bos gaurus</i> (N=6)																		
Max	135.46	154.89	110.89	96.12	56.49	395.40	99.32	353.80	391.50	2.99	3.46	3.82	4.20	1.28	1.61	1.22	1.15	1.13
Min	117.31	96.43	94.21	85.01	43.22	333.20	87.12	302.10	321.50	2.79	2.55	3.49	3.64	1.21	1.05	0.86	1.04	1.06
Mean	124.31	123.64	99.99	91.03	49.09	362.02	91.55	325.98	355.32	2.91	3.00	3.62	3.98	1.24	1.35	1.03	1.10	1.09
<i>Bubalus arnee</i> (N=6)																		
Max	102.11	106.03	87.29	77.75	50.59	319.60	80.69	271.70	317.80	3.41	3.16	3.85	4.28	1.24	1.46	0.97	1.15	1.11
Min	92.71	101.13	82.33	72.58	38.44	310.50	73.89	262.10	305.40	3.04	2.93	3.66	4.07	1.10	1.33	0.88	1.06	1.04
Mean	97.08	103.83	83.98	75.75	42.93	315.92	77.86	266.88	312.07	3.26	3.04	3.76	4.17	1.16	1.37	0.94	1.11	1.08

Table A10. Measurements (in millimeters) of radii and ulnae of extant ruminants from Southeast Asia.

	Bp	Dp	Bd	Dd	SD	GL	GLL	BFD	BFP	BPC	PL	LI	SDO	DPA	LO
<i>Axis axis</i> (N=8)															
Max	37.72	18.84	34.78	26.20	23.88	241.10	236.80	29.93	33.07	20.72	171.20	177.70	30.96	34.01	49.28
Min	34.16	16.11	30.00	21.74	19.46	203.70	198.90	26.97	30.12	16.33	139.40	160.30	24.87	28.49	41.44
Mean	35.43	17.78	32.68	24.28	21.06	222.60	218.74	28.37	31.30	18.93	162.54	165.38	27.89	30.82	45.17
<i>Axis porcinus</i> (N=4)															
Max	31.15	15.78	25.09	24.81	16.45	165.70	162.80	24.02	27.11	15.44	126.03	132.09	25.17	26.16	40.22
Min	28.45	13.37	24.11	16.43	12.81	164.10	158.40	22.73	25.85	13.66	122.60	119.42	20.45	23.94	36.03
Mean	29.80	14.36	24.65	20.72	14.71	165.08	160.58	23.29	26.30	14.64	124.52	125.71	22.97	25.17	37.99
<i>Panolia eldii</i> (N=3)															
Max	42.22	20.72	39.16	26.63	23.31	276.60	271.80	36.15	37.87	24.74	212.80	217.50	33.98	34.91	54.59
Min	38.88	19.02	35.18	25.16	19.93	254.80	249.20	33.17	35.14	20.32	196.70	200.10	30.69	33.48	46.71
Mean	40.04	19.85	36.68	25.80	21.08	262.30	256.90	34.20	36.07	21.84	202.20	206.07	31.82	34.09	49.43
<i>Rusa unicorn</i> (N=4)															
Max	59.02	31.24	54.29	40.62	32.49	322.50	320.50	46.82	54.38	29.77	239.80	243.60	46.89	50.60	70.12
Min	51.89	24.21	44.25	34.29	29.10	296.30	291.30	41.82	46.02	23.81	217.80	222.20	39.89	42.37	57.71
Mean	55.35	27.73	49.20	37.52	30.66	309.45	305.83	44.26	50.07	26.34	228.53	232.90	43.18	46.18	63.96
<i>Bos sauveli</i> (N=4)															
Max	89.11	38.72	83.52	58.24	42.13	372.30	364.50	74.01	78.29	45.63	316.50	314.20	51.33	64.95	109.67
Min	78.88	35.44	68.52	56.47	36.54	329.40	324.80	66.14	72.13	44.24	285.40	274.10	46.46	64.32	93.75
Mean	83.99	37.14	76.06	57.41	39.35	350.90	344.63	70.21	75.22	44.99	300.95	294.05	48.89	64.59	101.67

Table A10 (continued). Measurements (in millimeters) of radii and ulnae of extant ruminants from Southeast Asia.

<i>Bos javanicus</i> (N=6)															
Max	93.83	43.24	90.23	57.23	50.34	420.90	421.30	70.11	81.49	47.56	293.50	283.40	61.20	73.76	114.89
Min	82.22	39.12	75.30	47.26	43.74	389.20	372.40	65.35	76.32	44.59	285.10	281.30	50.30	71.04	103.98
Mean	88.05	41.32	82.89	52.20	46.17	402.75	393.83	68.04	79.14	45.96	288.23	282.52	54.78	71.99	109.80
<i>Bos gaurus</i> (N=6)															
Max	107.54	56.43	103.42	69.94	60.98	470.60	461.70	88.76	96.43	58.43	345.60	328.60	67.68	90.12	137.40
Min	90.31	46.45	80.33	53.26	48.24	414.85	415.70	72.96	84.93	49.64	291.30	281.40	56.42	71.45	86.43
Mean	97.23	50.39	92.17	59.82	53.57	439.98	432.00	80.35	88.83	53.83	320.88	310.42	60.96	79.86	114.21
<i>Bubalus arnee</i> (N=6)															
Max	86.89	45.55	81.67	64.24	51.84	411.20	385.40	78.73	76.52	50.66	293.50	292.60	60.43	78.24	112.34
Min	77.01	41.45	73.23	53.10	43.07	377.40	372.30	70.68	70.91	46.32	283.10	281.20	48.44	68.09	95.47
Mean	81.86	43.36	77.95	58.93	46.51	393.25	380.40	74.37	73.89	48.47	288.32	287.23	54.81	72.12	104.12
	PL/Bp	PL/Dp	PL/Bd	PL/Dd	Bp/Bd	Dd/Dp	Bp/Dp	Bd/Dd	Bp/BFP	Bd/BFd	GL/LO				
<i>Axis axis</i> (N=8)															
Max	4.87	9.86	5.33	7.65	1.15	1.48	2.14	1.52	1.18	1.22	5.31				
Min	3.93	7.81	4.30	5.45	1.04	1.27	1.91	1.22	1.10	1.08	4.68				
Mean	4.59	9.16	4.98	6.73	1.09	1.37	2.00	1.35	1.13	1.15	4.93				
<i>Axis porcinus</i> (N=4)															
Max	4.42	9.43	5.13	7.53	1.29	1.86	2.17	1.47	1.16	1.09	4.59				
Min	3.97	7.77	4.89	5.08	1.16	1.08	1.94	1.00	1.10	1.00	4.11				
Mean	4.19	8.72	5.05	6.23	1.21	1.46	2.08	1.23	1.13	1.06	4.36				
<i>Panolia eldii</i> (N=3)															
Max	5.06	10.34	5.59	7.99	1.11	1.32	2.04	1.47	1.11	1.08	5.47				

Table A10 (continued). Measurements (in millimeters) of radii and ulnae of extant ruminants from Southeast Asia.

Min	5.04	9.95	5.43	7.70	1.08	1.29	1.97	1.39	1.11	1.06	5.07		
Mean	5.05	10.19	5.51	7.84	1.09	1.30	2.02	1.42	1.11	1.07	5.32		
<i>Rusa unicolor</i> (N=4)													
Max	4.20	9.01	4.92	6.35	1.18	1.43	2.14	1.34	1.14	1.17	5.15		
Min	4.04	7.63	4.42	5.87	1.07	1.30	1.88	1.28	1.08	1.06	4.60		
Mean	4.13	8.32	4.67	6.11	1.13	1.36	2.01	1.31	1.11	1.11	4.86		
<i>Bos sauveli</i> (N=4)													
Max	3.62	8.93	4.17	5.60	1.15	1.59	2.51	1.48	1.14	1.13	3.97		
Min	3.55	7.38	3.79	4.90	1.06	1.50	2.04	1.18	1.09	1.03	3.01		
Mean	3.59	8.13	3.97	5.25	1.11	1.55	2.27	1.33	1.12	1.08	3.49		
<i>Bos javanicus</i> (N=6)													
Max	3.49	7.32	3.81	6.16	1.11	1.46	2.17	1.78	1.15	1.29	3.74		
Min	3.13	6.75	3.18	5.01	0.99	1.10	2.10	1.32	1.07	1.15	3.59		
Mean	3.28	6.99	3.49	5.56	1.06	1.27	2.13	1.60	1.11	1.22	3.67		
<i>Bos gaurus</i> (N=6)													
Max	3.58	6.97	4.03	6.08	1.12	1.25	1.96	1.64	1.12	1.17	4.80		
Min	3.13	5.99	3.18	4.94	1.01	1.14	1.90	1.48	1.06	1.09	3.42		
Mean	3.31	6.38	3.51	5.40	1.06	1.18	1.93	1.54	1.09	1.15	3.96		
<i>Bubalus arnee</i> (N=6)													
Max	3.68	6.84	3.87	5.39	1.06	1.55	1.95	1.48	1.17	1.07	3.96		
Min	3.38	6.44	3.59	4.41	1.03	1.21	1.84	1.14	1.07	1.04	3.50		
Mean	3.53	6.66	3.70	4.92	1.05	1.36	1.89	1.33	1.11	1.05	3.79		

Table A11. Measurements (in millimeters) of metacarpi of extant ruminants from Southeast Asia.

	Bp	Dp	Bd	Dd	SD	GL	GLL	LL	DD	GL/Bp	GL/Dp	GL/Bd	GL/Dd	Bp/Bd	Dp/Dd	Bp/Dp	Bd/Dd
<i>Axis axis</i> (N=8)																	
Max	28.75	19.36	28.03	17.75	18.20	174.30	172.80	169.00	17.55	6.52	9.77	7.69	12.69	1.26	1.36	1.59	1.88
Min	25.13	17.23	22.56	13.59	14.18	162.10	159.50	156.70	12.33	6.06	8.74	6.22	9.52	1.03	1.02	1.35	1.30
Mean	26.94	18.25	24.86	16.24	15.66	169.30	167.04	164.05	14.58	6.29	9.28	6.83	10.52	1.09	1.13	1.48	1.54
<i>Axis porcinus</i> (N=4)																	
Max	23.14	15.71	23.60	14.61	14.18	120.80	116.88	118.82	11.76	5.68	7.92	5.81	8.82	1.06	1.14	1.59	1.76
Min	21.28	14.43	20.79	13.38	12.63	111.00	109.20	107.80	9.42	4.83	7.45	4.70	7.66	0.97	1.03	1.36	1.50
Mean	22.18	15.11	21.77	13.86	13.39	115.99	113.35	113.52	10.62	5.25	7.68	5.35	8.38	1.02	1.09	1.47	1.57
<i>Panolia eldii</i> (N=4)																	
Max	34.01	20.89	29.98	20.66	18.08	224.80	222.50	221.30	17.58	7.18	11.33	7.82	11.20	1.18	1.06	1.72	1.49
Min	30.61	19.81	28.11	19.64	17.60	219.80	216.20	214.40	15.06	6.60	10.52	7.50	10.87	1.08	0.96	1.47	1.40
Mean	32.22	20.32	28.83	20.04	17.82	222.25	219.48	217.63	16.45	6.91	10.95	7.71	11.09	1.12	1.01	1.59	1.44
<i>Rusa unicorn</i> (N=4)																	
Max	42.02	28.45	41.13	27.81	24.99	234.30	230.40	226.70	22.07	5.77	8.24	5.96	8.84	1.03	1.11	1.48	1.54
Min	36.43	26.66	35.35	24.08	22.19	210.20	205.10	203.50	19.54	5.55	7.83	5.70	8.43	1.02	1.02	1.36	1.46
Mean	39.22	27.58	38.11	25.60	23.42	221.95	217.60	214.95	20.69	5.67	8.04	5.83	8.68	1.03	1.08	1.42	1.49
<i>Bos sauveli</i> (N=2)																	
Max	65.72	36.61	57.43	32.87	36.44	249.10	246.40	241.50	29.43	3.81	6.82	4.35	7.68	1.15	1.13	1.80	1.77
Min	65.44	36.54	57.09	32.45	36.23	248.40	245.30	241.20	29.22	3.78	6.79	4.34	7.56	1.14	1.11	1.79	1.74
Mean	65.58	36.58	57.26	32.66	36.34	248.75	245.85	241.35	29.33	3.79	6.80	4.34	7.62	1.15	1.12	1.79	1.75

Table A11 (continued). Measurements (in millimeters) of metacarpi of extant ruminants from Southeast Asia.

<i>Bos javanicus</i> (N=6)																	
Max	66.76	40.44	60.38	39.84	39.86	225.20	214.30	215.10	27.71	3.76	6.46	4.09	6.86	1.11	1.16	1.74	1.69
Min	59.28	34.48	54.45	32.45	34.21	215.30	206.10	205.70	26.03	3.37	5.53	3.73	5.65	1.09	1.01	1.58	1.51
Mean	62.88	37.73	57.30	35.67	37.25	222.10	212.44	211.66	26.84	3.54	5.92	3.88	6.27	1.10	1.06	1.67	1.61
<i>Bos gaurus</i> (N=6)																	
Max	75.52	43.88	69.11	40.81	51.55	251.50	247.20	239.10	33.49	3.78	6.24	4.14	6.61	1.12	1.11	1.76	1.75
Min	66.25	39.22	60.68	37.86	39.04	226.50	218.20	215.10	28.44	3.28	5.73	3.35	5.87	1.02	1.02	1.60	1.59
Mean	70.36	41.52	65.83	39.08	44.16	242.95	235.85	230.37	31.13	3.46	5.85	3.70	6.22	1.07	1.06	1.70	1.68
<i>Bubalus arnee</i> (N=6)																	
Max	68.11	42.38	74.01	38.81	45.12	195.20	186.60	180.60	28.92	2.97	6.08	2.79	5.43	0.97	1.10	2.12	1.98
Min	61.63	31.14	66.52	33.77	30.97	182.80	170.70	172.40	24.32	2.87	4.57	2.61	4.99	0.91	0.85	1.58	1.91
Mean	65.18	33.89	69.73	35.89	36.91	189.60	178.42	176.14	25.74	2.91	5.66	2.72	5.29	0.93	0.94	1.94	1.94

Table A12. Measurements (in millimeters) of femora of extant ruminants from Southeast Asia.

	Bp	Dp	Bd	Dd	SD	GL	GLC	DC	GL/Bp	GL/Dp	GL/Bd	GL/Dd	Bp/Bd	Dd/Dp	Bp/Dp	Dd/Bd
<i>Axis axis</i> (N=6)																
Max	55.93	27.30	47.01	65.81	18.53	219.70	209.20	24.02	4.24	8.93	4.94	3.52	1.26	2.56	2.15	1.49
Min	49.76	23.63	43.72	59.88	17.31	210.90	198.20	22.35	3.90	8.05	4.63	3.32	1.11	2.35	2.02	1.33
Mean	53.26	25.66	45.37	63.15	18.09	215.97	204.03	23.32	4.06	8.43	4.76	3.42	1.17	2.46	2.08	1.39
<i>Axis porcinus</i> (N=2)																
Max	47.14	23.25	38.75	56.33	16.43	183.60	173.40	19.77	3.89	8.14	4.84	3.26	1.24	2.50	2.10	1.49
Min	46.71	22.26	37.91	55.71	16.04	181.20	172.70	19.36	3.88	7.90	4.68	3.25	1.21	2.42	2.03	1.44
Mean	46.93	22.76	38.33	56.02	16.24	182.40	173.05	19.57	3.89	8.02	4.76	3.26	1.22	2.46	2.06	1.46
<i>Panolia eldii</i> (N=4)																
Max	66.06	30.81	52.98	73.65	22.92	267.70	253.10	26.77	4.05	8.83	5.06	3.63	1.25	2.43	2.18	1.44
Min	60.54	30.30	49.74	71.12	21.50	241.40	225.30	24.54	3.99	7.85	4.85	3.39	1.22	2.31	1.97	1.39
Mean	63.29	30.55	51.36	72.45	22.19	254.63	239.35	25.63	4.02	8.34	4.96	3.51	1.23	2.37	2.07	1.41
<i>Rusa unicorn</i> (N=4)																
Max	91.36	44.39	76.39	102.41	32.56	354.80	336.20	38.43	4.27	8.15	4.75	4.18	1.21	2.35	2.08	1.34
Min	74.13	42.25	66.99	76.12	26.90	316.30	296.70	32.08	3.87	7.45	4.64	3.46	1.09	1.78	1.75	1.13
Mean	82.68	43.23	71.67	88.78	29.58	335.80	316.10	35.29	4.08	7.76	4.69	3.83	1.15	2.05	1.91	1.23
<i>Bos sauveli</i> (N=4)																
Max	131.83	69.02	99.92	132.22	46.31	408.20	389.50	48.12	3.44	5.92	4.09	3.11	1.32	2.04	1.91	1.33
Min	106.60	62.94	96.44	128.62	31.30	366.20	347.10	46.27	3.10	5.79	3.80	2.85	1.11	1.90	1.69	1.31
Mean	118.88	66.04	98.18	130.18	38.61	387.23	368.30	47.09	3.27	5.86	3.94	2.97	1.21	1.97	1.80	1.33

Table A12 (continued). Measurements (in millimeters) of femora of extant ruminants from Southeast Asia.

<i>Bos javanicus</i> (N=6)																
Max	134.88	72.44	105.98	135.67	48.37	427.30	395.10	55.28	3.30	6.12	4.09	3.17	1.32	1.94	1.98	1.30
Min	124.52	63.45	94.81	122.95	38.89	387.10	363.70	51.97	3.09	5.76	3.94	3.10	1.22	1.86	1.85	1.25
Mean	128.18	67.43	100.88	129.08	43.23	406.38	381.20	53.46	3.17	6.03	4.03	3.15	1.27	1.92	1.90	1.28
<i>Bos gaurus</i> (N=6)																
Max	151.32	93.76	124.94	156.78	49.63	483.20	458.70	59.27	3.68	6.69	4.19	3.18	1.31	2.26	1.90	1.32
Min	115.19	63.46	108.35	142.42	43.55	423.70	428.70	37.88	3.19	5.15	3.77	2.96	1.04	1.67	1.61	1.25
Mean	135.93	77.41	115.22	147.53	45.77	452.82	440.95	54.42	3.35	5.94	3.93	3.07	1.18	1.94	1.77	1.28
<i>Bubalus arnee</i> (N=6)																
Max	131.65	69.14	105.25	134.59	47.78	386.20	378.10	51.44	2.95	5.73	3.68	3.04	1.25	1.98	1.95	1.29
Min	123.63	67.17	101.98	125.25	39.52	353.70	336.50	49.23	2.86	5.22	3.46	2.81	1.21	1.86	1.82	1.21
Mean	128.81	67.82	104.06	129.11	42.99	374.52	361.50	50.72	2.91	5.52	3.60	2.90	1.24	1.90	1.90	1.24

Table A13. Measurements (in millimeters) of tibiae of extant ruminants from Southeast Asia.

	Bp	Dp	Bd	Dd	SD	GL	LL	GL/Bp	GL/Dp	GL/Bd	GL/Dd	Bp/Bd	Dp/Dd	Bp/Dp	Bd/Dd
<i>Axis axis</i> (N=6)															
Max	52.61	49.43	34.89	24.24	19.97	222.20	240.10	4.51	4.97	7.07	9.61	1.65	2.16	1.14	1.56
Min	48.92	42.77	30.03	22.11	17.98	209.60	226.40	4.09	4.44	6.17	9.14	1.45	1.89	0.99	1.33
Mean	50.12	46.99	32.48	23.06	18.62	216.52	232.87	4.32	4.62	6.68	9.39	1.55	2.04	1.07	1.41
<i>Axis porcinus</i> (N=4)															
Max	43.79	43.73	28.22	22.21	17.11	207.90	198.30	4.77	5.18	7.88	9.42	1.66	2.08	1.08	1.35
Min	41.22	40.05	26.36	20.53	16.80	182.70	192.30	4.41	4.18	6.47	8.65	1.46	1.82	0.94	1.19
Mean	42.51	41.84	27.15	21.47	16.98	195.33	195.55	4.59	4.68	7.21	9.09	1.57	1.95	1.02	1.27
<i>Panolia eldii</i> (N=4)															
Max	58.99	59.38	37.56	29.35	21.62	294.80	285.40	5.02	5.14	7.86	10.35	1.68	2.03	1.03	1.32
Min	58.01	57.40	34.96	28.46	20.65	274.30	258.00	4.66	4.62	7.83	9.36	1.56	2.01	0.98	1.19
Mean	58.63	58.29	36.27	28.88	21.09	284.65	271.75	4.85	4.89	7.85	9.86	1.62	2.02	1.01	1.26
<i>Rusa unicorn</i> (N=4)															
Max	84.53	83.90	51.92	43.54	30.12	334.60	354.40	4.00	4.47	6.66	8.22	1.68	1.97	1.12	1.35
Min	73.20	65.43	47.48	35.53	28.83	291.90	316.80	3.96	3.97	6.06	7.68	1.53	1.83	0.99	1.15
Mean	78.67	74.36	49.45	39.37	29.44	313.13	335.33	3.98	4.24	6.33	7.97	1.59	1.88	1.06	1.26
<i>Bos sauveli</i> (N=4)															
Max	102.24	92.12	73.59	49.56	44.92	398.30	364.90	3.90	4.55	5.82	8.20	1.55	1.86	1.17	1.51
Min	98.75	87.54	63.92	48.58	38.54	372.20	311.60	3.76	4.04	5.40	7.51	1.39	1.80	1.07	1.29
Mean	100.51	89.86	68.80	49.12	41.72	384.98	338.15	3.83	4.29	5.61	7.84	1.47	1.83	1.12	1.40

Table A13 (continued). Measurements (in millimeters) of tibiae of extant ruminants from Southeast Asia.

<i>Bos javanicus</i> (N=6)															
Max	106.11	97.35	69.35	56.17	46.06	414.50	364.70	3.91	4.28	6.23	7.63	1.61	1.81	1.10	1.24
Min	100.05	96.02	64.88	53.01	38.60	385.30	354.80	3.83	3.96	5.80	6.86	1.51	1.73	1.03	1.18
Mean	103.61	96.78	66.86	55.09	42.05	401.23	360.73	3.87	4.15	6.00	7.29	1.55	1.76	1.07	1.21
<i>Bos gaurus</i> (N=6)															
Max	130.17	107.70	75.51	60.10	57.06	449.70	396.30	3.66	4.22	5.99	7.81	1.73	1.87	1.21	1.31
Min	113.50	98.40	72.50	57.60	46.00	415.40	351.70	3.45	4.18	5.69	7.10	1.56	1.69	1.15	1.23
Mean	120.97	103.27	74.01	58.39	50.25	432.45	373.75	3.58	4.19	5.84	7.41	1.63	1.77	1.17	1.27
<i>Bubalus arnee</i> (N=6)															
Max	107.80	103.58	71.90	53.37	48.92	367.20	340.50	3.53	4.40	5.30	7.07	1.56	1.99	1.25	1.44
Min	101.53	82.14	67.68	47.10	40.71	324.10	294.70	3.11	3.45	4.77	6.78	1.41	1.58	1.04	1.30
Mean	104.67	93.55	69.57	50.67	45.08	350.18	316.90	3.35	3.77	5.03	6.91	1.51	1.85	1.13	1.38

Table A14. Measurements (in millimeters) of metatarsi of extant ruminants from Southeast Asia.

	Bp	Dp	Bd	Dd	SD	GL	GLL	LI	DD	GL/Bp	GL/Dp	GL/Bd	GL/Dd	Bp/Bd	Dp/Dd	Bp/Dp	Bd/Dd
<i>Axis axis</i> (N=6)																	
Max	24.36	26.28	26.56	18.15	17.76	187.80	185.40	182.50	15.25	8.00	7.74	7.53	12.97	0.96	1.80	0.98	1.72
Min	23.38	24.26	24.86	14.43	13.97	180.10	179.60	175.50	13.48	7.50	6.95	6.91	10.06	0.90	1.42	0.90	1.40
Mean	23.81	25.46	25.78	16.72	15.32	184.22	182.05	179.68	14.31	7.74	7.24	7.15	11.12	0.92	1.53	0.94	1.55
<i>Axis porcinus</i> (N=4)																	
Max	23.95	22.96	24.00	15.63	13.45	143.46	139.93	139.08	13.56	6.69	6.74	6.25	9.32	1.02	1.53	1.08	1.55
Min	21.44	21.27	22.94	15.01	12.37	130.90	129.40	128.30	12.56	5.48	5.70	5.52	8.47	0.93	1.37	1.01	1.48
Mean	22.70	21.96	23.32	15.41	13.08	137.47	134.71	133.73	13.15	6.09	6.28	5.90	8.92	0.97	1.43	1.03	1.51
<i>Panolia eldii</i> (N=4)																	
Max	30.76	29.92	29.58	19.81	17.68	237.80	235.30	230.80	18.82	8.39	8.22	8.06	12.18	1.04	1.53	1.04	1.52
Min	27.27	27.84	28.52	19.49	16.88	228.10	224.80	218.80	17.02	7.72	7.95	7.99	11.51	0.96	1.41	0.98	1.44
Mean	29.01	28.80	29.04	19.60	17.28	232.95	229.80	224.73	17.80	8.05	8.09	8.02	11.89	1.00	1.47	1.01	1.48
<i>Rusa unicolor</i> (N=4)																	
Max	40.63	36.93	42.15	29.40	24.01	258.20	254.60	246.60	28.47	6.52	6.99	6.19	8.83	0.96	1.38	1.11	1.44
Min	34.82	35.34	36.63	25.66	23.56	226.70	223.50	220.10	24.56	6.32	6.34	6.08	8.64	0.95	1.25	0.97	1.40
Mean	37.68	36.16	39.38	27.66	23.69	241.93	238.58	233.05	26.40	6.43	6.69	6.15	8.75	0.96	1.31	1.04	1.42
<i>Bos sauveli</i> (N=2)																	
Max	53.65	51.21	52.82	33.45	31.96	282.60	273.50	263.70	32.34	5.28	5.53	5.36	8.47	1.02	1.53	1.05	1.58
Min	53.44	51.07	52.67	33.36	31.85	282.40	273.10	263.40	32.20	5.27	5.51	5.35	8.44	1.01	1.53	1.04	1.57
Mean	53.55	51.14	52.75	33.41	31.91	282.50	273.30	263.55	32.27	5.28	5.52	5.36	8.46	1.02	1.53	1.05	1.58

Table A14 (continued). Measurements (in millimeters) of metatarsi of extant ruminants from Southeast Asia.

<i>Bos javanicus</i> (N=6)																	
Max	54.98	51.89	55.74	37.28	35.52	257.80	246.40	246.90	32.40	5.14	5.56	5.12	7.58	1.00	1.49	1.08	1.55
Min	48.30	46.33	50.31	33.94	30.30	243.00	234.00	230.80	29.05	4.59	4.78	4.53	6.77	0.90	1.35	0.95	1.46
Mean	51.13	49.68	53.05	35.21	33.34	250.98	238.20	236.65	30.41	4.92	5.07	4.74	7.14	0.96	1.41	1.03	1.51
<i>Bos gaurus</i> (N=6)																	
Max	60.25	59.22	64.81	41.66	42.06	273.10	265.70	261.20	36.04	4.85	5.33	4.34	7.18	0.94	1.50	1.14	1.66
Min	52.35	50.30	61.89	37.36	35.48	254.00	245.70	239.10	32.84	4.43	4.61	3.92	6.10	0.81	1.21	1.02	1.56
Mean	57.31	53.27	63.77	39.75	38.00	265.57	257.70	251.92	34.65	4.64	5.00	4.17	6.70	0.90	1.34	1.08	1.61
<i>Bubalus arnee</i> (N=6)																	
Max	57.42	49.56	66.93	37.74	37.03	226.40	213.50	206.80	33.13	4.05	4.67	3.41	6.47	0.86	1.41	1.20	1.91
Min	52.56	46.69	62.34	34.87	32.31	212.80	198.20	200.80	30.30	3.91	4.54	3.34	5.92	0.84	1.27	1.13	1.76
Mean	55.45	48.13	65.28	36.01	34.84	221.17	208.05	203.58	31.39	3.99	4.59	3.39	6.15	0.85	1.34	1.15	1.81

Table A15. Measurements (in millimeters) of mandibles of large bovids from Khok Sung. Numbers within the parentheses refer to the numbers used in von den Driesch's metrical methods (1976: fig. 21). * indicates measurements of the maximum length of the preservation according to incomplete specimens. "es" refers to an estimated value of the full length due to incomplete specimens.

Taxon	<i>Bos sauveli</i>		<i>Bos gaurus</i>		<i>Bubalus arnee</i>				
	DMR-KS-05-03-9-1	DMR-KS-05-04-9-1	DMR-KS-05-03-00-1	DMR-KS-05-04-3-1	DMR-KS-05-03-20-10	DMR-KS-05-03-20-20	DMR-KS-05-03-20-2	DMR-KS-05-03-10-3	DMR-KS-05-03-20-1
Mandible no.			1						
Metrical parameters (mm)									
(1) Length from the angle: Gonion caudale–infradentale	450*	446.21	–	–	Juvenile	–	–	461.14	464.54
(2) Length from the condyle: aboral border of the condyle process–infradentale	483.55	478.08	–	–	371.28*	–	–	490.82	493.34
(3) Length: Gonion caudale–aboral border of the alveolus of m3	132.51	122.31	–	137.11	83.57	–	94.92	126.23	127.48
(4) Length of the horizontal ramus: aboral border of the alveolus of m3–infradentale	313.60	312.1	–	–	278.91*	–	–	324.52	325.67
(5) Length: Gonion caudale–oral border of the alveolus of p2	307.52	289.11	–	305.44	245.18	–	–	301.04	299.77
(6) Length: Gonion caudale–the most aboral indentation of the mental foramen	397.32	356.52	–	–	311.78	–	–	375.44	374.89
(7) Length of the cheek tooth row; measured along the alveoli on the buccal side	169.58	165.66	–	171.58	–	–	–	173.72	174.52
(8) Length of the molar row; measured along the alveoli	107.01	103.86	101.01	109.10	–	–	–	111.57	113.69

Table A16. Measurements (in millimeters) of crania of *Bubalus arnee* from Khok Sung. Numbers within the parentheses refer to the numbers used in von den Driesch's metrical methods (1976: fig. 8). * indicates measurements of the maximum length of the preservation according to incomplete specimens. "es" refers to an estimated value of the full length due to incomplete specimens.

Taxon	<i>Bubalus arnee</i>			
	DMR-KS-05-03-16-3	DMR-KS-05-03-21-1	DMR-KS-05-03-11-1	DMR-KS-05-03-20-1
Cranium no.				
Metrical parameters (mm)				
(1) Total length: Akrokranium–Prosthion	-	-	-	568.97
(2) Condylbasal length: aboral border of the occipital condyles–Prosthion	-	-	-	565.98*
(3) Basal length: Basion–Prosthion	-	-	-	553.31
(4) Short skull length: Basion–Premolare	-	426.18	-	381.21
(5) Premolar–Prosthion	-	-	-	185.07
(6) Neurocranium length: Basion–Nasion	-	230 (es)	-	246.53
(7) Viscerocranium length: Nasion–Prosthion	-	-	-	344.25
(8) Median frontal length: Akrokranium–Nasion	-	-	-	206.61
(9) Greatest frontal length: Akrokranium–the median point of intersection of the line joining the oral points of the frontals	-	-	-	248.82
(10) Short upper cranium length: Akrokranium–Rhinion	-	-	-	440.31
(11) Akrokranium–Infraorbitale of one side	-	-	-	385.55
(12) Greatest length of the nasals: Nasion–Rhinion	-	-	-	230.87
(13) From the aboral border of one occipital condyle to the Entorbitale of the same side	-	263.18	-	243.75
(14) Lateral facial length: Entorbitale–Prosthion	-	-	-	389.11
(15) From the aboral border of one occipital condyle to the Infraorbitale of the same side	-	-	-	390.16

Table A16 (continued). Measurements (in millimeters) of crania of *Bubalus arnee* from Khok Sung. Numbers within the parentheses refer to the numbers used in von den Driesch's metrical methods (1976: fig. 8). * indicates measurements of the maximum length of the preservation according to incomplete specimens. "es" refers to an estimated value of the full length due to incomplete specimens.

(16) Infraorbitale-Prosthion	168.66	-	-	181.36
(17) Dental length: Postdentale-Prosthion	-	-	-	341.43
(18) Oral palatal length: Palatinoorale-Prosthion	-	-	-	272.03
(19) Lateral length of the premaxilla: Nasointermaxillare-Prosthion	-	-	-	197.68
(20) Length of the cheek tooth row (measured along the alveoli)	-	-	169.58 (right)	165.56 (left)
(21) Length of the molar row (measured along the alveoli on the buccal side)	-	110 (es) (right)	98.06 (right)	102.63 (left)
(22) Length of the premolar row (measured along the alveoli on the buccal side)	62.56 (right), 62.09 (left)	-	70.34 (right)	65.76 (right), 68.70 (left)
(23) Greatest inner length of the orbit: Ectorbitale-Entorbitale	-	-	-	67.73 (right), 68.26 (left)
(24) Greatest inner height of the orbit	-	-	-	55.51 (right), 61.44 (left)
(25) Greatest mastoid breadth: Otion-Otion	-	188.71	-	-
(26) Greatest breadth of the occipital condyles	-	106.59	-	-
(27) Greatest breadth at the bases of the paraoccipital processes	-	154.23	-	-
(28) Greatest breadth of the foramen magnum	-	47.38	-	-
(29) Height of the foramen magnum: Basion-Opisthion	-	40.96	-	-
(30) Least occipital breadth: the distance between the most medial points of the aboral borders of the temporal grooves	-	117.35	-	93.06
(31) Least breadth between the bases of the horn cores	-	129.32	-	151.45
(32) Least frontal breadth: breadth of the narrowest part of the frontal aboral of the orbits	-	210 (es)	-	222.23
(33) Greatest breadth across the orbits = Greatest frontal breadth = greatest breadth of skull: Ectorbitale-Ectorbitale	-	-	-	231.78
(34) Least breadth between the orbits: Entorbitale-Entorbitale	-	-	-	165.52

Table A16 (continued). Measurements (in millimeters) of crania of *Bubalus arnee* from Khok Sung. Numbers within the parentheses refer to the numbers used in von den Driesch's metrical methods (1976: fig. 8). * indicates measurements of the maximum length of the preservation according to incomplete specimens. "es" refers to an estimated value of the full length due to incomplete specimens.

(35) Facial breadth: across the facial tuberosities	-	-	-	167.42
(36) Greatest breadth across the nasals	-	-	-	64.01
(37) Breadth across the premaxillae on the oral protuberances	-	-	-	112.89
(38) Greatest palatal breadth: measured across the outer borders of the alveoli	-	-	-	148.14
(39) Least inner height of the temporal groove, roughly from the middle of one bone edge to the other	-	40.08	-	24.57
(40) Greatest height of the occipital region: Basion-highest point of the intercornual ridge in the median plane	-	139.25	-	-
(41) Least height of the occipital region: Opisthion-highest point of the intercornual ridge in the median plane	-	115.68	-	138.74
(42) Distance between the horn core tips	-	540 (es)	-	607.18
(43) Greatest tangential distance between the outer curves of the horn cores	-	-	-	341.38 (right), 333.17 (left)
(44) Horn core basal circumference	-	199.91 (left)	-	341.38 (right)
(45) Greatest (oro-aboral) diameter of the horn core base	-	72.03 (right), 70.77 (left)	-	132.71 (right), 131.53 (left)
(46) Least (dorso-basal) diameter of the horn core base	-	44.67 (right), 49.49 (left)	-	56.05 (right), 53.45 (left)
(47) Length of the outer curvature of the horn core	-	102.21 (right), 258.17 (left)	-	164* (right), 215* (left)

Table A17. Fauna lists of large mammalian species from the Middle Pleistocene of Central eastern and South China. Locality abbreviations: **YCK**, Yenchingkou; **KLS**, Koloshan; **WM**, Wuming; **DX**, Daxin; **HJ**, Hejiang; **GX**, Ganxian; **PXDD**, Panxian Dadong; **WY**, Wuyun; **MB**, Maba; **HST**, Hoshantung; **HG**, Hsingan. The fauna lists and ages follow Colbert and Hooijer (1953) for YCK; Kahlke (1961) for KLS, HST, and HG; Rink et al. (2008) for WM and DX; Zhang et al. (2014) for HJ; Wang et al. (2014) for GX; Han and Xu (1985), Bekken et al. (2004), and Schepartz et al. (2005) for PXDD; Chen et al. (2002), Rink et al. (2008), and Wang et al. (2014) for WY; Han and Xu (1985), Wu et al. (2011), and Shen et al. (2014) for MB. The subspecies-level identifications are not taken into account.

Region	Central eastern China				South China							
	YCK	KLS	WM	DX	HJ	GX	PXDD	WY	MB	HST	HG	
Locality												
Approximate age (ka)			745 to 481	380 to 308	400 to 320	>350	300 to 130	279 to 76	>230			
Taxa												
PRIMATES												
<i>Macaca</i> sp.			+	+	+			+	+	+		
<i>Macaca assamensis</i>							cf.					
<i>Macaca robustus</i>		+										
<i>Macaca arctoides</i>							+					
Colobinae indet.							+					
<i>Presbytis</i> sp.								+				
<i>Rhinopithecus</i> sp.				+								
<i>Rhinopithecus roxellana</i>	+								+			
<i>Trachypithecus</i> sp.					+							
<i>Nomascus</i> sp.					+							
<i>Hylobates</i> sp.				+								
<i>Bunopithecus sericus</i>	+											
<i>Szechuanopithecus yangtsensis</i>		+										
<i>Pongo</i> sp.				+			+		+			
<i>Pongo pygmaeus</i>						+		+		+		+

Table A17 (continued). Fauna lists of large mammalian species from the Middle Pleistocene of Central eastern and South China. Locality abbreviations: **YCK**, Yenchingkou; **KLS**, Koloshan; **WM**, Wuming; **DX**, Daxin; **HJ**, Hejiang; **GX**, Ganxian; **PXDD**, Panxian Dadong; **WY**, Wuyun; **MB**, Maba; **HST**, Hoshantung; **HG**, Hsingan. The fauna lists and ages follow Colbert and Hooijer (1953) for YCK; Kahlke (1961) for KLS, HST, and HG; Rink et al. (2008) for WM and DX; Zhang et al. (2014) for HJ; Wang et al. (2014) for GX; Han and Xu (1985), Bekken et al. (2004), and Schepartz et al. (2005) for PXDD; Chen et al. (2002), Rink et al. (2008), and Wang et al. (2014) for WY; Han and Xu (1985), Wu et al. (2011), and Shen et al. (2014) for MB. The subspecies-level identifications are not taken into account.

Locality	YCK	KLS	WM	DX	HJ	GX	PXDD	WY	MB	HST	HG
<i>Palaeoloxodon namadicus</i>	+								+		
PERISSODACTYLA											
<i>Tapirus</i> sp.									+		
<i>Tapirus indicus</i>					+						+
<i>Tapirus sinensis</i>								+			
<i>Megatapirus augustus</i>	+	+		+			+	+	+		
Rhinocerotidae indet.											
<i>Rhinoceros</i> sp.											
<i>Rhinoceros unicornis</i>	?									+	
<i>Rhinoceros sinensis</i>	+	+	+	+	+		+		+		
<i>Rhinoceros fusuiensis</i>						+		+			
ARTIODACTYLA											
<i>Sus</i> sp.		+	+	+			+		+	+	+
<i>Sus scrofa</i>	+		+		+	+		+	+		
<i>Sus xiaozhu</i>					+	+					
<i>Sus bijianhanensis</i>			+	+							
<i>Dicoryphochoerus ultimus</i>				+							
Cervidae indet.		+					+			+	
<i>Cervus</i> sp. or <i>Rusa</i> sp.				+		+		+			
<i>Cervus yunnanensis</i>						+					

Table A17 (continued). Fauna lists of large mammalian species from the Middle Pleistocene of Central eastern and South China. Locality abbreviations: **YCK**, Yenchingkou; **KLS**, Koloshan; **WM**, Wuming; **DX**, Daxin; **HJ**, Hejiang; **GX**, Ganxian; **PXDD**, Panxian Dadong; **WY**, Wuyun; **MB**, Maba; **HST**, Hoshantung; **HG**, Hsingan. The fauna lists and ages follow Colbert and Hooijer (1953) for YCK; Kahlke (1961) for KLS, HST, and HG; Rink et al. (2008) for WM and DX; Zhang et al. (2014) for HJ; Wang et al. (2014) for GX; Han and Xu (1985), Bekken et al. (2004), and Schepartz et al. (2005) for PXDD; Chen et al. (2002), Rink et al. (2008), and Wang et al. (2014) for WY; Han and Xu (1985), Wu et al. (2011), and Shen et al. (2014) for MB. The subspecies-level identifications are not taken into account.

Locality	YCK	KLS	WM	DX	HJ	GX	PXDD	WY	MB	HST	HG
<i>Rusa unicolor</i>	+				cf.		+		+		
<i>Elaphodus cephalophus</i>	+										
<i>Muntiacus</i> sp.				+	+		+			+	
<i>Muntiacus muntjak</i>	+								+		
<i>Muntiacus szechuanensis</i>		+									
<i>Hydropotes</i> sp.									+		
<i>Mochus</i> sp.							+				
<i>Mochus moschiferus</i>	+										
Bovidae indet.			+			+		+		+	+
<i>Bos</i> sp. or <i>Bubalus</i> sp.				+	+		+		+		
<i>Bos gaurus</i>	+										
<i>Bubalus arnee</i>	+										
<i>Bubalus brevicornis</i>		+									
Caprinae indet.		+		+						+	
<i>Capricornis sumatraensis</i>	+		cf.				+	+			
<i>Naemorhedus goral</i>	+						+				
<i>Megalotivis guangxiensis</i>				+	+		+				

Table A18. Fauna lists of large mammalian species from the Middle Pleistocene of Southeast Asia. Locality abbreviations: **KS**, Khok Sung; **TWN**, Thum Wiman Nakin; **TPKP**, Thum Phra Khai Phet; **KPN**, Kao Pah Nam; **TPD**, Thum Phedan; **TK**, Tham Khuyen; **TH**, Tham Hai; **TO**, Tham Om; **MG**, Mogok Caves; **PNL**, Phnom Loang; **BDB**, Boh Dambang; **BDC**, Badak Cave; **TB**, Tambun (Kinta Valley); **KDBB**, Kedung Brubus; **TNHK**, Trinil Hauptknochenschicht; **ND**, Ngandong. The fauna lists and ages follow Tougard (2001) and Esposito et al. (1998, 2002) for TWN; Tougard (1998) and Filoux et al. (2015) for TPKP; Pope et al. (1981) for KPN; Yamee and Chaimanee (2005) for TPD; Olsen and Ciochon (1990), Ciochon et al. (1996), and Ciochon (2009) for TK, TH, and TO; Colbert (1938, 1943) and Takai et al. (2006) for MG; Beden and Guérin (1973) for PNL; Demeter et al. (2013) for BDB; Ibrahim et al. (2013) for BDC; Hooijer (1962) and Medway (1972) for TB; van den Bergh et al. (2001) for KDBB; van den Bergh et al. (2001) and Joordens et al. (2015) for TNHK; and Santa Luca (1980), van den Bergh et al. (2001), and Indriati et al. (2011) for ND. The subspecies-level identifications are not taken into account.

Country	Thailand				Vietnam			Myanmar		Cambodia		Malaysia		Indonesia		
	KS	TWN	TPKP	KPN	TPD	TK	TH	TO	MG	PNL	BDB	BDC	TB	KDBB	TNHK	ND
Locality	213 to 120	>169 ± 11	≈TWN	≈690		475 ± 125	≈TK	250 to 140		>TWN	≈PNL	274 to 208		800 to 700	540 to 430	>143
Approximate age (ka)																
Taxa																
PRIMATES																
<i>Macaca</i> sp.	+		+			+	+				+					
<i>Macaca assamensis</i>						cf.										
<i>Macaca nemestrina</i>												+				
<i>Macaca fascicularis</i>															+	+
<i>Trachypithecus</i> sp.																
<i>Trachypithecus cristatus</i>															+	
Hominoidea indet.						+	+									
<i>Nomascus concolor</i>						cf.										
<i>Hylobates</i> sp.																
<i>Pongo</i> sp.			+	?								+				
<i>Pongo pygmaeus</i>						+	+			+	+					
<i>Gigantopithecus blacki</i>						+	?									
<i>Homo</i> sp.								+								
<i>Homo erectus</i>														+	+	+

Table A18 (continued). Fauna lists of large mammalian species from the Middle Pleistocene of Southeast Asia. Locality abbreviations: **KS**, Khok Sung; **TWN**, Thum Wiman Nakin; **TPKP**, Thum Phra Khai Phet; **KPN**, Kao Pah Nam; **TPD**, Thum Phedan; **TK**, Tham Khuyen; **TH**, Tham Hai; **TO**, Tham Om; **MG**, Mogok Caves; **PNL**, Phnom Loang; **BDB**, Boh Dambang; **BDC**, Badak Cave; **TB**, Tambun (Kinta Valley); **KDBB**, Kedung Brubus; **TNHNK**, Trinil Hauptknochenschicht; **ND**, Ngandong. The fauna lists and ages follow Tougaard (2001) and Esposito et al. (1998, 2002) for TWN; Tougaard (1998) and Filoux et al. (2015) for TPKP; Pope et al. (1981) for KPN; Yamee and Chaimanee (2005) for TPD; Olsen and Ciochon (1990), Ciochon et al. (1996), and Ciochon (2009) for TK, TH, and TO; Colbert (1938, 1943) and Takai et al. (2006) for MG; Beden and Guérin (1973) for PNL; Demeter et al. (2013) for BDB; Ibrahim et al. (2013) for BDC; Hooijer (1962) and Medway (1972) for TB; van den Bergh et al. (2001) for KDBB; van den Bergh et al. (2001) and Joordens et al. (2015) for TNHNK; and Santa Luca (1980), van den Bergh et al. (2001), and Indriati et al. (2011) for ND. The subspecies-level identifications are not taken into account.

Locality	KS	TWN	TPKP	KPN	TPD	TK	TH	TO	MG	PNL	BDB	BDC	TB	KDBB	TNHNK	ND
CARNIVORA																
<i>Cuon</i> sp.	+					+		+			+				+	
<i>Cuon alpinus</i> (=javanicus)							+				+					
<i>Ursus thibetanus</i>		+	+			+	+				+					
<i>Helarctos malayanus</i>						+						+				
<i>Alluropoda melanoleuca</i>		+	+			+			+							
<i>Martes</i> sp.										+						
<i>Martes flavivula</i>		+														
<i>Arctonyx collaris</i>		+				+		+								
<i>Viverra zibetha</i>								cf.								
<i>Lutrogale palaeoleptonyx</i>													+			
<i>Cynogale</i> sp.													+			
<i>Felis</i> sp.								+								
<i>Panthera pardus</i>							+									
<i>Panthera tigris</i>			cf.	+			+	+		+				+		+
<i>Paradoxurus hermaphroditus</i>		+				cf.										
<i>Prionailurus bengalensis</i>											+				+	
<i>Paguma larvata</i>		+						cf.						+		
<i>Hyaena brevirostris</i>																
<i>Crocuta</i> sp.				+												
<i>Crocuta crocuta</i>	+	+	+		+					+						

Table A18 (continued). Fauna lists of large mammalian species from the Middle Pleistocene of Southeast Asia. Locality abbreviations: **KS**, Khok Sung; **TWN**; Thum Wiman Nakin; **TPKP**, Thum Phra Khai Phet; **KPN**, Kao Pah Nam; **TPD**, Thum Phedan; **TK**, Tham Khuyen; **TH**, Tham Hai; **TO**, Tham Om; **MG**, Mogok Caves; **PNL**, Phnom Loang; **BDB**, Boh Dambang; **BDC**, Badak Cave; **TB**, Tambun (Kinta Valley); **KDBB**, Kedung Brubus; **TNHK**, Trinil Hauptknochenschicht; **ND**, Ngandong. The fauna lists and ages follow Tougard (2001) and Esposito et al. (1998, 2002) for TWN; Tougard (1998) and Filoux et al. (2015) for TPKP; Pope et al. (1981) for KPN; Yamee and Chaimanee (2005) for TPD; Olsen and Ciochon (1990), Ciochon et al. (1996), and Ciochon (2009) for TK, TH, and TO; Colbert (1938, 1943) and Takai et al. (2006) for MG; Beden and Guérin (1973) for PNL; Demeter et al. (2013) for BDB; Ibrahim et al. (2013) for BDC; Hooijer (1962) and Medway (1972) for TB; van den Bergh et al. (2001) for KDBB; van den Bergh et al. (2001) and Joordens et al. (2015) for TNHK; and Santa Luca (1980), van den Bergh et al. (2001), and Indriati et al. (2011) for ND. The subspecies-level identifications are not taken into account.

Locality	KS	TWN	TPKP	KPN	TPD	TK	TH	TO	MG	PNL	BDB	BDC	TB	KDBB	TNHK	ND
<i>Bos gaurus</i>	+	+		cf.		+								+	+	
<i>Bibos palaeosondaicus</i>																
<i>Bubalus arnee</i>	+	+				+				cf.	+					
<i>Bubalus palaeokerabau</i>													+	+	+	
<i>Duboisia santeng</i>													+	+	+	
<i>Epileptobos groeneveldii</i>														+		
Caprinae indet.										+						
<i>Capricornis sumatraensis</i>	+	+	+		+			+			+	+				
<i>Neomohedus</i> sp.			+													
<i>Hippopotamus</i> sp.				+												
<i>Hexaprotodon</i> sp.													+			
<i>Hexaprotodon sivalensis</i>														+		+

Table A20 (continued). Fauna lists of extant large mammalian species from Southeast Asia and South China. The biogeographic affinities of the mammalian species are given and abbreviated as (I) for Indochinese taxa, (S) for Sundaic taxa, (O) for other geographic taxa (e.g., Palearctic and Indian regions), and (W) for widespread taxa. Data are compiled from Lekagul and McNeely (1988), Corbet and Hill (1992), and Nowak (1999). The binomial nomenclature is modified from categories of IUCN (2015) and from Groves and Leslie Jr (2011)

Country	South China	Myanmar	Laos	Cambodia	Vietnam	North (TH)	South (TH)	Malaysia	Sumatra	Java	Borneo
<i>Hemigalus derbyanus</i> (S)		+					+	+	+		+
<i>Chrotogale owstoni</i> (I)	+		+		+						
<i>Diplogale hosei</i> (S)											+
<i>Cynogale bennettii</i> (S)									+		+
<i>Herpestes brachyurus</i> (S)								+	+		+
<i>Herpestes javanicus</i> (I, S, O)	+	+	+	+	+	+	+	+		+	
<i>Herpestes semitorquatus</i> (S)									+		+
<i>Herpestes urva</i> (I)	+	+	+	+	+	+	+	+			
<i>Felis chaus</i> (W)	+	+	+	+	+	+					
<i>Prionailurus bengalensis</i> (W)	+	+	+	+	+	+	+	+	+	+	+
<i>Prionailurus planiceps</i> (S)							+	+	+		+
<i>Prionailurus viverrinus</i> (W)	+	+	+	+	+	+			+	+	
<i>Catopuma badia</i> (S)											+
<i>Catopuma temminckii</i> (I, S)	+	+	+	+	+	+	+	+	+		
<i>Paradofelis marmorata</i> (I, S)	+	+			+		+	+	+		+
<i>Neofelis nebulosa</i> (I, S)	+	+	+	+	+	+	+	+	+		+
<i>Panthera pardus</i> (W)	+	+	+	+	+	+	+	+		+	
<i>Panthera tigris</i> (W)	+	+	+	+	+	+	+	+	+	+	
PHOLIDOTA											
<i>Manis javanica</i> (S)		+					+	+	+	+	+

Table A21. The average body mass of Khok Sung mammals used for the cenogram analysis. The body mass estimation of *Elephas* sp. is obtained from the literature (Sreekumar and Nirmalan, 1989).

Rank	Taxa	Body mass (g)	Ln body mass (g)
1	<i>Elephas</i> sp.	3642000	15.10804354
2	<i>Stegodon</i> cf. <i>orientalis</i>	2436300	14.70599105
3	<i>Rhinoceros unicornis</i>	2012700	14.51498766
4	<i>Rhinoceros sondaicus</i>	1171900	13.97413692
5	<i>Bubalus bubalis</i>	944700	13.88242126
6	<i>Bos gaurus</i>	873200	13.68540187
7	<i>Bos sauveli</i>	720500	13.47076418
8	<i>Rusa unicolor</i>	255400	12.45058622
9	<i>Sus barbatus</i>	204500	12.22832325
10	<i>Panolia eldii</i>	133500	11.80185676
11	<i>Capricornis sumatraensis</i>	103600	11.54829261
12	<i>Axis axis</i>	90800	11.40199390

